1-1-2021

Protein Phosphatase 2a In Metformin's Action In Primary Human Skeletal Muscle Cells

Aktham H. Mestareehi
Wayne State University

PROTEIN PHOSPHATASE 2A IN METFORMIN'S ACTION IN PRIMARY HUMAN SKELETAL MUSCLE CELL

by

AKTHAM MESTAREEHI

DISSERTATION

Submitted to the Graduate School

of Wayne State University,

Detroit, Michigan

in partial fulfillment of the requirements

for the degree of

DOCTOR OF PHILOSOPHY

2021

MAJOR: PHARMACEUTICAL SCIENCES

Approved by:

_____

Advisor Date

_____

Co-Advisor Date

_____

_____

_____

_____

DEDICATION

I give all the glory to God for blessing me with an abundance of protection, grace, and much more than I deserve. Even during my most challenging obstacles and setbacks, He has given me my strength and encouragement to preserver. I proudly dedicate this thesis to God, my beloved mother, my siblings, and to the memory of my father.

To my family, I am truly thankful for the never-ending support, prayers and unconditional love you have given me throughout my life. Without your love and support, this chapter of my life would not have been possible.

To my mother, many thanks for teaching me that it's never too late to alter careers and pursue my passion and dreams. I could have not been blessed with a more loving, selfless, and dedicated mother. I truly thank you, from the bottom of my heart.

ACKNOWLEDGEMENTS

First and foremost, I would like to express my sincere gratitude and most profound appreciation to my advisor Prof. Zhengping Yi and my Co-advisor Prof. Anjaneyulu Kowluru for the consistent and continuous support of my Ph.D. project, for their motivation, enthusiasm, patience and immense knowledge. Their guidance helped me in all the research time and gave me the golden opportunity to do this amazing project. I could not have visualized having a better robust mentor and advisor for my Ph.D. project.

In addition to my advisor, from the bottom of my heart, I would like to thank my thesis committee: Prof. Fei Chen, Dr. Wanqing Liu, and Dr. Kyle Burghardt, for their insightful comments, encouragement, guidance, and feedback throughout this project, but for the most challenging question which incentivized me to sharpen my thinking, widened my research from several perspectives and brought my work to a higher and next level.

I would like to thank the school of medicine faculty members, especially Prof. Jian-Ping Jin and Christine Cupps from “Detroit Cardiovascular Training Program” for supporting me not only by providing a predoctoral fellowship award funded by the National Institutes of Health for two years, but also academically and emotionally through the bumpy road to finish this project, without their precious support it would not be possible to conduct this thesis.

I would also like to extend my deepest gratitude to Dr. Xiangmin Zhang for enlightening me at the first glance of research, and I remember he accustomed to say, "You are always the first one in and the last one out working in our lab".

I take this opportunity to express my profound gratitude to all of the pharmacy department faculty members for their support, help, and who gave me access to the laboratory and research facilities. My sincere thanks and appreciation also go to Prof. George Corcoran, Dr. David Pitts and Ms. Angela Bumphus for unceasing encouragement, support, and availability when I needed them the most.

I am also grateful to Dr. Chunna Guo, who encouraged me through this venture; thank you very much for your loyalty and friendship. I am deeply grateful to my fellow lab-members for the stimulating discussions, meeting, and working together for long hours and devoting much effort to our research before deadlines, and for all the fun and laughter we have had in the last four years. In particular, I need to especially thank our current lab members: Mr. Majed Alharbi, Ms. Lana Alghanem, Ms. Ruchi Jaiswal and Ms. Norah Krayem. I greatly look forward to having all of you as colleagues and friends in the years ahead. I give a profound sense of gratitude to one and all who indirectly or directly have lent their hand during this venture.

Finally, I am very grateful to all students, nurses, and physicians who helped in clinical research studies. Also, I am extremely and incredibly thankful to all participants that took part in the project and enabled this research to be possible.

TABLE OF CONTENTS

LIST OF FIGURES

LIST OF TABLES

LIST OF ABBREVIATIONS

Braf	Serine/threonine-protein kinase B-raf
AMP	Adenosine monophosphate
AKT	RAC-alpha serine/threonine-protein kinase
AS160	AKT substrate of 160 kDa
AMPK	AMP-activated protein kinase
AK1	Adenosine kinase 1
CaMKII	Ca2+/calmodulin-dependent protein kinase II
DMEM	Modification of Basal Medium Eagle
DTT	Dithiothreitol
EDTA	Ethylenediaminetetraacetic acid
EGFR	Epidermal growth factor receptor
EIF3A	Eukaryotic translation initiation factor 3 subunit A
COPD	Chronic obstructive pulmonary disease
FBS	Fetal Bovine Serum
FDR	False discovery rate
FN1	Fibronectin
FoxO1	Forkhead box O1
FYN	Tyrosine-protein kinase Fyn
GLUT4	Glucose transporter type 4
GRB2	Growth factor receptor-bound protein 2
GSK3	Glycogen synthase kinase-3
GSK3β	Glycogen synthase kinase-3 beta
HbA1C	Hemoglobin A1c
HDL	High-density lipoprotein
LDL	Low-density lipoprotein
IAA	Iodoacetamide
IFN-γ	Interferon gamma
IKK	IκB kinase
IL-1	Interleukin-1
IL-6	Interleukin-6

ILK	Integrin-linked protein kinase
IR	Insulin receptor
IRS	Insulin receptor substrate
JNK	Mitogen-activated protein kinase 8
KEGG	Kyoto Encyclopedia of Genes and Genomes
UPLC	Ultra-performance liquid chromatography instruments
LTQ	Linear iontrap quadrupole
MS	Mass spectrometry
mTOR	Mammalian target of rapamycin kinase
mTORC1	Mammalian target of rapamycin complex 1
MYH1	Myosin heavy chain 1
NEK6	Serine/threonine-protein kinase Nek6
NF-κB	Nuclear factor of kappa light polypeptide gene enhancer in B cells
NSCLC	Non-small cell lung cancer
OGTT	Oral glucose tolerance test
PA	Peak area
PBS	Phosphate-buffered saline
PFK2	6-phosphofructo-2-kinase
PIP2	Phosphorylates phosphatidylinositol-4,5-bisphosphate
PIP3	Phosphatidylinositol-3,4,5-trisphosphate
PKA	Protein Kinase A
AGC	Containing PKA, PKG, PKC families
PPM	Parts per million
PPP1CA	Serine/threonine-protein phosphatase PP1-alpha catalytic subunit
PPP1R12A	Protein phosphatase 1 regulatory subunit 12A
PPP2R2A	Serine/threonine-protein phosphatase 2A 55 kDa regulatory subunit B alpha isoform
PRKAB2	5'-AMP-activated protein kinase subunit beta-2
PRKACA	cAMP-dependent protein kinase catalytic subunit alpha
PRKAR2A	cAMP-dependent protein kinase type II-alpha regulatory subunit

PRKG1	cGMP-dependent protein kinase 1
Co-IP	Co-immunoprecipitation
ESI	Electrospray ionization
MAP2K1 /MEK1	Dual specificity mitogen-activated protein kinase kinase 1
MAP2K2 /MEK2	Dual specificity mitogen-activated protein kinase kinase 2
MAP2K6/MEK6	Dual specificity mitogen-activated protein kinase kinase 6
MAPK1/ERK	Mitogen-activated protein kinase 1
MAPK12/p38γ	Mitogen-activated protein kinase 12
MAPK13/p38δ	Mitogen-activated protein kinase 13
MAPT	Microtubule-associated protein tau
MAST2	Microtubule-associated serine/threonine-protein kinase 2
RTK	Receptor tyrosine kinases
SDS-PAGE	Sodium dodecyl sulfate polyacrylamide gel electrophoresis
SHP2	SH2 domain-containing protein tyrosine phosphatase-2
T1D	Type 1 diabetes
T2D	Type 2 diabetes
TK	Tyrosine kinase
TKL	Tyrosine kinase–like
TNF-α	Tumor necrosis factor alpha-like
GO	Gene ontology
PTM	Protein post-translational modifications
ROS	Reactive oxygen species
IPA	Ingenuity Pathway Analysis
BMI	Body fat index
CDK2	Cyclin-dependent kinase 2
CAMK	Calcium/calmodulin-dependent protein kinase
CK1	Casein kinase 1
iNOS	Inducible nitric oxide synthase
PSG	Penicillin-Streptomycin-Glutamine
RPS6	Ribosomal protein S
RPS6KA3/RSK2	Ribosomal protein S6 kinase alpha-3
STK11/LKB1	Serine/threonine-protein kinase STK11

CML	Chronic myelogenous leukemia
IMAT	Intermyocellular and perimuscular adipose tissue
CAMK2G	Calcium/calmodulin-dependent protein kinase type II sub-unit gamma
CDK2	Cyclin-dependent kinase 2
CACNB1	Voltage-dependent L-type calcium channel subunit beta-1
CSNK1A1	Casein kinase I isoform alpha
TP53RK	TP53-regulating kinase
PSMA1	Proteasome subunit alpha type-1
CMGC	Containing CDK, MAPK, GSK3, CLK families
PSMC3	26S proteasome regulatory subunit 6A
YES1	Tyrosine-protein kinase Yes
PSMD11	26S proteasome non-ATPase regulatory subunit 11
PSMD14	26S proteasome non-ATPase regulatory subunit 14
PSMD7	26S proteasome non-ATPase regulatory subunit 7
RAP1B	Ras-related protein Rap-1b
RPS3	40S ribosomal protein S3
RPS6	40S ribosomal protein S6
HSPA2	Heat shock-related 70 kDa protein 2
ACTG1	Actin, cytoplasmic 2
CSNK2A1	Casein kinase II subunit alpha
SRC	Tyrosine-protein kinase Src
NANA	Nascent polypeptide-associated complex alpha subunit
VIM	Vimentin

CHAPTER 1 INTRODUCTION

1.1 INTRODUCTION TO DIABETES AND INSULIN SIGNALING PATHWAY

1.1.1 DEFINITION AND DIAGNOSTIC CRITERIA FOR DIABETES

Diabetes is a group of metabolic diseases of various etiology characterized by chronic hyperglycemia resulting from defects in insulin action, insulin secretion, or both[1]. The chronic hyperglycemia of diabetes is linked with damage, dysfunction, and failure assorted organs like eyes, heart, kidneys, and brain[1]**.** Diabetes characteristic symptoms include unexplained weight loss, thirst, fatigue, slow healing, sores, blurring of vision, polydipsia, and polyuria. Ketoacidosis is the most severe form that may develop, lead to coma and death in the absence of effective treatment[2]. The number of people with diabetes rose from 108 million in 1980 to 422 million in 2014, according to a global diabetes report presented by the World Health Organization in 2020[2]. 10.5% of the US population (34.2 million people of all ages) have been diagnosed with diabetes by 2020 based on their fasting glucose and A1C[3]. 1.6 million deaths were directly caused by diabetes in 2016 [2]. The underlying cause of diabetes varies by type, and this increase in people diagnosed with diabetes requires the immediate attention of researchers, healthcare providers, and also the general public worldwide. The long-term effects of diabetes include the progressive development of retinopathy with potential blindness, nephropathy that may drive to renal failure, and/or neuropathy with a risk of foot ulcers, amputation, and autonomic dysfunction, as well as cerebrovascular, peripheral vascular, and cardiovascular diseases [2].

Diabetes is mainly classified into type 1 (T1D) and type 2 diabetes (T2D). The main reason for T1D is absolute insulin deficiency caused by autoimmune destruction

of the β-cell. Comparatively, T2D is caused by the combination of relative insulin deficiency and insulin resistance. T2D is the most popular types of diabetes and accounts for 90-95% of all diabetic patients, one of the largest epidemics around the world. T1D can develop at any age, and often appears during childhood or adolescence, and accounts for 5-10% of those with diabetes. T2D is common in people older than 40. There are major factors contributing to T2D, such as genes and lifestyle. Gestational diabetes is another type of diabetes that can appear in pregnant women with no medical history of the disease. The estimated cost of diabetes in 2017 was $327 billion for diagnosed diabetes compared to 2012 ($245 billion), which is more than 33 % increase in merely 5 years[4].

Diabetes is diagnosed by hyperglycemia through physical assessment, medical history, and blood glucose tests such as FPG, OGTT, and A1C[4]. The oral glucose tolerance test (OGTT) is a time-intensive diagnostic test, where the patients are required to fast at least eight hours before the 75-g oral glucose load followed by two hours blood draw every 30 minutes up to 2 hours for plasma glucose measurement using a glucose analyzer[4]. The current diagnostic criteria for diabetes and prediabetes are summarized in Figure 1.

1.1.2 PHYSIOLOGY OF NORMAL GLUCOSE HOMEOSTASIS

Glucose is an essential source of energy for mammalian cells; Glucose needs to leave the bloodstream and get inside the cells to provide energy. In humans, glucose is directly gained from the diet or by synthesis in the kidney and the liver. There are several classes of glucose transporters such as the sodium-glucose cotransporters, and the facilitative glucose transporters and SemiSweet facilitative hexose transporters (SWEETs). Blood glucose concentrations must be maintained within narrow ranges

(glucagon and insulin are hormones that make it happen). The process of maintaining and preserving blood glucose level is called glucose homeostasis[4].

After a carbohydrates-rich meal, carbohydrates are broken down into simple sugars and primarily glucose, then glucose will be absorbed into the bloodstream and plasma glucose will start to rise. Insulin is produced by beta cells of the pancreas to maintain the plasma glucose levels. Insulin is a peptide hormone that consists of two polypeptide chains containing 51 amino acids, which are linked together by disulfide bonds and has a molecular mass of 5808 Da[5].

The combined hyperglycemia and insulin effects to enhance glucose disposal include stimulation of glucose uptake by peripheral tissues (primarily muscle); stimulation of glucose uptake by the splanchnic (hepatic & gastrointestinal) tissues; and inhibition of endogenous (mainly hepatic) glucose production. Many tissues contribute to optimize and maintain glucose levels in the whole human body, which is represented in Figure 2.

1.1.3 OVERVIEW OF SKELETAL MUSCLE

The skeletal muscle system is the largest organ/tissue in the human body, about 40% of the total body weight of a young man, which stores energy in the form of proteins. It is significant and important for glucose homeostasis, movement, and metabolism[6].

The skeletal muscle is attached to the bones by bundles of collagen via tendons and it's a form of striated muscle tissue that is under voluntary control by the somatic nervous system, unlike the other two human muscle tissue types, smooth and cardiac muscle[7]. Skeletal muscle refers to a number of muscle fiber bundles (fascicles) that can differ in fiber type. Based on the skeletal muscle metabolic characteristics, fibers can

be divided into fast-twitch Type 2 and slow-twitch Type 1 fibers, and are defined by their myosin heavy chain (MHC) isoform expression[8].

Skeletal muscle plays important role in metabolic diseases, such as diabetes, obesity, aging, and insulin-resistance. In addition, skeletal muscle releases myokines to promote tissue cross talk. Insulin stimulates glucose uptake in various tissues and organs in the body such as adipose tissue, brain, and skeletal muscle. Skeletal Muscle is the major site of insulin-stimulated glucose clearance and is responsible for ~80% of insulin-stimulated glucose uptake. Under the hyperinsulinemic-euglycemic condition, insulin-stimulated glucose uptake is similar between non-diabetic controls and T2D patients in brain, liver, and adipose tissue but is markedly diminutive in skeletal muscle[9] as shown in Figure 3. Glucose uptake occurs in skeletal muscle through multiple signaling events that lead to the translocation of GLUT4.

1.1.4 NORMAL INSULIN SIGNALING PATHWAYS IN SKELETAL MUSCLE

The main actions of (direct & indirect) insulin on cells include stimulation of glucose uptake, protein synthesis, and glycogen synthesis through activation of various pathways in skeletal muscle cells[5].

The two major pathways of insulin signaling emerging from the insulin receptor are phosphatidylinositol 3-kinase (PI3K, a lipid kinase)/AKT (also known as protein kinase B or PKB) pathway and the Raf/Ras/MEK/ MAPK (mitogen activated protein kinase, also known as extracellular signal-regulated kinase or ERK) pathway[10] as shown in Figure 4. The PI3K pathway is responsible for the major metabolic effects of insulin. Insulin binds to tyrosine kinase insulin receptor present on the cell membrane and activates it, leading to phosphorylation of its substrates, such as IRS-1, and start the intracellular signal transduction cascade[5].

Activation of PI3K pathway is triggered by the binding of the IRS1 and IRS-2 to p55 or p85 regulatory subunit of PI3K (which has 8 isoforms), resulting in activation of the p110 catalytic subunit (which has three isoforms) and increases in phosphatidyl-inositol-3,4,5-triphosphate (PIP3), which leads to the activation of PDK (phospho-inositide-dependent protein kinase) 1 and -2 (as shown in Figure 5)[5]. PDK1 then phosphorylates and activates AGC protein kinase family proteins, which include isoforms of p70 ribosomal S6 kinase (S6K), AKT/protein kinase B (PKB), and several isoforms of protein kinase C (PKC), as well as serum-glucocorticoid-induced protein kinase (SGK), which are responsible for PI3K-PIP3 downstream effects. The AKT/PKB family consists of three different isoforms, AKT2 is most abundant in insulin-sensitive tissues and plays a predominant role in mediating insulin action on metabolism. AKT is phosphorylated at Thr-308 by PDK-1 and at Ser-473 by mammalian target of rapamycin complex 2 (mTORC2)[11]. There are multiple downstream substrates of AKT/PKB including glycogen synthase kinase 3 (GSK3), involved in the regulation of glycogen synthesis; mammalian target of rapamycin (mTOR), involved in the regulation of protein synthesis; forkhead box-containing protein O subfamily (FoxO), transcription factors, especially FoxO1, involved in the regulation of gluconeogenic and adipogenic genes, and AS160 (AKT substrate of 160kDa), engaged in glucose transport (Figure 6). mTOR is a serine/threonine kinase (mTORC1 and mTORC2) that acts as a nutrient sensor; it induces protein synthesis by phosphorylating eukaryotic translation initiation factor 4E-binding protein 1 (4EBP1) and p70 ribosomal protein S6 kinase (p70S6K)[5].

The MAPK-ERK pathway emanates from both Shc and IRS, regulating gene expression, proliferation, cytoskeletal reorganization, and differentiation. Activated receptor and IRS proteins bind to adaptor molecules like Grb2; and exist in a complex with SOS (son of sevenless). SOS is a Guanine nucleotide exchange factor, activates

Ras-GDP to Ras-GTP, and stimulates downstream target MEK1 & 2 that phosphorylate and activate the cascade of serine/threonine kinases Raf/MEK/ ERK1-2[11].

Glucose disposal into muscle is the major component of insulin action that prevents postprandial hyperglycemia, through the translocation of the insulin-sensitive glucose transporter GLUT4 from intracellular vesicles to the plasma membrane. The molecular mechanism is still not entirely and fully understood. GLUT4 is highly expressed in skeletal muscle, adipose tissue, and is one of 13 human glucose transporter isoforms (GLUTs). PI3K/PDK1/AKT2 pathway is the major insulin signaling pathway involved in GSVs translocation, through phosphorylation of the AS160 substrate (GTPase-activating protein). When AS160 is phosphorylated, it activates small G proteins called RAB, by blocking the exchange of GTP for GDP. PKCs isoforms appear to be involved in downstream of PDK1 but not through AKT (Figure 7). In addition to insulin, exercise also stimulates glucose transport and GLUT4 translocation through an insulin-independent and AMPK-dependent mechanism[5].

Plenty of mechanisms are in place to diminish or terminate the signal increased by insulin, both at the receptor and post-receptor level that can lead to negative regulators of insulin signaling and insulin resistance. The insulin receptor and IRS proteins are negatively regulated by ligand-induced downregulation, serine phosphorylation and tyrosine protein phosphatases. Many IRS kinases are activated by insulin such as S6 kinase, c-Jun-N-terminal kinase (JNK), and ERK, indicating that IRS serine phosphorylation is a negative feedback mechanism in the insulin signaling network[5]. Serine/threonine phosphatases have been implicated in insulin action such as PP2A, PP2B, PP1 and two novel members of PP2C. Transmembrane phosphatases, such as LAR, and protein tyrosine phosphatases, such as PTP1B, have been shown to dephosphorylate the tyrosine residues on activated IR. Lipid phosphatases such as PTEN and SHIP1

dephosphorylates PIP3. Proteins of the suppressor of cytokine signaling (SOCS) family, Tribbles homolog 3 (Trb3), Grb, inositol phosphate (IP7) are among the other negative regulators[11]. The insulin signaling pathways can be influenced by many factors such as hyperglycemia, cytokines, fatty acids, ER stress and mitochondrial dysfunction. These negative regulators of insulin signaling are summarized in Figure 8.

1.1.5 TYPE 2 DIABETES AND OBESITY IN SKELETAL MUSCLE INSULIN RESISTANCE

Type 2 diabetes (non-insulin-dependent) is one of the major common metabolic disorders, characterized by relative insulin insufficiency and insulin resistance. Most patients with T2D are obese, and obesity causes higher risk of insulin resistance[7]. About 80% of glucose uptake takes place in skeletal muscle and insulin resistance is a characteristic feature of T2D. In T2D, one of the earliest detectable metabolic defect is impaired glycogen synthesis secondary to decrease glycogen synthase activity[9].

Obesity increases the risk for many diseases, particularly insulin resistance, cardiovascular disease, T2D, and the mechanisms linking these diseases with obesity remain unclear. Obesity defined as Body Mass Index $\geq$ 30 kg/m^2, is one of the global epidemics and it has tripled globally since 1975. On the other hand, severe obesity is defined as a BMI $\geq$ 40 kg/m^2. More than 1.9 billion adults were overweight, of these over 650 million adults were obese and over 340 million adolescents and children (aged 5-19 years) were overweight or obese in 2016. In 2019, 38 million children under the age of 5 years were obese or overweight[12]. In the United States, more than 93 million adults, ~42.4% of the adult population, and ~20% of children and adolescents (aged 6 to 19 years) were obese in 2017 to 2018[13]. Obesity is associated with chronic low-grade inflammation in several tissues, including skeletal muscle, adipose tissue, liver, pancreas islet, brain, and intestine, which contributes to insulin resistance and T2D[14].

T2D and obesity are becoming global epidemics, increasing the health burden that affects a large portion of the human population in the world and in the United States. However, molecular links between T2D, obesity, and insulin resistance remain to be elucidated.

1.1.6 MECHANISMS OF INSULIN RESISTANCE IN SKELETAL MUSCLE

Numerous studies have reported possible dysregulation of the insulin receptor signaling network in causing insulin resistance both *in vitro* in cell lines, and *in vivo* in animal models and humans. Many factors influence insulin sensitivity and lead to insulin resistance such as any defect steps in normal insulin singling pathway and activation/abnormal function of negative regulators of insulin signaling pathway. Research over the years has explored the role of the individual or combined role of these regulators in molecular mechanisms of insulin resistance network, which include inflammation, genetic mutations, hyperglycemia, lipotoxicity, hyperinsulinemia, ER stress, and mitochondrial dysfunction. Gene mutations in the insulin receptor gene IRS-1, AKT2, PI3K, PTEN, AS160, and Trb3 have been identified to severe insulin resistance. Ectopic accumulation of lipids (especially fatty acids) is believed to cause insulin resistance through multiple mechanisms such as activation IKK, PKC, Ser-307, IRS-1 phosphorylation, and JNK[11].

Increased plasma concentration of the sphingolipid ceramide is associated with insulin resistance and noticed in diabetic and obese patients. Ceramides inhibit AKT activation by inducing the interaction of PP2A with AKT, and phosphorylation of AKT at Thr-34 by PKC ζ, resulting in increased binding of PIP3 to AKT[15]. Increased TNF-α, IL1β, or IL-6 is observed in obesity and leads to induced insulin resistance through multiple mechanisms of activation of Ser/Thr kinases, decreasing IRS-1, GLUT4, and PPARγ expression[16].

Skeletal muscle insulin resistance appears before the onset of β-cell failure and symptomatic T2D. The desensitization of muscle causes insulin resistance to the insulin released by the pancreas to elicit glucose uptake, increasing in blood glucose levels. Skeletal muscle is considered the primary driver of whole-body insulin resistance, although skeletal muscle insulin resistance is reversible. Moreover, there is a delay in glucose uptake and insulin action in insulin resistance and T2D causing reduced overall glucose uptake by the skeletal muscle[7].

Sarcopenia is known as reduced muscle mass and a gradual decline in mitochondrial function in human skeletal muscle as aging (40-50 years), while aging is a main risk factor of T2D. This age-associated muscle dysfunction can lead to other diseases especially combined increased fat mass (obesity) and decreased skeletal muscle mass (sarcopenia)[17].

There are several methods available clinically to determine insulin resistance or insulin sensitivity, such as Hyperglycemic Clamp, Insulin Tolerance Test (ITT), the Insulin Modified frequently Sampled Intravenous Glucose Tolerance Test (FSGIT), Fasting Surrogates, the Oral Glucose Tolerance Test (OGTT), and the Hyperinsulinemic-Euglycemic Clamp that used where insulin sensitivity measurement and maintenance of steady-state conditions is crucial[18]. All the methods have their importance and validity. From these, the hyperinsulinemic-euglycemic clamp should be the first choice to determine insulin sensitivity, which is considered the golden standard to assess the action of insulin in *vivo*[9].

1.1.7 MECHANISMS OF INFLAMMATION IN SKELETAL MUSCLE

There is an essential relationship between insulin resistance and weight that has been demonstrated by nondiabetic and lean studies, suggesting that obesity increases the risk of insulin resistance. The chronic inflammation resulting from obesity is a main

significant contributor to insulin resistance and T2D pathogenesis. T2D is associated with elevated blood glucose, elevated circulating pro-inflammatory cytokines, and increased free fatty acids, which can all lead to insulin-resistance[19].

The skeletal muscle acts as an endocrine organ, secreting factors called "myokines." Myokines are proteins emitted by skeletal muscle that are masterful of cross-talk with other organs such as the adipose tissue, bone, and brain. Obesity-induced insulin-resistance and inflammation by the release of particular cytokine hormones from both tissues (adipo-myokines). Skeletal muscle secretes interleukin-8 (IL-8), interleukin-6 (IL-6), interleukin-15 (IL-15), myostatin, irisin, and myonectin. The release can either reduce or increase inflammation, insulin-resistance, and obesity[20]. One theory of skeletal muscle insulin-resistance development is the activation of immune cells such as T cells and macrophages, in both mouse models and humans, they can become pro-inflammatory during obesity or T2D. The intramuscular adipose tissue depots are the main contributors of pro-inflammatory immune cells to the skeletal muscle (e.g. M1-like macrophages). They account for up to 10% of the total skeletal muscle mass which expands with obesity and T2D[21]. The cross-talk between skeletal muscle and adipose tissue drives the pro-inflammatory phenotype in skeletal muscle and is a primary contributor to the development of insulin-resistance[22]. Pro-inflammatory cytokine (IL-6) is released by skeletal muscle with TNFα contributes to insulin-resistance. Myonectin activates the AMP-activated protein kinase (AMPK) pathway in myocytes, resulting in increased translocation of the GLUT4 glucose transporter and glucose uptake. In addition, myostatin signaling can inhibit the AKT-mediated mTOR pathway leading to activation of the ubiquitin-proteasome pathways and autophagy via the FOXO pathway, which is involved in protein degradation[23]. The cytokines, including IFN-γ and TNF-α, can activate IκB kinase/NF-κB (IKK/NF-κB) and JNK pathways as shown in Figure 9.

There is growing research evidence showing that the IKK/NF-κB pathway was increased in obesity and T2D[12].

Interleukin 15 (IL-15) can decrease inflammation, obesity, increase glucose uptake, and enhance mitochondrial oxidative functions in cultured skeletal muscle cells and rat skeletal muscle, via the AMPK and STAT3 pathways[24]. O-GlcNAcylation (O-GlcNAc) is a posttranslational modification of serine or threonine hydroxyl groups, has been proposed to enhance IL-15 expression in skeletal muscle. O-GlcNAcylation is elevated in the skeletal muscle of T2D and obesity. Moreover, O-GlcNAc inhibits the activity of insulin-stimulated glucose uptake pathways including the insulin receptor (IR), PI3K, and AKT. In addition, O-GlcNAc synthesis through the hexosamine biosynthesis pathway (HBP) is enhanced under hyperglycemic conditions and leads to insulin-resistance through the modulation of AKT signaling[25]. In addition, there is cross-talk between O-GlcNAc and AMPK, indicating that more work needs to be done to understand the molecular mechanism underlying T2D, obesity, and insulin-resistance in skeletal muscle.

1.1.8 MECHANISMS OF GLUCOSE UPTAKE IN SKELETAL MUSCLE

There are several glucose transporters to facilitate glucose movement across the plasma membrane. This membrane-spanning SLC2A family is integral to the transportation of other hexoses and glucose either to outside or inside of the cell. More than 14 SLC2A-family glucose transporters are expressed in human cells and categorized based on sequence similarity as a class (I, II, and III). The GLUT proteins have 12 membrane-spanning domains and are included in ~500 amino acid residues[26].

There are three GLUTs in skeletal muscle responsible for facilitating glucose uptake; GLUT1, GLUT4, and GLUT3 (expressed in neonatal and fetal muscle

only). GLUT4 is known as the insulin-regulated glucose transporter and primarily localizes to intracellular vesicles, and is transported to the cell surface. It is highly abundant in adipose tissue, skeletal muscle and is encoded by the SCL2A4 gene[7]. There are two pathways (Canonical insulin signaling pathway and Noncanonical insulin signaling pathway) in the skeletal muscle to insulin stimulates GLUT4 vesicle translocation, once insulin binds to the α-subunit of IR and activates the intracellular signaling cascade. This leads to a conformation change and tyrosine phosphorylation of the IR ß-subunit.

These two pathways are involved by the activating of the Rho-family GTPase Rac1 in the noncanonical insulin signaling pathway or the serine/threonine kinase AKT in the canonical insulin signaling pathway. As shown in Figure 10, both pathways function autonomously and independently to activate GLUT4 translocation[7].

1.2 INTRODUCTION TO KINASES AND PHOSPHATASES

In a normal cell, one-third of proteins are regulated by phosphorylation. It is one of the most important post-translational modifications and is vital to control numerous biological functions such as proliferation, cell division, apoptosis, and survival. Proteins shift from a dephosphorylated to a phosphorylated state and vice versa; and are controlled specifically by protein phosphatases and kinases. The reversible phosphorylation of proteins including threonine (Thr), tyrosine (Tyr), and serine (Ser) amino acids, is shown in Figure 11. Dephosphorylation is catalyzed by the protein phosphatases, whereas the phosphorylation of these hydroxyl- amino acid side chains is catalyzed by the protein kinases[27]. The degree of phosphorylation between these phosphorylated amino acids, phosphoserine (pSer) predominates with 86.4% of the total phosphorylation, followed by phosphothreonine (pThr) at 11.8%, then phosphotyrosine (pTyr) with 1.8%[28].

The researchers have identified many protein kinases and classified them into protein tyrosine kinases and protein serine-threonine kinases. Protein serine/threonine phosphatases (PSPs) and protein tyrosine phosphatases (PTPs) are two major classes of protein phosphatases. PSPs are divided into three sub-families[29]:

Phosphoprotein phosphatases (PPPs), such as PP4, PP5, PP6, PP1, calcium-activated PP2B (also known as calcineurin), PP7, and PP2A.

Metal (Mg^{+2} and Mn^{+2}) dependent protein phosphatases (PPMs), catalyze the reaction, comprised of PP2C and pyruvate dehydrogenase phosphatases.

Aspartate based phosphatase, use an aspartic acid signature (DXDXT/V). Halo acid dehydrogenases (HAD) enzyme family and the phosphatases are transcription initiation factor II are examples of this group

The human genome sequence contains 25000 total proteins, 518 total protein kinases (385 Protein serine/threonine kinase, 90 Protein tyrosine kinase, and 43 PTK like protein), and 119 total protein phosphatases (21 Protein serine/threonine phosphatase and 98 Protein tyrosine specific phosphatase)[30].

We aimed to investigate and study protein phosphatase 2A (PP2A) in human skeletal muscle cells in lean insulin-sensitive and obese insulin-resistant groups.

1.2.1 PROTEIN PHOSPHATASE 2A (PP2A), REGULATION, MODIFICATION, AND INTERACTING PROTEINS

PP2A is one of the main serine-threonine protein phosphatases. It plays a pivotal role in cellular processes, like signal transduction, cell proliferation, and apoptosis, by dephosphorylating key signaling molecules such as AKT, AMPK, p53, c-Myc, etc[31]. It constitutes 0.3 - 1% of the total protein in the mammalian cell[31]. The majority of the soluble phosphatases activity at phosphoserine and phosphothreonine is catalyzed by

PP2A. PP2A structurally; is a heterotrimeric complex with a dimeric core enzyme, as shown in Figure 12, consisting of a 55kda B regulatory subunit (PP2Ab), a 65kda scaffold subunit A (PP2Aa), and a 36kda catalytic subunit C (PP2Ac). PP2A exists in two forms; a dimer form ($PP2A_D$) or a trimer complex ($PP2A_T$)[32].

PP2A plays a role in numerous signaling pathways, such as mTOR and MAPK deregulation and dysfunction of PP2A affect various physical processes.

1.2.2 PP2A SUBUNITS

PP2A (A scaffold subunit) has two isoforms, alpha (Aα) and beta (Aβ), and are encoded by two different genes PPP2R1B and PPP2R1A. They are both share 86% sequence similarity. The dimer core, in most cases (90%), is composed of A alpha isoform. Both the isoforms are located within the cytoplasm and account for 0.1% of the total protein[31]. Structurally, PP2A-A consists of HEAT sequence (Huntington-elongation-A-subunit-TOR) including 15 tandem repeats of 39 amino acids[28]. The various isoforms of several subunits of PP2A and their subcellular distribution are shown in Table 1[28].

PP2A (B regulatory subunit) regulates activity, localization, and substrates for the complex. PP2A-B is encoded by 15 different genes and has a minimum of 26 different splice variants and transcripts. It is the master regulator of PP2A. PP2A-B is classified into four different families known as B (B55/PR55), B' (B56/PR61), B'' (PR48/PR72/PR130), and B''' (PR93/PR110). B55 has four different isoforms (α, β, γ, and δ), B56 has five isoforms (α, β, γ, δ, and ε), B'' contains PR72 (expressed in skeletal muscle & heart) & PR130 (expressed in all tissues and is abundant in muscle & heart) and B''' is found by yeast two-hybrid screening[28].

PP2Ac (catalytic subunit) is most abundant in (the brain & heart) and expressed in almost all tissue. PP2Ac (37kDa) exists in two isoforms (Cα & Cβ) shares

40% identical sequences with PP2B, 50% amino acid sequences with PP1, and 86% identical in humans and yeast. Both isoforms share 97% sequence similarity and consist of 309 amino acids, Cβ is expressed in the (nucleus & cytoplasm), and Cα is expressed in the plasma membrane. PP2Acβ is less abundant than PP2Acα because of the lower degree of mRNA translation and week promoter activity. An interesting feature of PP2Ac is C terminal tail is conserved (^{304}TPDYEL^{309}) and the tail binds to the regulatory and scaffold subunits (PR61γ)[28,32].

1.2.3 REGULATION OF PP2A

The activity and specificity of PP2A can be influenced by the presence and the binding of the other regulators against a particular substrate such as binding of α4 to PP2A is important to stabilize PP2Ac in its inactive conformation[33]. In addition, it reports an important regulator called Phospho tyrosyl phosphatase activator (PTPA), which facilitates its Serine/Threonine phosphatase activity by stabilizing PP2A in an active conformation[34]. PP2A is also being regulated by subunit diversity, autoregulation, post-translational modifications, and substrate protein interaction. The two major modifications that modulate PP2A efficiency are methylation and phosphorylation. The phosphorylation on Tyr^{307} decreases PP2A activity, by preventing its interaction with the regulatory subunit of PP2Ac and PP2A-PR55/PR61. In addition, PP2A undergoes carboxyl methylation on the carboxyl group of the C-terminal residue of Leu^{309}. Leucine Carboxyl MethylTransferase1 (LCMT1), also known as PP2A-Methyltransferase (PPMT), is responsible for methylation of PP2Ac; meanwhile, PP2A Methyl Esterase (PPME) is responsible for PP2Ac de-methylation. Several investigators reported that, the addition of a methyl group by LCMT1 at Leu^{309} increases the binding affinity of the core dimer (A & C subunit) and provides a specific activity to the holoenzyme[35].

1.2.4 INHIBITORS OF PP2A

$I1_{PP2A}$ and $I2_{PP2A}$ are two inhibitors found to inhibit PP2A through *in vitro* and *in vivo* experiments[36]. Okadaic acid (a microbial toxin), inhibits the enzymatic activity of PP2Ac at low concentration < 10nM. Other inhibitors are commercially available to inhibit PP2A activity such as calyculin A, tautomycin, microcystins, nodularm, fostriecin, and cantharidin at IC_{50} values.

1.2.5 ROLE PP2A IN DIABETES

IRS-1 interacts with PP2Ac on human skeletal muscle biopsies that were confirmed by our lab. This interaction was increased in T2D patients and obese insulin-resistant nondiabetic controls compared to lean nondiabetic controls[37]. Several studies have shown that insulin inactive PP2A *in vitro* and *in vivo* experiments. Srinivasan and Begum are reported that insulin deactivated PP2A in the differentiated rat L6 cells and the phosphatase activity decreased relatively with the increased concentrations of insulin and the incubation time[38]. PP2A is phosphorylated (Tyr^{307}) *in vitro* by the tyrosine kinases and leads to the deactivation PP2A as reported by Jian Chen., et al.[36]. Rosanna Cazzolli., et al. reported that insulin treatment reduced the glycogen synthesis by inhibition of phosphorylation on PKB of C2C12 skeletal my tube cells, which is extremely very important for the INS/IRS-1/AKT pathway [39]. Hojlund K., et al. reported that PP2Ac protein levels in control subjects decreased compared to the basal levels but not in T2D upon insulin stimulation in human skeletal muscle. Indeed, they also reported an increase in lipid oxidation, reduction in glucose oxidation, and glucose disposal[40]. Palmitate negatively regulates the insulin signaling pathway by enhancing PP2A, leading to dephosphorylate AKT and ERK1/2, as reported by Nardi, F., et al.[41]. Furthermore, Mandavia, C. & Sowers, J.R. demonstrated that PP2A has a positive impact on

the INS signaling pathway by diminishing the excessive serine phosphorylation on the IRS-1 in cardiomyocytes[42].

1.3 TREATMENT OF DIABETES

Physical inactivity is the primary cause of most chronic diseases such as T2D and obesity. The main goal to control blood sugar (glucose) levels within the normal range in treating type 1 and T2D. Moreover, most T2D patients can achieve their target blood glucose levels with exercise and diet alone but might need insulin therapy or oral medication depends on several factors. Appropriate pharmacologic therapy is available on the market and it is important to determine if the patients are insulin-deficient, insulin-resistant, or both. Treatments are classified into different mechanisms such as enhancing glucose absorption, decreasing hepatic glucose production, increasing insulin-sensitivity, and stimulating insulin secretion.

There are numerous treatments to help people with their diabetes; maintain glucose levels, and these drugs have several different mechanisms to lower glucose levels. Figure 13 shows several sites of action of the pharmacological therapies for theT2D treatment[43].

Sulfonylureas, it helps the body secrete more insulin such as glimepiride (Amaryl), glyburide (DiaBeta, Glynase), and glipizide (Glucotrol). The side effects include weight gain and low blood sugar.

Meglitinides, it works by stimulating the pancreas to secrete more insulin, they're faster acting, and the duration of their effect in the body is shorter than sulfonylureas, like nateglinide (Starlix) and repaglinide (Prandin). The side effects include weight gain and low blood sugar.

Thiazolidinediones, similar to metformin, it makes the body's tissues more sensitive to insulin. These medications include pioglitazone (Actos) and rosiglitazone (Avandia). It also has been linked to weight gain, an increased risk of heart failure and anemia. Because of these side effects, Thiazolidinediones aren't the first-choice treatments.

DPP-4 inhibitors, it helps decrease blood sugar levels. These medications include sitagliptin (Januvia), linagliptin (Tradjenta), and saxagliptin (Onglyza). Their side effects increasing the risk of pancreatitis and joint pain.

GLP-1 receptor agonists, it helps lower blood sugar levels and the side effects include nausea and an increased risk of pancreatitis. These medications are injectable and their use is associated with weight loss. Exenatide (Byetta, Bydureon), semaglutide (Ozempic), and liraglutide (Victoza) are examples of GLP-1 receptor agonists.

SGLT2 inhibitors, it prevents the kidneys from reabsorbing sugar into the blood and it is excreted in the urine. Examples include empagliflozin (Jardiance), canagliflozin (Invokana), and dapagliflozin (Farxiga). These medications are linked to low blood pressure, urinary tract infections, vaginal yeast infections, and a higher risk of diabetic ketoacidosis.

Insulin, there are many types and each works differently. These medications are insulin detemir (Levemir) or insulin glargine (Lantus). Insulin is mainly used in type 1 diabetes treatment and also can be used in T2D.

Biguanides (such as Glucophage, Glumetza, Fortamet), it works by decreasing glucose production in the liver and increasing insulin-sensitivity so the body uses insulin more effectively. Metformin is the most common biguanide and the first line of drug to treat T2D, and particularly in obese patients. It has been shown to decrease mortality and complications compared to other medications. These medications are

linked to nausea and diarrhea. If lifestyle changes and metformin are not enough to maintain a blood glucose level, other injected medications can be added. Metformin can also combine with other T2D drugs such as, metformin-pioglitazone (Actoplus), metformin-rosiglitazone (Avandamet), metformin-alogliptin (Kazano), and metformin-glyburide (Glucovance). Metformin is used to treat polycystic ovary syndrome (PCOS) in insulin-resistance and enhance outcomes in assisted reproduction. The current clinical data and recent translational research link the effects of metformin on pregnancy, reproductive healthcare, prediabetes, aging, cancer, cardiovascular diseases, and neurodegenerative diseases[44].

We aimed here to investigate the precise molecular mechanisms of metformin in human skeletal muscle cells.

1.3.1 METFORMIN MECHANISM OF ACTION AND CLINICAL APPLICATION

Metformin (N, N-dimethylbiguanide) was first discovered to decrease glucose levels in the 1920s by Slotta and Tschesche. In 1957 metformin was used for diabetes treatment by French physician Jean Steme. A large clinical trial performed in the 1980-1990s by the United Kingdom Prospective Diabetes Study confirmed the effect of metformin on improving mortality and morbidity in T2D. Canada approved it in 1972 and by US-FDA in 1994. It is a hydrophilic base and exists at physiological pH as the cationic species (>99.9%). The chemical formula of metformin is $C_4H_{11}N_5$ and the chemical structure is shown in Figure 14. Metformin oral bioavailability (F) is 55 ± 16 % (mean± SD) and has acid dissociation constant (pKa) of 2.8 and 11.5. Metformin peak plasma concentrations occur ~3 hours after 500mg dosage, and it ranges from 1.0 to 1.6 mg/L; this leads to an increase after 1500 mg dose to 3 mg/L. The elimination half-life of metformin is ~5 hours in plasma and 18 hours in red blood cells. Metformin has been

used with an excellent safety record and has been an effect on several organs and/or tissues such as adipose tissue, kidney, liver, and skeletal muscles[45].

Several molecular mechanisms of action of metformin have been proposed but more remain to be investigated. We focus on human skeletal muscle and insulin-resistance in this chapter. It is widely accepted that metformin can reduce glucose production in the liver by inhibiting gluconeogenesis, increasing insulin-sensitivity (i.e., decreasing insulin-resistance) and enhancing glucose uptake in skeletal muscles, and diminishing intestinal glucose absorption. The potential mechanisms of metformin action involve multiple pathways. Metformin inhibits the mitochondrial respiratory chain (complex I), which enhances the AMP/ATP ratio, resulting in an increase in the phosphorylation of AMP-activated protein kinase (AMPK) at Thr-172, which has a variety of effects on energy homeostasis and cellular metabolism[46]. The increase of AMP/ATP leads to inhibiting the activity of adenylate cyclase, which leads to the inhibition of gluconeogenesis[47]. Metformin diminishes mitochondrial glycerol -3 phosphate dehydrogenase activity, which thus leads to the suppression of gluconeogenic[48].

Metformin enhances the AMPK pathway which improves glucose uptake GLU4 through SLC2A4 in skeletal muscle, as reported by Li Gong., et al.[49]. Furthermore, some papers have been published indicating that metformin treatment reduces NADH: O_2 activity in skeletal muscle tissue[48]. Metformin can enhance insulin receptor tyrosine kinase activity, increase glycogen synthesis, and increase the activity of GLUT4 glucose transporters. As reported in insulin-resistant rats, metformin enhances insulin-sensitivity of skeletal muscle, vascular, increased glucose uptake, and diminishes the level of circulating branched-chain amino acids in insulin-resistant skeletal muscle[49]. Recent studies indicate that metformin lowers asymmetric dimethylarginine (ADMA) plasma concentrations, which is associated with T2D patients[50].

Metformin treatment significantly increases AMPK α2 activity in skeletal muscle in participants with T2D, and this is associated with enhanced phosphorylation of AMPK on Thr172 and decreased acetyl-CoA carboxylase-2-activity. Moreover, phosphocreatine and ATP concentrations are lower after metformin treatment in T2D participants, and therefore the increase in activity of AMPK α2 is likely because of a change in muscle energy status. These results strongly suggest that the metabolic effects of metformin in T2D could be mediated by AMPK α2 activation, as reported by Nicolas Musi., et al[51]. In addition, metformin increases glucose uptake in human cultured muscle cells[52], muscle strips from diabetic participants[53], and muscle from streptozotocin-treated rodents[54].

Metformin is also reported to inhibit lipogeneses, which is linked to cancer development, and hyperinsulinemia has been known as a risk factor in cancer development of numerous types of cancers such as breast cancer, prostate cancer, and colon cancer[55,56]. Metformin can induce apoptosis in several cancerous cell lines such as glioma, endometrial cancer, and triple-negative breast cancer[57]. Furthermore, metformin activates Bcl-2-associated X protein (BAX) and p53, and increases the cells to undergo apoptosis through the extracellular receptor kinase (ERK) signaling pathway[58]. Additionally, metformin activates adenosine monophosphate-activated protein kinase (AMPK), leading to active the tumor suppressor protein p53 and increase apoptosis and subsequently diminish cell division[59]. Another metformin mechanism of action is the inhibition of inflammation by the suppression of multiple mediators such as tumor necrosis factor-alpha (TNF-α), hypoxia-inducible transcription factor-1 alpha through inhibition of the mTOR signaling pathway[60].

Interestingly, metformin is receiving extensive attention as a potential anti-cancer treatment that showed enhanced survival rates in several cancer types for diabetic patients. Deng et al. reports that metformin significantly decreases both tyrosine and serine phosphorylation of STAT3 (P-STAT3 at Tyr705 or Ser727), decreases (P-mTOR) and increases (P-AMPK/AMPK). Furthermore, the authors showed that metformin inhibits STAT3 activation, directly or indirectly in triple-negative breast cancer[61].

Various studies have shown that phosphatidylinositol-3-kinase/protein kinase B protein (PI3K/PKB) signaling pathway is vital for insulin stimulation of glucose transport. It is associated with insulin-resistance in the cells. PIP3 binds to PDK1 and AKT, and PDK1 phosphorylates AKT at Thr308/309 of AKT1/AKT2, respectively. The pAKT2 recruits GLUT4 and GLUT1, and leads to increased glucose uptake. Metformin treatment can restore PI3K/AKT/GLUT4 signaling and reduce insulin resistance in the hepatocytes of rats T2D[62]. Metformin improves insulin-resistance through the AMPKα-SIRT1 pathway in a PCOS rat model and can serve as a therapeutic target[63].

Thioredoxin interacting protein (TXNIP) is considered a novel mediator of insulin resistance, improved glucose uptake, and increased insulin-sensitivity in adipose and skeletal muscle knockout mice[64]. In human cultured skeletal muscle cells, the reduction of TXNIP expression by RNA gene-silencing significantly enhances insulin induced glucose uptake[65]. Recently, a study by Lesley T. et al. shows that metformin affects gut microbiota, resulting in enhancing the cAMP-induced agmatine production and Akkermansia spp, leading to reduce absorption of glucose from the gastrointestinal tract and enhance lipid metabolism[66].

Several studies have been carried out examining the role of metformin in retinal injury in diabetic mice. More importantly, metformin decreases TXNIP, OGT, ChREBP, NF-κB, and PARP in diabetic mouse retinas. Notably, metformin inhibits the interaction of OGT with ChREBP and inhibits the interaction of OGT with NF-κB leading to decrease retinal cell death[67]. Moreover, metformin has been investigated in the theca cells taken from women (ovaries) with PCOS and was found to inhibit androgen production by repressing the steroidogenic enzymatic activities of 17α-hydroxylase/17,20 lyase (CYP17A1) and 3β-hydroxysteroid dehydrogenase type 2 (HSD3B2), which are overexpressed in ovary syndrome women[68].

Aging has been targeted by metformin to enhance healthspan and lifespan in several models. Beyond these, metformin inhibits mitochondrial complex 1 in the electron transport chain and decreases endogenous production of reactive oxygen species (ROS). In addition, metformin decreases IGF-1 signaling, insulin levels, DNA damage, and leads to activation of AMP-activated kinase (AMPK)[69]. Importantly, metformin influences cellular and metabolic processes associated with age development, such as autophagy, inflammation, and cellular senescence[70].

It has been reported that metformin reduces inflammation and protects against acute lung injuries in animal models. The pandemic of coronavirus disease 2019 (COVID-19), causes severe lung injury, several organ damage and linked to excessive inflammation[71]. Furthermore, clinical studies have been reported that metformin treatment is involved with a reduction of mortality in diabetic and obesity patients with severe COVID-19. Therefore, metformin is a potential drug candidate to treat or prevent severe COVID-19[72]. A recent study has identified protein interaction between human proteins and SAR-CoV2 proteins using mass spectrometry analysis in HEK-293T kidney cells[73]. The results revealed that metformin may target the interaction between

host factors and viral proteins, such as human protein NDUFAF1 or NDUFB9 and viral protein Orf9c, and human protein NDUFA2 and viral protein Nsp7[73].

Metformin has immunomodulatory and a potential antiviral activities by restoring AMPK activity, decreases the viral replication of Coxsackievirus B3 (CVB3) and protects mice from CVB3-induced myocarditis, thereby increases the survival rate of infected mice[74,75]. In addition, metformin diminishes infectious virion production and viral gene expression of Kaposi sarcoma herpesvirus[76]. Furthermore, several studies have shown that metformin may also directly inhibit severe acute respiratory syndrome coronavirus (SARS-CoV-2) infection by interfering with angiotensin-converting enzyme 2 (ACE2) interaction through the activation of AMPK. AMPK phosphorylates ACE2 (Ser680) and induces ACE2 expression in human endothelial cells by increasing its stability. Metformin also increase the expression and phosphorylation of ACE2, which leads to functional changes and conformational in the ACE2 receptor and reduce the binding of SARS-CoV-2[77,78]. Moreover, ACE2 plays significant role in antifibrosis and anti-inflammation. The binding of SARS-CoV-2 and ACE2 in cells, leads to enhancing proinflammatory and imbalance in the renin-angiotensin-aldosterone system (RAS), which is likely averted through upregulation of ACE2 expression by metformin[79]. Thus, metformin would prevent the entry of SARS-CoV-2 in the cells and reduce its deleterious effects.

The precise molecular mechanisms of metformin's action in human skeletal muscle appear to be complex and remain unclear, and more work is required to truly understand it.

1.3.2 ROLE PP2A IN METFORMIN'S ACTION

To better clarify the effect of metformin treatment on PP2A within several types of tissues and cells, we precisely and deeply reviewed current and previous literature regarding to additional mechanisms for metformin actions. Sathyaseelan S. Deepa, et al. demonstrated that the interaction of APPL1 with protein kinase Cζ (PKCζ) and protein phosphatase 2A (PP2A) is increased in C2C12 myotubes with adiponectin treatment, leading to inactivation of PKCζ, and activation of PP2A. The author also reported that metformin treatment does not effect on APPL1-PP2A interaction, PKCζ and PP2A phosphorylation in the skeletal muscle C2C12 myotubes. In addition, metformin treatment enhanced AMPK and decreased LKB1 (Ser307) in C2C12 myotubes[80].

Furthermore, they reported that metformin inhibited the assembly of the complex MID1- α4 -PP2Ac, which regulated the PP2Ac degradation and influenced PP2A activity. Surprisingly, the author found that metformin decreased the GSK3β phosphorylation at position Ser9, thereby activating the enzyme[81].

Metformin significantly decreased invasive capacity, tumor formation, and cell growth in human lung cancer cells (A549 or H1651) in *vitro* as well as phosphorylation of AKT (Ser473), phosphorylation of Bax (Ser184), and phosphorylation of Myc (Ser62) partially by activating PP2A[82]. The tumor-suppressive of PP2A is partially p53 dependent, B56gamma-PP2A diminished cell proliferation and cell transformation in the absence of p53 by an unknown mechanism as summarized by Shouse et al.[83]. In breast cancer cells, metformin treatment enhanced the expression of PP2A by decreased the p70S6K-rpS6 axis in a PP2A dependent manner[84]. Surprisingly, recent research by Shinsuke et al. demonstrated that metformin treatment significantly decreased PP2A-B expression in endometrial cancer patients[85].

Lei Zheng et al. reported that the antidiabetic metformin significantly diminished NLRP3 protein expression and NLRP3 inflammasome activation in ox-LDL-stimulated macrophages through activation PP2A, AMPK, and PP2Ac activity required for inhibited NF-κB and Tristetraprolin activation induced by metformin[86]. Furthermore, metformin treatments in human renal epithelial cells significantly enhanced PRKN gene transcription, mitochondria integrity, mitophagy, cell viability and decreased nuclear factor kappa B (NF-κB) activation but not that of p53 or ATF4 through PP2A activation[87]. Notably, treatment with metformin in human subcutaneous white adipose tissues (scWAT) led to decrease lipolysis and remodel iWAT by activating PP2A in beige fat independently of adenosine monophosphate kinase (AMPK) activation, and decreased dephosphorylation of acetyl-CoA carboxylase (Ser 79) and hormone-sensitive lipase (Ser 660). Additionally, metformin treatment enhanced mitochondrial coupling control as summarized by Christopher et al.[88].

In myeloproliferative neoplasm cells (MPN), metformin diminished malignant cells growth by suppressing the mTOR pathway. In contrast, it had been reported that metformin significantly enhanced reactive oxygen species (ROS) levels, leading to the inhibition of SHP-2(a positive regulator of JAK2V617F) and activated PP2A (a negative regulator of JAK2V617F). Furthermore, the B56α subunit of PP2A complex is responsible for JAK2V617F inhibition. Finally, the author determined that metformin enhanced the antileukemic action of ruxolitinib in HEL and SET-2 cells by activating AMPK at Thr172 and diminishing mTOR. Indeed, the investigator confirmed that metformin activated PP2A by decreasing pTyr 307 of PP2A complex in C subunit (which had a negative role in the action of PP2A). These results suggested that metformin inhibited the JAK-STAT pathway inset-2 and HEL cells[89].

Gang et al. demonstrated that metformin treatment significantly enhanced PP2A activity by decreasing its phosphorylation (pY307) and association with α4 in Human and rat cardiac myocytes. Therefore, they reported that metformin activated PP2A in human and rat cardiomyocytes apoptosis by decreasing NF-κB signaling activation that was elicited by high-glucose stimulation. Moreover, metformin decreased apoptosis, inflammatory, and ROS production in primary human and rat cardiomyocytes in *vitro* by activating PP2A[90].

Interestingly, Bor Luen et al. have shown that metformin had a beneficial effect in Huntington's disease (HD) in animal models and the two main pathways that cross-talk with each other as summarized in Figure 15. The first pathway is that metformin inhibited mitochondrial ETC (complex I), which enhanced the AMP/ATP ratio, resulting in increasing of the activation α1 isoform of AMP-activated protein kinase (AMPK-α1), which occurred in HD human and mouse brains. The activation of AMPK- α1 due to hyperactivity as Ca-activated Ca /calmodulin-dependent protein kinases and oxidative stress evoked by mHTT. The second pathway is metformin activated PP2A by disrupting the ribonuclear protein complex containing MID1, leading to inhibition of mTORC1 and thus attenuated the translation of CAG repeat expanded mHTT[91].

More work is needed to determine if PP2A plays an essential role in metformin's action and can allow better insight into the controversy of metformin's underlying molecular mechanisms in human skeletal muscle.

1.4 PHOSPHORYLATION, PROTEIN INTERACTIONS AND MASS SPECTROMETRY

1.4.1 MECHANISMS OF PROTEIN PHOSPHORYLATION

Protein phosphorylation is considered one of the major post-translational modifications involved in a broad of physiological functions. It plays an important role in gene expression, cell signaling, and differentiation. It is also implicated in DNA replication during the cell cycle. Protein phosphorylation provides a dynamic and sensitive way to regulate protein activity, protein interaction, stability, and subcellular localization.

A fundamental understanding of the mechanistic of signaling networks requires identification, quantification, analysis, and characterization of phosphorylation sites, both on the global and individual proteome. Analysis and quantification of phosphorylation-site provide ultimate information on functional relationships between signaling proteins. More than 100,000 phosphorylation sites have been reported in literature-curated databases PhosphoSitePlus, PHOSIDA, and Phospho.ELM. Phosphopeptide enrichment mapping is particularly important when obtaining quantitative information by a kinase. The stable-isotope tags (TMT) are the most common quantitative methods incorporated into sample peptides and provide relative quantification. The TMT reagents are available as kits with eleven labels, meaning up to eleven samples can be labeled, mixed, and analyzed by UPLC-ESI-MS/MS in a single run. Here we provide an overview for successful analysis and quantification of serine, threonine, and tyrosine phosphorylation events by mass spectrometry[92].

The following key steps are summarized for successful analysis and identification of phosphorylation sites on individual proteins[92].

1. Optimize the methods for detecting phosphorylation events *in vivo* and *in vitro*
2. Identification of the kinases that act directly on the protein of interest
3. Mapping of phosphorylation sites *in vitro* and *in vivo*
4. Interpretation data of mapping phosphorylation-site

5. Interpretation and analysis of phosphorylation site mutants

1.4.2 PROTEIN-PROTEIN INTERACTIONS ESSENTIALS

Protein-protein interactions are precisely defined as physical contacts with molecular docking between proteins that occur in a living organism or a cell *in vivo*[93]. It is vital and plays a crucial role in numerous cell functions, such as signal transduction, gene transcription, and cell cycle regulation. Eccentricity in protein-protein interactions cause aberrant cell signals and thereby cause diseases. The reason for focusing on protein-protein interaction is to analyze the signaling network pathways and to investigate the function of the specific target protein, which is significantly helpful in cases of unidentified protein interaction partners. Several previous publications describe that protein-protein interactions may result in changes in; downstream events, substrate specificity, substrate channeling, the activity of the complex, kinetic characteristics of the complexes, and a new binding site on the complex[94]. It is worthwhile and essential to compare the information and characteristics of a protein-protein interaction network with the information to the corresponding canonical pathway involving the same proteins. Direct and indirect interactions between proteins can be measured using co-complex methods; the most common approach is co-immunoprecipitation (Co-IP)[95]. In protein-protein interaction experiments, the mass spectrometry method can detect thousands of protein-protein interaction partners, and identify novel partners that have not been identified by the western blotting techniques.

We can improve our understanding of cellular systems and their interaction by finding protein-protein interactions in normal, infected, and diseased cells.

1.4.3 MASS SPECTROMETRY BASED QUANTITATIVE PROTEOMICS

Mass spectrometry (MS) based proteomics is emerging as a broadly effective and the most promising approaches for a global identification, characterization, and quantification of proteins, phosphorylation events, protein-protein interactions, and protein-post translational modifications (PTMs) in a single experiment, which help us to understand fundamental aspects of biology[96]. The typical workflow for quantitative proteomic and phosphoproteomic in MS-based bottom-up begin with starting material (e.g., tissue, body fluid, cell lysates, etc.) and followed by protein (or peptide) separation (e.g., liquid chromatography, affinity capture, electrophoresis, etc.). Therefore, the resulting peptides and phosphopeptides are often fractionated and analyzed by a high resolution, high sensitivity, high accuracy, and high reproducibility mass spectrometer UPLC-MS/MS. Mass spectrometric raw files are processed using a MaxQuant software version containing protein sequencing information (e.g., Uniprot) to identify and quantify thousands of proteins, peptides, protein phosphorylation events, and other post-translational modifications (PTMs).

In the present work, the quantitative phosphoproteomic and proteomic approaches were developed in our laboratory to investigate global phosphorylation profiles, phosphorylation changes for known PP2A substrates, novel PP2A substrates, and novel PP2Ac interaction partners in human skeletal muscle cells derived from lean insulin sensitivity and obese insulin-resistant non-diabetic participants under several conditions (with/without metformin, with/without insulin and/or with/without okadaic acid) by using high mass accuracy and high mass resolution UPLC-ESI-MS/MS. In addition, no large-scale proteome and phosphoproteome studies have been reported on the effect of PP2A substrate and protein interactions in response to metformin treatment in primary human skeletal muscle cells from obese insulin resistant. The goal of the

study is to address the knowledge gaps regarding molecular mechanisms by which metformin increases the insulin-sensitivity in skeletal muscle, using a combination of clinical studies (for direct measurements of human pathophysiology), in *vitro* cell studies (for causal mechanisms), and cutting-edge proteomics (for global analysis of cell signaling & unbiased discovery).

1.5 SPECIFIC AIMS

We have formulated, developed, and combined an excellent technical reproducibility and high throughput method with highly selective enrichment of phosphopeptides using high accuracy and precision mass spectrometric UPLC-ESI-MS/MS using an Orbitrap Tribrid MS to measure PP2A activity, a novel PP2Ac interaction partners, and a novel PP2A substrates. The three specific aims are described in the overall experimental design flowchart demonstrated in our strategy and research plan are presented in Figure 16.

1.5.1 SPECIFIC AIM 1: DETERMINE THE EFFECT OF METFORMIN ON PP2AC ACTIVITY IN PRIMARY HUMAN SKELETAL MUSCLE CELLS DERIVED FROM LEAN INSULIN-SENSITIVE AND OBESE INSULIN-RESISTANT PARTICIPANTS

We performed a hyperinsulinemic-euglycemic clamp to assess insulin-sensitivity, obtained human skeletal muscle biopsy samples, and cultured the primary skeletal muscle cells (shown to retain donors metabolic characteristics) derived from muscle biopsies from the two groups of subjects. We treated these cells with/without metformin 50 µM, insulin 100 nM, and/or okadaic acid 5 nM, and measured PP2Ac activity using a serine/threonine phosphatase activity assay from 8 lean insulin-sensitive non-diabetic

and 8 obese insulin-resistant non-diabetic participants. We hypothesized that metformin enhanced PP2Ac activity in primary human skeletal muscle cells.

1.5.2 SPECIFIC AIM 2: DETERMINE THE EFFECT OF METFORMIN ON PHOSPHOPROTEOME IN PRIMARY HUMAN SKELETAL MUSCLE CELLS DERIVED FROM LEAN INSULIN-SENSITIVE AND OBESE INSULIN-RESISTANT PARTICIPANTS

We treated the primary human skeletal muscle cells with/without metformin 50 μM, insulin 100 nM, and/or okadaic acid 5 nM (a specific PP2A inhibitor) and measured the phosphorylation changes for known PP2A substrates and global phosphorylation profiles using our quantitative phosphoproteomics and proteomics approach from 8 lean insulin-sensitive non-diabetic and 8 obese insulin-resistant non-diabetic participants. We hypothesized that metformin enhanced insulin stimulated-phosphorylation of PP2A substrates (e.g. AKT, AMPK, etc.).

1.5.3 SPECIFIC AIM 3: DETERMINE THE EFFECT OF METFORMIN ON PROTEIN-PROTEIN INTERACTIONS OF PP2AC IN HUMAN SKELETAL MUSCLE CELLS DERIVED FROM LEAN INSULIN-SENSITIVE AND OBESE INSULIN-RESISTANT PARTICIPANTS

A hyperinsulinemic-euglycemic clamp was performed to assess insulin-sensitivity and obtained human skeletal muscle biopsy samples. The primary human skeletal muscle cells were treated with/without metformin 50 μM, insulin 100 nM, and/or okadaic acid 5 nM. We identified and quantified binding partners of PP2A via Co-immunoprecipitation using our proteomic approach for novel PP2Ac interaction partners from 8 lean insulin-sensitive non-diabetic and 8 obese insulin-resistant non-diabetic participants. We hypothesized that; metformin improved PP2Ac interactions and rendered them similar to those in lean insulin-sensitive participants.

CHAPTER 2 EXPERIMENTAL DESIGN AND METHODS

2.1 ANTIBODIES AND REAGENTS

The PP2A activity assay kit (EMD Millipore, cat:17313) contains protein A agarose, anti-PP2A, C subunit, clone 1D6 (Catalog # 05-421), Threonine Phosphopeptide (K-R-pT-I-R-R) (Catalog # 12-219), pNPP Ser/Thr Assay Buffer (Catalog # 20-179), Normal mouse IgG (Catalog # 12-371) , Protein A Agarose (Catalog # 16-125D), Phosphate Standard (Solution C) (Catalog # 20-103), Malachite Green Additive (Solution A & B) (Catalog # 20-105& Catalog # 20-104), and 96-Well Microtiter Plate (½ volume flat bottom plate), C18 ZipTip (Millipore, Billerica, MA), Titansphere TiO_2 5µm (Lot No. ZQ5-4436, were purchased from GL Sciences (Tokyo, Japan)), Urea (catalog # BP169-500, Fisher scientific, Hampton, NH), Protease/Phosphatase Inhibitor Cocktail (catalog # 78440, Thermo Fisher Scientific, Waltham, MA), Trypsin Protease (0.40 µg/mL) MS Grade (catalog # PI90058, Fisher scientific, Hampton, NH). HPLC grade acetonitrile (ACN, catalog #134035), trifluoroacetic acid (TFA, catalog # LS119 1, Fisher Scientific, Hampton, NH), and formic acid (FA) were from Sigma. Metformin hydrochloride (Tocris Bioscience, Bristol, UK) was prediluted in purified water as 10× stock and preserved under –80°C before use. Bradford reagents from Sigma. Tandem Mass Tag (TMT) isobaric reagents (LOT# TH273420, ThermoFisher Scientific). Urea 99.5 %(lot # A0377566, ACROS), TCEP HCl (lot# UE278965, Thermo Scientific), Iodoacetamide (lot# SLB55004, SIGMA), HPLC grade H2O (lot#168195, Thermo Scientific), Methanol HPLC grade (lot# 165353, Thermo Scientific), Mini-PROTEAN TGX gels (cat# 4561034, BIO-RAB), 0.1% FA in H2O (lot# 163350, Fisher chemical), 0.1% FA in ACN (lot# 180905, Fisher chemical).

2.2 THE CLINICAL STUDIES AND HUMAN SUBJECTS

This protocol was approved by the Institutional Review Board of Wayne State University. The clinical studies started with participant recruitment by phone and comprehensive screening tests to exclude participants with significant diseases, followed by scheduling them for an onsite visit (Visit 1). All participants were instructed to stop any form of exercise for at least two days and stop anticoagulants medication (seven days prior to the Visit 2); before each visit and none of them had any significant medical problems. On Visit 1 day, the participants arrived at the clinical research service center in the morning after a 10-hour overnight fast. Written consent was obtained before their participation, and the purpose, potential risks of the study were explained to all participants. The exclusion criteria are based on if the participants had diseases such as significant pulmonary diseases (e.g., COPD), diabetic coma, heart diseases and extreme obesity (BMI>40). Measurement of vitals, urine analysis, 2-hour oral glucose tolerance test (OGTT), which is a test for diabetes diagnosis, pregnancy test if a female participant, and 12 lead electrocardiogram (ECG) were performed at the site. HbA1c and blood chemistry were measured by the Detroit Medical Center (DMC). The participants were grouped (non-diabetic, pre-diabetic or diabetic) based on three criteria, HbA1C value, 2h-OGTT, and fasting glucose[4] as shown in Figure 1. The eligible participants (a total of 16 volunteers) were scheduled for Visit 2 after successfully passing all tests.

2.2.1 HYPERINSULINEMIC-EUGLYCEMIC CLAMP AND MUSCLE BIOPSIES

The qualified participants were asked to fast at least 10 hours overnight and stop any anticoagulant medications. A hyperinsulinemic-euglycemic clamp study was performed to measure insulin-sensitivity and access the participant's muscle biopsy, as described in a previous study[9]. The study began at approximately 8 am (time −60 min)

after 10 hours of an overnight fast. A catheter was placed in an antecubital vein and maintained throughout the study for infusions of insulin and glucose. A second catheter was placed in a vein in the contralateral arm for the sampling of arterialized venous blood. Blood glucose was measured and reported every 15 minutes before insulin infusion started, and every 5 minutes after insulin infusion started. Around 8:30 am (time −30 min), a licensed physician performed the muscle biopsies from the vastus lateralis muscle from the thigh using the modified Bergstrom technique under local anesthesia (lidocaine)[97]. The collected biopsies were immediately blotted free of blood and cleaned of connective tissue and fat (~30sec), submerged in ice-cold media containing proteases and phosphatases inhibitors, and transported directly to the laboratory for primary skeletal muscle cell culturing as described previously[98]. At 9 am (time 0 min), a primed, continuous infusion of human regular insulin (Humulin R; Eli Lilly, Indianapolis, IN). The hyperinsulinemic-euglycemic clamp took two hours, and the procedure was done by clamping the participant's insulin at a high concentration (80 mU/kg/min) via IV infusion. Plasma glucose was measured at 5-min intervals throughout the clamp, and glucose was also infused to maintain normal glucose levels at approximately 90 mg/dL, and the average rate of glucose infusion during the last 30 minutes is the indicator of insulin sensitivity (M-value). The lower M value is lower insulin-sensitivity, and higher insulin-resistance, vice versa. The overall theory of hyperinsulinemic-euglycemic clamp is shown in Figure 17.

2.2.2 CLINICAL CHARACTERIZATION OF THE 16 PARTICIPANTS

Total 16 subjects, 8 (4 males & 4 females) lean healthy insulin-sensitive nondiabetic ($20 \leq$ BMI < 25 kg/m^2) and 8 (4 males & 4 females) obese insulin-resistant participants ($30 \leq$ BMI < 40 kg/m^2) were enrolled in this project. All participants were

asked to fast overnight for at least 10 hours. The clinical characteristics of these participants are presented in Table (2 & 3). No significant difference in age, fasting plasma glucose, and HbA1c between lean healthy insulin-sensitive and obese insulin-resistant nondiabetic participants. In contrast, 2h OGTT and BMI of these two groups were significantly deference (p-value < 0.01). In addition, the M-value, an assessment for insulin sensitivity obtained during the hyperinsulinemic-euglycemic clamp, is much higher for the lean insulin-sensitive group than the obese insulin-resistance group (p-value < 0.01).

2.3. PRIMARY CELL CULTURE AND METFORMIN TREATMENT

Human skeletal muscle biopsies were immediately blotted free of blood cleaned of connective tissue (~30sec), and transferred immediately to the lab. The biopsies were washed three times with Phosphate Buffer Saline (PBS) (from Glibco) and placed in a 10 cm Petri plate under the hood. The biopsies were cut and minced into fine and small pieces using sterilized scissors. The minced tissues were transferred into a 50 ml tube with PBS, centrifuged and the supernatant was removed entirely. Trypsin-EDTA (0.05 %) was added to the 50ml tube containing minced tissues and kept in a water bath at 37°C for one hour with shaking every 15 minutes. The minced tissues were centrifuged at 1000 rpm for 5 minutes, and the supernatants were entirely removed from the tubes. 10 ml of growth media was added to the tubes and filtered through a nylon mesh. The resulting human skeletal muscle cells were cultured in a growth medium (Dulbecco modified Eagle's medium) supplemented with 10% FBS, 1% PSG, 10 ng/mL EGF, 0.4 μg/mL dexamethasone, 50 μg/mL fetuin, 1% sodium pyruvate and 1% NEAA, and maintained in a humidified atmosphere at 37°C and 5% CO_2. The human skeletal muscle cells expanded to eight dishes, and the culture medium was completely changed every other day. Once the myoblasts cells reached 95% confluence, the growth medium

was replaced with a differentiation medium (DMEM containing 2% horse serum and 1% PSG) on the following day. The cell cultures were incubated for 72 hours, during which myotube differentiation occurred, and the differentiation medium changed every other day as shown in Figure 18. The primary myotubes were starved for 4 hours and treated with eight different conditions, with vehicle or 50μM Metformin for 24 hours, with /without 100nM insulin for 15 minutes, and/or with/without 10nM okadaic acid for 30 minutes (Figure 19), and washed three times with ice-cold PBS, lysed and protein concentrations will be quantified via Bradford method. The protein standard curve was measured by reading different concentrations for known BSA 2mg/mL.

2.4 SPECIFIC AIM 1: DETERMINE THE EFFECT OF METFORMIN ON PP2AC ACTIVITY IN PRIMARY HUMAN SKELETAL MUSCLE CELLS DERIVED FROM LEAN INSULIN-SENSITIVE AND OBESE INSULIN-RESISTANT PARTICIPANTS

The primary cells were cultured to reach 95% myoblasts cells, myotubes were differentiated, starved, and treated (± Metformin 50 μM), (± insulin 100 nM), (±Okadaic acid 5nM) in 10-mm Petri dishes, and the myotube cells were harvested and homogenized in 1 ml of lysis activity buffer included (20 mM imidazole-HCl, 2 mM EDTA, 2 mM EGTA, pH 7.0, with 10 mg/mL each of aprotinin, leupeptin, 1 mM benzamidine, and 1 mM PMSF). The PP2A activity was performed according to the manufacturer's protocol. The cell lysates were collected in Eppendorf tubes, homogenized for 10 minutes at 4°C, and were centrifuged at 11000 x g for 15 minutes at 4°C. The protein concentrations were measured using the Bradford protein assay method. 200 mg of total protein of each sample were transferred to new Eppendorf tubes, including 30 mL of protein A agarose, 4 mL of normal mouse IgG and the volumes were topped off to 1000 mL with pNPP assay buffer. The NIgG immunoprecipitates were incubated

for one and a half hours at 4°C with constant rocking and followed by centrifugation at 3000 x g for 3 minutes at 4°C. The supernatants were transferred to new Eppendorf tubes, including 30 mL of protein A agarose, 4 mL of anti-PP2Ac antibody and the volumes were topped off to 1000 mL with pNPP assay buffer. All tubes were incubated at constant rotation for 2 hours at 4°C and centrifuged at 3000 x g for 3 minutes at 4°C. The immunoprecipitated PP2Ac and NIgG beads were washed three times with 700 mL tris buffered saline (TBS) (3000 x g for 3 minutes at 4°C), once with 500 mL pNPP Ser/Thr Assay Buffer, followed by incubation with 60 mL of 750 mM of threonine phosphopeptide (K-R-pT-I-R-R) and 20 mL of pNPP Ser/Thr assay buffer at 30°C for 10 minutes in a shaking incubator. The beads were centrifuged 3000 x g for 3 minutes at 4°C, and 25 mL of the supernatants were mixed with 100 mL of Malachite green phosphate detection solution into each well to a 96-well plate to terminate the reaction, and the color was allowed to develop for 15 minutes at room temperature. The sample absorbance was read using a microplate reader at 650 nm and the workflows are presented in Figure 20. The amount of free phosphate released was determined from a standard curve (according to the manufacturer's protocol, Product. No 17-313) and normalized to that of the controls. The phosphatase activity was calculated as mean fold change ±SEM from the untreated samples of n=16 independent experiments.

2.4.1 STATISTICAL ANALYSIS

All data were represented as the mean ± standard error of the mean (SEM) from sixteen independent experiments. The significances between the control, insulin, okadaic acid, and metformin-treated groups were analyzed by independent student's t-test.

2.5 SPECIFIC AIM 2: DETERMINE THE EFFECT OF METFORMIN ON PHOSPHOPROTEOME IN PRIMARY HUMAN SKELETAL MUSCLE CELLS DERIVED FROM LEAN INSULIN-SENSITIVE AND OBESE INSULIN-RESISTANT PARTICIPANTS

The human skeletal muscle cells were treated for 24 hours with metformin 50 µM or left untreated, with okadaic acid 5nM for 30 minutes or left untreated and with insulin 100 nM for 15 minutes or left untreated. Cell lysates were collected from eight different conditions from 8 lean insulin-sensitive non-diabetic and 8 obese insulin-resistant non-diabetic participants. The cells were lysed in one mL of 8 M urea buffer (pH=8) in 50 mM TEAB (triethylammonium bicarbonate) containing Protease Inhibitor, phosphatase inhibitor cocktail 2 (1:100, sigma), and phosphatase inhibitor cocktail 3 (1:100, sigma). Samples were homogenized for 10 minutes at 4°C then centrifuge at 12000 rpm for 15 minutes at 4°C, and supernatants were transferred into 2mL microcentrifuge tubes. Protein concentrations were measured through the Bradford Protein Assay (product No. 23236). For protein digestion, 250 µg proteins of each condition were transferred into 1.5mL microcentrifuge tubes, reduced by adding 5µL of 200 mM tris (2-carboxyethyl) phosphine (TCEP) followed by a one-hour incubation at 55°C. Samples were allowed to cool before alkylation at room temperature in the dark with the addition of 5 µL of 375mM iodoacetamide (IAA) for 30 minutes. Proteins were precipitated in six times of ice-cold acetone overnight at -20°C and centrifuged at 8000g for 10 minutes at 4°C. The supernatants were removed and sample tubes were inverted and allowed to dry for 3 minutes without disturbing the protein pellets. Protein pellets were suspended with 200mL of 100mM TEAB and digested overnight with 12.5 µL of trypsin (1:50 w/w) at 37°C with shaking at 600rpm. The following day, TMT reagents (Thermo Scientific A34808, Lot No for TMT 10- plex: SI258088, and 131C channel:

SJ258847) were suspended in 41µL 100 % anhydrous ACN, the peptides were quantified using Quantitative Colorimetric Peptide Assay (Product No.23275) and labeled using 41 µL of TMT 11 Label Reagent to 100 µL of protein digested followed by 2 hours incubation at room temperature. 2 µL of each TMT labeled peptide samples were mixed with 28µL of 0.1%TFA in H_2O and injected into UPLC-ESI-MS/MS to determine the labeling efficiency (>95%) followed by 8 µL of 5% hydroxylamine (Pierce) added to the samples for 15 minutes to quench the reaction at room temperature. The TMT labeled peptides were combined, speedvac till 100 µL left, and phosphopeptide enrichment using titanium dioxide (TiO_2) performed and modified as described previously[99]. The appropriate amount of (400µg beads/100µg peptides) and briefly, 100mg of TiO_2 were dissolved with a loading buffer containing (65%ACN, 2%TFA, and saturated glutamic acid) for 15 minutes. The pH of TMT labeled peptide samples were adjusted then mixed with TiO_2 beads (1:1); the volume completed to 500 µL with loading buffer and incubated with gentle rotation for 20 minutes. The samples were centrifuged at 3000 rpm for 2 minutes, the supernatants were incubated again with another TiO_2 beads for 20 minutes and the beads were saved and combined into one 1.5 mL microcentrifuge tubes. Two more times of TiO_2 beads were incubated with the same supernatants for 20 minutes each and the beads were collected from all four runs. The TMT incubated beads were then washed twice with 500 µL washing buffer I (65% ACN, 0.5% TFA) and two times with 500 µL washing buffer II (65%ACN, 0.1% TFA). The bound peptides were eluted once with 100 µL elution buffer I (300 mM NH_4OH, 50% ACN) and two times with 100µL elution buffer II (500 mM NH_4OH, 60% ACN). The eluates were combined (300 µL) and speedvac till 10 µL left to process through a high pH reversed-phase peptide fractionation kit (Product No.84868). The spin columns provided from the kit were conditioned and activated by ACN and 0.1%TFA, and the

phosphopeptide samples were dissolved with 300 µL 0.1% TFA. The elution solutions were prepared according to manufacturer protocol (Product No. 84868) and the phosphopeptide samples were eluted with different concentrations (5%ACN, 7.5%ACN, 10%ACN, 12.5%ACN, 15%ACN, 17.5%ACN, 20%ACN, 22.5%ACN, 25%ACN, 50%ACN, and 80%ACN) according to their protocol. The samples were evaporated to dryness using vacuum centrifuge and suspended with 0.1% TFA before being analyzed on an Orbitrap Fusion Mass spectrometer UPLC-ESI-MS/MS as illustrated in Figure 21.

In addition, we subjected a100 µg of total TMT peptide mixture samples without TiO_2 procedure, followed by high pH reversed-phase peptide fractionation to UPLC-ESI-MS/MS analysis to obtain the relative quantification of protein abundance for the identified phosphoproteins. MaxQuant was used to process the raw mass spectra and generate protein group intensities and phosphosites for the database search using human protein FASTA files, followed by bioinformatics analysis as described in Figure 21.

2.5.1 UPLC-ESI-MS/MS ANALYSIS (ORBITRAP FUSION LUMOS)

Mass spectrometric raw files were collected from Orbitrap Fusion Lumos (ThermoFisher) equipped with a nano-LC based electrospray ionization source and coupled on-line to a Dionex Ultimate 3000 UPLC system (Thermo Fisher Scientific). Each phosphopeptide fractions and total peptide fractions were individually loaded into a 50 cm column with 75 µm inner diameter, packed in house with 1.9 µm C18 with 10 µm emitter PicoTip (New Objective) and the column temperature was maintained at 70°C. The phosphopeptides and peptides were separated with a binary buffer system of 0.1% FA in water (buffer A) and 0.1% FA in acetonitrile (buffer B), at a constant flow rate

of 300 nL/mL. The samples were eluted with a linear gradient chromatography ranging from 5 to 35% buffer B (0.1% FA in acetonitrile) for 180 minutes followed by 35% to 90% buffer B for 15 minutes, and 2% buffer B for 25 minutes, resulting about four hours gradients. For each analysis, we injected 5 µL into the column and used an MS^2 based TMT method.

The mass spectrometer was operated in top speed mode with a cycle time (3sec) strategy, and the global parameters are 2kv for spray voltage and 250°C for ion transfer tube temperature. The full survey scan began with an MS^1 spectrum (mass range 400-1600 m/z, Orbitrap resolution at 120000, automatic gain control (AGC) target 2×10^5, data type is profile, and maximum injection time 50 ms). The most abundant ions per full MS were selected and fragmented by high collision dissociation (HCD) at 35 and analyzed in the quadrupole ion trap resolution at 30000. MS^2 analysis consisted of automatic gain control (AGC) target 5×10^5, isolation window of 1.3 Th, and maximum injection time of 200 ms. The MS/MS analysis rejected ions processing unknown or a charge state of 1; only, +2 to +7 charge states were chosen for MS/MS. All scan events were recorded in profile mode, with 10 ppm mass tolerance and a dynamic exclusion at 30 seconds following data collection.

2.5.2 DATA PROCESSING AND ANALYSIS

Raw files obtained from Orbitrap Fusion Lumos mass spectrometer were processed using a MaxQuant software version (1.6.17.0) and filtered to 0.01 FDR (commonly used threshold in phosphoproteins) at the protein levels. The samples were searched using a Homo-sapiens database, which is downloaded from (www.uniprot.org ,released on 01/17/2020), allowing for a variable modification of lysine and N-termini

with TMT 11, phospho (STY), oxidation (M), acetylation (protein N-term), and carbamidomethylation of cysteine as fixed modifications. Search parameters were set to an initial precursor mass tolerance of 20 ppm. First search mass accuracy tolerance is 20 ppm, main search mass accuracy tolerance is 4.5 ppm and fragment mass tolerance is 0.5 Da. Two missing trypsin cleavage site was allowed for protease digestion. Protein quantification and identification were based on a minimum of two ratio counts, originating from unique or razor peptides only, and the minimum peptide length was set to 7. For phosphopeptide identification and quantification, and Andromeda minimum score and minimum delta score threshold of 40 and 6, respectively. In addition, only phosphosites with a localization probability filter greater than 0.75 were considered as confidently localized.

2.5.3 IDENTIFICATION AND QUANTIFICATION PHOSPHOPEPTIDES USING TMT 11PLEX REAGENTS

The data from all sixteen participants were analyzed using MaxQuant and the FDR threshold was set to 0.01 for each respective phosphosites and protein levels. All proteins were marked as “Potential Contaminations”, “Reverse”, and “less than 0.75 localization probability” or “only identified by sites” were filtered out. Reporter ion intensities were extracted from MS^2 spectra for quantitative analysis and we included a protein ID Column, unique peptide, gene symbol, and phosphosites.

For phosphoproteomics data, the TMT 11plex quantitative data were summarized by total protein levels to correct the sample loading differences. The reporter intensities were normalized to the median of each reporter ion channel across total proteins and phosphorylation sites.

$$\mathrm{NP} = \frac{\mathrm{P}i}{\sum_1^{\mathrm{n}} \mathrm{P}i}$$

NP is the normalized quantification value and P is the original quantification intensities. To compare the phosphorylation sites between lean insulin-sensitive and obese insulin-resistance samples, phosphorylation sites were considered if it satisfied the following criteria, quantified at least half of the samples in one group and the fold change greater than 1.5 (i.e., 1.5 fold increase) or less than 0.667 (i.e.,1.5 fold decrease). All the analyses were based on log2-scaled protein concentrations and normalized by sample median. T-test analyses were performed to quantify proteome and phosphoproteome significantly between group changes.

2.5.4 Identification and quantification of signaling pathways

To analyze and interpret high-throughput proteomics data, pathway analysis with many software is a powerful tool in biological research, and facilitates novel insights in several fields. Pathway analyses led to organizing a list of proteins into a solid list of pathways to elucidate and interpret proteomics results. Several biological pathways have been linked to insulin-resistance and T2D.

Bioinformatics data analysis were performed using Ingenuity Pathway Analysis (Ingenuity Systems, Redwood City, CA, www.ingenuity.com) and DAVID Bioinformatics Resources 6.8 to access gene ontology (GO) and pathway enrichment analyses. The results were exported from DAVID, and organized using Microsoft Excel and manually curated. The DAVID analysis revealed that many kinases and phosphatases involved in insulin signaling were significantly enriched and logarithmized P-Values for significant overrepresentation are shown. We have indicated how many proteins in each pathway were identified to be phosphorylated, significantly enriched and P-values were calculated using a hypergeometric test and corrected with Benjamini (cut-off of 0.01 was applied).

2.6 SPECIFIC AIM 3: DETERMINE THE EFFECT OF METFORMIN ON PROTEIN-PROTEIN INTERACTIONS OF PP2AC IN HUMAN SKELETAL MUSCLE CELLS DERIVED FROM LEAN INSULIN-SENSITIVE AND OBESE INSULIN-RESISTANT PARTICIPANTS

The primary skeletal muscle cells were cultured, differentiated, starved, and treated (± Metformin 50 µM), (± Insulin 100nM), (±Okadaic acid 5nM) in 15-mm Petri dishes. The myotube cells were harvested and homogenized in 1.5 mL of lysis activity buffer included (20 mM imidazole-HCl, 2 mM EDTA, 2 mM EGTA, pH 7.0, with 10 mg/mL each of aprotinin, leupeptin, 1 mM benzamidine, and 1 mM PMSF). The samples were centrifuged at 14000 rpm for 15min followed by protein quantification using Bradford assay and the supernatants were transferred into new microcentrifuge tubes. One mg of protein of each condition was first incubated with 30 µl of protein A beads conjugated to 4 µg of mouse NIgG and the volumes were topped off to 1000 mL with activity assay buffer for three hours at 4°C with constant rocking and followed by centrifugation at 3000 x g for 3 minutes at 4°C. The supernatants from NIgG beads were incubated with 30 µl of protein A beads conjugated to 4 µl of anti-PP2Ac antibody overnight at 4°C with constant rocking. The immunoprecipitated PP2Ac and NIgG beads were washed 3 times with 700 mL tris buffered saline (TBS) (3000 x g for 3 minutes at 4°C) and the beads were treated with 30 µl of 2 x SDS buffer comprising 50 mM DTT at 95^{o}C for 5 minutes and iodoacetamide (IAA) for 30 minutes. The eluates were resolved on 4-15% SDS-PAGE, and the gels were stained with (45% methanol, 10% acetic acid, 0.0025% coomassie blue) for 5 minutes, and destained with (50% methanol, 10% acetic acid). The protein bands of each lane of the gel were cut into five slices horizontally using a sterilized blade, followed by in-gel trypsin digestion. The resulting peptides from the gel were extracted using formic acid and acetonitrile. The

peptides were purified and enriched using the C-18 column ziptip. The resulting peptides were analyzed by UPLC-ESI-MS/MS using an Orbitrap Elite mass spectrometry as illustrated in Figure 21. MaxQuant was used to process the raw mass spectra and generated protein group intensities and peptides for the database search using human protein FASTA files, followed by bioinformatics study[100].

2.6.1 UPLC-ESI-MS/MS ANALYSIS (LTQ-ORBITRAP ELITE)

Mass spectrometric raw files were collected from LTQ Orbitrap Elite equipped with a nano-LC based electrospray ionization source and coupled on-line to a Dionex Ultimate 3000 UPLC system (Thermo Fisher Scientific). The peptides were individually loaded into a 50 cm column with 75 µm inner diameter, packed in a house with 1.9 µm C18 with 10 µm emitter PicoTip (New Objective) and the column temperature was maintained at 70°C. The peptides were separated with a binary buffer system of 0.1% FA in water (buffer A) and 0.1% FA in acetonitrile (buffer B); at a constant flow rate of 300 nL/mL. The samples were eluted with a linear gradient chromatography ranging from 5 to 35% buffer B (0.1% FA in acetonitrile) for 295 minutes followed by 35% to 90% buffer B for 15 minutes; and 2% buffer B for 20 minutes, resulting about 5hours and half gradients. For each analysis, we injected 5 µL into the column and used an MS^2 based label-free method.

The mass spectrometer was operated in a positive mode in a top 20 method to identify peptides in the samples and the global parameters are 2kv for spray voltage and 250°C for ion transfer tube temperature. The precursor spectra full scan began with an MS^1 spectrum (mass range 400-1650 m/z, orbitrap resolution at 240000, automatic gain control (AGC) target 3×10^4; data type is profile and maximum injection time 50 ms. The top 20 peaks per full MS were selected, fragmented by collision-induced dissociation (CID) at 33, 1.0 m/z isolation window and activation Q is 0.25 and analyzed in the

linear ion trap resolution at 30000. MS^2 analysis consisted of automatic gain control (AGC) target 3×10^6, isolation window 1.3 Th, and maximum injection time 200 ms. The MS/MS analysis rejected ions processing unknown or a charge state of 1. All scan events were recorded in profile mode, with 10 ppm mass tolerance and a dynamic exclusion at 30 seconds following data collection.

2.6.2 DATA PROCESSING AND ANALYSIS

Raw files obtained from Orbitrap Elite mass spectrometer were processed using a MaxQuant software version (1.6.17.0) and filtered to 0.01 FDR at the protein levels. The MS/MS samples were matched using the Human Uniprot FASTA database (released on 01/17/2020) allowing for a variable modification of acetylation (protein N-term), oxidation (M), and carbamidomethylation of cysteine as fixed modifications. The parameters were set to an initial precursor mass tolerance of 20 ppm, first search mass accuracy tolerance of 20 ppm, main search mass accuracy of tolerance 4.5 ppm and fragment mass tolerance is 0.5 Da. Two missing trypsin cleavage site was allowed for protease digestion. Protein quantification was based on a minimum of two ratio counts, originating only from unique or razor peptides. The minimum peptide length was set to a 7 score threshold of 40 and 6, respectively. In addition, LFQ was selected for the label-free proteome quantification option in MaxQuant.

2.6.3 QUANTIFICATION AND STATISTICAL ANALYSIS OF PP2Ac

Proteins identification and quantification were performed using the MaxQuant software version (1.6.17.0). All proteins were labeled as “Potential Contaminations”, “Reverse”, “Keratin”, ”Albumin”, ” Hemoglobin” and “IgG” were discarded. Proteins with a minimum of 2 unique peptides and with a false discovery rate (FDR) at 0.01

were selected for the analysis. Protein has to meet the following criteria to be categorized as a potential PP2Ac interaction partner; the peak area of protein is identified with label-free quantification (LFQ) in more than half samples of the PP2Ac immunoprecipitates and the proteins have an enrichment ratio (PP2Ac/NIgG) larger than 10, or only identified in PP2Ac samples not identified in all of the NIgG control samples. Previous publication by our lab had described the calculation of enrichment ratio[101] as follows, the peak area of identified protein in a gel lane was normalized to the sum of the peak areas for all proteins identified in the same gel lane to obtain a normalized ratio for each protein, Norm:*i*,

$$\text{Norm: } i = \frac{\text{PA}i}{\sum_1^{\text{n}} \text{PA}i}$$

Then, the average normalized ratio for individual protein in the PP2Ac co-immunoprecipitates (Average_Norm:*i*_PP2Ac) divided by the average normalized ratio for the same protein in the NIgG co-immunoprecipitates (Average_Norm:*i*_NIgG)

$$\text{Enrichment\_Ratio: } i = \frac{\text{Average\_Norm: } i\text{\_PP2Ac}}{\text{Average\_Norm: } i\text{\_NIgG}}$$

A higher peak area will be assigned to this protein in the PP2Ac samples than in the NIgG samples to truly identify this protein as a PP2A complex and the cutoff of enrichment ratio higher than 10.

Next, the proteins were identified with LFQ PAs in more than half of the PP2Ac Co-immunoprecipitation samples. To determine the relative quantities of PP2Ac interaction partners in human skeletal muscle cells among lean insulin-sensitive controls and obese insulin-resistant non-diabetic. The peak area for an individual protein identified in a specific group was normalized against the peak area for PP2Ac identified in the same group, which results in Norm:*j*.

$$\text{Norm: } j = \frac{\text{PA}j}{\text{PA\_PP2Ac}}$$

The normalization strategy is very important in protein-protein interaction studies. The $\log_2$ form was calculated for the normalized peak area (Norm:j) for each PP2Ac interaction partner and compared within the group to estimate the effects of insulin, metformin, and okadaic acid on PP2Ac protein-protein interactions. To be considered as Metformin responsive PP2Ac interaction partners, the fold change of normalized peak areas should be >1.5 and $P < 0.05$ by independent Student's *t*-test. ANOVA with post hoc independent *t*-tests used for group comparisons for statistically significant P<0.01.

Bioinformatics and pathway analysis were performed on PP2Ac interaction partners using DAVID Bioinformatics Resources 6.8. This pathway is considered significantly enriched if the P-value < 0.01 and contained at least four identified PP2Ac partners.

CHAPTER 3 RESULTS

3.1 SPECIFIC AIM 1: DETERMINE THE EFFECT OF METFORMIN ON PP2AC ACTIVITY IN PRIMARY HUMAN SKELETAL MUSCLE CELLS DERIVED FROM LEAN INSULIN-SENSITIVE AND OBESE INSULIN-RESISTANT PARTICIPANTS

The summary of clinical characteristics of all the 16 human subjects (8 lean insulin-sensitive non-diabetic and 8 obese/overweight insulin-resistance non-diabetic participants) is listed in Table 4. These participants without a family history of T2D and are healthy. Myotube human skeletal cells were treated, harvested, and homogenized in 1 mL of lysis activity buffer. The PP2A activity was performed according to the manufacturer's protocol and measured for each condition (with/without metformin, with/without insulin, and/or okadaic acid) to analyze if metformin directly affects PP2A activity. The amount of free phosphate released from each condition (reflecting phosphatase activity) was calculated from a standard curve with R^2 at 0.999. The slope and intercept were used to calculate the amount of phosphate released by PP2Ac immunoprecipitates incubated with the standard phosphopeptide, as shown in Figure 22.

3.1.1 EFFECT OF METFORMIN AND INSULIN ON PP2A ACTIVITY

PP2A activity measurements as presented in Table 5 and Table 6 indicated that metformin treatment significantly increased the activity of PP2A in the myotubes derived from eight lean insulin-sensitive and eight obese insulin-resistant non-diabetic participants (fold increase Metformin/basal: 1.54±0.11 and 1.68±0.16, $P<0.001$, respectively.) as presented in Figure 23. These results provided the first evidence that metformin promotes activation of PP2A in human skeletal muscle cells derived from lean insulin-sensitive and obese insulin-resistant non-diabetic participants. Insulin increased PP2A activity by 8% without metformin and okadaic acid treatments in lean

insulin-sensitive participants (P-value=0.006) and insulin could not increase PP2A activity without metformin and okadaic acid in obese insulin-resistant participants (P-value=0.062). In addition, insulin decreased PP2A activity by 27% when the human skeletal muscle cells were treated with metformin in lean insulin-sensitive participants (P-value=0.001) and by 24% if the human skeletal muscle cells were treated with metformin in obese insulin-resistant participants (P-value=0.002). Furthermore, insulin decreased PP2A activity by 14% if the human skeletal muscle cells were treated with metformin and okadaic acid in lean insulin-sensitive participants (P-value=0.032) and could not decrease it in obese insulin-resistant participants (P-value=0.064) when the human skeletal muscle cells treated with metformin and okadaic acid. Notably, the PP2A inhibitor okadaic acid treatments significantly decreased PP2A activity in lean insulin-sensitive participants (P-value=0.02) and in obese insulin-resistant participants (P-value=0.003) by 21% and 24%, respectively, as demonstrated in Figure 24.

3.2 SPECIFIC AIM 2: DETERMINE THE EFFECT OF METFORMIN ON PHOSPHOPROTEOME IN PRIMARY HUMAN SKELETAL MUSCLE CELLS DERIVED FROM LEAN INSULIN-SENSITIVE AND OBESE INSULIN-RESISTANT PARTICIPANTS

Many cellular responses to drugs are mediated by changes in cellular phosphosignaling. Protein phosphorylation is mainly observed on serine, tyrosine, and threonine. In human cells, phosphorylation is regulated by > 500 kinases and 200 phosphatases. UPLC-ESI-MS/MS analysis of the TMT 11-labeled and high pH reverse-phase fractionated samples generated a total proteome (n= 198 fractions) and phosphoproteome (n=198 fractions) across 16 participants. TMT 11plex reporter ions were quantified from MS^2 scans. The raw MS files were processed using the MaxQuant software version (1.6.17.0). The precursor MS signal intensities were measured and data-dependent

Orbitrap HCD-MS/MS spectra were filtered and deisotoped. Sample throughput is essential for analyzing high numbers of samples using UPLC-ESI-MS/MS in quantitative phosphoproteomics and proteomics experiments. Our TMT 11-plex proteome analysis identified a total of 96,569 peptides, of which 37,164 were unique. These peptides were assigned to a total of 7,037 non-redundant proteins at 0.01 FDR on the peptide spectrum match (PSM) levels, of which 6,064 were unique with two unique peptides. We identified a total of 24,741 phosphorylation events from our phosphoproteome analysis, of which 16,413 were confidently localized with 75%, and 10,890 phosphorylation events were quantified. These phosphorylation events were assigned to a total of 5,557 non-redundant phosphoproteins at 0.01 FDR, of which 4,178 were unique with two unique peptides. The ratio of pS: pT: pY (19,481:4804:450 sites) phosphorylation for TiO_2 enriched dataset about 79:19:2. Using 75% localization, we identified 1,958 phosphorylation events that were not reported in humans; among them, 1,756 were not reported in any species in the phosphositePlus database and thus appeared to be novel sites, as shown in Table 7. The phosphoproteome and proteome measurements demonstrated high reproducibility and accuracy with Pearson correlation coefficients from 0.90 and 1.0. The confidence of quantifications for protein and phosphorylation events is high with more than 88% ± 3% and 76% ± 5% (Mean ±SEM), respectively. We developed a new strategy to map metformin-dependent changes in the phosphoproteome and proteome profiles to known signaling networks to interpret these results. In addition, to gain insight into the molecular mechanism underlying metformin, we identified and quantified 291 unique kinases. Furthermore, we quantified 75 unique phosphatases, and 18 protein phosphatases 2A in human skeletal muscle cells from sixteen participants as reported in Table 8.

In total, after metformin treatments, we quantified 10,543 and 10,397 phosphorylation site changes in lean insulin-sensitive and obese insulin-resistant participants, respectively. To quantify these changes, we performed t-test analysis and found 4,455 and 1,966 phosphorylation sites were significantly modulated ($P<0.05$) in lean insulin-sensitive and obese insulin-resistant participants, respectively. In addition, 445 phosphorylation sites were significantly changes ($P<0.05$) between two groups after metformin treatments. We quantified 5,146 phosphorylation sites in lean insulin-sensitive participants and 967 phosphorylation sites in obese insulin-resistant participants were significantly changes ($P<0.05$) under insulin stimulation as. In addition, we quantified 842 phosphorylation sites were significantly different ($P<0.05$) upon insulin stimulation between two groups.

To gain insights into the processes regulated by metformin treatment, we quantified the phosphatases and the kinases, that significantly enriched ($P<0.05$) by changing the phosphoproteome profile. 88 protein phosphatases were significant changes in lean insulin-sensitive participants after metformin treatments as shown in Table 9. Furthermore, 31 protein phosphatases were significantly changes after metformin treatments in obese insulin- resistant participants as reported in Table 10. While 7 protein phosphatases (PPP1R12A, PPP2R3A, PPP1R9B, PTPN12, DUSP27) were significantly different ($P<0.05$) between two groups after metformin treatments as presented in Table 11. Furthermore, 94 protein phosphatases (PPP1R12A, PPP1R12B, PPP1R12C, PPP1R3F, PPP2R5E, PPP1R3D, PPP2R5D, PPP1R7, PPP1R18, etc.) were significant differences ($P<0.05$) in lean insulin-sensitive participants and 18 protein phosphatases (PPP1R12A, PPP1R12B, etc.) were significant difference in obese insulin-resistant participants upon insulin stimulation as reported in Table 12 and in Table 13 . In addition, 32 protein phosphatases were significant changes ($P<0.05$) in both

groups upon insulin stimulation, such as PPP1R12A, PPP2R5D, PPP2R5D, PPP2R5D, PPP6R3, and SSH1 as shown in Table 14. Furthermore, PP2A subunits quantified in our phosphoproteome experiment were significant changes after metformin treatment as illustrated in Table 15.

We quantified 99 protein phosphatases, among them 7 protein phosphatases 2A were significantly change ($P<0.05$) in lean insulin-sensitive after okadaic acid treatments. Moreover, 56 protein phosphatases included 4 protein phosphatases 2A were significantly different ($P<0.05$) after 30 minutes of okadaic acid treatments in obese insulin-resistant participants. 9 protein phosphatases and one protein phosphatase 2A were significantly different ($P<0.05$) when comparing both groups after okadaic acid treatments.

We quantified 1,344 protein kinases, among them 398 and 139 protein kinases were significantly different ($P<0.05$) after metformin treatments in lean insulin-sensitive and obese insulin-resistant participants, respectively as shown in Table 16. In addition, 46 protein kinases were significant differences, when comparing two groups after metformin treatments as presented in Table 17. 465, 93 and 602 protein kinases were significant changes upon insulin-stimulations in lean insulin-sensitive, obese insulin-resistant, and comparing two groups, respectively. These significant changes either increased or decreased in metformin-treated cells. Next, we overlaid the phosphoproteome and proteome level changes we quantified after insulin-stimulation and metformin treatments.

To determine enriched cellular functions following metformin treatment and insulin, we utilized the samples using DAVID bioinformatics. We then constructed graphs to visualize these data by protein number and P-value per function annotation. The "cellular component", "molecular function", "biological process" or "pathway

analysis" which have a unique identification number were significantly enriched in identified phosphoproteins in primary skeletal muscle cells and P-values were calculated using a hypergeometric test and corrected with Benjamini (cut-off of 0.01 was applied). The complete list is shown graphically in Figures (25, 26, 27& 28). Moreover, our DAVID analysis result revealed that the molecular function most affected included, poly (A) RNA binding, protein binding, actin-binding, nucleotide binding, protein serine/threonine kinase activity, and protein kinase binding. The cellular components associated with metformin treatment were cytoplasm, nucleoplasm, cytosol, cell-cell adherens junction, nucleus, and membrane, and actin cytoskeleton. The biological processes included cell-cell adhesion, mRNA splicing, RNA splicing, GTPase activity, protein phosphorylation, and muscle concentration. A total of 93 pathways were significantly ($p<0.05$) altered by metformin treatment, as shown in Table 18. These pathways were categorized according to KEGG pathway analysis included insulin signaling, ErbB signaling, mTOR signaling, AMPK signaling, MAPK signaling, and glucagon singling pathways. We chose to study insulin signaling pathway, AMPK pathway, insulin resistance pathway because metformin was known to affect cellular metabolism and process through AMPK activation.

Mitochondrial proteins accounts for approximately 20% of the human skeletal muscle proteome and several of these mitochondrial proteins are phosphorylated[102]. Furthermore, we identified 375 phosphoproteins that could be localized to the mitochondrion, accounting for 9% of all identified phosphoproteins such as PANK2, SPARC, CXORF23, VARS, RPL34, ARAF, ATP5C1, MTFR1L, DCAF5, PHB2, ELK1, IFIT3, GLS, ELK3, RPS14, GJA1, RPS6KA6, SCP2, PPP2R1A, DPYSL2, DHX57, FTH1, BSG, FAM110B, LONP1, AKT1, FAM65B, VPS35, ATP6V1E1, PRKACA, GLUL, ACOT9, GSTK1, GABARAPL1, ACOT7, STARD7, ACSL1,

ECH1, CD3EAP, PRKCA, BCS1L, SND1, HCFC1, ARMC1, POR, KARS, MTHFD1, ACOT2, UQCRC1, VDAC3, VDAC2, SUCLG1, VDAC1, UQCRC2, LAP3, ALDH7A1, PI4K2A, URI1, SHMT2, STXBP1, TXN, ATP5H, SDSL, ATP5O, MRPL12, HACD3, PPL, ADH5, ATP5L, PRDX3, LDHB, DHX30, ATP5B, CYB5R1, PRDX5, PPP3R1, CYB5R3, PRDX4, GRPEL1, HLCS, PRDX1, ATP5D, TP53BP2, TNRC18, SFN, ARGLU1, TRMT1L, DECR1, FIS1, TRAP1, RMDN3, BRAF, RMDN1, GPN1, CS, GLUD1, QARS, FASN, NMT1, OGDH, ALDH18A1, DHX29, AARS, SLC35F6, FEN1, CLIC4, MRPS15, CLTC, IDE, MYOM2, MECP2, PPP3CA, MAP1LC3B, AKAP10, ATIC, AIFM1, C1QBP, RARS, ANXA6, TSPO, KIF1B, NEFH, CLIC1, RAB8B, CTSB, LYPLA1, MRPS27, PARP1, TNNC1, ATPIF1, DYNLL1, SIRT1, HADHB, HADHA, MRPS9, BDH2, PACS2, IVD, AGPS, PGAM5, ALDOC, DLD, CRYAB, KANK2, FH, DTYMK, MYCBP, OAT, ECHS1, STX17, GSTP1, HEATR1, ATP5A1, MRPS31, AKAP8, TIMM13, DLST, HSD17B4, MIEF1, NOL3, COX5B, NAPG, AKAP1, PPP2CA, RPS15A, PSMB3, EMC2, HS1BP3, CKB, BRD8, HARS, BID, CCT7, DCPS, YKT6, RANBP2, BCAP31, SLC16A1, MDH1, CDKN2A, MDH2, MTX2, GSR, RAB11A, LRPPRC, RAB11B, LETM1, APEX1, NBR1, HSPA1B, HSPA1A, ACAA2, TACO1, PARK7, COMT, TOMM22, NARS, CHCHD4, PROSC, PPP1CC, COL4A3BP, AKR7A2, CHCHD3, SACS, MACROD1, CAPN1, HADH, PTRF, AP2M1, TGM2, SH3GLB1, MAP2K1, MAP2K2, LIG1, ACYP2, LIG3, TRNT1, SDHA, TUFM, COX6B1, C12ORF10, ILF3, RAB35, FKBP4, ISCU, ATP6V1A, DDX6, DIABLO, AK3, PSEN1, PHB, FOXO3, SPATA5, ACAT2, FOXO1, ACAT1, SLC9A1, BCL2L13, UBB, PITRM1, PSAP, ABL1, NDUFV3, NDUFV2, MYH10, TBC1D15, MARK2, HSPA9, MPST, FDPS, NOP14, PDHA1, HSPA5, GOT1, IDH1, GOT2, IDH2, HSPA2, NFKB1, QDPR, MAVS, CDK7, P4HA1, CHMP2B, PIN1, CYCS, ACO1, UBA1, TPP1, ACO2, ACBD3, NIT2, MCU,

YWHAE, GSK3B, ACADVL, SLC25A3, GSK3A, HSP90AB1, YWHAB, COX4I1, HSPB7, ETFA, ATP2A1, ETFB, HK1, HEBP2, FUNDC2, ATP7B, MRPL1, YWHAQ, OPA1, ME1, DNM1L, YWHAG, IDH3A, YWHAH, TSFM, ADSL, HSDL2, GPX1, NCBP1, ELAC2, IQCE, ATP5F1, REXO2, YWHAZ, PKM, DDAH1, RRM2B, DDAH2, ACOX1, PALLD, DNAJC5, CAT, NDUFS2, PFDN2, NDUFS1, BCAT1, PFDN4, SLC25A5, SLC25A6, SRC, PNKP, RAB1B, GLRX, PDHB, SRI, MAT2B, UACA, HSD17B10, TBRG4, HSPD1, CKMT2, HMGCL, CLN3, ALDH1B1, C6ORF203, MAPK1, STOM, IARS2, ABCF2, MAPK3, TIMM8B, TIMM8A, DUT, TXNRD3, BAD, TXNRD1, BNIP3, TXNL1, RPL35A, IMMT, PTPN11, HSPE1, MAPK14, SOD2, GDAP1, OXR1, SOD1, DNAJA1, GOLPH3, SUCLA2, PC, RPS6KB1, GLOD4, OCIAD1, BAX, DRG2, SSBP1, SLIRP, SLC25A31, ABCE1, MMACHC, and FSIP2.

Using phosphoproteomic approach, we identified 25 phosphoproteins covering all components of the skeletal muscle sarcomere. This included phosphorylation sites on muscle and fiber-type specific isoforms of thick filament proteins (myosins, myosin regulatory light chains, myosin light chains, myosin light chain kinase 2, and myosin-binding protein C) and thin filament proteins (R-actin, tropomyosins, and troponins), such as ARF1, LMOD1, ILK, LMOD2, SYNE1, LMAN1, CAPZB, MYO18B, HABP4, ANKRD1, ANKRD2, MYOZ2, TMOD1, PSMA6, ACTA1, MYH2, ACTC1, MYH3, MYL1, MYL2, TNNT2, MYL3, MYH8, MYH4, and MYH7. We identified phosphorylation sites on the three known giant muscle proteins, titin (126 sites), nebulin (26 sites) and obscurin (61 sites), and the M-band-specific proteins, myomesin-1(4 sites). Furthermore, we detected 65 phosphoproteins on several Z-disc proteins including FHOD3, RYR1, FHL2, HSPB1, JPH1, FBXO22, MYPN, PPP3CA, JPH2, CSRP3, CAPZB, CFL2, MYO18B, PGM5, SCN5A, SYNPO, MYOZ2, PPP1R12A, DST,

GLRX3, ACTN1, ANK2, ANK3, ACTN4, OBSCN, SYNPO2L, MYOT, PALLD, CASQ2, ITGB1BP2, PPP1R12B, SYNC, CRYAB, MYL9, OBSL1, TRIM54, MYH7, HDAC4, SYNPO2, PSEN2, NEXN, SRI, MYL12A, MYL12B, TTN, PDLIM3, PAK1, DNAJB6, BAG3, FLNA, XIRP2, FLNB, DMD, FLNC, SMN1, AHNAK2, SORBS2, PARVA, NEB, FKBP1A, DES, HRC, CTNNB1, STUB1, and MURC.

We have reported several phosphorylation sites on the main proteins in the Ca2+-signaling apparatus (the Ca2+-cycle) such as CACNA1S (9 sites), AHNAK (152 sites), ATP2B1; ATP2A2 (13 sites), HRC (18 sites), JPH1(9 sites), JPH2 (8 sites), RYR1 (4 sites) and 21 of CAMK2B, CAMK2D and CAMKK2. Furthermore, we detected 66 phosphoproteins involved in insulin signaling pathway such as PYGB, GSK3B, IRS1, INPPL1, PRKAG1, ARAF, PYGM, IRS2, CBLB, PYGL, ELK1, PRKAG3, HK1, CRKL, RPTOR, IKBKB, PPP1CB, GYS1, PPP1CC, AKT2, AKT3, FLOT1, FLOT2, AKT1, PRKACA, PRKACB, PRKAB2, MAP2K1, MAP2K2, PDPK1, EXOC7, RPS6, TSC2, TSC1, PRKAB1, PPP1R3F, PPP1R3C, PRKAR1B, PRKAR1A, PPP1R3D, RAPGEF1, RAF1, EIF4E2, SOS1, PRKAA1, PRKAA2, SHC1, CBL, FOXO1, PRKAR2A, EIF4EBP1, MAPK1, EIF4E, SH2B2, MAPK3, BAD, PHKB, BRAF, SORBS1, MTOR, PPP1CA, RPS6KB1, RHEB, FASN, TRIP10, and GRB2 as shown in Figure 29. Moreover, 40 phosphoproteins were linked to insulin resistance pathway such as PYGB, GSK3B, CRTC2, PRKAA1, PRKAA2, IRS1, PRKAG1, PYGM, IRS2, PYGL, PRKAG3, FOXO1, RELA, IKBKB, PPP1CB, GYS1, RPS6KA3, PPP1CC, RPS6KA6, AKT2, AKT3, RPS6KA1, AKT1, MGEA5, PRKAB2, PDPK1, GFPT2, PRKCD, GFPT1, STAT3, PTPN11, PRKAB1, MTOR, NFKB1, PPP1CA, CREB1, PPP1R3C, TBC1D4, RPS6KB1, and PPP1R3D.

The results revealed effect metformin on mitotic cell cycle. The data showed decreased expression of Cyclin-dependent kinase CDKs (CDK1, CDK2, and CDK7)

after treating the human skeletal muscle cells with 50 μM metformin, while CDK11B, CDK16, and CDK18 were upregulated with metformin. The transcription factor of E2F is one of the downstream of CDKs that is regulated by Rb. These quantified phosphoproteins are RB1, YWHAE, GSK3B, HDAC2, CDKN1B, PCNA, CCNH, PRKDC, YWHAB, HDAC1, CUL1, SMC3, CDC20, FZR1, CDC23, YWHAQ, CDC26, RAD21, CDC27, ABL1, EP300, E2F3, SFN, BUB3, YWHAG, SKP1, YWHAH, SMAD2, CREBBP, SMAD3, CDKN2A, SMC1A, YWHAZ, RBX1, RBL2, CDK7, STAG2, CCNE1, CDK4, MCM3, ANAPC1, MCM2, and ANAPC2 as reported in Figure 30.

The insulin signaling pathway is one of the survival pathways that is initiated via growth factor ligand resulting in cellular processes such as motility, survival, proliferation and morphology. About 66 phosphoproteins were associated with this pathway such as PYGB, GSK3B, IRS1, INPPL1, PRKAG1, ARAF, PYGM, IRS2, CBLB, PYGL, ELK1, PRKAG3, HK1, CRKL, RPTOR, IKBKB, PPP1CB, GYS1, PPP1CC, AKT2, AKT3, FLOT1, FLOT2, AKT1, PRKACA, PRKACB, PRKAB2, MAP2K1, MAP2K2, PDPK1, EXOC7, RPS6, TSC2, TSC1, PRKAB1, PPP1R3F, PPP1R3C, PRKAR1B, PRKAR1A, PPP1R3D, RAPGEF1, RAF1, EIF4E2, SOS1, PRKAA1, PRKAA2, SHC1, CBL, FOXO1, PRKAR2A, EIF4EBP1, MAPK1, EIF4E, SH2B2, MAPK3, BAD, PHKB, BRAF, SORBS1, MTOR, PPP1CA, RPS6KB1, RHEB, FASN, TRIP10, and GRB2. We focused to study insulin receptor pathway to reveal the effect of metformin on human skeletal muscle cells. mTOR was downregulated after metformin treatment leading to decreased protein synthesis. The PI3K/Akt signaling pathway were downregulated as shown in Figure 31.

We have reported several phosphoproteins associated with AMPK signaling pathway such as CRTC2, IRS1, PRKAG1, PPP2R2A, IRS2, ELAVL1, PRKAG3,

RPTOR, GYS1, EEF2K, PPP2R1A, PPP2R5E, AKT2, AKT3, AKT1, MAP3K7, RAB8A, RAB2A, PRKAB2, PDPK1, TSC2, PPP2R5D, TSC1, PRKAB1, SIRT1, TBC1D1, CREB1, AKT1S1, PFKFB2, PRKAA1, PRKAA2, CAB39, FOXO3, FOXO1, PPP2CA, PPP2CB, EIF4EBP1, PPP2R3A, EEF2, MTOR, RAB11B, RAB10, PFKL, RPS6KB1, RAB14, RHEB, FASN, PFKM, and PFKP as shown in Figure 32. Furthermore, 35 phosphoproteins were associated with mTOR signaling pathway such as PRKAA1, PRKAA2, CAB39, IRS1, IKBKB, RPTOR, RPS6KA3, RPS6KA6, AKT2, AKT3, RPS6KA1, EIF4EBP1, AKT1, MAPK1, RICTOR, EIF4E, EIF4B, MAPK3, PDPK1, RPS6, TSC2, PRKCA, TSC1, BRAF, MTOR, RRAGA, RPS6KB1, RRAGC, RRAGB, RHEB, AKT1S1, ULK3, ULK2, ULK1, and EIF4E2 as shown in Figure 33.

We observed phosphoproteins were associated with ERBB pathway such as CAMK2B, GSK3B, CAMK2D, CDKN1B, SHC1, SRC, ARAF, CBLB, CBL, ELK1, EGFR, CRKL, PAK1, ERBB3, AKT2, AKT3, ERBB2, ABL1, EIF4EBP1, AKT1, MAPK1, ABL2, PLCG1, PAK2, NCK1, MAPK3, PAK4, MAP2K4, JUN, MAP2K1, MAP2K2, BAD, GAB1, PRKCA, NRG1, BRAF, MTOR, PTK2, RPS6KB1, GRB2, RAF1, and SOS1 as shown in Figure 34.

MAPK signaling pathway was detected in the our phosphoproteomics and these phosphoproteins such as ATF2, ZAK, HSPB1, ARRB1, ELK1, CRKL, IKBKB, PPP3CA, RPS6KA3, RPS6KA6, CASP3, AKT2, AKT3, RPS6KA1, STMN1, RAC2, AKT1, IKBKG, RAC1, PRKACA, PRKACB, MAP3K7, MAP3K4, MAP3K5, PDGFRB, MAP2K3, MAP2K4, MAP4K2, DAXX, MAP2K1, MEF2C, DUSP3, MAP2K2, CACNA2D1, RRAS2, PRKCA, DUSP9, MAPK8IP3, DUSP6, DUSP7, CACNB1, PPM1A, CACNB3, PPM1B, RASA1, RAPGEF2, MAPT, RAF1, SOS1, MAX, SRF, CACNA1B, EGFR, CACNA1H, RELA, STK3, RELB, RAP1B, CDC42, PPP3R1,

PAK1, MAPK7, FLNA, MAPK1, FLNB, CACNA1S, FLNC, PAK2, MAPK3, MAP4K4, MAP2K6, MAP3K2, HSPA8, MAP3K3, JUN, JUND, MAP3K1, HSPA1L, NFATC3, BRAF, NFATC1, HSPA2, MAPK14, GNG12, NFKB1, NFKB2, PPP5C, TAOK1, NF1, GRB2, TAB2, FGF13, MAP3K11, HSPA1B, and HSPA1A as reported in Figure 35.

We further studied the upregulated and downregulated proteins in metformin-treated human skeletal muscle cells to identify novel of molecular protein targets from lean insulin-sensitive and obese insulin-resistant participants as shown in Figures 36 &37, that could utilized to develop a new therapeutic strategy for obesity and T2D in the future. Among the upregulating proteins, we detected proteins such as PPP1R12B, FOXO4, EP300, TP53BP1, PRPF4B, CDK13, DCLK1, MYLK, ARHGAP21, TTN, AKT3, PPP2R5C, and PPP2R5E. Some interesting proteins were found highly significant upregulated such as TBX3, PPP1R12B, NFX1, LMOD2, and RAB40B. Among the downregulated proteins, we quantified proteins such as FREM1, PDXDC1, SPEG, PI4KA, PPP1R3F, RNF34, and SIK2. Among the interesting downregulated proteins found in treated cells are TBC1D1, DEPTOR, GPS1, MAP3K2, ARAF, and SASH1. Furthermore, we observed the upregulated and downregulated proteins in insulin-stimulation human skeletal muscle cells from lean insulin-sensitive and obese insulin-resistant participants as shown in Figures 38 &39. We identified the top 100 significant upregulated proteins and the bottom 100 significant downregulated proteins. We deeply studied the significant pathway ($P<0.05$) in lean insulin-sensitive and obese insulin-resistant participants for these unique downregulated and upregulated phosphoproteins after metformin treatment and upon insulin-stimulation as reported in Figure 40.

This comprehensive human skeletal muscle phosphoproteome and proteome dataset would render valuable resources for identification and help researchers elucidate

cellular signaling pathways and might provide novel targets for drug development for insulin-resistance and T2D.

3.3 SPECIFIC AIM 3: DETERMINE THE EFFECT OF METFORMIN ON PROTEIN-PROTEIN INTERACTIONS OF PP2AC IN HUMAN SKELETAL MUSCLE CELLS DERIVED FROM LEAN INSULIN-SENSITIVE AND OBESE INSULIN-RESISTANT PARTICIPANTS

To characterize the phosphatase complex, we created a high-density interaction network surrounding PP2Ac. The protein-protein interactions approach was developed by our lab using Co-IP to identify PP2Ac partners[101]. The raw MS files were processed using the MaxQuant software version (1.6.17.0), and the peak area of protein was identified with label-free quantification (LFQ). PP2Acα and PP2Acβ were identified and detected in PP2Ac Co-immunoprecipitant from all human skeletal muscle cell participants. We identified 3,377 total proteins with FDR at 0.01 and 2 unique peptides from all PP2Ac Co-immunoprecipitation lean insulin-sensitive samples. Additionally, 3,091 total proteins were identified from all PP2Ac Co-immunoprecipitation obese insulin-resistant samples. Quantification and statistical analysis were performed to determine potential PP2Ac interaction partners, and these might interact directly or indirectly with PP2Ac. We confirmed that 805 proteins from the lean insulin-sensitive group and 378 proteins from the obese insulin-resistant group had met our criteria for PP2Ac interaction partners (enrichment ratio more than 10 and a peak area (PA) identified in more than half PP2Ac co-immunoprecipitation samples). Furthermore, we identified interaction partners proteins, using STRING, and BioGRID-4.2 databases, and these proteins were appeared to be known PP2A partners, and 9 proteins (DDX3Y, IGKC, RPS4Y1, C4AMC7, WASH3P, 7SEP, 11SEP, and 9SEP) were not identified in these databases and considered novel PP2Ac interaction partners.

We quantified several proteins that were previously known to interact with PP2A, such as PPP1R12B, PPP6R2, PPP2R1B, PPP2R5C, PPP2R2D, PPP1R18, PPP1R21, PPP3CA, PPP2R4, PPP1R7, PPP4R1, TPPP3, PPP4R2, CCDC88A, CCT2, STRN4, STRIP2, STRIP1, STRB, MYH8, MYH9, PSMD11, PSMD14, PSMA7, PSMD3, PSMB1, PSMA2, PSMA3, PSMB5, PSMD8, GPSM2, PSMC6, PSMD1, PSME2, GAK, AKR7A2, AKAP10, EIF2AK2, AKR1C3, AK2, AKAP12, AHNAK, PAK2, AAK1, AHNAK2, ZAK, AKAP2, TRAPPC3, TRAPPC5, TUBB4A,TUBG1, TUBGCP3, OTUB1, TUBGCP6, TUBGCP2, TUBB6, TUFT1, TUBA8, STUB1, MTCH1, TMTC3, RTCA, CLTC, TTC9, TCF25, MOB4, HMOX2, DCTN3, ACTN1, CTPS1, CTNNA2, CTNNA1, CCT6A, CCT3, CCT8, CCT2, RICTOR, CCT7, DCTN5, ACTR10, MCTS, DYNC1LI2, DYSF, DYNC1I2, DYNC1H1, DYM, FOXO1, FOCAD, TRAPPC3, TRA2B TRAP1, TRAF2, TRAPPC5, TSC2, TSN, ITSN1, MTSS1L, TSG101, TSC1, ITSN2, MCTS1, RRAS2, GRASP, RASSF4, RASAL2, NME3, DNMBP, CAMK2G, CAMK2D, CAMSAP1, ZC3HAV1, ZC3H15, RSU1, RAB11B, PARP4, RAB21, RAPH1, ARPC2, ARPC3, ACTN1, SPAG9, ARPC5L, ARHGAP1, DNM1L, ROCK2, AAK1, TARDBP, PTPN12, FABP5, FASN and CKAP4. In addition, we also quantified many proteins that interact with PP2Ac potentially. These results demonstrated that our approach to identify and quantify PP2Ac-interacting proteins were successful.

There were more than 26 ribosomal proteins were reported in this study (enrichment ratio more than 10 and a peak area (PA) identified in more than half PP2Ac co-immunoprecipitate samples) such as, MRPL40, MRPL1, MRPL13, NMD3, MRPL49, RPL18, RPL6, RPL18A, RPL19, RPL24, MRPS35, MRPS22, RPL32, FAU, RPS6, RPL7A, MRPL11, MRPL22, RPL15, DAP3, MRPL19, RPS9, RPL28,

RPL27A, RPL4, and RPL13. Moreover, we identified and quantified translation initiation factors, including EIF3J, EIF2D, EIF1, EIF2B2, EIF6, and EIF2B1and EIF2B4. Many of the newly identified potential PP2Ac-binding proteins were known to be involved in vesicle trafficking including, VPS16, VPS4B, VMA21, VPS11, VPS52, VPS36, VPS37A, VPS53, TSG101, VPS18, VPS29, and VPS35. The interactions of several candidate proteins, such as STAT6, ILF3, DDX17, HIST1H1B, and LIMD1 were confirmed to be involved in the regulation of transcription.

We identified and quantified more than 30 different kinases that met our requirement for potential PP2Ac interaction partners such as, 5-AMP-activated protein kinase subunit gamma-1, Rho-associated protein kinase 2, serine/threonine-protein kinase OSR1, cAMP-dependent protein kinase catalytic subunit alpha, serine/threonine-protein kinase PAK 2, 5-AMP-activated protein kinase catalytic subunit alpha-, serine/threonine-protein kinase Nek7, serine/threonine-protein kinase WNK1, STE20-like serine/threonine-protein kinase, cAMP-dependent protein kinase catalytic subunit beta, calcium/calmodulin-dependent protein kinase type II subunit delta , serine/threonine-protein kinase TBK1, SH3 domain-containing kinase-binding protein 1 and epidermal growth factor receptor kinase substrate 8. In addition, more than 14 protein phosphatases were identified and quantified such as, Type II inositol 3,4-bisphosphate 4-phosphatase (INPP4B), serine/threonine-protein phosphatase 2A 65 kDa regulatory subunit A beta isoform (PPP2R1B), dual specificity protein phosphatase 3 (DUSP3), tyrosine-protein phosphatase non-receptor type 12 (PTPN12), serine/threonine-protein phosphatase 2B catalytic subunit alpha isoform (PPP3CA), serine/threonine-protein phosphatase 2A 56 kDa regulatory subunit gamma isoform (PPP2R5C), serine/threonine-protein phosphatase 2A 55 kDa regulatory subunit B delta isoform (PPP2R2D), serine/threonine-protein phosphatase 4 regulatory subunit 3A (SMEK1), serine/threonine-

protein phosphatase 4 regulatory subunit 1(PPP4R1), protein phosphatase 1 regulatory subunit 21 (PPP1R21) and protein phosphatase 1 regulatory subunit 14B (PPP1R14B).

DAVID bioinformatics were performed on the 880 PP2Ac interaction partners to determine numerous pathways that were significantly enriched, such as mTOR, AMPK, AKT and MAPK signaling as illustrated in Table 19.

3.3.1 METFORMIN RESPONSIVE PP2AC INTERACTION PARTNERS

In total, 1377 and 903 PP2Ac interaction partners were quantified in lean insulin-sensitive non-diabetic participants and obese insulin-resistant non-diabetic participants after metformin treatments, respectively. Additionally, 899 and 405 were quantified with a fold change greater than 1.5 (i.e., 1.5-fold increase) or less than 0.6667 (i.e., 1.5-fold decrease) from lean insulin-sensitive non-diabetic participants and obese insulin-resistant non-diabetic participants, respectively, by comparing metformin-treated samples to untreated samples as shown in Table 20 &21. We performed a t-test analysis to quantify the changes in both groups and found that 12 and 7 were significantly modulated after treating the human skeletal muscle cells with metformin ($P < 0.05$). These 12 and 7 PP2Ac partners were considered as metformin responsive interaction partners and were previously reported to interact with PP2Ac from both groups as shown in Table 22.

We found the interaction of PPP2R4, PPP1R18, PPP1R14B, and PPP2R5E with PP2Ac was increased by 2.43, 2.00, 2.43, and 2.43 folds, respectively, in response to metformin treatment in lean insulin-sensitive participants. Conversely, the interaction of PPP2R1A, PPP2R1B, PPP2R2A, PPP2R3A, PPP2R5C, PPP2R5D, PPP2R4, PPP2R4, PPP3CA, and PPP2R2D with PP2Ac have decreased by 1.36, 0.87, 1.095,

1.43, 1.36, 0.98, 0.419, 0.38 and 1.14 folds, respectively. Moreover, Protein phosphatase 1A (PPM1A) and Protein phosphatase 1F (PPM1F) were decreased with metformin treatment with fold changes 1.26 and 1.37, respectively.

3.3.2 INSULIN RESPONSIVE PP2AC INTERACTION PARTNERS

We quantified and identified 450 proteins from lean insulin-sensitive group and 225 proteins from obese insulin-resistant group had met our criteria for PP2Ac interaction partners (enrichment ratio more than 10 and a peak area (PA) identified in more than half PP2Ac Co-immunoprecipitate samples) upon insulin-stimulation as shown in Table 23&24. These interaction partners were previously reported in the SRING database, except RPS4Y1 was not reported. In addition, most of these pathways are related to protein synthesis and degradation, cytoskeleton dynamics, and AMPK signaling. Interestingly, a few glucoses-responsive were detected in these pathways such as, PPP2R1B, PPP2R5C, PPP2R2D, ARPC4, and RHOA. We also quantified voltage-dependent anion-selective channel protein 1 (VDAC1), insulin-degrading enzyme (IDE), UDP-glucose: glycoprotein glucosyltransferase 1 (UGGT1), Insulin-like growth factor 2 mRNA-binding protein 3 (IGF2BP3), Insulin receptor substrate 1(IRS1), Insulin-like growth factor 2 mRNA-binding protein 1(IGF2BP1), Insulin receptor substrate 2 (IRS2) and Insulin-like growth factor 2 mRNA-binding protein 2 (IGF2BP2) as PP2Ac partners. Additionally, we quantified and identified several proteins such as, DCC-interacting protein 13-alpha (APPL1), Transforming protein RhoA (RHOA), 85/88 kDa calcium-independent phospholipase A2 (PLA2G6), and Ras-related protein Rab-10 (RAB10), which have been shown to regulate insulin secretion.

We quantified nine proteins in lean insulin-sensitive control group that were significantly decreased ($P < 0.05$) upon insulin-stimulation, including VWA5A, TRIO, URI1, AP1S2, AP3S2, C1QBP, NAV3, RIN1, and EIF3K. Furthermore, PPP2R5E

were significant increased during insulin-stimulation. In contrast, insulin-stimulation in obese insulin-resistant control group significantly decreased in GDI2 and RAB14, and ZYX, AP2A2, and HDAC7 were significantly increased.

3.3.3 PP2Ac INTERACTION PARTNERS WITH SIGNIFICANT DIFFERENCE BETWEEN LEAN INSULIN-SENSETIVE AND OBESE INSULIN-RESISTANT NON-DIABETIC PARTICIPANTS

Given the relevance of the structure of protein complexes in the biological functions of PP2A, it is important to identify, quantify and characterize many PP2Ac interaction partners by comparing the normalized peak areas of PP2Ac between both groups. We found 230 proteins showed a significant decrease in obese insulin-resistant controls when compared with lean insulin-sensitive controls such as, GTPBP1, IGF2BP3, PRKAR2A, PRKACA, ATP2B1, TUBG1, MYH10, MAP2K2, MTOR, RPL28, GDI2, PPP2R2A, PPP2R3A, PPP1R7, PKN1, PPP2R2D, PPP4R1, TUBGCP2, PTPN23, PRRC2C, and PPME1. While 20 proteins showed a significant decreased in obese insulin-resistant treated with metformin when compared with lean insulin-sensitive treated with metformin such as AKR7A2, ATP2B1, HNRNPA2B1, RPL14, HNRNPM, EIF5, RPL19, HNRNPU, PLCB3, EIF2B5, DDX39B, LPIN1, GPNMB, SLC1A5, FUBP1, FKBP10, ARL8A, SRR, and MAD1L1. Upon insulin-stimulation, we quantified 29 proteins were significant decreased in obese insulin-resistant when compared with lean insulin-sensitive such as, AKR7A2, UGDH, CNOT3, EIF3J, COL3A1, PYGB, ATP2B1, HNRNPA2B1, MYH10, NSF, RPL28, CARS, HNRNPM, GPNMB, HNRNPU, DDX39B, TJP1, PPP4R1, FKBP15, EIF2B5, SLC1A5, CSRP2, GBF1, and ILF3.

CHAPTER 4 DISCUSSION

4.1 SPECIFIC AIM 1: DETERMINE THE EFFECT OF METFORMIN ON PP2AC ACTIVITY IN PRIMARY HUMAN SKELETAL MUSCLE CELLS DERIVED FROM LEAN INSULIN-SENSITIVE AND OBESE INSULIN-RESISTANT PARTICIPANTS

To examine our hypothesis that activation of PP2A is involved in the antidiabetic activity of metformin's treatment, we measured the PP2A activity of primary human skeletal muscle cells with and without Metformin for changed the catalytic activity of PP2A cells, followed by phosphatase assay immunoprecipitated. In the present study, our data demonstrated that Metformin's increased the activity of PP2A in the myotubes derived from all eight lean insulin-sensitive non-diabetic participants, and eight obese insulin-resistant non-diabetic participants and average fold increase were (Metformin/basal): 1.54±0.11 and 1.68±0.16, $P<0.001$, respectively). The molecular mechanisms of metformin are not fully understood. Metformin inhibits complex I in the mitochondrial electron transport chain in liver and muscle cells as well as skeletal muscle[103]. Another potential molecular mechanism is the activation of AMPK in skeletal muscle after metformin treatment[51].

Several studies have reported the effect of metformin on PP2A activity and associated pathways. Deepa et al., reported that metformin has no effect on PP2A activity in C2C12 myotube (a mouse cell line)[80], others have demonstrated that metformin induces PP2A activity in several cell systems. For example, in lung cancer cells (A549 and H1651), metformin activated PP2A to reduce tumor formation *in vivo* and decrease tumor cell growth and invasion capacity *in vitro* as well as serine phosphorylation level of Bax (Ser184), Myc (Ser62), and Akt (Ser473)[82]. Sacco et al. reported that metformin treatment induced the protein expression of PP2A catalytic and regulatory subunit in

breast cancer cells in *vitro*[84]. Notably, Auger et al. have reported that metformin activated PP2A in human subcutaneous white adipose tissue (scWAT), resulting in dephosphorylation of acetyl-CoA carboxylase (Ser79) and hormone-sensitive lipase (Ser660), and metformin also lowered lipolysis in beige fat[88]. Kawashima et al. demonstrated that metformin treatment activated PP2A in myeloproliferative neoplasm (MPN) cells to suppress the oncogenic kinase JAK2V617F by increasing reactive oxygen species levels leading to the inhibition of SHP-2, a positive regulator of JAK2V617F. Furthermore, the results indicated that metformin suppressed phosphorylation of the PP2Ac at Tyr307 in a dose-dependent manner. These results revealed that metformin activated PP2A independent of AMPK activation[89]. PP2A is one of the major tau phosphatases, and it has been demonstrated that metformin works through PP2A to reduce tau phosphorylation in primary cortical neuron cells[81]. Metformin treatment-induced PRKN gene transcription, mitochondria integrity, mitophagy, cell viability and decreased activation of nuclear factor kappa B (NF-kB) but not p53 or ATF4 in human renal epithelial cells[87]. Zhang et al. reported that metformin decreased NLRP3 protein expression and NLRP3 inflammasome activation in ox-LDL-stimulated macrophages through AMPK and PP2A. PP2A catalytic activity was required for NF-κB inhibition and Tristetraprolin activation induced by metformin in ox-LDL-stimulated macrophages[86].

Despite the existing evidence (albeit indirect), on potential regulation of protein phosphorylation-dephosphorylation of key cellular proteins and functions by metformin, putative mechanisms underlying metformin-mediated activation of PP2A remain unclear at this time. PP2A is regulated by the mTOR kinase, and both enzymes affect the phosphorylation status of the ribosomal protein S6 and p70S6K. PP2A has been

shown to dephosphorylate the mTOR substrate S6K1 and be involved in mTOR-mediated phosphorylation of insulin receptor substrate 1 (IRS1) through modulation of PP2A activity by mTOR[104]. Along these lines, Kickstein and coworkers have reported that metformin directly affected PP2A independently of AMPK/TOR signaling[81]. Based on the data accrued in these studies, the authors have proposed that metformin interferes with the association of PP2Ac with MID1-α4 complex leading to regulation of PP2A activity. On the other hand, activation or phosphorylation of AMPK by metformin leads to the inhibition of mTOR signaling, and subsequent dissociation of PP2A and α4 and resulting in PP2A activation[105]. It has also been proposed that metformin could dissociate the binding of PP2A and MID1, resulting in decreased PP2A degradation and enhanced phosphatase activity[81,105]. Additionally, metformin could likely promote interaction between the structural (A subunit), regulatory (B subunit), and catalytic C subunits, leading to the enzyme's functional activation. Such interactions may be influenced by post-translational modification of individual subunits, including the methylation of the catalytic subunit at Leucine-309 residue 4, which has been shown to promote PP2A activation.

A limitation of the present study is the lack of comprehensive functional characterization. Additional mechanistic experiments such as inhibition PP2A activity using specific inhibitors, knockdown of PP2Ac or α4 are warranted to explore the functional role of the activation of PP2A by metformin in skeletal muscle insulin signaling and insulin-resistance in primary muscle cells derived from both lean healthy insulin-sensitive and obese insulin-resistant participants. Nonetheless, primary skeletal muscle cells from well-characterized live human participants were used, which provides information more relevant to human physiology than L6 rat or C2C12 mouse skeletal muscle cell

lines. The potential mechanisms of metformin action involved several biological pathways are presented in Figure 41. Our results provided the first evidence to suggest that metformin promotes activation of PP2A in human skeletal muscle cells derived from lean insulin-sensitive and obese insulin-resistant non-diabetic participants. The results indicate potential new targets for mechanistic studies on skeletal muscle insulin resistance in humans.

4.2 SPECIFIC AIM 2: DETERMINE THE EFFECT OF METFORMIN ON PHOSPHOPROTEOME IN PRIMARY HUMAN SKELETAL MUSCLE CELLS DERIVED FROM LEAN INSULIN-SENSITIVE AND OBESE INSULIN-RESISTANT PARTICIPANTS

We present a large-scale quantitative proteome and phosphoproteome approach to quantified metformin-induced changes from human skeletal muscle cells. We used TMT 11 labeling approach followed by a high-resolution UPLC-ESI-MS/MS to measure protein expression levels and peptide phosphorylation events. This method quantified more than 7,000 proteins and 24,700 phosphorylation events. Of these, about 10% phosphorylation sites (1,958) were not previously reported in four large protein phosphorylation site databases (www.phospho.elm.eu.org, www.uniprot.org, www.phosphosite.org, and www.phosida.com). We quantified more than 10,300 phosphorylation site changes in lean insulin-sensitive and obese insulin-resistant participants. 4,455 and 1,966 phosphorylation sites were significant changes ($P<0.05$) in lean insulin-sensitive and obese insulin-resistant participants, respectively. In addition, we quantified 5,146 phosphorylation sites in lean insulin-sensitive and 967 phosphorylation sites in obese insulin-resistant participants were significant changes upon insulin-stimulation. We

found a phosphoserine/phosphothreonine/phosphotyrosine ratio of about 79:19:2 in human skeletal muscle cells, suggesting tissue-specific differences in protein phosphorylation.

This study employed human skeletal cell cultures and protein extracts for our phosphoproteomics and proteomics analysis to investigate the possible mechanisms of metformin on human skeletal muscle cells in comparison to lean insulin-sensitive healthy cells. We aimed to study proteins resulting from metformin treatment to investigate the possible signaling pathways that might elucidate explanations behind the effect of metformin on skeletal muscle cells. These analyses provided an unbiased picture of metformin's effect on the phosphoproteome and proteome; we also inspected sites phosphorylated by mTOR and AMPK. Metformin is well known to increase AMPK activity and diminish mTOR activity[51]. PP2A is regulated by mTOR and both affect the phosphorylation of p70S6K and ribosomal protein S6. AMPK playing essential roles in a variety of growth, autophagy, cell polarity, and metabolism processes. The phosphorylation of the AMPK on activating residue Ser183 was detected by our phosphoproteome experimental analysis; we observed the phosphorylation state, gene, and protein of the known AMPK substrates. We reported more than 95% phosphorylation of these AMPK substrates was reported in the four large protein phosphorylation site databases and were reproducibly hyperphosphorylated after metformin treatment in our phosphoproteome experimental conditions as shown in Table 25. The kinase that phosphorylates the activation loop of Thr172 of AMPK is LKB1 (STK11) and AMPK directly phosphorylates the same residue by CAMKK2b in response to calcium flux[106]. Additional studies reported that MAPKKK family members such as TAK1/MAP3K7

might phosphorylate Thr172[107]. LKB1 phosphorylated and activated twelve kinases related to AMPK, included the SIKs (1-3), MARKs (1-4), NUAKs (1-2), and BRSK/SADs (1-2) sub-families of kinases[108].

We quantified Calcium/calmodulin-dependent protein kinase kinase 2 (CAMKK2) in our phosphoproteome results, and the phosphorylation sites are (S495, S452, S522, S479, S511, and S468); these phosphorylation sites were significantly increased ($P<0.05$) after metformin treatment in lean insulin-sensitive participants. CAMKK2 activates AMPK in response to calcium increase, which leads to phosphorylate several of AMPK substrates to impact growth and metabolism acutely. Furthermore, we quantified 19 Calcium/calmodulin-dependent protein kinase type II subunits (CAMK2B, CAMK2D, and CAMK2A), and we observed that CAMK2D (S334 and S348) were significant increased ($P<0.05$) in lean insulin-sensitive participants after metformin, meanwhile CAMK2D (T287) were significantly increased ($P<0.05$) after metformin treatment in obese insulin-resistant participants. Calcium/calmodulin-dependent protein kinase type II subunit delta CAMK2D (S334, T331, and T351) were significantly increased ($P<0.05$) upon insulin-stimulation in lean insulin-sensitive participants and CAMK2D (S315 and S319) were significant decreased upon insulin stimulation in obese insulin-resistant participants. Mitogen-activated protein kinase kinase kinase (MAP3K7, MAP3K11, MAP3K3, MAP3K1, MAP3K2, MAP3K5, MAP3K7, MAP3K4, and MAP3K11) were quantified in our experiment, and MAP3K7 (S378, S454, and S427) were significantly decreased ($P<0.05$) after metformin treatment and insulin stimulation in lean insulin-sensitive participants. Moreover, MAP3K7 (T444 and T417) were decreased in obese insulin-resistant participants after metformin treatment and insulin-stimulation.

Two genes are encoding the AMPK α catalytic subunit (α1 and α2), two β genes (β1 and β2) and three γ subunit genes (γ1, γ2, and γ3)[109]. 5'-AMP-activated protein kinase subunit beta-1 (PRKAA1; S496, S486, T490, T488, S506, S498, S508, T482, S524, S527, S523, &T526), 5'-AMP-activated protein kinase catalytic subunit alpha-2 (PRKAA2; S377), 5'-AMP-activated protein kinase subunit beta-1 (PRKAB1; S108, S182, S181, S24, S25), 5'-AMP-activated protein kinase subunit beta-2 (PRKAB1; S39, S182, Y194, T40, S184, Y189, S108, S183, S44), 5'-AMP-activated protein kinase subunit gamma-2 (PRKAG2; S195), and 5'-AMP-activated protein kinase subunit gamma-3 (PRKAG3; S162, S65) were quantified in our phosphoproteome results. Furthermore, we quantified 34 AMPK substrates such as PPP1R12C, PPP1R3C, PAK2, GFPT1, KLC1, LIPE, HDAC4, HDAC9, HDAC5, VASP, RB1, TBC1D1, RAF1, ACACA, TSC2, PIKFYVE, RPTOR, TBC1D1, SNX17, YAP1, CTNNB1, EEF2K, CSNK1E, BAIAP2 and PFKFB2 were significant changes after metformin treatment. One mechanism by which AMPK controls the mTORC1 is by direct phosphorylation of the tumor suppressor TSC2 on serine 1387 (Ser1345 in rat TSC2)[110]. AMPK directly phosphorylates Raptor (regulatory associated protein of mTOR), which blocks the ability of the mTORC1 kinase complex to phosphorylate its substrates[111]. We found that the phosphorylation of Tuberin (TSC2; S1779) was significantly decreased ($P<0.05$) after metformin and insulin-stimulation in both groups. Furthermore, Metformin treatment and insulin-stimulation resulted in a significant decrease of (TSC2; S1449) in lean insulin-sensitive participants, while (TSC2; S1454) was significantly decreased ($P<0.05$) after metformin treatment in obese insulin-resistant participants. This observation is consistent with an inactivation of the serine/threonine-protein kinase (mTOR). We identified mTOR in this study and phosphorylation sites at S2120, S2127, S2478, S2481, S1261, S2448, S2450, S2454, T2119, T1262, T2446, and Y2125. We observed

that mTOR kinase (S1261) was not significantly change by metformin treatment in lean insulin-sensitive participants and was significantly decreased ($P<0.05$) in obese insulin-resistant participants by metformin treatment and insulin-stimulation. Furthermore, we identified and quantified several of mTOR substrates in our phosphoproteome studies such as RPTOR (S877, S881, S882, S884, S886, S887, S722, S859, S863, T883, T889, T857, and T865), BAG family molecular chaperone regulator (BAG 2&3; S31, S177, S291, S377, S386, and S106), Eukaryotic translation initiation factor 4E-binding protein 1(EIF4EBP1; T77), and Ribosomal protein S6 kinase beta-1 (RPS6KB1; S427, S441, S447, S452, S15, T444, and T11), we observed that (RPTOR; S877) was significantly decreased ($P<0.05$) in lean insulin-sensitive participants and decreased in obese insulin-resistant participants after insulin-stimulation and metformin treatment. Moreover, (EIF4EBP1; T77) was significantly increased ($P<0.05$) after metformin treatment in lean insulin-sensitive participants and increased in obese insulin-resistant participants after metformin treatment. We have investigated eukaryotic translation initiation factor 4B (EIF4B; S497, S498, S504, and T500) after metformin treatment and observed that the phosphorylation significant increased ($P<0.05$) in both groups, while the phosphorylation of (EIF4B; S504) was significant increased ($P<0.05$) upon insulin-stimulation in both groups. In addition to unbiased mass spectrometry studies, several studies reported AMPK could directly phosphorylate several sites in ULK1[112], we identified 15 phosphorylation sites of Serine/threonine-protein kinase (ULK1; S758, S477, S479, S556, S583, S588, S281, S450, S623, S544, S469, S403, T755, T401, and T636). We only observed that S623 and T636 were significantly increased ($P<0.05$) in lean insulin-sensitive participants after insulin-stimulation and metformin treatment, while S623 and T636 were significantly decreased after metformin treatment in obese insulin-

resistant participants. We investigated the effect of metformin on mTOR substrate Serine/arginine repetitive matrix protein (SRRM 1, 2 &4), we found 332 phosphorylation sites. Among them, 74 phosphorylation sites were significantly modulated ($P<0.05$) after metformin treatment and 102 phosphorylation sites were significantly changed ($P<0.05$) after insulin-stimulation in lean insulin-sensitive participants. Furthermore, 28 and 13 phosphorylation sites were significantly modulated ($P<0.05$) in obese insulin-resistant participants after metformin and insulin-stimulation, respectively.

AMPK is an upstream kinase for the metabolic enzymes Acetyl-CoA carboxylase (ACC1 & ACC2) and HMG-CoA reductase. In muscle, AMPK regulated glucose uptake by effects on the RabGAP TBC1D1 and its homolog TBC1D4 (AS160), which play roles in GLUT4 trafficking following insulin-stimulated glucose uptake[113]. We found 83 phosphorylation sites of TBC1 domain family members (TBC1D) were significant changed after metformin treatment in both groups. The phosphorylated TBC1D1 increases the plasma membrane localization of glucose transporter 4 (GLUT4) and regulates glycogen synthases (GYS1 and GYS2) to prevent the glycogen storage[114]. In the present study, we found that the phosphorylation of (TBC1D1; S237 & S668) significantly increased in lean insulin-sensitive participants, while S627 increased in obese insulin-resistant participants after metformin treatment. Unexpectedly, Metformin treatment significantly decreased S614, S627, and S237 of TBC1D1 in lean insulin-sensitive and obese insulin-resistant participants, respectively. Moreover, we observed that the phosphorylation of Hydroxymethylglutaryl-CoA synthase (HMGCS1; S495 & T490) was significant increased after metformin treatment lean insulin-sensitive participants. AMPK has been reported to regulate and phosphorylate several transcription factors, coactivators, a subfamily of histone deacetylases, the

acetyltransferase p300, and even histones themselves[115]. It has been reported that metformin mainly affects hepatic glucose production through activating AMPK but our results supported its effect in skeletal muscle. No research studies have been done on PRKAB1 (S108) and PRKAB2 (S108) for diabetes study using skeletal muscle. A significant increase of S108 phosphorylation in PRKAB1 (AMPK-beta-1) and PRKAB2 (AMPK-beta-2) after metformin treatment is shown in Figure 42.

We have identified and quantified highly predicated AMPK substrates in our phosphoproteome that are involved in excitation-contraction coupling, vesicle transport, and mitochondrial function such as A-kinase anchor protein (AKAP1), (AKAP10), and their phosphorylation sites are S445, S592, S429, and S52, S187, respectively. AKAP1 was shown to regulate mitochondrial respiration via AMPK-dependent phosphorylation and is highly expressed in human muscle, heart, and adipose tissue[116]. We found a member of the AKAP family and is expressed in endothelial cells, cultured fibroblasts, and osteosarcoma cells. It associates with protein kinases A and C and phosphatase and serves as a scaffold protein in signal transduction. We observed 4 phosphorylation sites of (AKAP12; S648, S651, S514, and T1116) and 17 sites of (AKAP13; S2398; S2378; S1297; S1909; S1929; S1911; S1932; S1914; S1565; S1876; S1858 S1647 ;T1611 ;T1930; T1912; T1607 and T1589) that were significantly increased ($P<0.05$) after metformin and insulin-stimulation in lean insulin-sensitive participants. In addition, (AKAP13; S1876, and S1858) showed a significant decrease ($P<0.05$) after metformin in obese insulin-resistant participants. PRKAB1 is a known AMPK substrate and a regulatory subunit; we detected one of the proteins whose phosphorylation and concentration are increased by metformin treatment. The phosphorylation of the PRKAB1 beta subunit at Ser108 is required to activation of the alpha cata-

lytic subunit; the upregulation of PRKAB1 in its active form may constitute a metformin-dependent mechanism that boosts the activity of AMPK[117]. The anti-type 2 diabetes metformin has been shown to inhibit mTOR activity[104]. We also confirmed that metformin inhibits the mTOR pathway by monitoring the reduced phosphorylation of p70S6kinase, another target of mTORC1/PP2A, and its downstream substrate ribosomal protein (rpS6) at Y234 in lean insulin-sensitive participants.

To gain extra insight into the molecular mechanism underlying the inactivation of the p70S6K-rpS6 axis by metformin treatment, we investigated the expression and activity levels of known p70S6K phosphatases. P70S6K/S6K1 is a vital negative feedback molecule in the insulin signaling pathway through phosphorylating IRS1. PHLPP (PH domain leucine-rich repeat phosphatase) is well known to dephosphorylate p70S6K[84] and was not upregulated in metformin-treated cells (T409). The results suggested that another phosphatase is more likely responsible for the inactivation of p70S6K-rpS6 in metformin-treated cells. PPP2R5C is the regulatory subunit gamma isoform of PP2A phosphatase has been previously shown to target p70S6K[118]. The results confirmed that (PPP2R5C; S497) were significantly increased ($P<0.05$) in lean insulin-sensitive participants after insulin-stimulation and metformin treatment. Hein et, al. reported that the interaction between PPP2R5C, PPP2R1A, and PPP2CB catalytic subunit of PP2A increased after metformin treatments[119]. Metformin treatment significantly increased ($P<0.05$) phosphorylation of S497 of PPP2R5C that triggers PP2A activity and dephosphorylation of p70S6K as revealed by our phosphoproteomic experimental approach. Moreover, Metformin treatment significantly increased ($P<0.05$) phosphorylation of S33 of PPP2R5E in lean insulin-sensitive participants and increased in obese insulin-resistant participants after metformin treatment. PPP2R5D, another

PP2A regulatory subunit, and importantly, (PPP2R5D; S89, S90, and S573) were increased after metformin treatment in lean insulin-sensitive participants, while S89 and S90 were significant increased ($P<0.05$), and S573 was significant decreased ($P<0.05$) after metformin treatment in obese insulin-resistant participants. Moreover, insulin-stimulation significantly increased ($P<0.05$) phosphorylation of S89, S88, and S90 of PPP2R5D in obese insulin-resistant participants and these phosphorylation sites (S89 and S90) were significant increased ($P<0.05$) after metformin treatments in the same group. The results demonstrated that insulin-stimulation significantly increased ($P<0.05$) phosphorylation of S497, S89, and S90 of PPP2R5C, PPP2R5D, PPP2R5D, respectively, in lean insulin-sensitive participants. Interestingly, we observed that (PPP2R5E; S32) were significantly decreased ($P<0.05$) in lean insulin-sensitive participants after insulin-stimulation and metformin treatment.

To show that metformin requires PP2A activity, the human skeletal muscle cells were incubated with or without 5 nM okadaic acid for 30 minutes before metformin treatment. In confirmation of our results, the phosphorylation of PPP2R3A (S181), PPP2R5C (S497), and PPP2R5D (S88, S89, S90, and S573) were significant increased ($P<0.05$) after okadaic acid treatment in lean insulin-sensitive participants and the phosphorylation for S88, S89, S90 were significant increased ($P<0.05$) in obese insulin-resistant participants after okadaic acid treatment. By contrast, the phosphorylation of S573 significantly decreased ($P<0.05$) after okadaic acid treatment and significantly increased ($P<0.05$) after metformin treatment in obese insulin-resistant participants. Metformin had been shown to activate AMPK; we assumed that metformin would activate PP2A via AMPK activation. The phosphorylation of Acetyl-CoA carboxylase 1(ACACA; S25, S62, S29 & S66) significantly decreased ($P<0.05$) after metformin treatment in obese insulin-resistant participants.

The glucagon released in response to starvation or fasting and acting through cyclic AMP (cAMP) and PKA (cAMP-dependent protein kinase), enhances hepatic glucose production by diminishing glycolysis and activating gluconeogenesis. Miller et al. reported that metformin rapidly decreased cAMP levels induced by glucagon in primary hepatocytes, and decreased phosphorylation of PKA substrates, including the 6-phosphofructo-2-kinase isoform PFKFB1[120]. Decreasing cAMP would inhibit the switch from glycolysis to gluconeogenesis triggered by glucagon. Although the metformin activated AMPK as reported in insulin-resistant mice, decreased cAMP, phosphorylation of PKA targets including PFKFB1, and blood glucose[120]. Metformin treatment significantly decreased ($P<0.05$) the phosphorylation of PFKFB2 at S466 in obese insulin-resistant participants. Activation of the cAMP-PKA pathway is negatively regulated AMPK activity by phosphorylating AMPKα subunit at S485, which leads to reduce net phosphorylation at Thr-172 and AMPK activity[121]. Metformin-activated AMPK decreased hepatic PPP1R3C expression, leading to the suppression of hepatic gluconeogenesis via blocking cAMP-stimulated TORC2 dephosphorylation[122]. We identified more than 77 cAMP and cAMP subunits in our phosphoproteome experiment. Among them, 11 phosphorylation sites of cAMP-regulated phosphoprotein 21 (ARPP21) were not reported in four large protein phosphorylation site databases and these phosphorylation sites are S303, S347, S293, S313, S349, S295, S315, S413, S359, S379, S348, S294, and S314. In addition, no research studies have been reported on these phosphorylation sites in human skeletal muscle. Metformin treatment significantly increased ($P<0.05$) the phosphorylation of PRKAR1A (S77), PRKAR2A (S78), PRKAR2A (S80), PRKACA (T202), PRKACA (Y205), and PRKAR1B (S77), and significantly decreased ($P<0.05$) the phosphorylation of PRKAR2A (S99), PRKACB

(S399), PRKAR1B (S3), PRKAR2B (S114), and PRKACA (Y331) in lean insulin-sensitive participants. Furthermore, PRKACA (T198) and PRKACA (Y205) were decreased after metformin treatment in obese insulin-resistant participants. Interestingly, PRKAB2 (S183), PRKAR2A (S99), PRKACB (S339), and PRKAA1 (S486) were significantly decreased, while PRKAB2 (T40), PRKACA (T198 and T202) were significant increased after insulin-stimulation in lean insulin-sensitive participants. Insulin-stimulation in obese insulin-resistant participants resulted in an insignificant increase in phosphorylation of PRKAB1 (S24 and S108).

Recent reports indicated that metformin diminished the cell cycle progression in G0/G1 and G2/M phases via unknown mechanism[123]. We found that the cyclin-dependent kinase (CDK1; CDK2; CDK3) is inactivated after metformin treatments; this kinase is known to control the cell cycle in the G2/M[84]. We observed the phosphorylation of (CDK16; S138) was significantly increased ($P<0.05$) in lean insulin-sensitive participants upon insulin-stimulation and metformin treatment, while the phosphorylation of (CDK16; S138) was significantly decreased ($P<0.05$) after metformin in obese insulin-resistant participants. Moreover, we quantified proteins that are known to promote cell cycle progressions, such as MAX (S2, S11), MCM2 (S139, S27, S40, and S41), MCM3 (S672 and T674), and RAD9A (S375 and S387). Metformin treatment significantly increased ($P<0.05$) the phosphorylation of MAX (S2) and MCM3 (S672 and T674) in obese insulin-resistant participants. Metformin reduced the activity of mitogen-activated protein kinase (ERK1). In contrast, we found metformin increased mRNA and protein concentrations of mitogen-activated protein kinase (MAP3K7 & MAP3K3), the upstream kinases of JNK and p38, respectively[124]. In our phosphoproteomic experimental conditions, MAP3K7 and MAP3K3 results enhanced the phos-

phorylation of p38 and the JNK substrate (JunD). These observations suggested metformin might increase a pro-apoptotic state by leading to activation of p38 and JNK signaling and inhibition of ERK1/2.

Hyperinsulinemia has been shown to develop insulin resistance in cell culture models. Insulin-stimulated tyrosine phosphorylation of insulin receptor (IR) and insulin receptor substrate-1 (IRS-1), activation of phosphatidylinositol 3-kinase (PI 3-kinase), and glucose uptake is impaired by chronic treatment with insulin[125]. To determine if metformin could directly decrease insulin-resistant skeletal muscle and enhance the insulin-signaling pathway, we treated the human skeletal muscle cells with metformin (50μm) for 24 hours and/or insulin (100 nM) for 15 minutes. Moreover, we also examined the effect of metformin on tyrosine phosphorylation of IR and IRS-1 and all three mitogen-activated protein kinases (MAP kinases) in human skeletal muscle cells. From our phosphoproteome experimental analysis, a total of 35 phosphorylation sites of IRS1 and IRS2 were modulated after insulin-stimulation and metformin treatment. Insulin receptor substrate 1 (IRS1) at S636 and S270 were significantly increased ($P<0.05$) after insulin-stimulation, and metformin treatment in lean insulin-sensitive participants and were unchanged in obese insulin-resistant participants. Metformin decreased insulin levels and decreased IGF-1 signaling[57]. Similarly, we observed that Insulin-like growth factor 2 mRNA-binding protein 2 (IGF2BP2) at S161 and S162 were significantly decreased ($P<0.05$) in lean insulin-sensitive participants after insulin-stimulation and metformin treatment.

Akt (protein kinase B (PKB)) has three isoforms Akt1, Akt2, and Akt3. Their domain structures are similar, and they share many substrates. Akt2 is specific for the insulin signaling pathway. Thomas et al. reported that Akt1 deficient mice did not ex-

hibit diabetes phenotypes while Akt2 deficient mice had insulin resistance, loss of pancreatic cells, and hyperglycemia[126]. Recent studies indicated that the PI3K/PKB signaling pathway is involved with insulin resistance and plays an essential role in insulin stimulation of glucose transport into cells[127]. PIP3 binds to PDK1 and Akt protein and recruited Akt protein to the plasma membrane. PDK1 phosphorylated Akt at Thr308/309 of Akt1/Akt2, respectively. The second PI3K phosphorylation of Akt at S473/474 of Akt1/Akt2 is associated with full Akt activation[126]. The phosphorylated Akt2 recruited insulin-regulated GLUT1 and GLUT4 from the cytoplasm onto the cell membrane surface, thus increasing glucose uptake[128]. Any defect in the Akt pathway with the downstream molecules could result in insulin resistance[129]. Inhibition of PP2A can induce the activation of Akt. It has been reported that metformin diminished insulin resistance by restoring PI3K/Akt/GLUT4 signaling. We identified 33 phosphorylation sites of Akt and Akt substrates that were modulated after treatments. Proline-rich AKT1 substrate 1 (AKT1S1) at S267, S223, and S231 were significantly increased ($P<0.05$) after metformin and insulin-stimulation in lean insulin-sensitive participants. In addition, AKT1S1 (S267) and AKTIP (S16) were significant increased upon insulin-stimulation, while AKT1S1 (S267) and (S222) were significantly increased ($P<0.05$) after metformin in obese insulin-resistant participants. The analysis of the mTOR upstream regulatory events confirmed that metformin treatment turns off the PI3K-mTOR pathway, we found that insulin-stimulation and metformin treatment significantly increased ($P<0.05$) AKT kinase (S476), and hyperphosphorylation of its substrates such as PFKFB2 (S493), ZFP36L (S54), BRAF (S151), and PDCD4 (S94) in lean insulin-sensitive participants. In contrast, Metformin treatment and insulin-stimulation significantly decreased ($P<0.05$) of NDRG2 (S332 &S338), DNMT1 (S154), DNMT3A

(S105), ZFP36L1 (S92), PDCD4 (S76), and PDCD4 (S457) in lean insulin-sensitive participants.

PP2A is an essential player in several cellular functions and consists of three subunits: catalytic (PP2Ac), scaffold (PP2AA), and regulatory subunits (PP2AB). The catalytic subunit of PP2A is represented by two genes in humans (PP2Acα and PP2Acβ) and shares 97% identity at the protein level[28]. The scaffold subunit of PP2A is encoded by two distinct genes (PPP2R1A and PPP2R1B). The PP2A regulatory subunit consists of four families of B subunits (B, B‘, B", and B′; the B′ members are known as striatins) that exist in human cells and are coded for by at least 15 genes[130]. Hahn et al. reported the level of S6K phosphorylation elevated in PP2A-B′ (regulation submit of PP2A) knockout flies, and they also reported S6K and PP2A-B′ interact physically, which suggests that PP2A-B′ might act directly on S6K[118]. The dysfunction of PP2A leads to several diseases, including diabetes, tumors, immune-related disorders, and Alzheimer’s disease. We quantified several of the PP2A regulatory subunits; STRN (S245& S233), STRN3 (S257 & S229), STRN4 (S53, S276, S157 & T377), PPP2R5E (T7, S32, S34, & S33), PPP2R3A (S181, S687, S686, S179, S65, S66 & S180), PPP2R5D (S90, S89, S573, S60, S62, S88, S541, S467 & T63), PPP2R5C (S497, S513, S528, & S458) and PPP2R5A (S42). These regulatory subunits are expressed in the cytoplasm, nucleus, centrosome, and Golgi complex. Furthermore, several families of the B subunits are believed to be associated in the stabilization of holoenzyme via binding with the A or C subunit, involved in the regulation of the A or C subunit for its further activities, involved in modulations of substrate selectivity, and catalytic activity and associated in cell growth and apoptosis [28,131]. No studies on their role in human skeletal muscle cells have been reported for all phosphorylation sites after metformin treatment. Metformin treatment and insulin-stimulation significantly increased

($P<0.05$) phosphorylation of S257 of STRN3 in lean insulin-sensitive participants and increased in obese insulin-resistant participants after metformin treatment and insulin stimulation. In addition, we observed significant decreased ($P<0.05$) phosphorylation of T377 of STRN4 in lean insulin-sensitive participants and decreased in obese insulin-resistant participants after metformin treatment and insulin-stimulation. Insulin-stimulation significantly decreased ($P<0.05$) phosphorylation of S229 of STRN3 in obese insulin-resistant participants. Significant changes ($P<0.05$) in PP2A were observed with metformin treatments in our phosphoproteome experiment has been shown in Figure 43.

Doublecortin-like kinase 1 (DCLK1) is a serine-threonine kinase of the calmodulin kinase (CAMK) family. DCLK1 has been identified as a tuft cell marker in the small intestine and reported to mark tumor stem cells in the pancreas and intestine[132.] Most of the research on DCLK1 within humans has been done on nervous tissue, which is primarily thought to be involved in cell differentiation and neurogenesis. Berggard, T. et al. reported that DCLK1 interacted with calmodulin 1 (CALM1), tyrosine 3-monooxygenase/tryptophan 5-monooxygenase activation protein (YWHAE), and doublecortin (DCX) in mouse brain[133,134]. We quantified more than 32 phosphorylation sites in human skeletal muscles that were associated with DCLK1, such as S36, S307, S358, S294, S313, S413, S332, S330, S334, S337, S25, S355, S310, S164, S172, T336, T168, T311, T354, T317, T296, and T34. DCLK2 was quantified in our phosphoproteome experiment, and more than 16 phosphorylation sites such as S688, S687, S705, S6, S362, S379, S308, S317, S308, S341, T683, T682, T700, T692, T693, and T710. Moreover, the role of DCLK1 in skeletal muscle and/or insulin signaling is not determined and needed more investigations. Phosphorylation of DCLK1 S330, S334, T336, and S337 has been identified in multiple cell types including embryonic stem cells [135-137] or

in brain tissue. Notably, DCLK1 along with multiple phosphorylation sites observed here have been detected in mouse cardiac muscle[138]. The phosphorylation of S330, S334, and S337 was reported in 3T3-L1 adipocytes upon insulin-stimulation[139]. The results demonstrated that all phosphorylation sites of DCLK1 in this aim fall between the 2nd doublecortin domain and the protein kinase domain, which suggested that the phosphorylation might regulate the binding of DCX and/or kinase activity/specificity. In addition, 14 phosphorylation sites (S1779, S720, S294, S310, S688, S705, S6, S362, S379, S308, S317, T317, T311, and T296) of DCLK were significant changes after metformin treatment in lean insulin-sensitive participants, while two phosphorylation sites (S298 and S308) of DCLK were significant changes after metformin in obese insulin-resistant participants.

Serine/threonine protein phosphatase 1 regulatory subunit 12A (PPP1R12A) modify the activity and specificity of the catalytic subunit of protein phosphatase 1 and regulating various cellular processes via dephosphorylation[140]. It has never been studied before in human skeletal muscle tissue or cells, and little is known about phosphorylation profiles controlled by PPP1R12A in skeletal muscle insulin signaling. Our lab found that PPP1R12A and the catalytic subunit of PP1 (PP1cδ) were identified as interaction partners of IRS-1 and this interaction may dephosphorylate IRS-1 to maintain proper insulin action in L6 cells[140]. Insulin-stimulation and metformin treatment significant increased ($P<0.05$) the phosphorylation of PPP1R12A (S299, S445, S871, and T453), PPP1R12B (S447 and S452), PPP1R12C (S452 and S451), PPP1R7 (S24 and S27), and PPP1R18 (S368) in lean insulin-sensitive participants. We observed that the phosphorylation of PPP1R12B (S375 and S452), PPP1R3D (S46, S74, and S78), PPP1R2 (S121, S122 and S127), and PPP1R7 (S24 and S27) were significant increased

after metformin treatment in obese insulin-resistant participants, and insulin-stimulation significant increased ($P<0.05$) the phosphorylation of PPP1R12A (S527), PPP1R12B (S735) and PPP1R2 (S121, S122, and S127) in obese insulin-resistant participants. Furthermore, we found PPP1R37 (S591 and S597), PPP1R18 (S125), PPP1R9B (S100), PPP1R3D (S74), and PPP1R12B (T646) were significantly decreased ($P<0.05$) upon insulin-stimulation and metformin treatment in lean insulin-sensitive participants. We also reported the phosphorylation of PPP1R12B (S452), PPP1R12 (T453 and T696), and PPP1R10 (T315) were significantly decreased after metformin treatment in obese insulin-resistant participants. Interestingly, some research has been reported on PPP1R2 (S121) phosphorylation using hepatic cell lines, cancer, renal cell lines, spermatozoa, lymphocytes, and leukemia cell lines, but not human skeletal muscle tissue or cells. Previous in *vitro* studies suggested that its inhibitory activity towards PP1 is regulated by phosphorylation at Thr72 by glycogen synthase kinase-3beta (GSK-3beta), and at S86, S120, and S121 by casein kinase 2 (CK2)[141]. In our experiment, PPP1R2 (S121, S122, and S127) phosphorylation has shown a significant increase ($P<0.05$) upon insulin-stimulation and metformin in obese insulin-resistant participants.

Glycogen synthase kinase-3 (GSK3) exists in GSK3α and GSK3β, which are an intermediate protein of the insulin signaling pathway and direct downstream protein AKT. Another remarkable characteristic of GSK3 is involved in many prevalent disorders, including inflammatory diseases, psychiatric neurological diseases, and cancer. The phosphorylated GSK3 can activate GS. Serine/threonine kinase (Akt/PKB) activation can phosphorylate the enzyme GSK-3 (S9 in GSK3β and S21 in GSK3α) in an N-terminal serine residue and then regulate the insulin pathway[114]. In our present study, we found five sites of GSK3α (S278, S282, S21, S39, and Y279) and eight sites of

GSK3β (S215, S219, S39, S9, S13, S21, S25, T390, and Y216). The phosphorylation of GSK3α (S21) and GSK3β (S9) had a statistically significant increase ($P<0.05$) after insulin-stimulation and metformin treatment in lean insulin-sensitive participants. In contrast, the phosphorylation of GSK3α (Y279) and GSK3β (Y216) had a statistically significant decreased ($P<0.05$) after insulin-stimulation and metformin treatment in lean insulin-sensitive participants. PP2A and GSK3β can regulate each other. Tianfeng et al. reported that PP2A could decrease phosphorylation of GSK3β (S9) and promote the kinase activity, while the upregulation of GSK3β can increase the activity of PP2Ac[142]. Y216 phosphorylation activates GSK3β and results from an autocatalytic activity or pyk2 action. In contrast, phosphorylation S9 inhibits GSK3β and results from the activity of PKB, PKA, and S6K through auto-inhibition[138].

Recent clinical and preclinical studies have confirmed that metformin improves chronic inflammation through the improvement of metabolic parameters such as insulin resistance, hyperglycemia, atherogenic dyslipidemia, and has a direct anti-inflammatory action. Several studies have suggested that metformin diminishes inflammatory response by inhibition of nuclear factor κB (NFκB) through AMP-activated protein kinase (AMPK) - independent and dependent pathways. Nuclear factor-κB (NF-κB) signaling is significantly recognized as a contributing factor to CVD and diabetes mellitus (DM)[143]. In the present study, we compared metformin with the specific IKKβ inhibitor and NF-κB. We observed that the phosphorylation of NF-κB (S937, S941, and S907) was decreased after metformin treatment in lean insulin-sensitive and obese insulin-resistant participants. Metformin significantly decreased ($P<0.05$) the phosphorylation of Inhibitor of nuclear factor kappa-B kinase subunit beta (IKBKB; S672) in lean insulin-sensitive participants. In addition, in an inactive state, STAT's exist as cytosolic proteins in an unphosphorylated state. Induced tyrosine phosphorylation of STATs by

stimulation cytokine or growth factors and leads to translocation to the nucleus. It has been reported that all STAT's are regulated by serine phosphorylation (PP2A being a serine/threonine phosphatase) and showed that phosphorylated STAT3 amounts are increased by two-fold in overweight T2D compared to overweight controls and is also shown to contribute to insulin resistance in various tissues like smooth muscle and liver [144]. This serine phosphorylation is facilitated by several serine/threonine kinases including JNK, ERK, p38, mTOR, IKKε, CaMKII, and PKCδ[145]. The phosphorylation of signal transducer and activator of transcription 3 (STAT3; S727) was significantly decreased ($P<0.05$) in obese insulin-resistant participants after metformin treatment.

Jablonski et al reported 23 candidate genes with variants showing a nominally significant interaction with the metformin intervention in the Diabetes Prevention Program (DPP), including HNF1B, ABCC8, HNF4A, MEF2A, SLC47A1, MEF2D, CAPN10, ADIPOR2, KCNJ11, SLC22A2, GCK, STK11, ITLN2, PCK1, PKLR, SLC22A1, GCG, PPARA, PRKAB2, PPARGC1A, PPARGC1B, PRKAA2, PRKAG2, and PRKAA1[146]. We detected phosphorylation sites in eight of these genes in our phosphoproteome experiment (i.e., MEF2A, MEF2D, PCK1, PKLR, PRKAA1, PRKAA2, PRKAB2, and STK11). Among them, S444 of Myocyte-specific enhancer factor 2D (MEF2D) and S31 of Serine/threonine-protein kinase STK11 (STK11) were significantly increased upon the treatment of metformin in OIR while did not change in Lean. This result suggests that some of these genetically identified genes may be involved in response to metformin treatment via functional interactions with metformin in the muscle tissue.

4.3 SPECIFIC AIM 3: DETERMINE THE EFFECT OF METFORMIN ON PROTEIN-PROTEIN INTERACTIONS OF PP2AC IN HUMAN SKELETAL MUSCLE CELLS DERIVED FROM LEAN INSULIN-SENSITIVE AND OBESE INSULIN-RESISTANT PARTICIPANTS

From our quantitative proteomics approach for protein-protein interaction that developed in our laboratory using high-performance liquid chromatography-electrospray ionization (ESI) high-resolution tandem mass spectrometry (UPLC-ESI-MS/MS) followed by proteomics analysis of the interacting proteins, we have quantified 1,290 PP2Ac interaction partners in human skeletal muscle cells from 8 lean insulin-sensitive and 8 obese insulin-resistant participants. Among them, 1,281 were known PP2Ac interaction partners and 9 were not reported before, thus appeared to be novel. We identified proteins that potentially interact with PP2Ac and several proteins previously known to interact with PP2Ac such as CaMK II and GSK3. Many of the newly identified PP2Ac-binding proteins were associated with growth control. Furthermore, characterization of the PP2A-interacting proteins might provide essential clues to understand the crosstalk and complicated signaling network between the signaling pathways related to the control of cell growth.

4.3.1 PP2Ac INTERACTION PARTNERS WITH PROTEINS INVOLVED IN INSULIN RECEPTOR

The effects of insulin are activated by binding to the insulin receptor (IR) that is located in the cell membrane. The receptor molecule includes an α- and β subunits, insulin binds to the α-subunits and the β subunits have tyrosine kinase enzyme activity which is triggered by the insulin binding. The phosphorylation of the IRS activates a signal transduction cascade and leads to the activation of other kinases and transcription

factors. The pathways activated are phosphatidylinositol 3-kinase (PI3K, a lipid kinase)/AKT (also known as protein kinase B or PKB) pathway and the Raf/Ras/MEK/MAPK (mitogen-activated protein kinase, also known as an extracellular signal-regulated kinase or ERK) pathway[11]. Activated PKB, resulting in enhance in GLUT4 transporters in the plasma membrane, glucose uptake, protein synthesis, and glycogen synthesis[5]. In the present study, we quantified 15 proteins are associated with insulin signaling pathways as PP2A interaction partners such as AKT2, MAP2K1/MEK1, eukaryotic translation initiation factor 2B subunit alpha (EIF2B1), protein tyrosine phosphatase non-receptor type 11, protein phosphatase 1 regulatory subunit 7, AMPK subunit gamma isoform (PRKAG1), and Ras. The G-proteins such as Rac1, Rho A, Rab5c were discovered in our experiment, and plays an essential role in glucose-stimulated insulin secretion, and also plays a pivotal role in traffic insulin stored vesicles to the cytoskeletal remodeling and cell membrane to allow fusion of these secretory granules with the plasma membrane for insulin secretion [147,148]. These findings suggest a close interaction between the PP2Ac and these signaling proteins. Furthermore, PP2A negatively regulate Akt2 in fibroblast cells[149] and might play an important role in terms of its interaction with Akt2 in lean health participants, while this interaction might be disrupted in cases of obese insulin-resistant and T2D participants. PP2A hyperactivation is linked with insulin resistance in response to saturated fatty acids like ceramide, shown with an associated Akt deactivation[150]. Moreover, several studies on liver hepatocytes in *vitro* and in *vivo* showed that PP2A activity is important for insulin-stimulated glycogen storage[151]. Our results confirmed that the interaction is significantly decreased in obese insulin-resistant non-diabetic control and insulin-stimulated when compared to lean insulin-sensitive and insulin-stimulated, respectively.

Several studies reported that PP2A is downregulated by mTOR, and degradation of IRS1 by mTOR is achieved by inhibiting PP2A[104]. mTOR pathway has an important impact on the metabolism, cell growth, proliferation, and regulated lipid synthesis, mitochondrial biogenesis, and protein biosynthesis. Laplante et, al. reported that growth factors like insulin-stimulated mTOR by enhanced phosphorylation of TSC2 protein by kinases like RSK1, PKB, and ERK1/2[152]. Activated AMPK carries the signal to the mTOR pathway. It phosphorylated mTOR inhibitor TSC2 and the mTOR interaction Raptor, which lead to a reduction of mTOR kinase activity and activation PP2A[81]. TSC 2 is a potential signaling molecule that functions downstream of the PI3K-Akt pathway and associates with several physiologies including proliferation. We found many PP2A interaction partners associated with the mTOR pathway including PRKAG1 (gamma 1) and PRKAB2 (beta 2) subunits of AMPK, small GTP proteins, Ribosomal protein S6 kinase alpha-1, transcription factors ELF3 and ELF4A, and ribosomal protein S15A that regulate protein synthesis.

PP2A can be regulated through dephosphorylating and phosphorylation on its Tyr307 site. Tyrosine-protein phosphatase non-receptor type 11 (PTPN11) has been shown to bind with several of intermediate signaling molecules such as IRS-1, p85 subunit of PI3 kinase, Grb2, and Gab1/2. We found the interaction between PTPN11 and PP2A significantly decreased in obese insulin-stimulated when compared to lean insulin-stimulated participants. Glycogen synthase kinase-3 (GSK3) exists in (GSK3α and GSK3β) and inhibits the activity of ELF2B by phosphorylating it under basal conditions. Elf2B is regulated through phosphorylation and (ELF2B1) is involved in protein synthesis. GSK3 is inactivated by Akt under insulin-stimulation, which leads to dephosphorylation and activation of ELF2B, thus increasing protein synthesis[153]. In the

present study, PP2A interacted with ELF2B, and interaction is decreased in obese insulin-resistant basal and insulin-stimulated compared to basal and insulin-stimulated in lean insulin-sensitive participants, respectively.

Insulin activates mitogen-activated protein kinases (MAPK) to increase gene expression, proliferation, cytoskeletal reorganization, and differentiation through the Grb2-SOS-Ras-MAPK pathway. Activation of insulin receptors and IRS proteins activates a signaling cascade that promotes activation of Ras-GDP to Ras-GTP and activates a series of downstream signaling molecules Raf/MEK/ERK1/2[15]. Boucher et al. reported that, ERK is associated with regulating cell proliferation, gene expression, differentiation, and cytoskeletal reorganization[11]. MAP2K1/MEK1 and Ras are identified as PP2A interaction partners. Nevertheless, these two molecules did not show any significant difference among groups. Furthermore, Protein phosphatase 1 (PP1) is reported to dephosphorylate, activate glycogen synthase, and enhancing glycogen synthesis. PP1 was activated in L6 rat skeletal muscle cells upon insulin-stimulation[154]. PP1 regulatory subunit (PPP1R12A, PPP1R12B, PPP1R21, and PPP1R12C) has shown to interact with PP2A and the interaction is decreased in the obese insulin-resistant and insulin-stimulated when compared to lean insulin-sensitive basal and insulin-stimulated.

cAMP-dependent protein kinase type I-alpha regulatory subunit (PRKAR1A), cAMP-dependent protein kinase type II-alpha regulatory subunit (PRKAR2A), cAMP-dependent protein kinase catalytic subunit beta (PRKACA), cAMP-dependent protein kinase catalytic subunit gamma (PRKACG), and cAMP-regulated phosphoprotein 21 (ARPP21) are involved in the hydrolysis of cAMP were seen as a PP2A partner interaction. In skeletal muscle, acute cAMP signaling has been implicated in the regulation of muscle contraction, glycogenolysis, and sarcoplasmic calcium dynamics[155].

4.3.2 PP2Ac KNOWN INTERACTION PARTNERS

AMPK is a protein kinase, exists of alpha, beta, and gamma subunits, and is activated in response to altered energy levels in the cell. AMPK isoforms identified in our study are PRKAA2 (alpha 2), PRKAA1 (alpha 1), PRKAG2 (gamma 2), PRKAB1 (beta 1), PRKAG1 (gamma 1), and PRKAB2 (beta 2). AMPK is known to have an essential role in skeletal muscle insulin sensitivity[156] and plays an important role in the activation of GLUT4 transporters[157]. PRKAB2 is found abundant in skeletal muscle cells whereas PRKAG1 is ubiquitously expressed[59]. Several studies reported that activation of AMPK is achieved by phosphorylation of AMPK at several serine and threonine sites. PP2A has been reported to dephosphorylate AMPK[31]. Both ADSL adenylosuccinate lyase and AMPK are found as PP2Ac interaction partners in our study, the interaction significantly increased in obese insulin-resistant participants after metformin treatment. The target of rapamycin (TOR) is a serine/threonine protein kinase that belongs to the phosphatidylinositol kinase-related kinase family and plays essential roles in cellular processes such as cell growth and proliferation. TIP41-like protein (TIPRL), negatively regulates TOR signaling[158]. Previous study reported the role of role of TIPRL in TOR signaling and the author observed that TIPRL facilitates TOR signaling via its association with PP2Ac in human cell lines[158]. In this study we reported that TIPRL as a PP2A partner in human skeletal muscle cells.

We observed many proteins involved in protein synthesis and degradation. Signal transducer and activator of transcription (STAT) proteins are transcription factors that regulate protein synthesis. Transcription factors STAT3, STAT1, STAT2, STAT6, and STAT5B were shown differences between lean insulin-sensitive and obese insulin-resistant participants and the interaction partners with PP2Ac increased in obese insu-

lin-resistant compared to lean insulin-sensitive participants. We also reported Calcium/calmodulin-dependent protein kinase type II (CAMK2B, CAMK2G, and CAMK2D) as a PP2A interaction partner. We observed both STAT1 proteins and CaMK2B showed a decreased interaction in lean insulin-sensitive participants and increased in obese insulin-resistant participants after metformin treatment. Furthermore, eukaryotic translation initiation factor 2B subunit alpha (EIF2B1), (EIF2B2; EIF2B3; EIF2B4; EIF2B5; and EIF2D), Glycine-tRNA ligase synthetase (GARS), and C-terminal-binding protein 1 (CTBP1) regulate protein synthesis at the transcription and translation level. All these proteins showed a decreased interaction in lean insulin-sensitive and increased in obese insulin-resistant participants after metformin treatment.

PP2Ac undergoes methylation at the carboxyl-terminal leucine (Leu-309) residue. Kowluru et al. reported that PP2A activity is increased under glucotoxicity conditions with a corresponding increase in C-terminal methylation of PP2Ac[159]. We identified protein methyl esterase-1 as a PP2A interaction partner in the present study. Leucine carboxyl methyltransferase (LCMT-1) is involved in transferring methyl onto leucine -309 of PP2Ac. The siRNA-mediated knockdown of LCMT-1 significantly decreased the carboxylmethylation of PP2Ac and the hyperactivation of PP2A under high glucose/glucotoxicity conditions, and the carboxylmethylation leads to sustained activation of PP2A[160,161]. We detect specific interaction of protein phosphatase methylesterase 1(PPME1), which catalyzes the demethylation of PP2A on leucine309. Moreover, PPME-1 is reported to protect PP2A from degradation[35].

Caveolin-1 (CAV1) is a scaffolding protein reported in most cell types as a main component of the caveolae plasma membranes. CAV1 plays a significant role in differentiation and cell proliferation. It has been reported that (CAV1) has antiapoptotic activities in prostate cancer cells and functions downstream of androgenic stimulation.

The interaction between CAV1 and PP2A is reported in human prostate cancer cells where CAV1 acts as a positive regulator in the Akt signaling pathway through inhibition of PP1 and PP2A[162]. Previously, it has been reported interaction of CAV1 with IRS1 in human skeletal muscle biopsies[37]. Likun Li et al. found CAV1 interacts with and diminishes serine/threonine protein phosphatases PP1 and PP2A via scaffolding domain binding site interactions, which leads to increased Akt, PDK1, and ERK1/2 activities[162]. Furthermore, the author demonstrates that CAV1 stimulated Akt activities to lead to enhanced phosphorylation of multiple Akt substrates, including GSK3, FKHR, and MDM2[162].

ATP synthase subunits, mitochondrial (ATP5L; ATP5F1; ATP5D; ATP5O; and ATP5I) are one of the subunits of the catalytic core of the ATP synthase enzyme and also known as ATP synthase-coupling factor B. This enzyme catalyzes the formation of ATP from ADP in the mitochondria[163]. The previous study was conducted on human skeletal muscle comparing the phosphorylation of this protein between basal and insulin-stimulated biopsies of lean, obese, and T2D. The result of ATP synthase in basal biopsies is found to be decreased in obese and T2D compared to lean[164]. In our experiment, we observed a decreased interaction of PP2Ac in lean insulin-sensitive after metformin treatment from all these proteins.

Small G-protein Rac1 is known to play important role in actin cytoskeleton remodeling, and insulin-stimulated GLUT4 translocation in L6 myotubes[165,166] and involved in the insulin signaling pathway. Moreover, experiments on human muscle and rats demonstrated the activation of Rac1 after exercise and its role in contraction-induced glucose uptake[167]. PP2A is reported to bind to the c-terminus of Rac1 in cell culture models[168].

Immunoglobulin-binding protein (Igbp1) was identified in our experiment as an important interaction partner of PP2A. Igbp1 is known as α4, is a non-canonical adaptor subunit of PP2A[169] and shown to interact with other phosphatases like PP4 and PP6[170]. PP2Ac has been shown to interact with α4 that regulates its abundance, localization, activity, and α4 is known to associate in PP2A biogenesis, activation, and stability[169,170]. McConnell, J. L. et al. reported that the PP2AC-α4 complex protected the catalytic subunit from proteasomal degradation[171]. We identified Igbp1 as an interacting partner of PP2Ac and the interaction decreased after metformin treatment in obese insulin-resistant participants.

Serine/threonine-protein kinase (LIMK1) plays an essential role in the regulation of dynamics of actin filament at the cell membrane and has been shown to regulate a few actin-dependent biological processes including cell motility, cell cycle progression, and cell differentiation[172]. Phosphorylation and activation of LIMK1 lead to activation of kinases like ROCK1, PAK1, and PAK4, which then phosphorylates and inactivates the actin-binding/depolymerizing factors[173,174]. This inactivation of the depolymerizing factors results in the prevention of the breakdown of F-actin and thereby actin cytoskeleton stabilization. This finding has significance considering that a glucose-responsive PP2Ac partner is associated with vesicle trafficking, actin cytoskeletal remodeling, and essential for glucose-stimulated insulin secretion.

Coiled-coil domain-containing protein 6 is a protein that in humans is encoded by the CCDC6 gene. Diseases associated with CCDC6 include differentiated thyroid carcinoma, papillary carcinoma, endometrial cancer, and retinoblastoma (RB) in Cancer[175]. CCDC6 plays an essential role in the maintenance of genomic stability, cell survival, and cell cycle control, extends a rationale of how disturbance of CCDC6 normal

function contributes to malignancy, and translates to a protein that is ubiquitously expressed, and its gene rearrangements are seen in many malignancies[176]. The interaction of CCDC6 with PP2Ac is seen in our experiments as an attempt to understand phosphatase interactions using human skeletal muscle cells.

Individual proteins in the cytosol, nucleus, endoplasmic reticulum (ER), and mitochondria are degraded at exceedingly differing rates that vary from minutes for some regulatory enzymes to days or weeks for proteins such as myosin and actin in skeletal muscle or months for hemoglobin in the red cell. Three enzymatic complexes are required to link chains of ubiquitin onto proteins that are destined for degradation. E1 (Ub-activating enzyme) and E2s (Ub-carrier or conjugating proteins) prepare Ub for conjugation, but the key enzyme in the process is the E3 (Ub-protein ligase)[177]. PP2A is well known to interact with molecules associated with these processes. In this study, we identified proteins like CCCT2, CCT61, CUL-1, PSMC6, PSMD1, and USP7. CCT2 and CCT6A are chaperone proteins. Ubiquitination is an important PTM that leads to protein degradation through the proteasome complex. We quantified several proteins that are involved in the ubiquitin-proteasome pathway through regulation of a E3ubiquitin-protein ligase complex family including, COP9 signalosome complex subunit 2 (COPS2), COP9 signalosome complex subunit 6 (COPS6), COP9 signalosome complex subunit 5 (COPS5), and COP9 signalosome complex subunit 7A (COP7A) and the interaction of these proteins with PP2Ac increased after metformin treatment in obese insulin-resistant participants. Furthermore, the interaction of all these proteins with PP2Ac decreased after metformin treatment in lean insulin-sensitive participants.

Ras homolog enriched in the brain (Rheb) is one of the Rho family of GTPases that regulates proliferation, motility, transcription, focal adhesion formation, transfor-

mation, and invasion. Rheb targets TSC2 molecule, and TSC2 stimulates GTP hydrolysis of Rheb and inhibits Rheb activity as a GTPase activating proteins[178]. Moreover, R-Ras is a small GTPase of the Ras family that regulates integrin activity and cell survival, and one of the potential PP2Ac interaction partners. It was reported that R-Ras interacts with several effecter proteins including the p110 subunit of PI3 kinase, RalGDS, and c-Raf[179].

Acyl-CoA thioesterase 9 (ACOT9) is a mitochondrial ACOT protein with homologous genes found from bacteria to humans, which catalyzes the hydrolysis of acyl-CoAs to form coenzyme A and free fatty acid. It is reported that mitochondrial dysfunction and free fatty acid induce skeletal muscle insulin resistance[180]. It has been reported that, ACOT9 activity is strongly regulated by CoA and NADH, suggesting that mitochondrial metabolic state regulates the function of ACOT9[181]. The main pathway for oxidation of fatty acids is the mitochondrial fatty acid oxidation (β-oxidation), producing the majority of ATP required for the cells where Coenzyme A (CoA) is an important co-factor[181]. Among ACOT9, glycyl-tRNA synthetase (GARS), hydroxysteroid 17-beta dehydrogenase 8 (HSD17B8), and superoxide dismutase 1, soluble (SOD1) are interacting with PP2AC. We observed that the interaction of PP2Ac with ACOT9, ACOT11, and ACO13 are decreased upon insulin-stimulation and metformin treatment in lean insulin-sensitive participants and this interaction increased in obese insulin-resistant participants.

We identified and quantified many proteins that are involved with post-translational modification (PTMs). These modifications include phosphorylation, ubiquitination, and methylation. Therefore, identifying and understanding PTMs are important in the study of cell biology and disease treatment. Sumoylation is another post-translational modification that regulates protein structure and intracellular localization through

the addition of small protein SUMO. We found SUMO-activating enzyme subunit 2 (UBA2) and SUMO-conjugating enzyme UBC9 in our study. UBA2 interaction increased by (2.3 and 1.6 fold changes) in obese insulin-resistant after metformin treatment and insulin stimulation, respectively. This protein forms a heterodimer with another protein SME-1 that acts as a SUMO-activating enzyme[182]. In contrast, metformin and insulin-stimulation decreased the interaction of PPP2Ac with UBA2 (0.38 and 0.26 fold changes, respectively) in lean insulin-sensitive non-diabetic participants. We observed protein involved in protein modification is cytosol aminopeptidase (LAP3), which catalyzes the hydrolysis of leucine residues from the amino-terminus of protein. The interaction with PP2A is decreased significantly in obese insulin-resistant participants and increased significantly in lean insulin-sensitive participants in response to metformin treatment.

Sterile alpha motif domain-containing 9 (SAM 9) and Deoxynucleoside triphosphate triphosphohydrolase (SAMHD1), SAMD4B, SAMD4A, and SAMM50 are playing an essential role in the regulation of the innate immune response, upregulated in response to viral infection and may be associated in the mediation of tumor necrosis factor-alpha proinflammatory responses. All these proteins interacts with PP2Ac were decreased in lean insulin-sensitive participants after metformin and increased in obese insulin-resistant participants. The role of this interaction or these proteins in skeletal muscle and insulin resistance is unknown and need more investigation.

Mapping the protein interactome has been a long goal of modern biology, we generated a high-density interaction map surrounding the PP2A catalytic subunit using quantitative proteomics. This approach revealed several protein-protein interactions including PPP2R1A, PPP2R1B, PPP2R2A, PPP2R3A, PPP2R5C, PPP2R5D, PPP2R5B, PPP2R4, PPP2R5E, PPP2R2D, PPP2R3B, STRN, STRN3, and STRN4. It

has also been reported to bind to the catalytic subunit of protein phosphatase 4 (PPP4C)[175]. We quantified protein phosphatase 2A regulatory subunit 4 (PPP2R4) with (2.4 fold increase) in the interaction between PP2Ac and its regulatory subunit (PR53). In addition to PP2A family trimers, several of additional proteins were quantified in our quantitative proteomics experiment as potentially interacting with PP2Ac. For example, the interactions of several candidate proteins, such as STRIP1, IGBP1, TCP1, tuberous sclerosis complex 2, RhoB, R-Ras, ACOT9, LRSAM1, CCT2, FOXO1, PKN2, NEDD1, APP, SLC2A1, CDKN1 and PPME1 with PP2Ac were confirmed by our co-immunoprecipitation experiments.

4.3.3 INTERACTION PARTNERS WITH SIGNIFICANT CHANGES IN THEIR INTERACTION TO PP2AC IN LEAN INSULIN-SENSITIVE AND OBESE INSULIN-RESISTANT PARTICIPANTS IN HUMAN SKELETAL MUSCLE CELLS.

4.3.3.1 PARTNERS WITH SIGNIFICANT CHANGE UPON INSULIN-STIMULATION AND METFORMIN TREATMENT.

In a total, 680 PP2Ac interaction partners were quantified in lean insulin-sensitive non-diabetic participants and met our criteria for PP2Ac interaction partners upon insulin-stimulation and 419 proteins has shown changes . Triple functional domain protein (TRIO) von Willebrand factor A domain-containing protein 5A (VWA5A) and calmodulin 3(CALM3) were significantly decreased ($P<0.05$; fold change < 0.666) and serine/threonine-protein phosphatase 2A 56 kDa regulatory subunit epsilon isoform (PPP2R5E), serine/threonine-protein kinase 3 (STK3), SH3 and PX domain-containing protein 2B (SH3PXD2B), 3-ketoacyl-CoA thiolase, mitochondrial (ACAA2), and myomesin-3 (MYOM3) were significantly increased ($P<0.05$; fold change > 1.5) after insulin-stimulation lean insulin-sensitive non-diabetic participants. Furthermore, 430

PP2Ac interaction partners met our criteria in obese insulin-resistant non-diabetic participants and 213 proteins has shown changes. We observed 32 proteins such as Rab GDP dissociation inhibitor beta (GDI2) and Ras-related protein Rab-14 (RAB14) were significantly decreased ($P<0.05$; fold change < 0.666) and AP-2 complex subunit alpha-2 (AP2A2), Zyxin (ZYX), Forkhead box protein O1 (FOXO1), TBC1 domain family member 15 (TBC1D15), activating signal cointegrator 1 complex subunit 2(ASCC2), and Histone deacetylase 7 (HDAC7) were significantly increased ($P<0.05$; fold change >1.5) after insulin stimulation.

We identified many proteins potentially interacting with PP2Ac after metformin treatment. 675 PP2Ac interaction partners were quantified in lean insulin-sensitive non-diabetic participants and met our criteria for PP2Ac interaction partners and 369 proteins have shown changes after metformin treatments. Interestingly, RNA 3-terminal phosphate cyclase (RTCA), PDZ domain-containing protein GIPC1 (GIPC1), kinesin-1 heavy chain (KIF5B), 60S ribosomal protein L31 (RPL31), kolyadenylate-binding protein 4 (PABPC4), dynactin subunit 2 (DCTN2), ARF GTPase-activating protein GIT2 (GIT2), Caprin-1, phosphatidate phosphatase LPIN1 (LPIN1), tyrosine-protein phosphatase non-receptor type 21 (PTPN21), vacuolar protein sorting-associated protein 53 homolog (VPS53), protein PBDC1 (PBDC1), alpha-parvin (PARVA), and ARF GTPase-activating protein GIT1 (GIT1) were significantly decreased ($P<0.05$; fold changes < 0.667) after metformin in lean insulin-sensitive participants. Moreover, protein S100-A9 (S100A9), protein S100-A4 (S100A4), cyclin-dependent kinase inhibitor 1 (CDKN1A), coiled-coil domain-containing protein 93 (CCDC93), serine/threonine-protein phosphatase 2A 56 kDa regulatory subunit epsilon isoform (PPP2R5E) were significantly increased ($P<0.05$; Fold changes >1.5) in lean insulin-sensitive partici-

pants after metformin as reported in Table 23. Interestingly, we observed several proteins are interacting with PP2Ac increased significantly (P<0.05) after metformin treatment, and these proteins were not quantified in basal/ control condition, such as SLC9A3, TPP1, ANKRD28, GGCT, CAT, APP, ASNS, COX5B, SLC2A1, COX5A, SCP2, TGM1, SERPINB3, TIA1, CDKN1A, KPNA1, PRAD, PPFIA1, CCDC93, ANKRD44, ACOTT11, RPRD1A, SEMA3C, TMEM165, LANCL2, LIN7C, CNPY2, and PPP2R5E.

In addition, 410 PP2Ac interaction partners met our criteria in obese insulin-resistant non-diabetic participants and 216 proteins have shown changes after metformin treatments. Protein pelota homolog (PELO) and DnaJ homolog subfamily B member 11 (DNAJB11) were significantly increased (P<0.05; fold change >1.5), while nucleoside diphosphate kinase B (NME2), peroxiredoxin-5 and mitochondrial (PRDX5) were significantly decreased (P<0.05; fold change <0.667) after metformin treatment. Furthermore, V-type proton ATPase catalytic subunit A (ATP6V1A), Trafficking protein particle complex subunit 3(TRAPPC3), and Vacuolar protein sorting-associated protein VTA1 homolog (VTA1) were diminished after metformin treatment. Interestingly, we observed several proteins are interacting with PP2Ac increased significantly (P<0.05) after metformin treatment, and these proteins were not quantified in basal/ control condition, such as IKBKB, SRC, DSCR3, COL6A2, APEH, CD81, CAMSAP1, CSNK2A, ZNRF2, TBC1D15, PLEKHO2, and MVB12A.

PP2A regulatory subunit is the only PP2A subunit that showed significant difference between lean and obese groups. We observed the interaction of PPP2R4, PPP2R2A, PPP2R1A, PPP2R5C, PPP2R3B, STRIN3, and STRIN4 with PP2Ac was decreased by 0.41, 0.91, 0.73, 0.74, 0.85, 0.87, and 0.79 folds, respectively, in response to metformin treatment in lean insulin-sensitive non-diabetic participants, while

PPP2RIB, PPP2R5D, and PPP2R5E were increased by 1.15, 1.01, and infinite folds, respectively, as shown in Table 26. Furthermore, we found the interaction of PPP2R3A, PPP2R5C, PPP2R5D, PPP2R3B, STRIN3, and PPP2R5B with PP2Ac was decreased by 0.98, 0.86, 0.91, 0.78, 0.86, and 0.79 folds, respectively, in response to metformin treatment in obese insulin-resistant non-diabetic participants, while PPP2R2A, PPP2R1A, PPP2R1B, STRIN4, and PPP2R5D were increased by 1.18, 1.11, 1.21, 1.11 and 1.36 folds, respectively, as reported in Table 27.

Several studies reported that insulin-stimulation leads to a rapid actin filament reorganization that corresponds with the recruitment of PI3-kinase subunits and glucose transporter proteins to regions of reorganized actin in culture muscle cells[183-185]. It has been reported that initiation of these effects of insulin requires an intact actin cytoskeleton and activation of PI 3-kinase[183-185]. Ras GTPase-activating-like protein (IQGAP1) is a protein associated with actin cytoskeleton organization, cellular adhesion, and is a downstream effector of Rac and Cdc42, small GTPases that regulate actin assembly, and is known to regulate MAPK and Wnt/β-catenin signaling pathways[186]. This cell adhesive function of integrin is regulated by its dephosphorylation or phosphorylation modulated by Ca^{2+}/calmodulin-dependent protein kinase II (CaMK) or protein phosphatase 2A[187]. Several studies were conducted to show that PP2A functions by recruitment of IQGAP1 to Rac-β1 integrin[188]. It has been reported that IQGAP1 can also directly recruit and sequentially activate B-Raf, Mek1/2(MAPK1/2), and Erk1/2 as a part of the MAPK signaling pathway[189]. We observed the interaction of PP2A with MAP2K1, IQGAP2, IQGAP3, RAC1, and CAM2KG in our study.

4.4 SUMMARY AND FUTURE DIRECTIONS

PP2A is one of the main serine-threonine protein phosphatases and plays a pivotal role in cellular processes, like signal transduction, cell proliferation, and apoptosis, by dephosphorylating key signaling molecules such as AKT, AMPK, p53, c-Myc, etc. The activity and specificity of PP2A can be influenced by the presence and the binding of the other regulators against a particular substrate such as binding of α4 to PP2A is important to stabilize PP2Ac in its inactive conformation. Metformin (N, N-dimethylbiguanide) is an effective oral biguanide antihyperglycemic drug and the most frequently prescribed as a first-line therapy for type 2 diabetes mellitus. We investigated the PP2A activity, novel interaction partners of PP2Ac and novel PP2A substrate in response to metformin treatment in human skeletal muscle cells. We reported the first evidence that metformin promotes activation of PP2A in human skeletal muscle cells derived from lean insulin-sensitive and obese insulin-resistant non-diabetic participant (fold increase Metformin/basal: 1.54±0.11 and 1.68±0.16, $P<0.001$, respectively). Furthermore, from our high throughput proteomics approach using UPLC-ESI-MS/MS, we identified and quantified PP2Ac interaction partners in human skeletal muscle cells. 230 proteins showed a significant difference in interacting with PP2Ac when compared among lean insulin-sensitive and obese insulin-resistant participants. In addition, 20 proteins that showed a significant difference between lean insulin-sensitive and obese insulin-resistant participants compared to metformin treatment. These interaction partners helped us understand the role and regulation of PP2A in human skeletal muscle cells. Furthermore, metformin reversed the abnormality in PP2Ac interaction partners and rendered them similar to lean.

We reported the first global analysis of the effect of metformin on phosphorylation events in human primary skeletal muscle cells derived from lean insulin-sensitive

and obese insulin-resistant participants. We identified a total of 24,741 phosphorylation events from our phosphoproteome analysis assigned to a total of 7,037 proteins. More importantly, 1,958 phosphorylation events that were not reported in humans; among them, 1,756 were not reported in any species in the phosphositePlus database and thus appeared to be novel sites. We found 4,455 and 1,966 phosphorylation sites were significantly modulated ($P<0.05$) in lean insulin-sensitive and obese insulin-resistant participants, respectively. In addition, 445 phosphorylation sites were significantly changes ($P<0.05$) between two groups after metformin treatments. We quantified 5,146 phosphorylation sites in lean insulin-sensitive participants and 967 phosphorylation sites in obese insulin-resistant participants were significantly changes ($P<0.05$) under insulin-stimulation. In addition, we quantified 842 phosphorylation sites were significantly different ($P<0.05$) upon insulin-stimulation between two groups. We confirmed that metformin treatment has significant modulated on the phosphorylation sites present in phosphatases and kinases which are important for insulin signaling or glucose uptake pathways. Furthermore, we demonstrated that PP2A plays an important role in metformin's action in primary human skeletal muscle cells, and identified novel metformin-responsive PP2A substrates and PP2Ac interaction partners that are significantly difference in cells derived from lean healthy and obese insulin resistant participants. These results allow us to better insight into molecular mechanisms for metformin's action in human skeletal muscle. Furthermore, we will validate the significantly change in protein phosphatase and protein kinases and their interaction partners by immunoblotting (i.e., western blots). We will perform the phosphoproteome and proteome in primary cell culture from obese insulin-sensitive and T2D participants to quantified novel metformin-responsive PP2A substrates and PP2Ac interaction partners. In addition, we will conduct functional studies for metformin responsive for site-specific phosphorylation

and PPP2Ac interaction partners. We will design metformin intervention in obese insulin resistant participants to determine whether findings in primary cell culture models can be translated into humans. Furthermore, we will investigate metformin resistance in obese insulin-resistant and T2D participants. We will make the data publically available after publication so that scientists worldwide can use them to design experiments to test hypothesis of their interests.

FIGURES AND TABLES

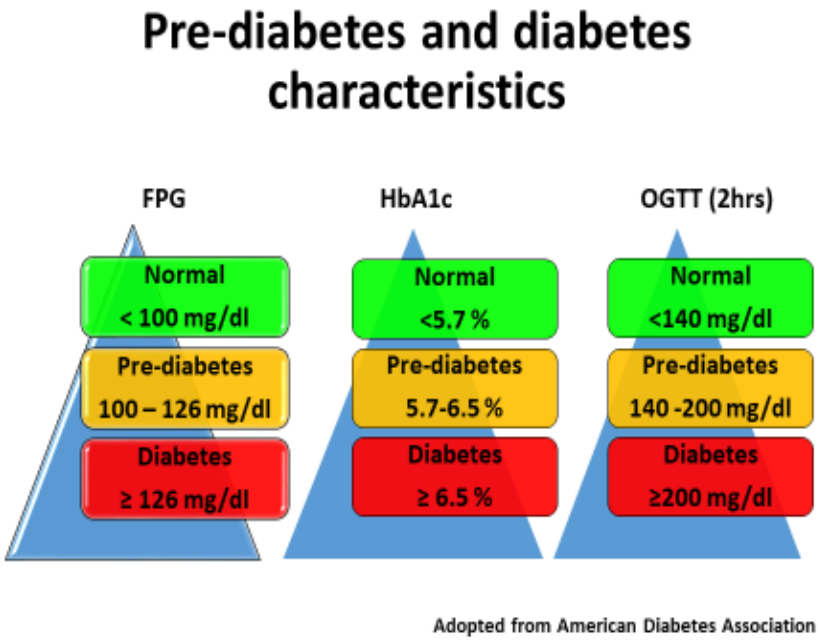

Figure 1. The current criteria for the diagnosis of prediabetes and diabetes[4]

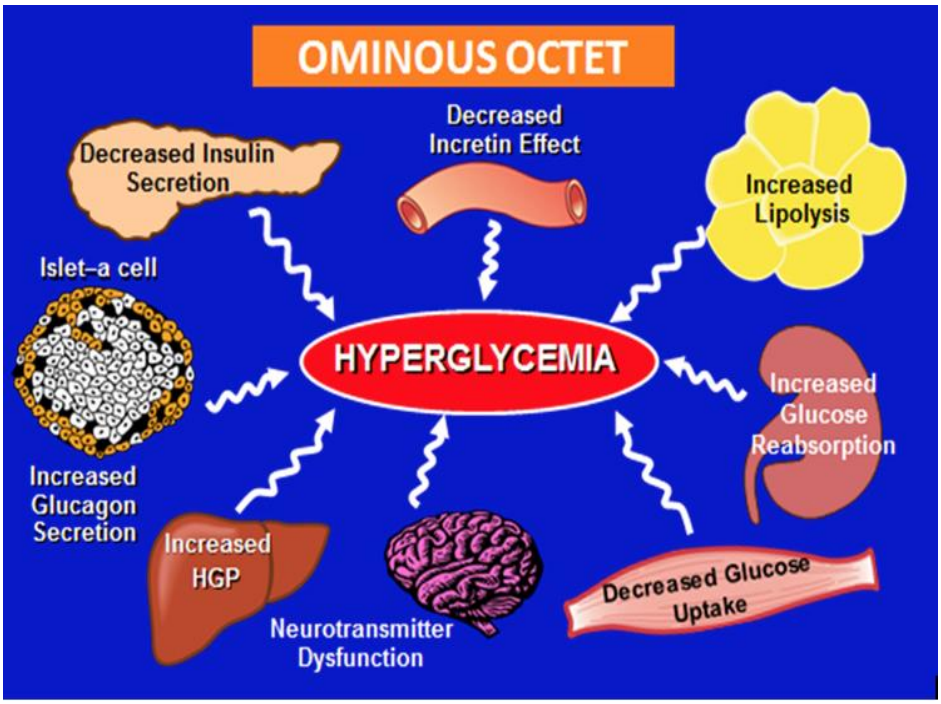

Figure 2. The eight principal mechanisms contributing to hyperglycemia[190]

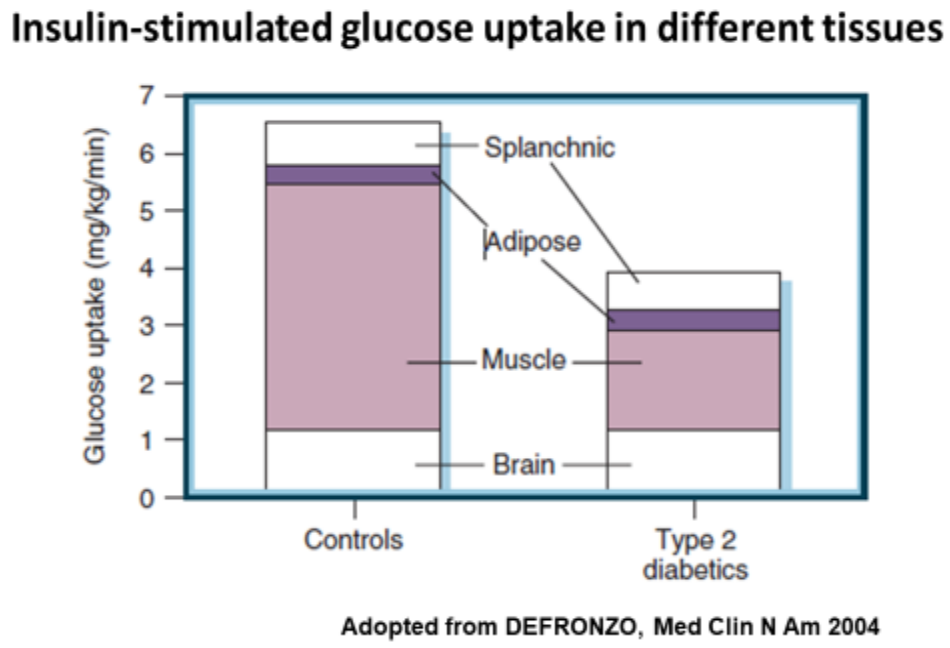

Figure 3. Glucose uptake in different tissues under hyperinsulinemic-euglycemic clamp comparing T2D to control (non-diabetic) patients[9]

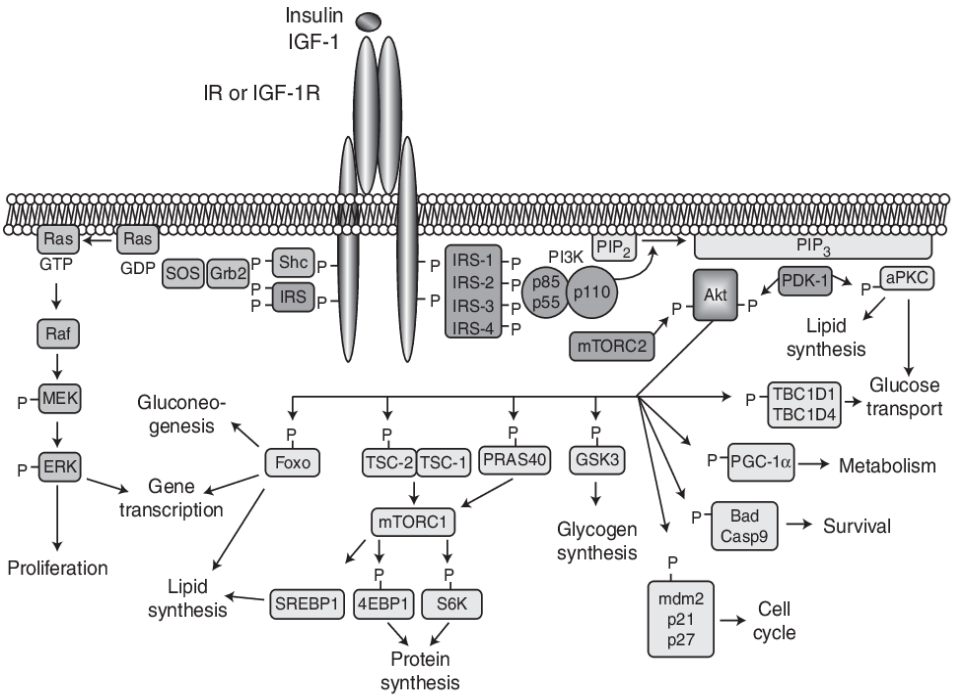

Figure 4. The two major insulin receptor signaling cascades (PI3K and ERK) are shown[5]

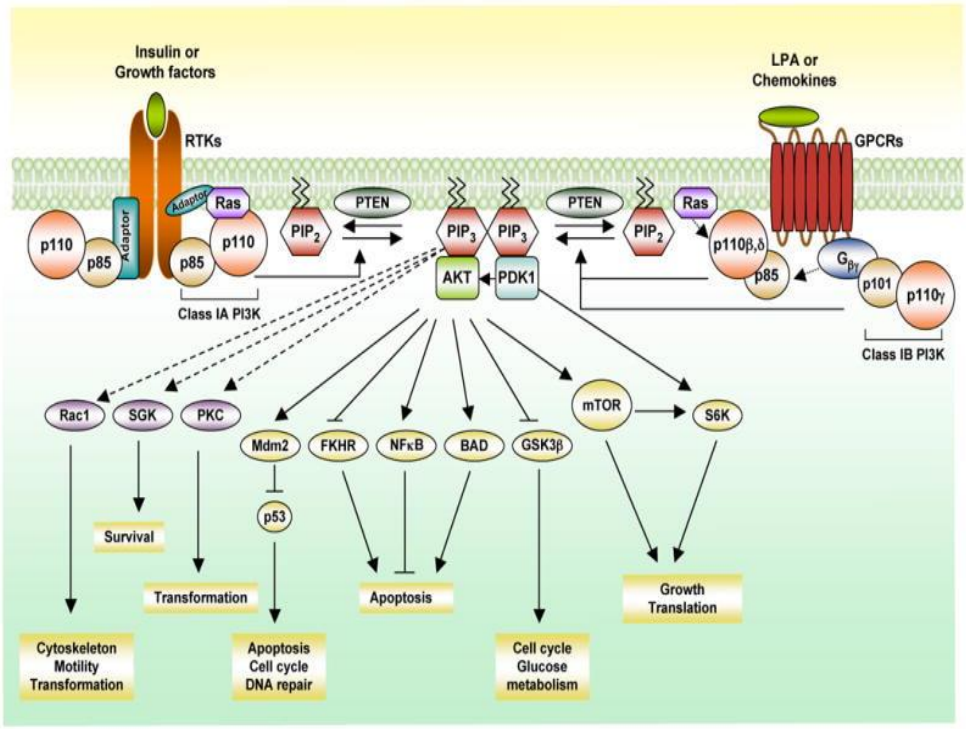

Figure 5. The phosphoinositide 3-kinase (PI3K) signaling pathway[7]

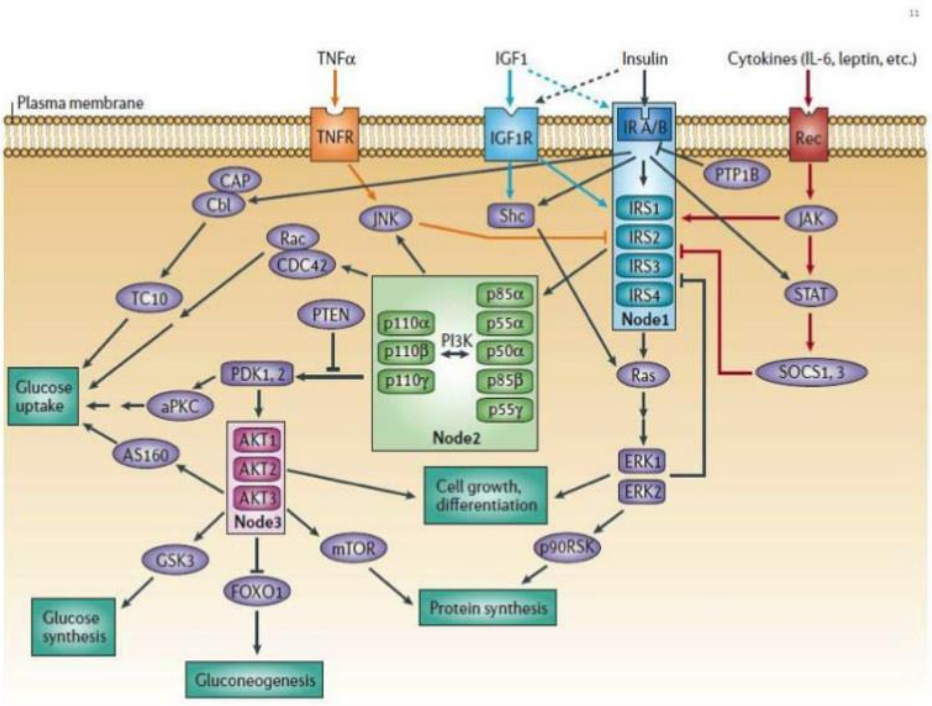

Figure 6. The critical nodes (IR/IRS, PI3K and AKT) are boxed of signal transduction network[5]

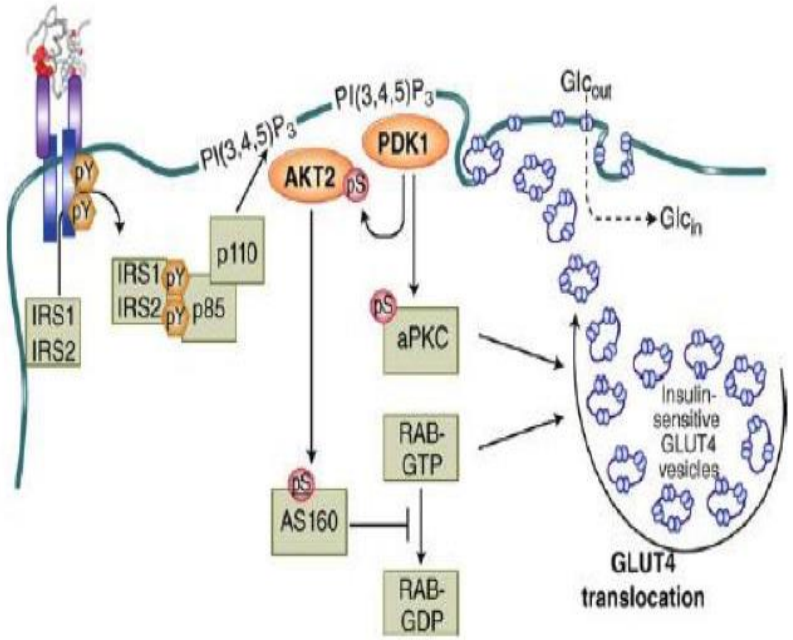

Figure 7. Mechanism of insulin-stimulated glucose transport and GLUT4 translocation[5]

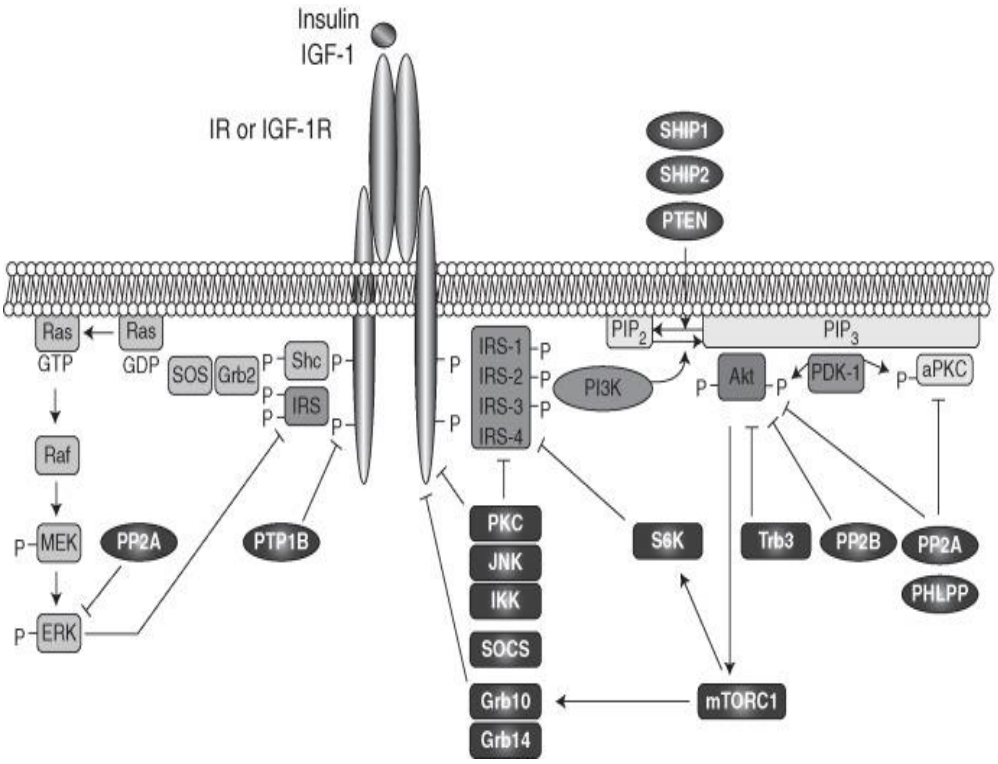

Figure 8. The negative regulators of insulin signaling pathway[11]

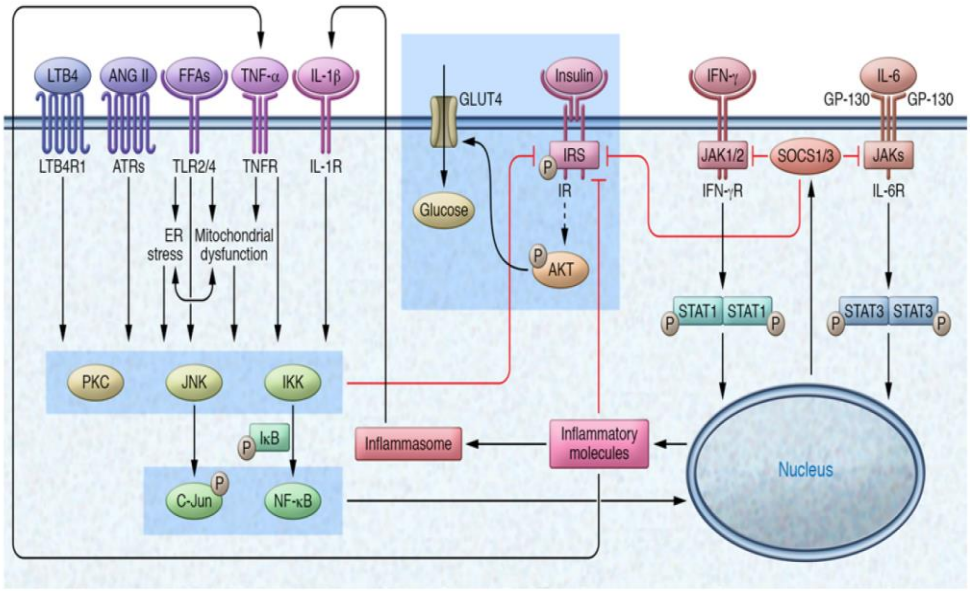

Figure 9. Inflammatory signaling mediates insulin resistance in myocytes via IRS/AKT pathway[14]

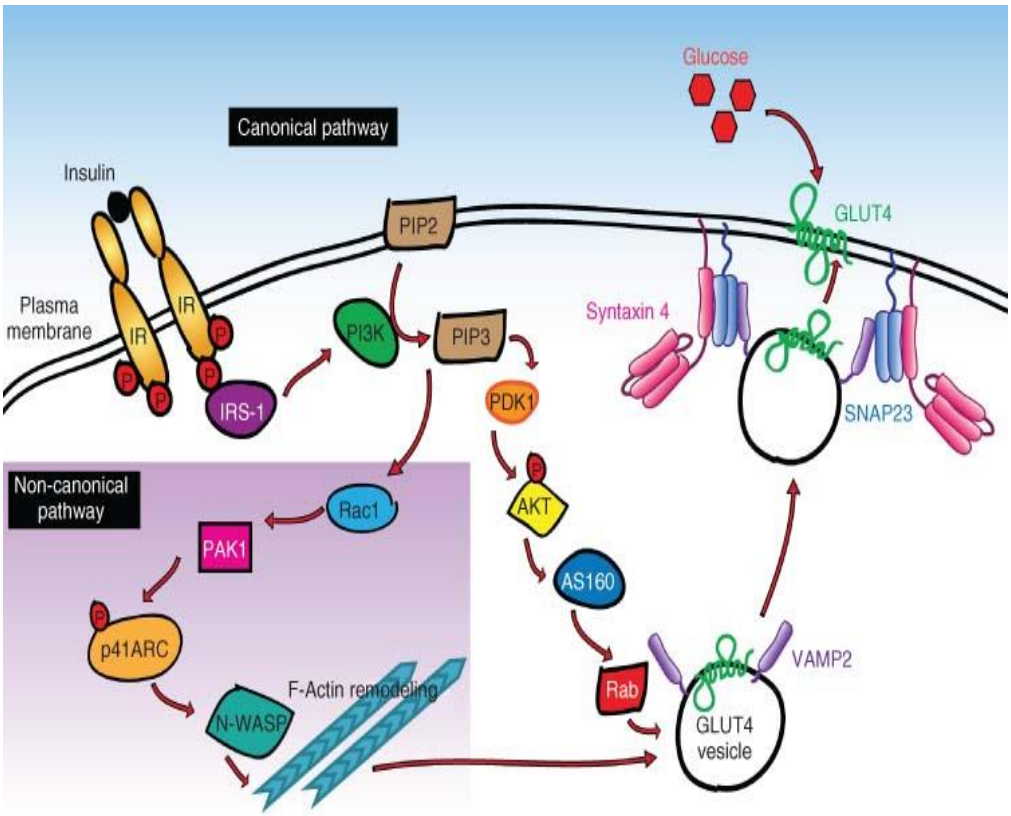

Figure 10. A simplified model of insulin-stimulated translocation of the GLUT4 glucose transporter in skeletal muscle[5]

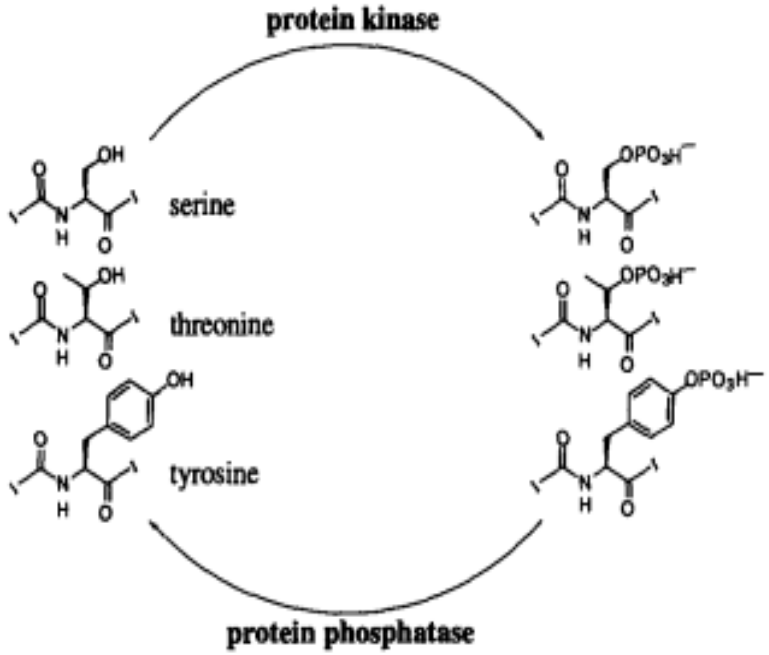

Figure 11. The reversible kinase /phosphatase cycle[27]

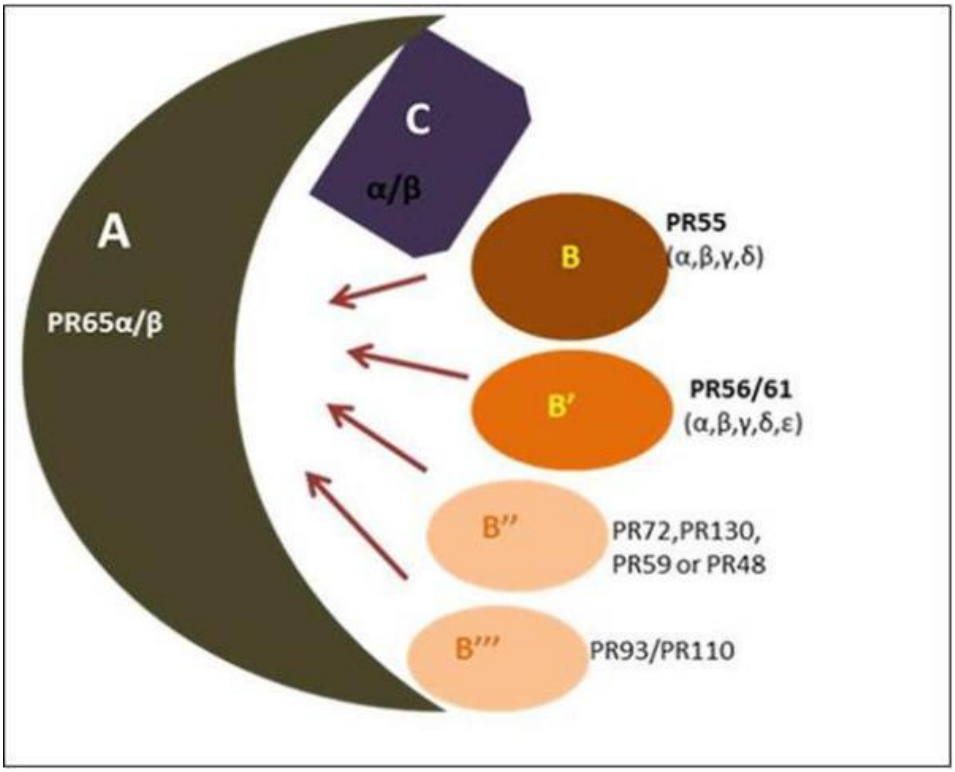

Figure 12. Schematic crystal structure of PP2A holoenzyme complex[31]

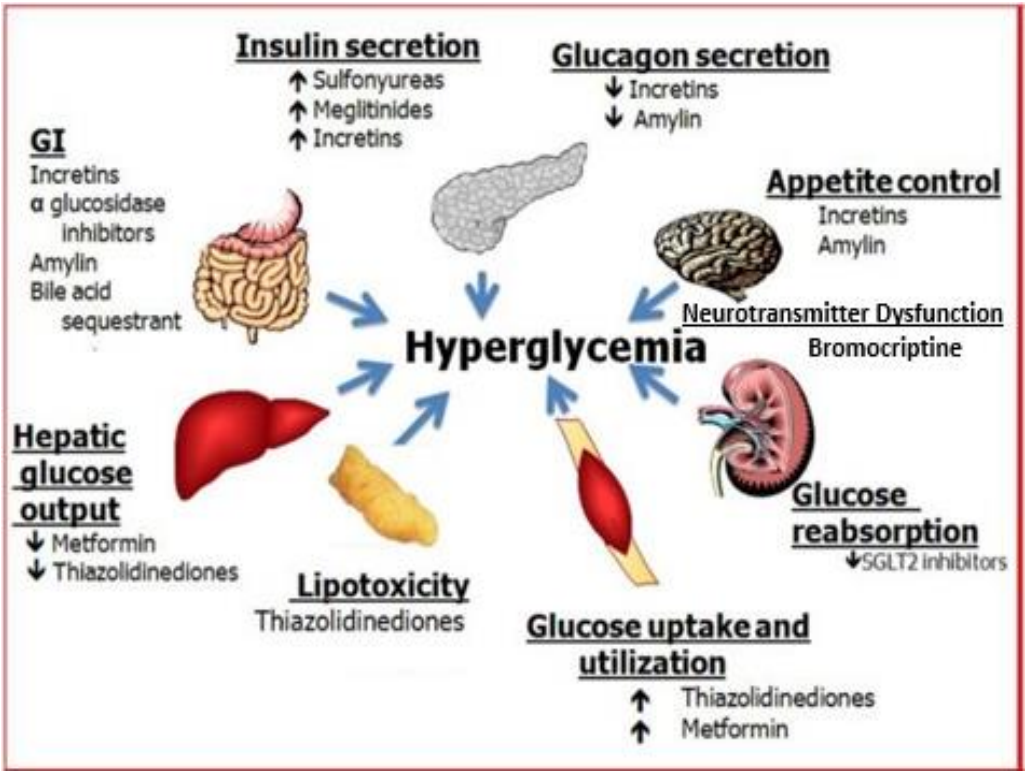

Figure 13. Pharmacological therapies action for the treatment of T2D[43]

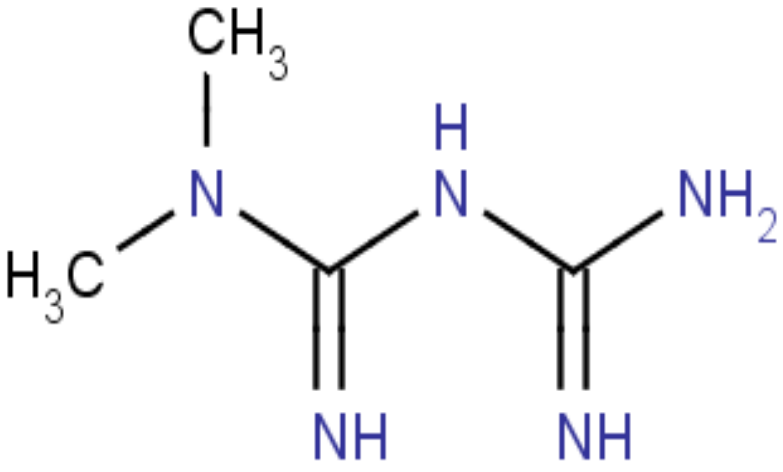

Figure 14. The chemical structure of metformin (molecular weight =129.1g/mol)[45]

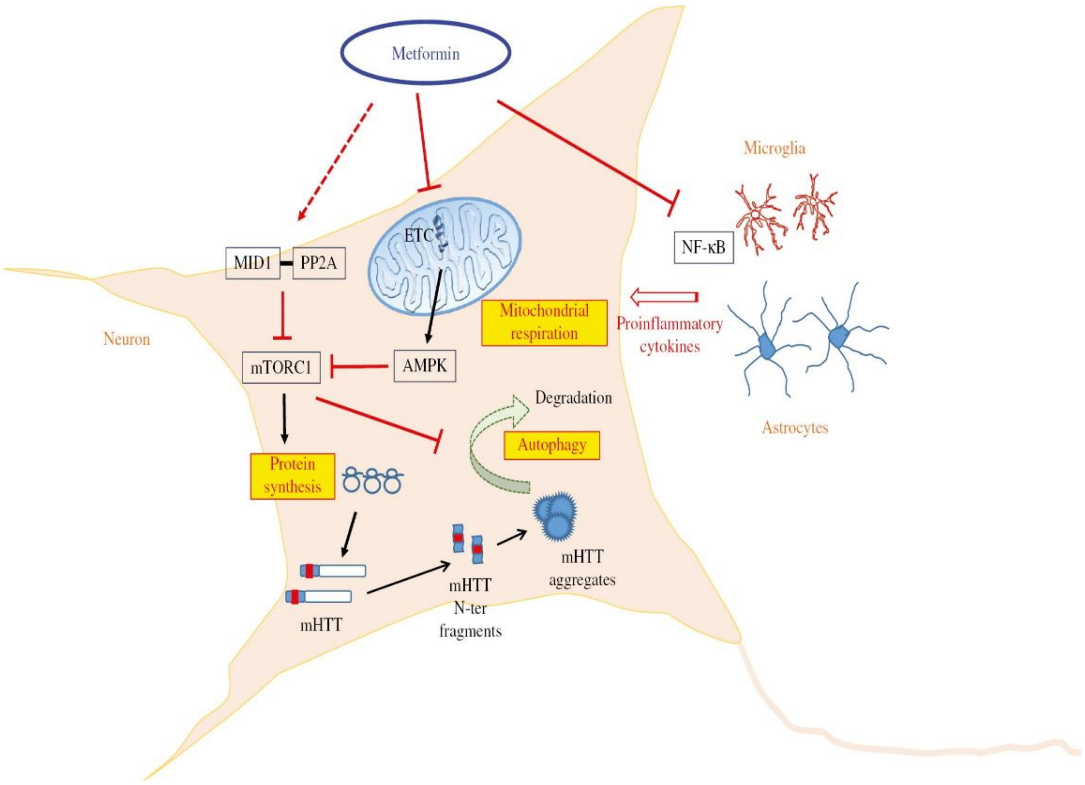

Figure 15. The potential action of metformin in Huntington's disease[91]

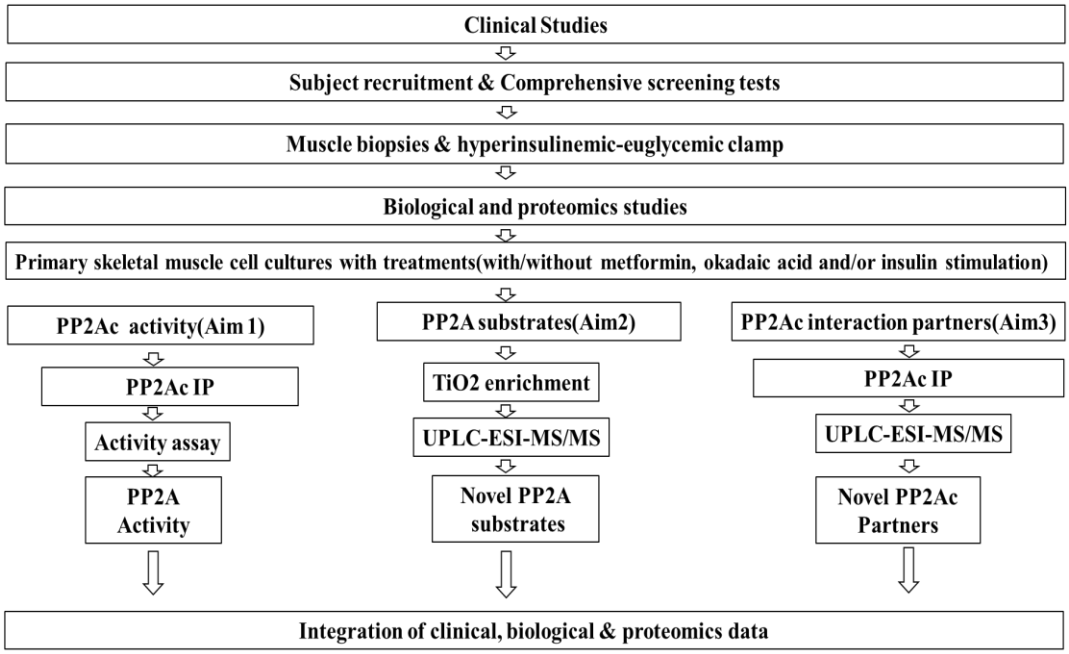

Figure 16. The overall experimental design flowchart for three specifi aims

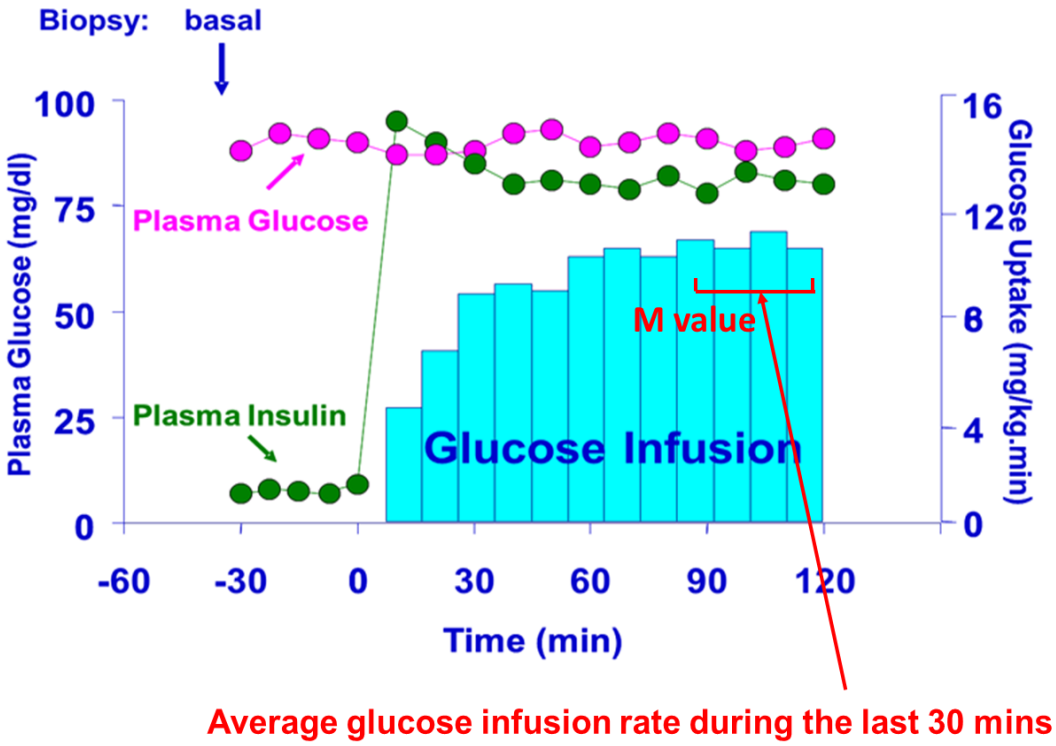

Figure 17. Diagram of the hyperinsulinemic-euglycemic clamp techinque[9]

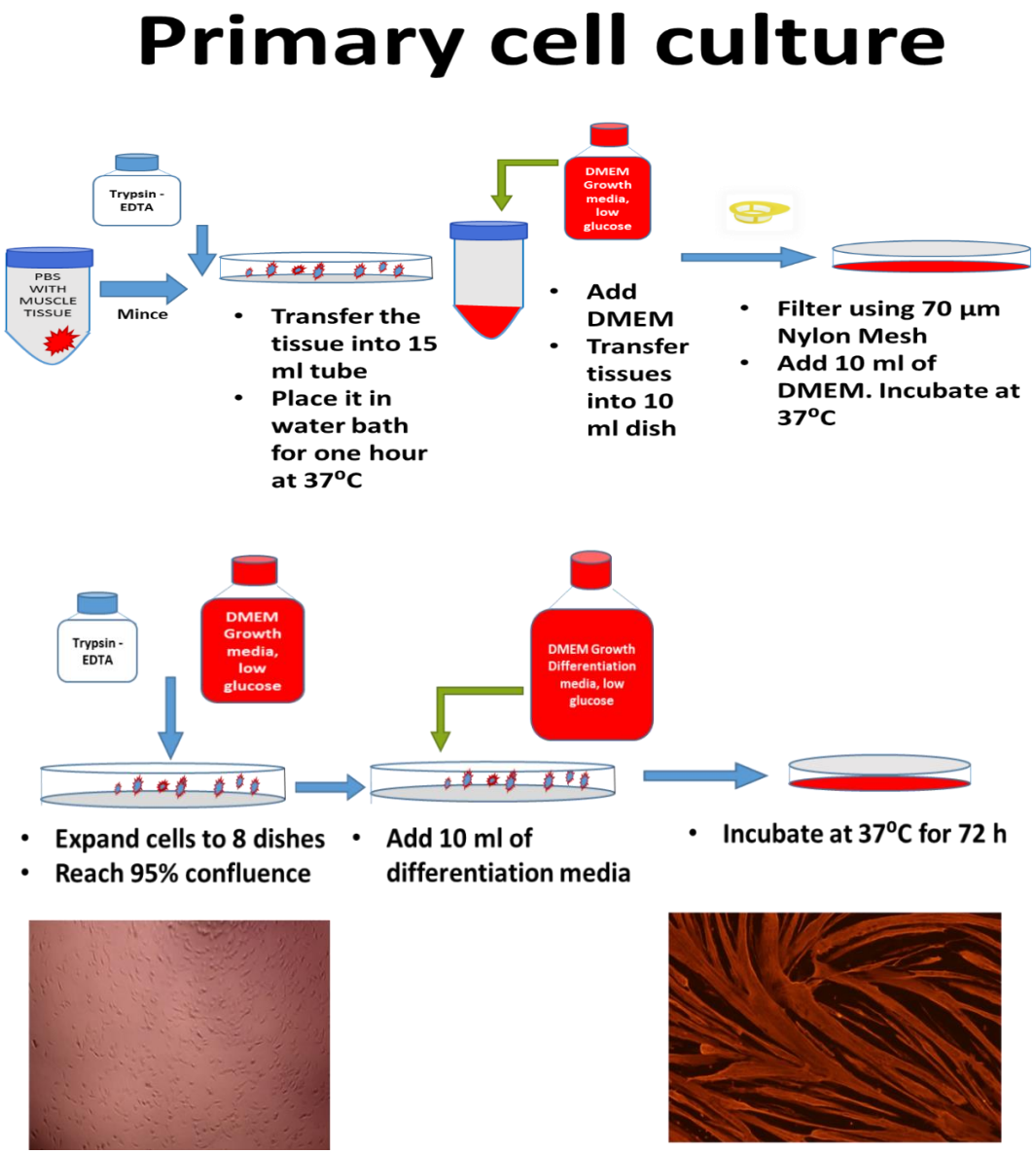

Figure 18. Schematic diagram of primary human skeletal muscle cell culture

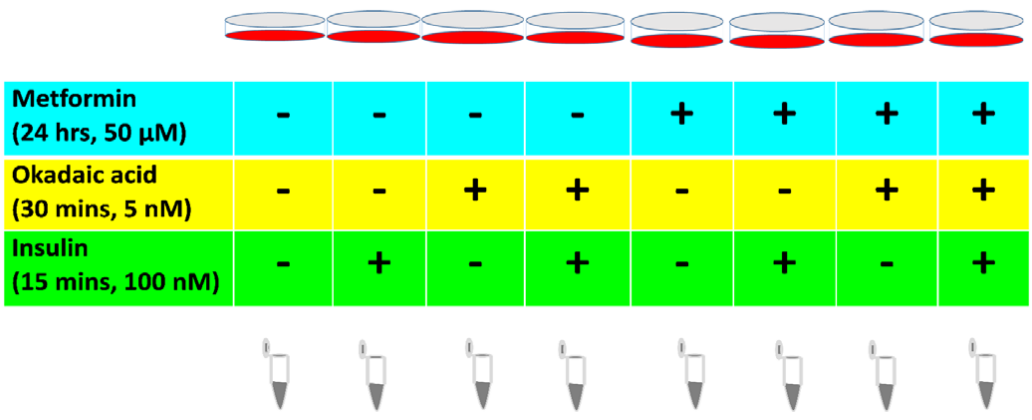

Figure 19. Primary human skeletal muscle cell culture and treatments

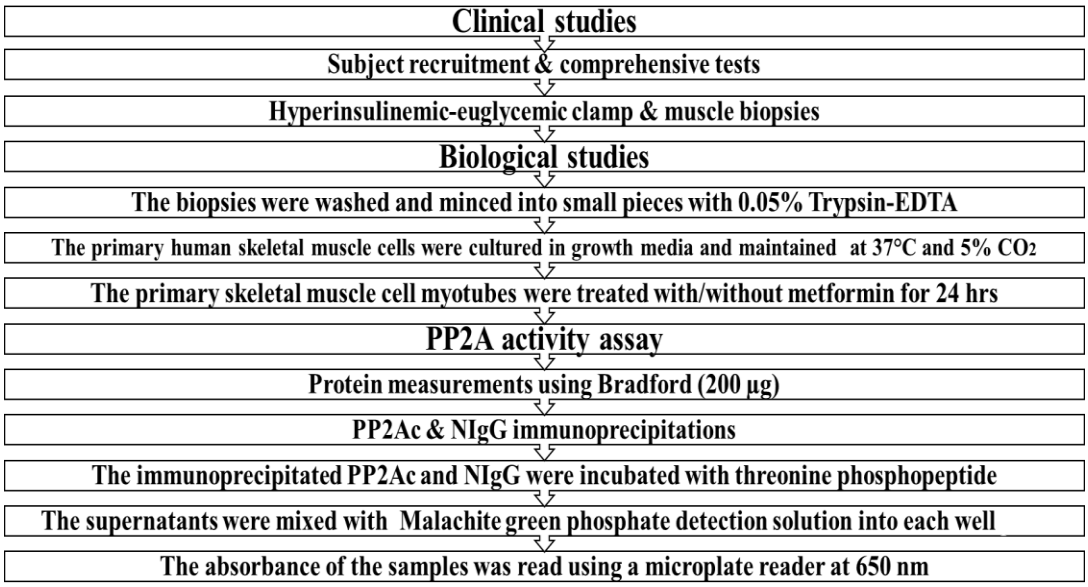

Figure 20. The overall flowchart to measure PP2A activity

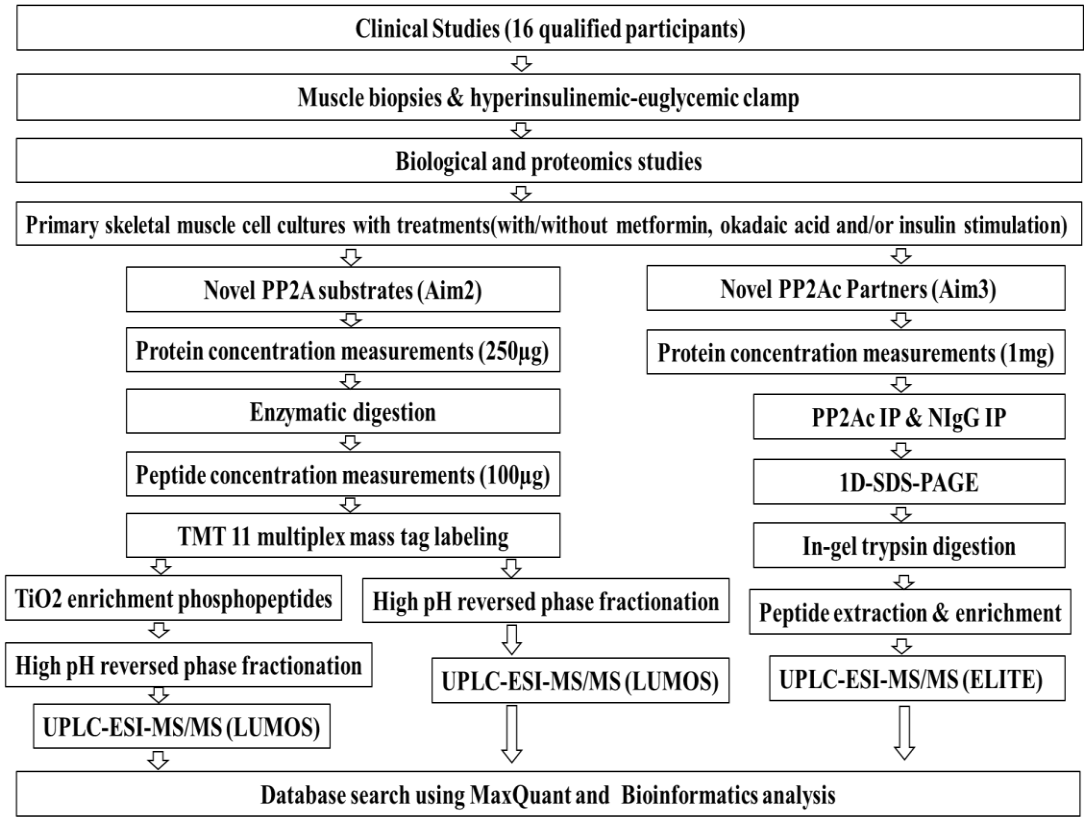

Figure 21. The overall detail experimental design flowcharts for identified and quantified Novel PP2Ac subtracts and Novel PP2Ac interaction partners

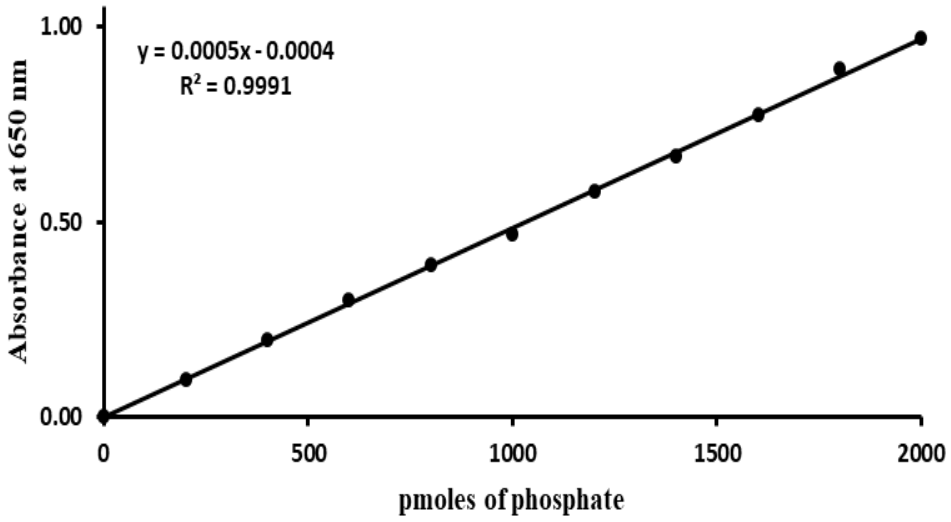

Figure 22. Measurement of phosphate concentration of the standard solutions (according to the manufacturer's protocol)

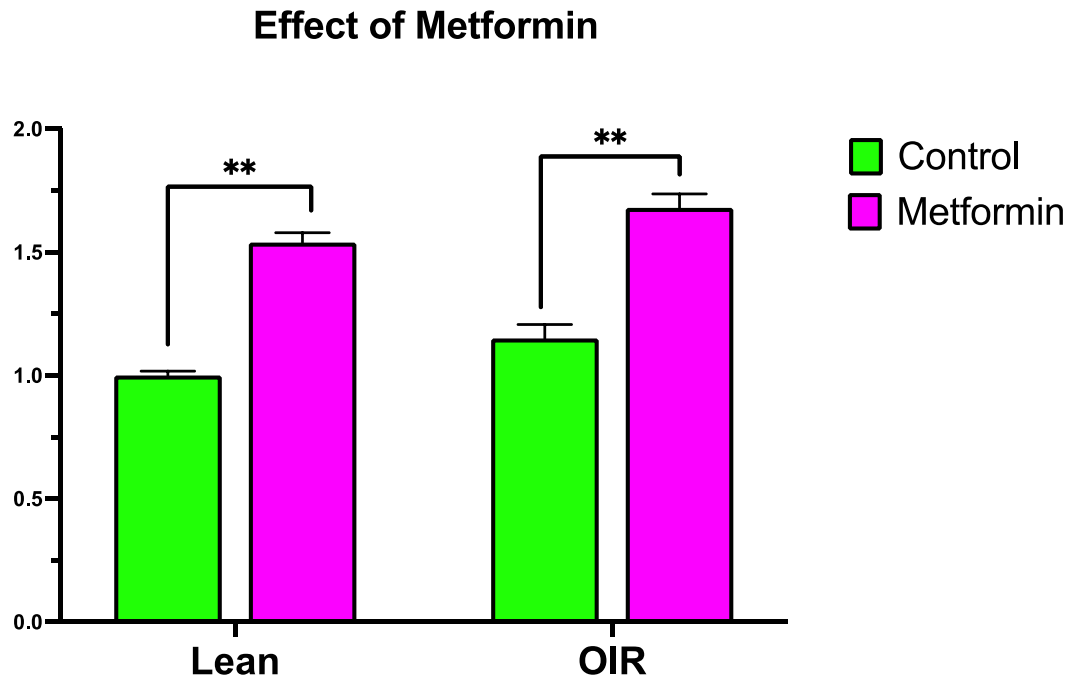

Figure 23. The significance between the basal and metformin-treated groups was analyzed by independent student's t-test. ** P<0.001

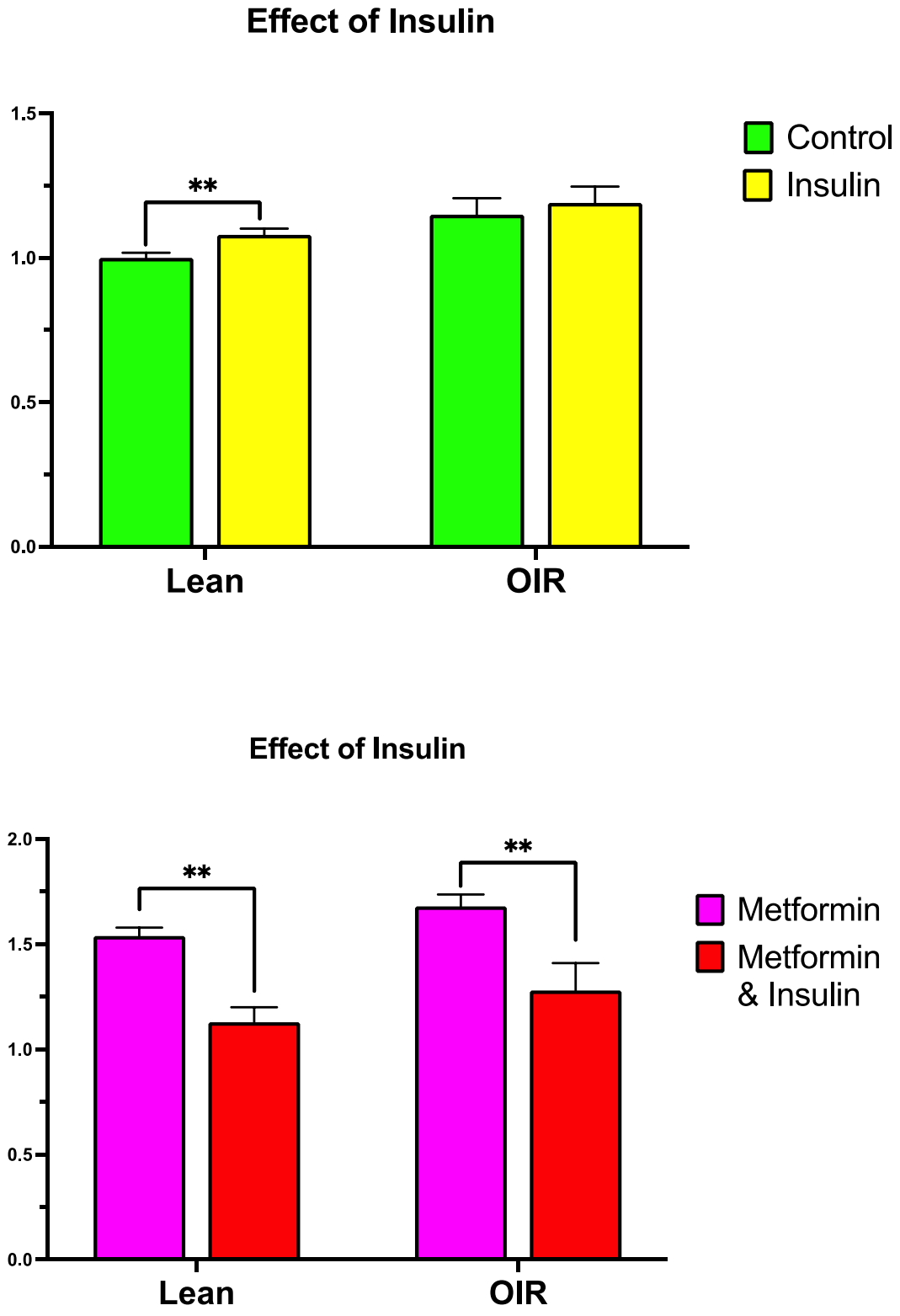

Figure 24. Summative PP2A activity. Data are given as fold changes (means ± SEM); **: P<0.01.

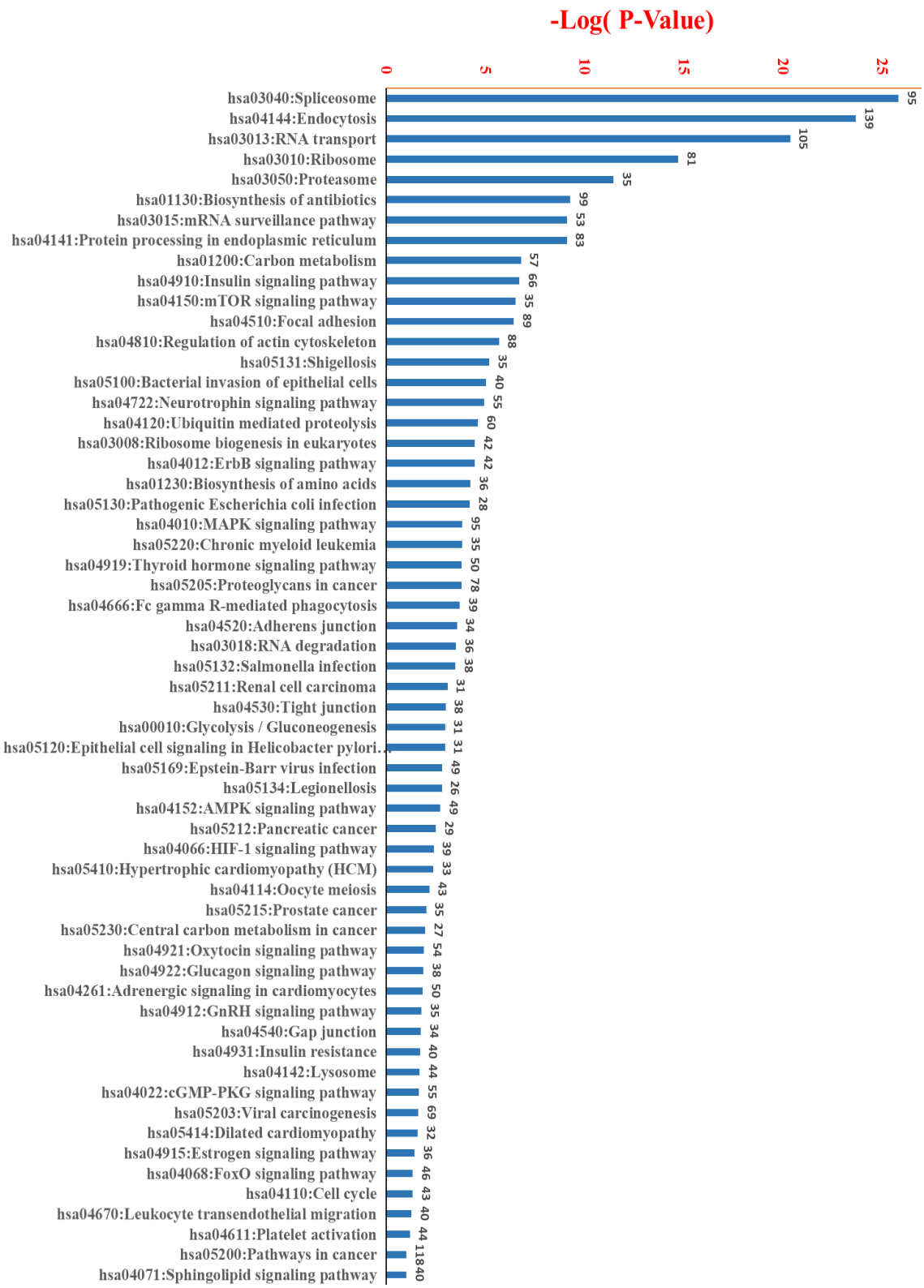

Figure 25. Significant enriched KEGG Pathways for the identified phosphoproteins in primary skeletal muscle cells revealed by DAVID. P-values were calculated using a hypergeometric test and corrected with Benjamin (cut-off of 0.01 was applied)

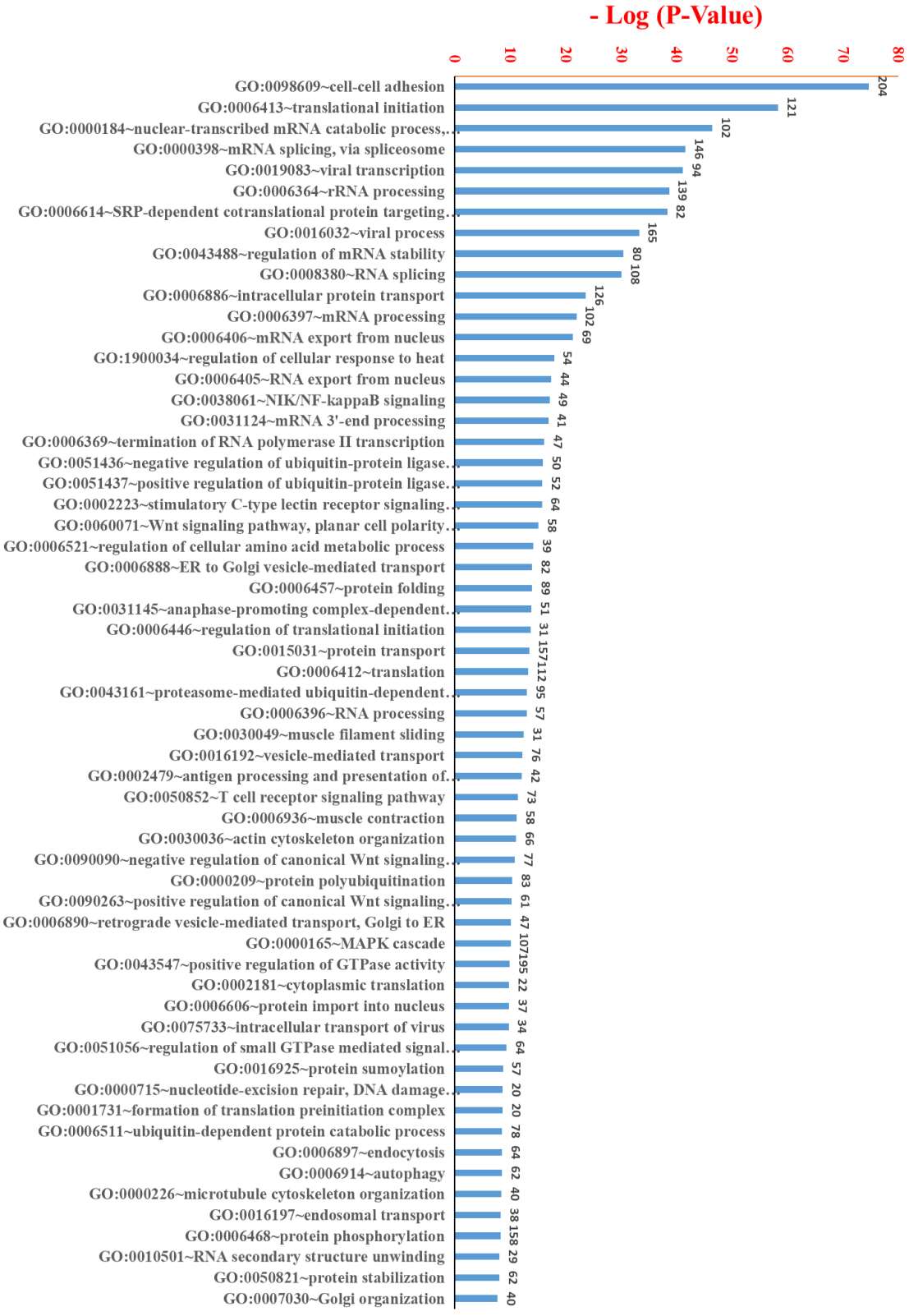

Figure 26. Significant enriched biological processes for the identified phosphoproteins in primary skeletal muscle cells revealed by DAVID. P-values were calculated using a hypergeometric test and corrected with Benjamini (cut-off of 0.01 was applied).

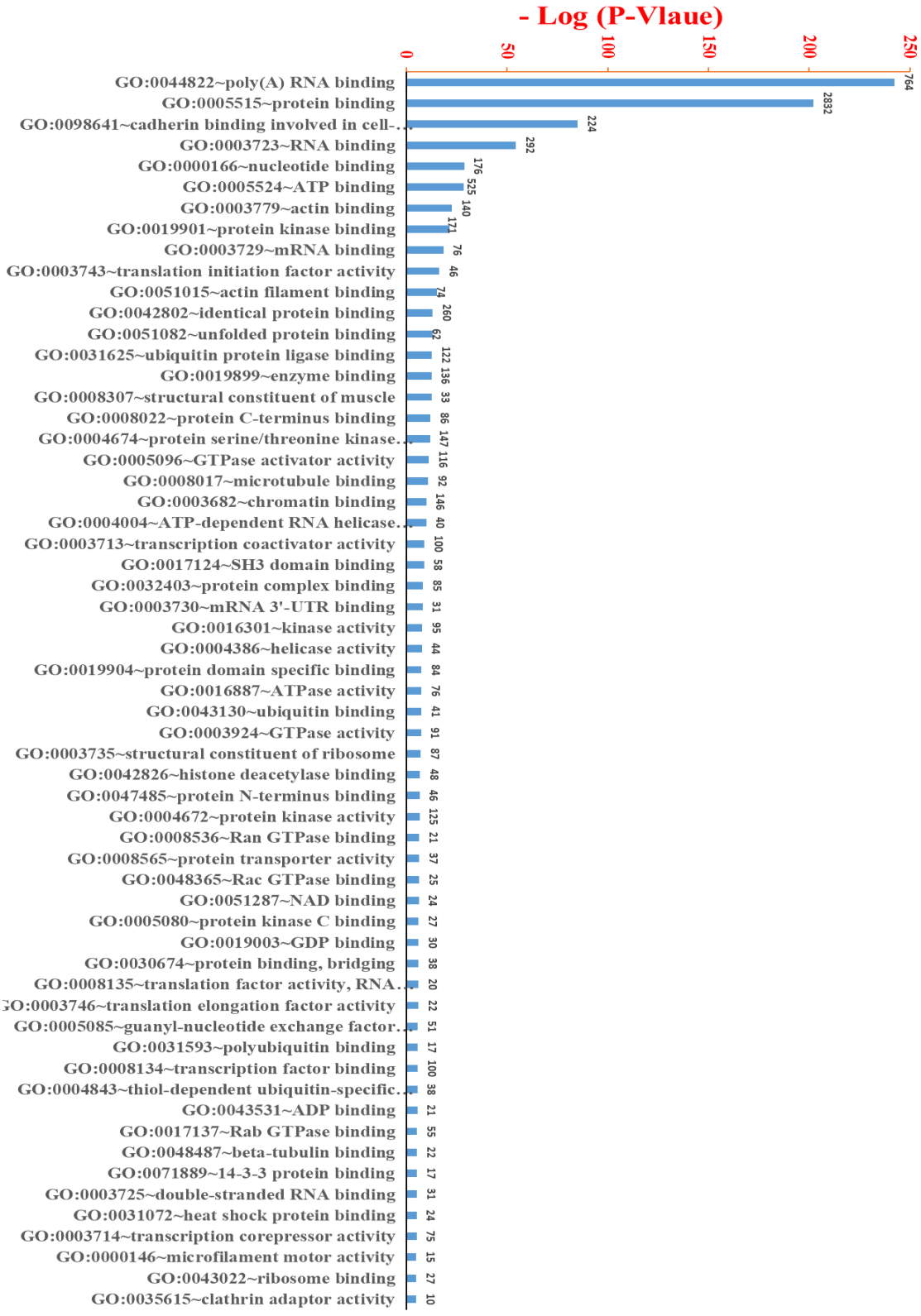

Figure 27. Significant enriched molecular functions for the identified phosphoproteins in primary skeletal muscle cells revealed by DAVID. P-values were calculated using a hypergeometric test and corrected with Benjamini (cut-off of 0.01 was applied).

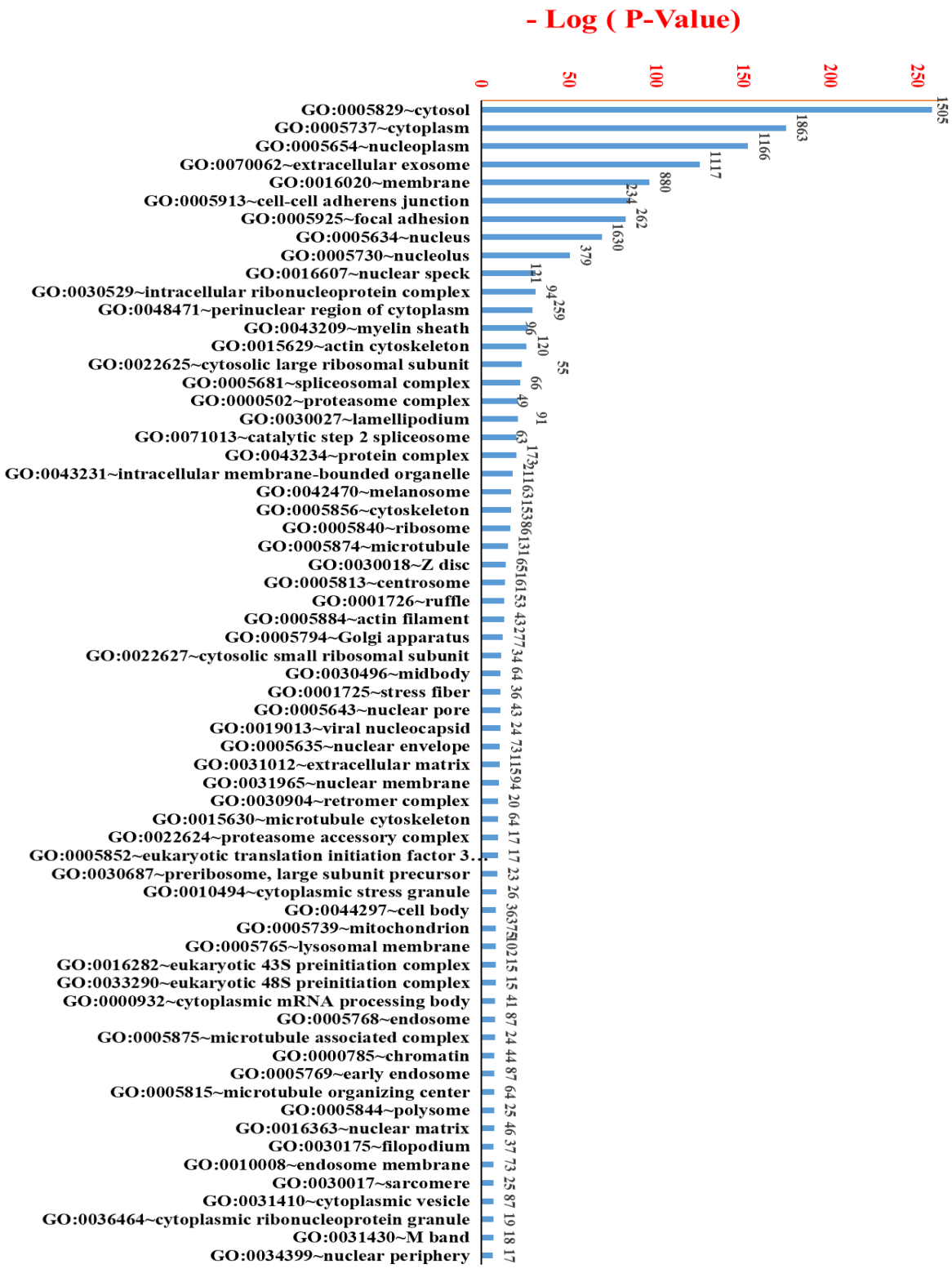

Figure 28. Significant enriched subcellular localizations for the identified phospho-proteins in primary skeletal muscle cells revealed by DAVID. P-values were calculated using a hypergeometric test and corrected with Benjamini (cut-off of 0.01 was applied).

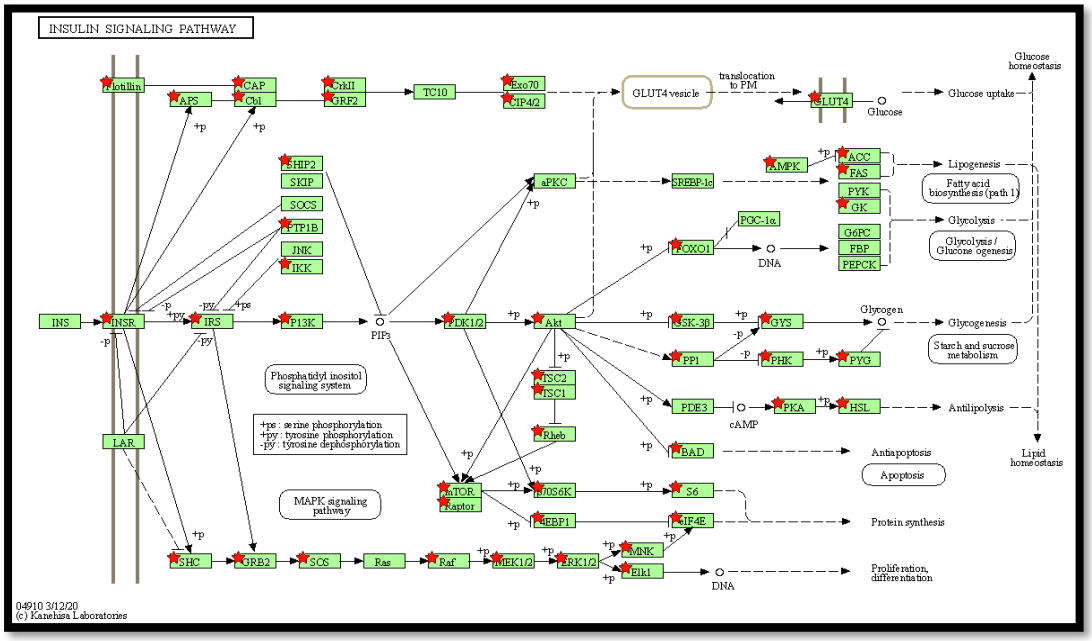

Figure 29. Color-coded insulin signaling pathway of phosphoproteins according to their differences in lean insulin-sensitive and obese insulin-resistant participants. Pathway map was downloaded from KEGG using David bioinformatics

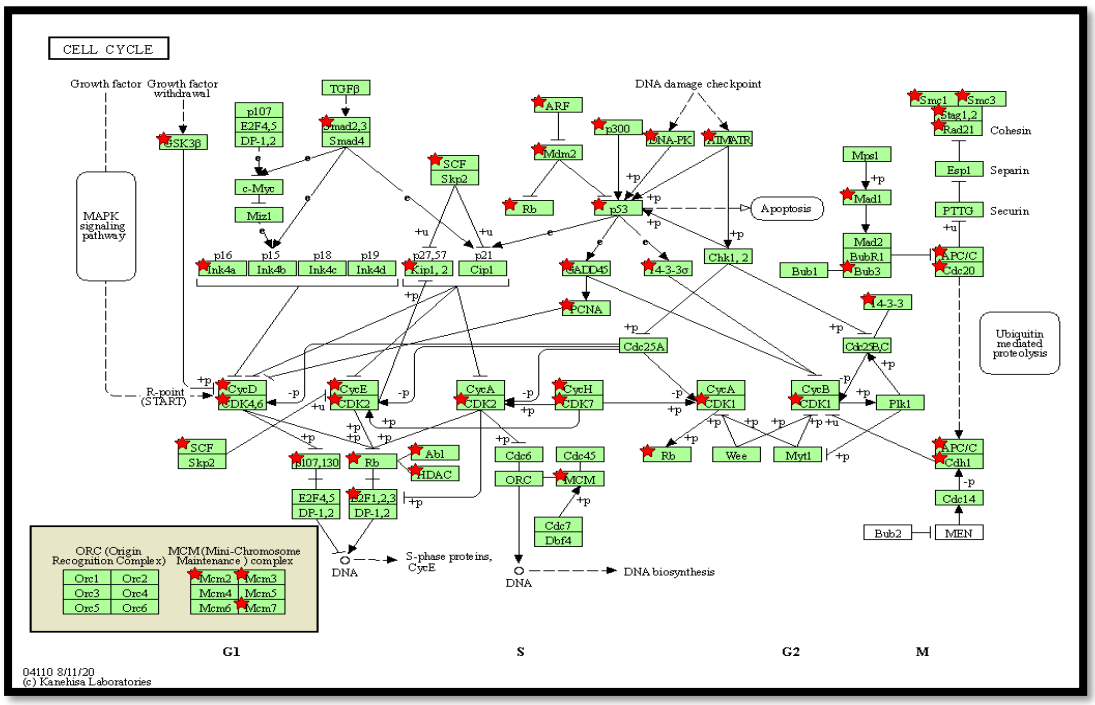

Figure 30. Color-coded cell cycle signaling pathway of phosphoproteins according to their differences in lean insulin-sensitive and obese insulin-resistant participants. Pathway map was downloaded from KEGG using David bioinformatics.

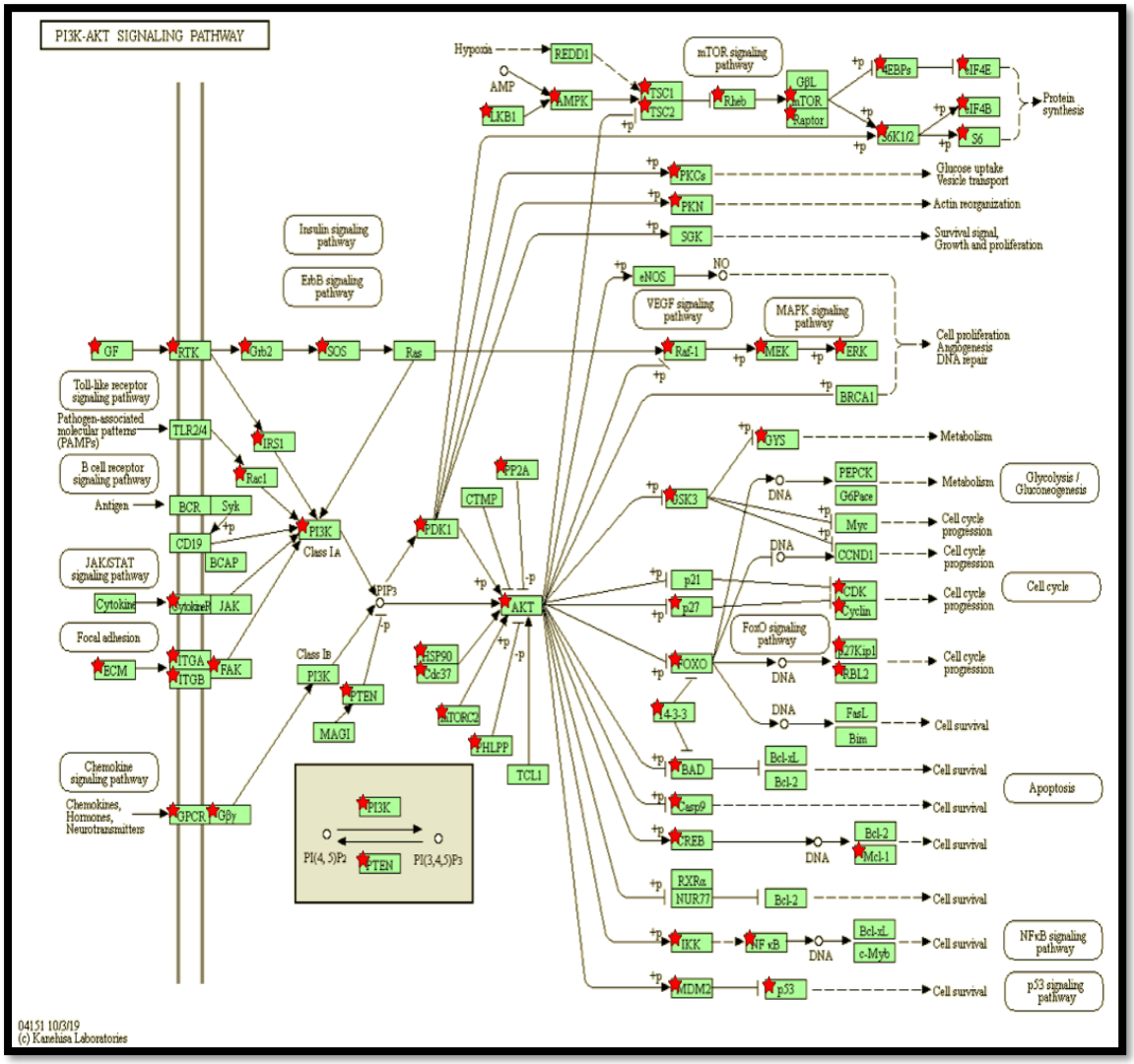

Figure 31. Color-coded PI3K-Akt signaling pathway of phosphoproteins according to their differences in lean insulin-sensitive and obese insulin-resistant participants. Pathway map was downloaded from KEGG using David bioinformatics.

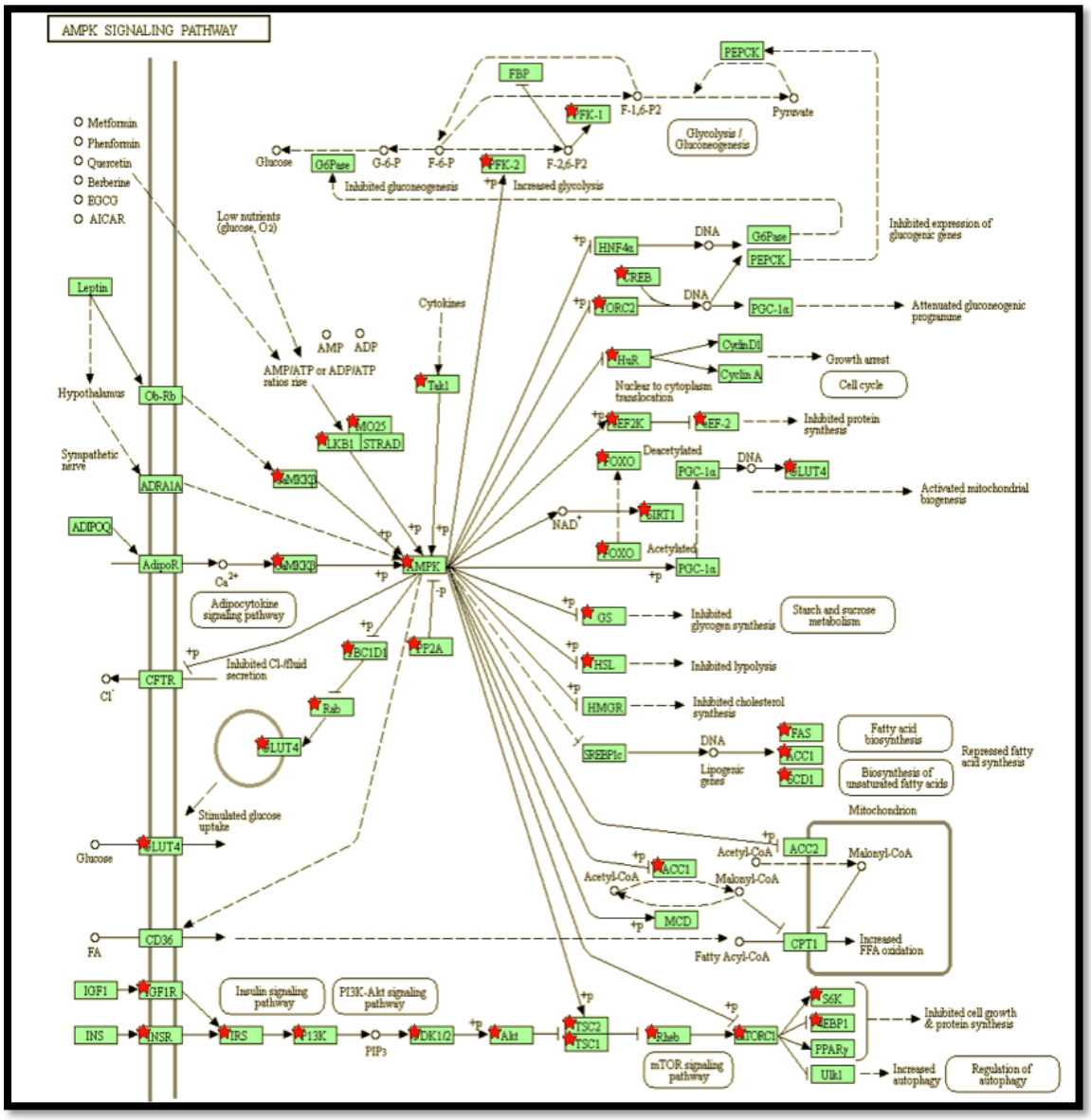

Figure 32. Color-coded AMPK signaling pathway of phosphoproteins according to their differences in lean insulin-sensitive and obese insulin-resistant participants. Pathway map was downloaded from KEGG using David bioinformatics

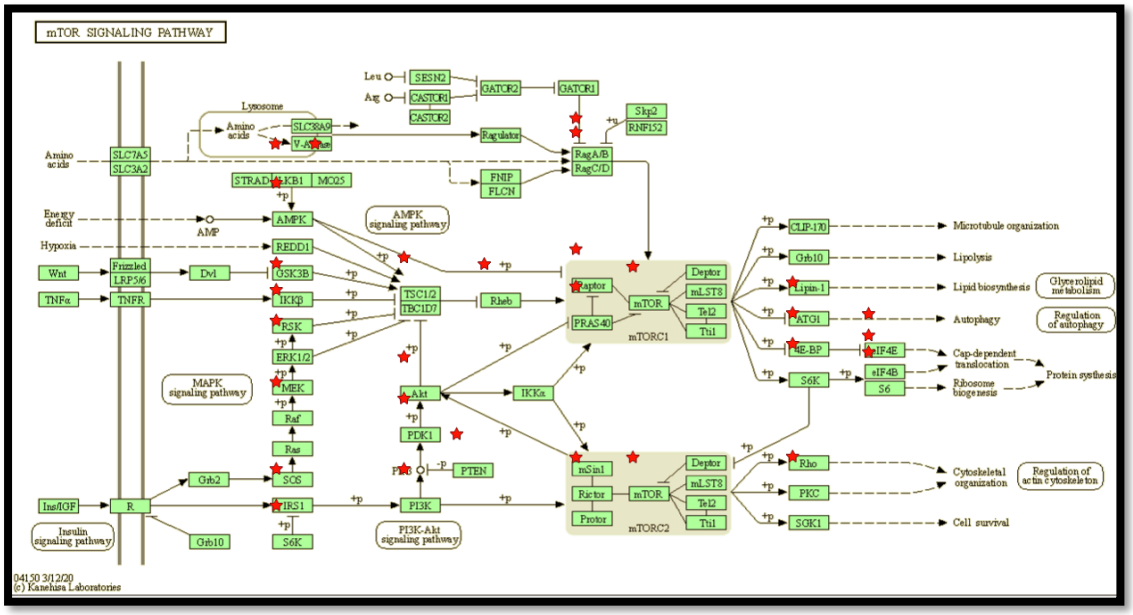

Figure 33. Color-coded mTOR signaling pathway of phosphoproteins according to their differences in lean insulin-sensitive and obese insulin-resistant participants. Pathway map was downloaded from KEGG using David bioinformatics.

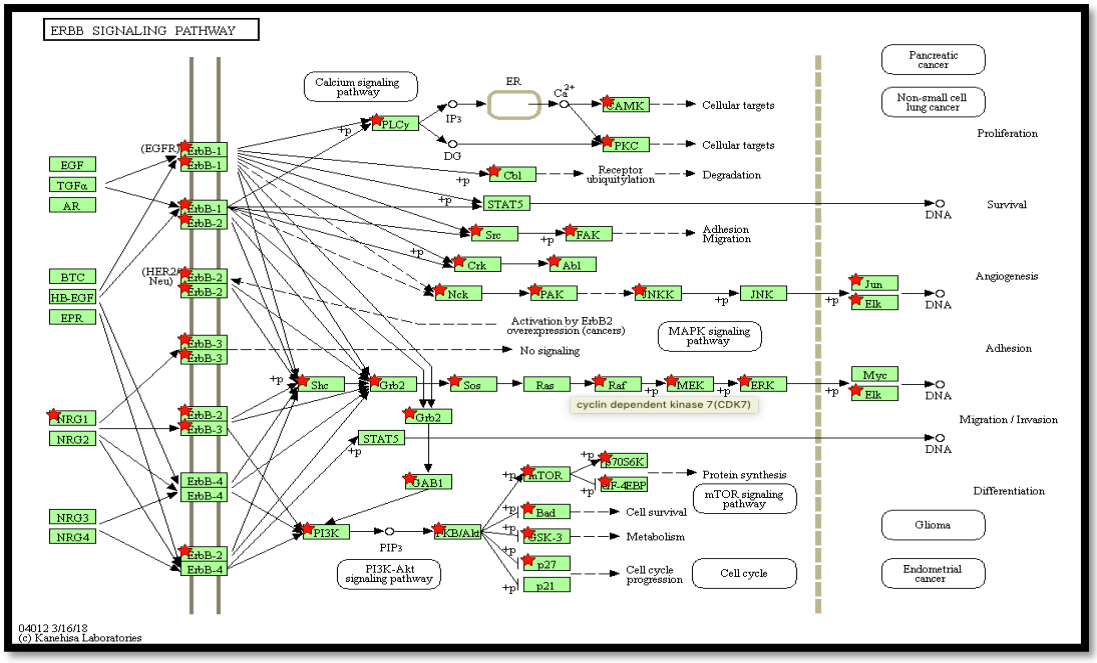

Figure 34. Color-coded ERBB signaling pathway of phosphoproteins according to their differences in lean insulin-sensitive and obese insulin-resistant participants. Pathway map was downloaded from KEGG using David bioinformatics.

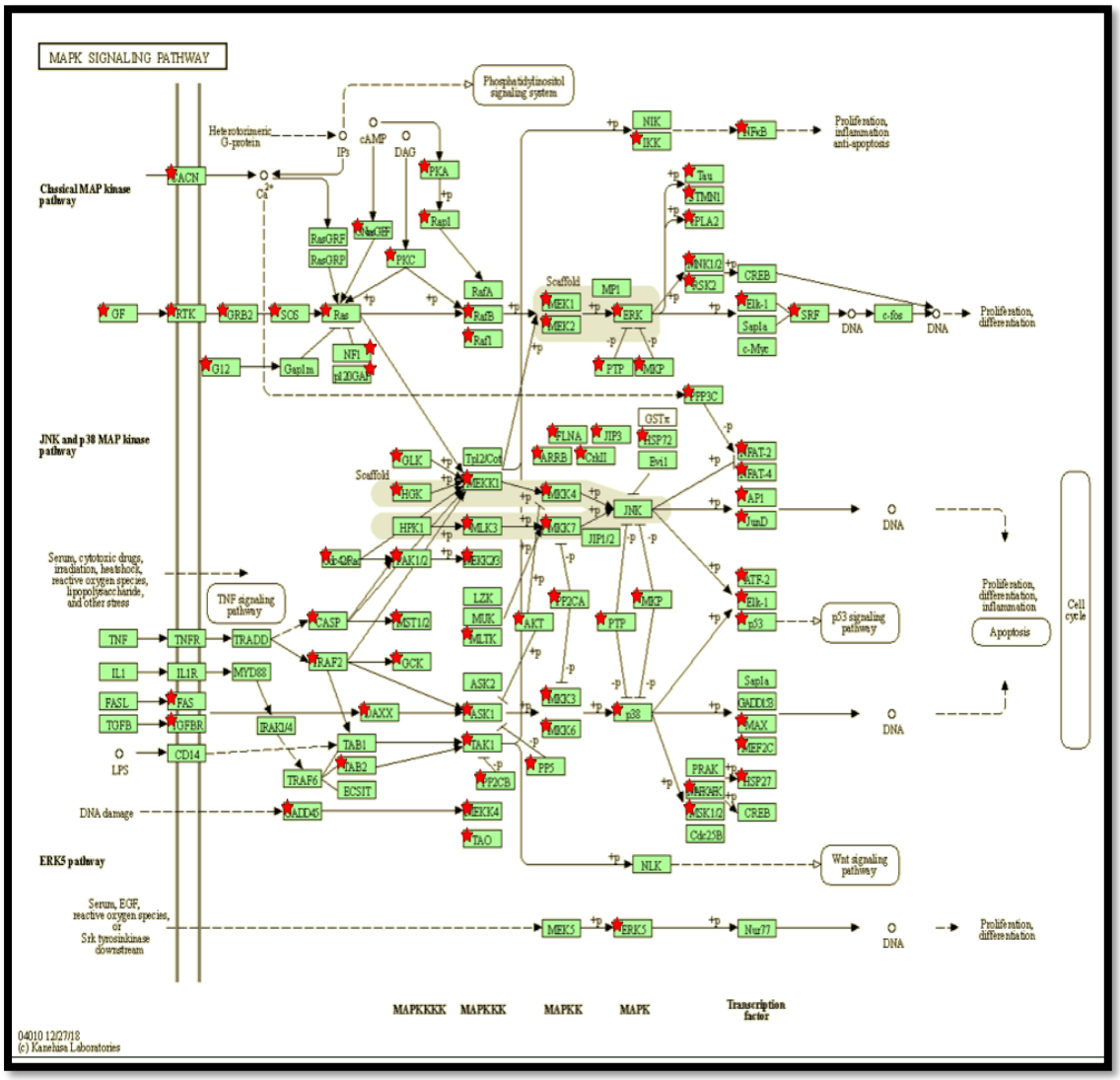

Figure 35. Color-coded MAPK signaling pathway of phosphoproteins according to their differences in lean insulin-sensitive and obese insulin-resistant participants. Pathway map was downloaded from KEGG using David bioinformatics.

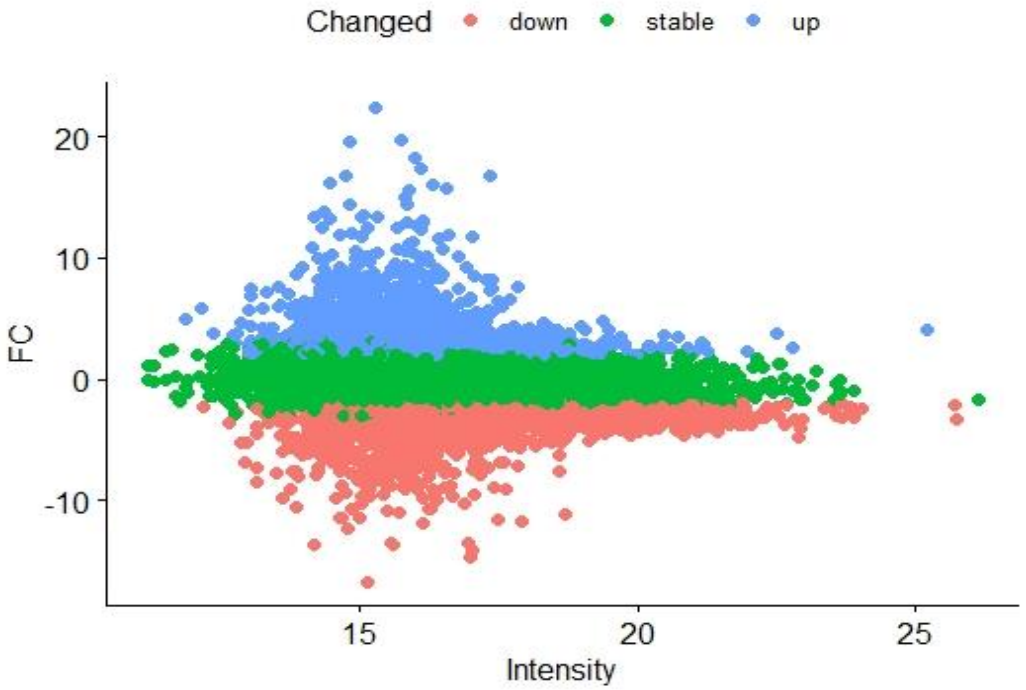

Figure 36. The upregulated and downregulated proteins in metformin-treated human skeletal muscle cells from lean insulin-sensitive participants

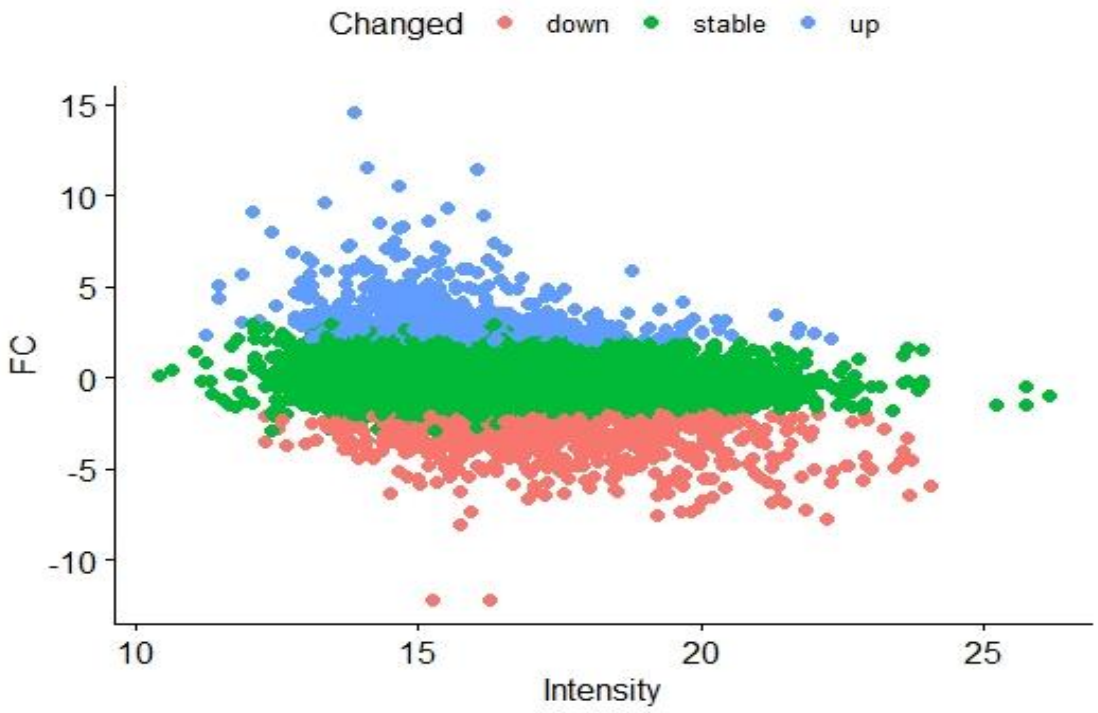

Figure 37. The upregulated and downregulated proteins in metformin-treated human skeletal muscle cells from obese insulin-sensitive participants

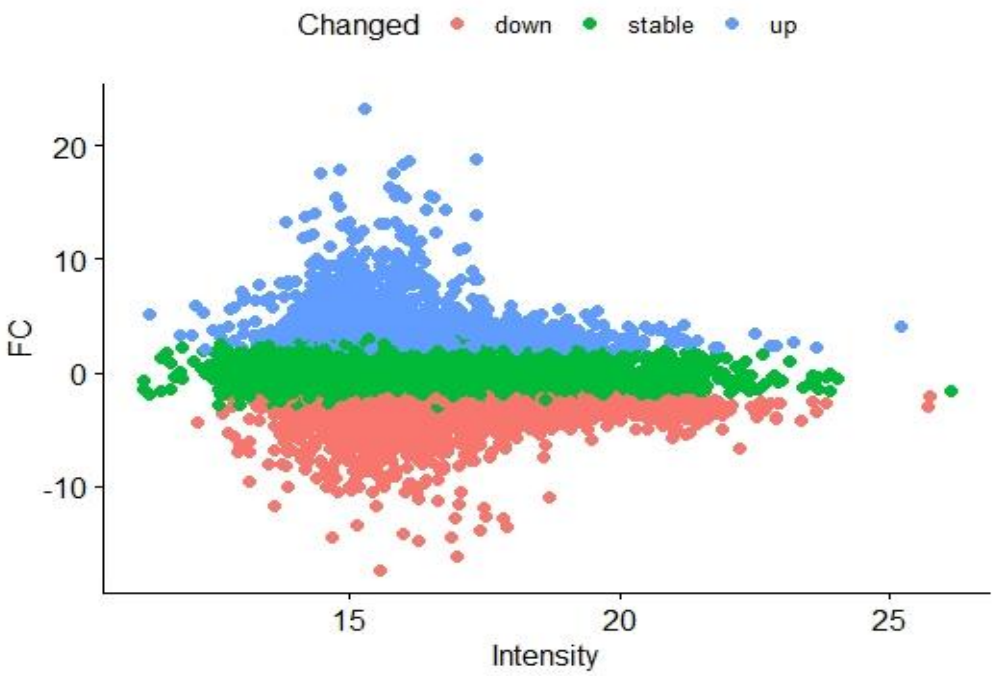

Figure 38. The upregulated and downregulated proteins in insulin-stimulation human skeletal muscle cells from lean insulin-sensitive participants

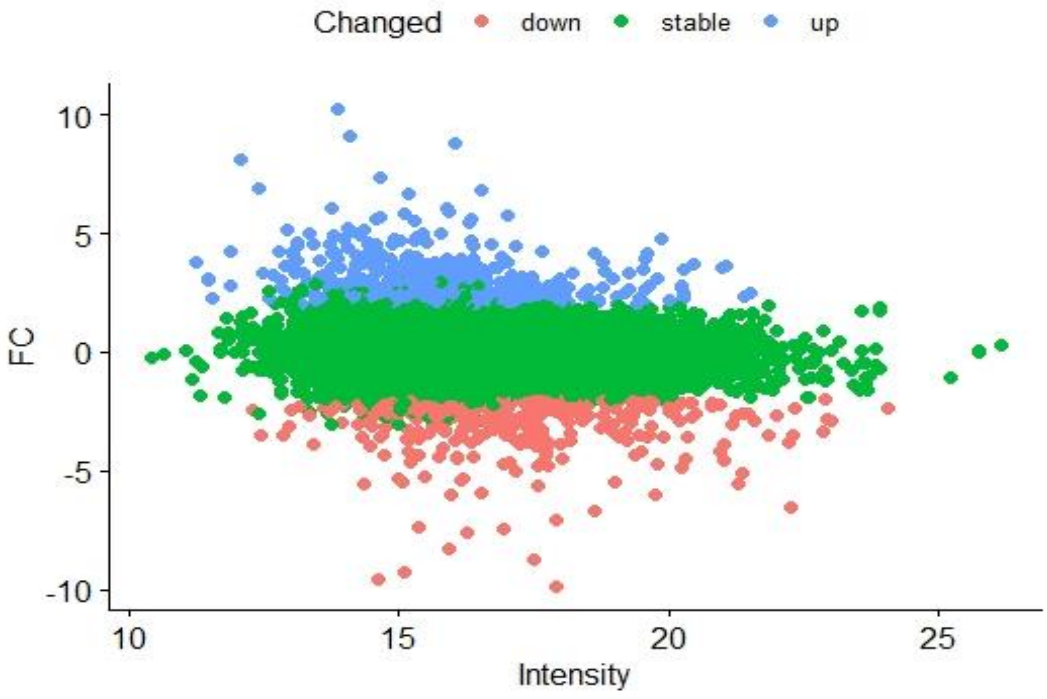

Figure 39. The upregulated and downregulated proteins in insulin-stimulation human skeletal muscle cells from obese insulin-sensitive participants

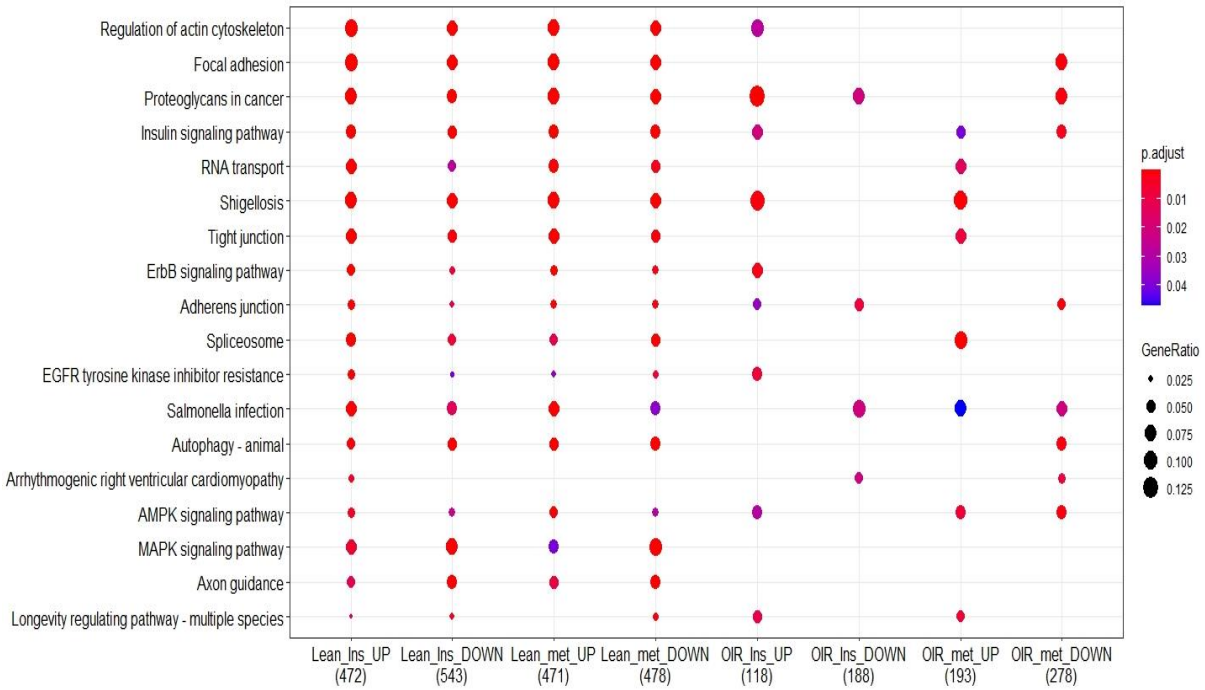

Figure 40. The significant pathways for the upregulated and downregulated phosphoproteins after metformin and upon insulin-stimulation

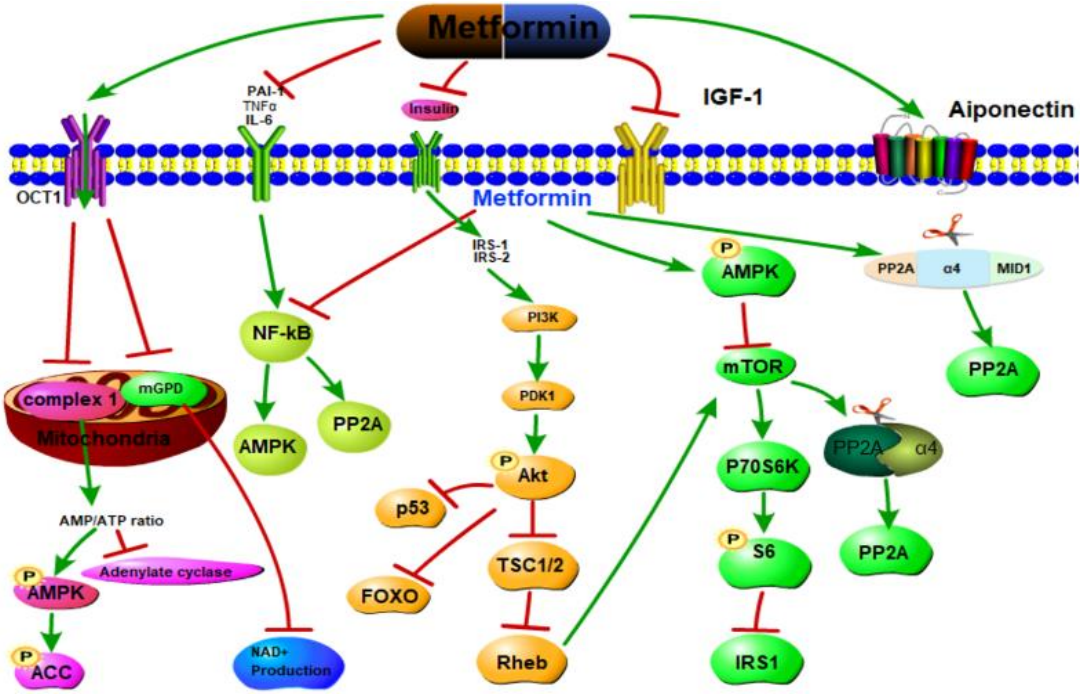

Figure 41. Integrative view of metformin molecular mechanism of action in multiple biological pathways

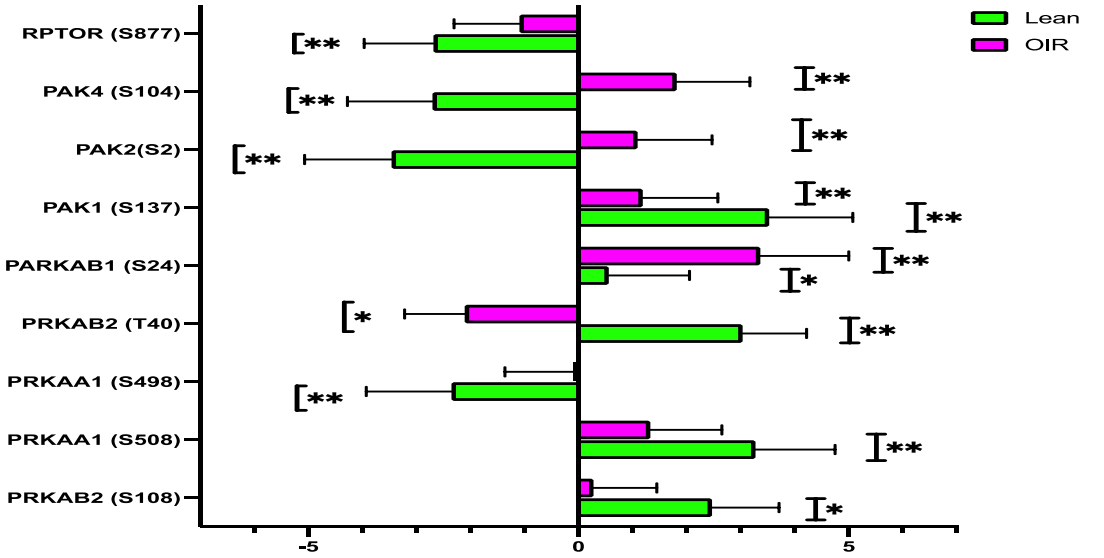

Figure 42. A significant changes of phosphorylation in PRKAB1 (AMPK-beta-1), PRKAA1 (AMPK-alpha-1), and PRKAB2 (AMPK-beta-2) after metformin treatment. Data are given as fold changes (means ± SEM); **: P<0.01, *: P<0.05

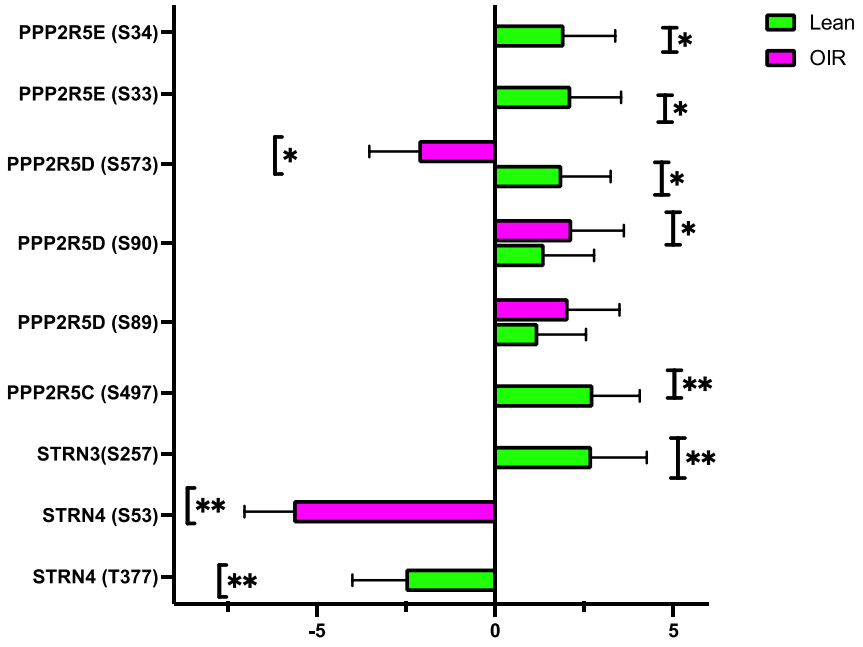

Figure 43. Significant changes in PP2A subunits were observed with after metformin treatments in our phosphoproteome experiment in both groups. Data are reported as fold changes (means ± SEM); **: P<0.01, *: P<0.05

Table 1. Numerous isoforms of different subunits of PP2A and their subcellular distribution in several tissues[28].

Subunit function	**Family**	**Protein**	**Isoform**	**Subcellular distribution**
Scaffolding A subunit		PPP2R1A	Aα	Cytosol
		PPP2R1B	Aβ	Cytosol
Catalytic C subunit		PPP2CA	Cα	Cytoplasm and Nucleus
		PPP2CB	Cβ	Cytoplasm and Nucleus
Regulatory B subunit	B (B55)	PPP2R2A	Bα	Cytosol, Membranes, Nucleus and Microtubules. Endoplasmic reticulum ,Golgi complex and Neurofilaments
		PPP2R2B	Bβ	Cytosol
		PPP2R2C	Bγ	Mainly in Cytoskeletal fraction
		PPP2R2D	Bδ	Cytosol
	B' (B56)	PPP2R5A	B'α	Cytoplasm
		PPP2R5B	B'β	Cytoplasm
		PPP2R5C	B'γ	Cytoplasm and Nucleus
		PPP2R5D	B'δ	Cytoplasm, Nucleus, Microsomes and Mitochondria
		PPP2R5E	B'ε	Cytoplasm
	B"	PPP2R3A	B"α	Centrosome and Golgi complex
		PPP2R3B	B"β	Cytosol and nucleus
		PPP2R3C	B"γ	Nucleus
		PPP2R3C	B"δ	Nucleus
		PPP2R3D	B"ε	Nucleus
	B"'	STRN		Cytoplasm and Membrane
		STRN3		Nucleus
		STRN4		Cytosol and Nucleus

Table 2. Clinical and metabolic characteristics of lean non-diabetic participants in the study. All measurements were done after an overnight fast

Participant #	1	2	3	4	5	6	7	8	**Mean**	**SEM**
Gender (M/F)	M	F	F	M	M	F	F	M		
Medical conditions	None	None	None	None	None	None	None	None		
Family history of T2D	None	None	None	None	None	None	None	None		
Age (years)	21	21	20	25	23	19	23	18	**21**	**1**
Blood pressure systolic (mmHg)	118	115	104	107	136	110	130	123	**118**	**4**
Blood pressure diastolic (mmHg)	56	76	63	66	88	63	73	63	**69**	**4**
Heart rate (beats/minute)	47	59	68	65	71	61	60	87	**65**	**4**
Respiratory Rate (breaths/minute)	18	18	20	20	16	20	20	16	**19**	**1**
Body Temperature (F)	97	98	98	98	96	98	98	98	**98**	**0**
Waist Circumference (cm)	80	79	69	96	77	71	80	81	**79**	**3**
Hip Circumference (cm)	88	86	92	99	100	79	87	103	**92**	**3**
Body height (inch)	71	64	66	69	74	61	68	70	**68**	**1**
Body weight (lb)	165	135	129	160	151	122	123	167	**144**	**7**
BMI (kg/m2) [a]	23.3	23.2	20.7	23.6	19.6	23	18.8	23.8	**22.0**	**0.7**
Blood chemistry										
HBA1c (%) [b]	5.2	5.4	5	5.4	5.4	5.5	5.2	5.6	**5**	**0**
Insulin (pmol/L)	38	36	107	45	36	28	35	32	**45**	**9**
Total Cholesterol (mg/dL)	109	121	121	163	109	160	149	142	**134**	**8**
Triglycerides (mg/dL)	42	92	68	105	49	66	54	56	**67**	**8**
HDL Cholesterol (mg/dL)	40	53	48	46	40	53	53	46	**47**	**2**
LDL Cholesterol (mg/dL)	61	50	59	96	59	94	85	85	**74**	**6**
Bioimpedance										
Percent fat mass (%)	19	11	22	27	3	23	17	16	**17**	**3**

Basal metabolic rate (calories)	1874	1714	1398	1559	2024	1330	1381	1931	**1651**	**96**
Bioresistance (Ohms)	518	334	633	639	355	580	624	501	**523**	**43**
OGTT										
Glucose 0 min (mg/dl) [c]	80	93	84	76	84	88	86	85	**85**	**2**
Glucose 30min (mg/dl)	119	140	122	137	151	167	139	112	**136**	**6**
Glucose 60min (mg/dl)	114	137	115	97	141	142	153	105	**125**	**7**
Glucose 90min (mg/dl)	85	114	100	109	89	116	114	113	**105**	**4**
Glucose 120 min (mg/dl) [d]	79	94	110	70	91	128	100	101	**97**	**6**
Hyperinsulinemic-euglycemic clamp										
Fasting plasma glucose before clamp (mg/dl) [c]	87	91	78	85	93	89	90	85	**87**	**2**
M value (mg/kgBW/min) [e]	12	9	16	10	11	10	11	9	**11**	**1**

[a] BMI: body mass index and criterion for overweight: ≥25 kg/m2

[b] criterion for normal HbA1c: <5.7%

[c] criterion for normal fasting plasma glucose: <100 mg/dl

[d] criterion for normal glucose tolerance: <140 mg/dl

[e] the average rate of glucose infusion during last 30 min of the hyperinsulinemic-euglycemic clamp, which is an index of insulin sensitivity.

Table 3. Clinical and metabolic characteristics of obese non-diabetic participants in the study. All measurements were done after an overnight fast.

Participant #	1	2	3	4	5	6	7	8	**Mean**	**SEM**
Gender (M/F)	M	M	F	F	M	M	F	F		
Medical conditions	None	None	None	None	None	None	None	None		
Family history of T2D	None	None	None	None	None	None	None	None		
Age (years)	56	18	20	22	24	22	48	21	**29**	**5**
Blood pressure systolic (mmHg)	125	130	109	132	135	136	126	111	**126**	**4**
Blood pressure diastolic (mmHg)	65	73	60	85	64	84	82	72	**73**	**3**
Heart rate (beats/minute)	77	87	70	85	101	83	92	92	**86**	**3**
Respiratory Rate (breaths/minute)	18	18	17	20	18	16	20	16	**18**	**1**
Body Temperature (F)	98	98.4	98.5	98	98.2	98.3	95.5	97.7	**98**	**0**
Waist Circumference (cm)	119.5	109.5	96	102	106	101	110	91	**104**	**3**
Hip Circumference (cm)	122	111.5	122	108	126	118	130	110	**118**	**3**
Body height (inch)	68.4	66	67.7	65.8	71	68.5	61.2	61.9	**66**	**1**
Body weight (lb)	252.4	235.7	218.7	193.1	241.1	238.7	204	167.4	**219**	**10**
BMI (kg/m2) [a]	35.5	38.1	33.5	31.4	33.7	35.8	38.3	30.7	**35**	**1**
Blood chemistry										
HBA1c (%) [b]	5.2	6.4	5.5	5.4	5.3	5.9	5.3	5.1	**5.6**	**0**
Insulin (pmol/L)	173	671	94	155.8	983.2	151.5	9.8	45.9	**320**	**123**
Total Cholesterol (mg/dL)	100	223	129	146	179	153	117	171	**150**	**14**
Triglycerides (mg/dL)	77	261	80	115	129	69	63	81	**113**	**23**
HDL Cholesterol (mg/dL)	46	39	44	42	44	54	52	50	**46**	**2**
LDL Cholesterol (mg/dL)	39	132	69	81	109	85	52	105	**81**	**11**
Bioimpedance										
Percent fat mass (%)	36.3	37.9	50.1	37.9	32.3	39.6	44.5	36.4	**40**	**2**
Basal metabolic rate (calories)	2202	1975	1496	1673	2289	2036	1670	1506	**1906**	**110**

Bioresistance (Ohms)	483	566	623	592	501	481	506	564	**536**	**19**
OGTT										
Glucose 0 min (mg/dl) [c]	84.6	88.7	81.8	84.9	82.8	89	82.9	78.6	**85**	**1**
Glucose 30min (mg/dl)	133	150	144	161.5	135	112	165	115	**143**	**7**
Glucose 60min (mg/dl)	129.5	145	150	178	147	145	200	136	**156**	**8**
Glucose 90min (mg/dl)	173	134	146	150.5	125	151	202	135	**155**	**9**
Glucose 120 min (mg/dl) [d]	178.5	126	100	156	99.5	134	169	128	**138**	**10**
Hyperinsulinemic-euglycemic clamp										
Fasting plasma glucose before clamp (mg/dl) [c]	96	97	82	87	81	97	87	76	**90**	**3**
M value (mg/kgBW/min) [e]	2.6	3.6	3	3	2.1	5.5	3	2.7	**3**	**0**

[a] BMI: body mass index and criterion for overweight: ≥30 kg/m^2

[b] criterion for normal HbA1c: <5.7%

[c] criterion for normal fasting plasma glucose: <100 mg/dl

[d] criterion for normal glucose tolerance: <140 mg/dl

[e] the average rate of glucose infusion during last 30 min of the hyperinsulinemic-euglycemic clamp, which is an index of insulin sensitivity.

Table 4. The clinical characteristics of lean and obese non-diabetic participants

Group	Gender (M/F)	Age (Years)	BMI (Kg/m²)	2h OGTT Glucose (mg/dl)	HBA1c (%)	Fasting plasma glucose (mg/dl)	M value (mg/kg/min)
Lean	**(4/4)**	**21.4±1.1**	**22.3±1.0 (<25)**	**96.5±6.0 (<140)**	**5.3±0.1 (<5.7)**	**87.2±2.2 (<100)**	**11.2±1.2**
Obese	**(4/4)**	**30.0±7.2**	**35.2±1.4* (>30)**	**137.6±14.7* (<140)**	**5.6±0.2 (<5.7)**	**89.6±4.0 (<100)**	**3.3±0.5***

- Data are presented as means±SEM, n=8
- In parenthesis: Criteria for obesity, normal glucose tolerance, normal HbA1c, and normal fasting plasma glucose
- All measurements were done after an overnight fast
- * P < 0.01

Table 5. Effect of metformin, insulin and okadaic acid on PP2A activity in primary human muscle cells derived from 8 Lean insulin-sensitive non-diabetic participants (n=8)

Participant #	**1**	**2**	**3**	**4**	**5**	**6**	**7**	**8**	**Mean**	**SEM**
	Amount of phosphate released by the PP2Ac immunoprecipitates (pmole) [#]									
Control	1089	1221	1255	1333	1638	1256	1217	1009	1,252	66
Metformin	1716	1866	1872	1767	1855	1816	2881	1620	1,924	140
Okadaic acid	672	1053	1044	561	1441	1145	1165	924	1,001	99
Insulin	1189	1255	1476	1413	1794	1274	1245	1142	1,349	75
Insulin & okadaic acid	874	940	910	1144	1484	1051	1202	985	1,074	71
Metformin & insulin	1053	1440	1405	1414	1561	1127	1803	1467	1,409	83
Metformin & okadaic acid	1299	1299	1085	1229	1343	961	1388	1334	1,242	52
Metformin, insulin & okadaic acid	946	856	896	1138	1339	822	1423	1263	1,085	83
	Normalized PP2A activity[#]									
Control	0.87	0.98	1	1.06	1.31	1	0.97	0.81	1.00	0.05
Metformin	1.37	1.49	1.5	1.41	1.48	1.45	2.3	1.29	1.54	0.11
Okadaic acid	0.54	0.84	0.83	0.45	1.15	0.91	0.63	0.74	0.76	0.08
Insulin	0.95	1	1.18	1.13	1.43	1.02	0.99	0.91	1.08	0.06
Insulin & okadaic acid	0.7	0.75	0.73	0.91	1.18	0.84	0.96	0.79	0.86	0.06
Metformin & insulin	0.84	1.15	1.12	1.13	1.25	0.9	1.44	1.17	1.13	0.07
Metformin & okadaic acid	1.04	1.04	0.87	0.98	1.07	0.77	1.11	1.07	0.99	0.04
Metformin, insulin & okadaic acid	0.76	0.68	0.72	0.91	1.07	0.66	1.14	1.01	0.87	0.07

- # Amount of phosphate released reflects the PP2A activity and the mean of the PP2A activity for the 8 samples without metformin treatment was set to 1.00.

Table 6. Effect of metformin, insulin and okadaic acid on PP2A activity in primary human muscle cells derived from 8 obese insulin resistant non-diabetic participants (n=8)

Participant #	**1**	**2**	**3**	**4**	**5**	**6**	**7**	**8**	**Mean**	**SEM**
	Amount of phosphate released by the PP2Ac immunoprecipitates (pmole) [#]									
Control	1520	1329	1047	1410	1349	2725	1067	1075	1,440	194
Metformin	2250	1952	1651	2165	2188	3345	1600	1662	2,102	200
Okadaic acid	1163	888	699	1155	1089	1909	895	952	1,094	129
Insulin	1553	1541	1088	1429	1369	2825	1081	1077	1,495	203
Insulin & okadaic acid	1079	1258	1033	1074	1131	2185	825	806	1,174	154
Metformin & insulin	1445	1430	1429	1292	1620	2703	1457	1481	1,607	160
Metformin & okadaic acid	1339	1323	1106	1290	1225	2231	763	741	1,252	163
Metformin, insulin & okadaic acid	957	898	1078	1184	1125	2325	695	660	1,115	185
	Normalized PP2A activity[#]									
Control	1.21	1.06	0.84	1.13	1.08	2.18	0.85	0.86	1.15	0.16
Metformin	1.8	1.56	1.32	1.73	1.75	2.67	1.28	1.33	1.68	0.16
Okadaic acid	0.93	0.71	0.56	0.92	0.87	1.52	0.72	0.76	0.87	0.10
Insulin	1.24	1.23	0.87	1.14	1.09	2.26	0.86	0.86	1.19	0.16
Insulin & okadaic acid	0.86	1	0.82	0.86	0.9	1.75	0.66	0.64	0.94	0.12
Metformin & insulin	1.15	1.14	1.14	1.03	1.29	2.16	1.16	1.18	1.28	0.13
Metformin & okadaic acid	1.07	1.06	0.88	1.03	0.98	1.78	0.61	0.59	1.00	0.13
Metformin, insulin & okadaic acid	0.76	0.72	0.86	0.95	0.9	1.86	0.56	0.53	0.89	0.15

- # Amount of phosphate released reflects the PP2A activity and the mean of the PP2A activity for the 8 samples without metformin treatment was set to 1.00.

Table 7. Identified and quantified novel sites from primary human skeletal muscle cells that were not reported in four large protein phosphorylation sites database.

Proteins	PhosphoSites	Protein Names	Gene Names
O43236	pS4	Septin-4	
Q9UHD8-5	pT200	Septin-9	
P49588	pS403	cytoplasmic	AARS
O15439	pS53	Multidrug resistance-associated protein 4	ABCC4
P08910	pT417	Abhydrolase domain-containing protein 2	ABHD2
O14639	pS214;pS498;pT504;pT653	Actin-binding LIM protein 1	ABLIM1
O94929	pS337;pS419;pS424;pS472;pS570;pT421;pT423	Actin-binding LIM protein 3	ABLIM3
Q12979-3	pT2	Active breakpoint cluster region-related protein	ABR
Q8N0Z2	pS153;pS156	Actin-binding Rho-activating protein	ABRA
Q9UKV3-5	pS828	Apoptotic chromatin condensation inducer in the nucleus	ACIN1
P35609	pS363	Alpha-actinin-2	ACTN2
P78563	pS10;pT73		ADARB1
O60503	pS1273;pT690	Adenylate cyclase type 9	ADCY9
P35611	pY419	Alpha-adducin	ADD1
Q9UEY8	pT653	Gamma-adducin	ADD3
Q16186	pS219	Proteasomal ubiquitin receptor ADRM1	ADRM1
Q6ZN18	pT6	Zinc finger protein AEBP2	AEBP2
Q8TED9	pS387;pS584;pS94	Actin filament-associated protein 1-like 1	AFAP1L1
Q9UPQ3	pT535	ANK repeat and PH domain-containing protein 1;Arf-GAP with GTPase	AGAP1
Q8N302	pS3	Angiogenic factor with G patch and FHA domains 1	AGGF1
Q5TGY3	pY1068		AHDC1
Q9UKA4	pS1177;pT462;pY1345		AKAP11
Q02952	pS1295;pT126;pT1475		AKAP12
Q12802	pT1947		AKAP13

Q12802-4	pS1584;pS1635;pS1927;pS2480;pT1893;pT1933		AKAP13
Q13023	pS1332;pS1653;pS424;pS610;pS746;pS908		AKAP6
Q96L96	pS1228;pS1401;pS1844;pS647;pT1190;pT1231;pT1392;pT597		ALPK3
Q96Q42	pT1472	Alsin	ALS2
Q8IY63	pS872	Angiomotin-like protein 1	AMOTL1
Q9Y2J4	pT679	Angiomotin-like protein 2	AMOTL2
Q01484	pT2719;pY2718	Ankyrin-2	ANK2
Q01484-5	pS1723;pS8;pS927;pS941	Ankyrin-2	ANK2
Q12955	pS2009;pS2625;pS3207;pS4352;pT4332	Ankyrin-3	ANK3
Q9P2G1	pS912	Ankyrin repeat and IBR domain-containing protein 1	ANKIB1
Q9GZV1	pS349;pT353	Ankyrin repeat domain-containing protein 2	ANKRD2
Q9UPS8	pS790;pS794	Ankyrin repeat domain-containing protein 26	ANKRD26
Q92625	pS381;pS382;pS589;pS676	Ankyrin repeat and SAM domain-containing protein 1A	ANKS1A
P08133	pS173	Annexin A6	ANXA6
O14617-2	pT786	AP-3 complex subunit delta-1	AP3D1
Q02410	pS575	Amyloid beta A4 precursor protein-binding family A member 1	APBA1
Q92870	pT125	Amyloid beta A4 precursor protein-binding family B member 2	APBB2
P25054	pS2468	Adenomatous polyposis coli protein	APC
Q6Q4G3	pY225	Aminopeptidase Q	AQPEP
Q9Y6D6	pT400	Brefeldin A-inhibited guanine nucleotide-exchange protein 1	ARFGEF1
Q9Y6D5	pT281	Brefeldin A-inhibited guanine nucleotide-exchange protein 2	ARFGEF2
Q07960	pT56	Rho GTPase-activating protein 1	ARHGAP1
Q8IWW6	pS114;pT581	Rho GTPase-activating protein 12	ARHGAP12
Q5T5U3	pS1568;pT1743	Rho GTPase-activating protein 21	ARHGAP21
Q9P227	pS545	Rho GTPase-activating protein 23	ARHGAP23
Q8N264	pS381	Rho GTPase-activating protein 24	ARHGAP24

Q9P2N2	pS629	Rho GTPase-activating protein 28	ARHGAP 28
Q2M1Z3	pS957	Rho GTPase-activating protein 31	ARHGAP 31
Q13017	pT1182	Rho GTPase-activating protein 5	ARHGAP 5
Q9BRR9	pT145	Rho GTPase-activating protein 9	ARHGAP 9
O15013	pS198;pS200;pS201	Rho guanine nucleotide exchange factor 10	ARHGEF 10
Q9NZN5	pS1394	Rho guanine nucleotide exchange factor 12	ARHGEF 12
Q96PE2	pS348;pS509;pS550;pS757;pS862;pT548	Rho guanine nucleotide exchange factor 17	ARHGEF 17
Q8TER5	pS984;pS997	Rho guanine nucleotide exchange factor 40	ARHGEF 40
Q12774	pS1394	Rho guanine nucleotide exchange factor 5	ARHGEF 5
Q15052	pT130	Rho guanine nucleotide exchange factor 6	ARHGEF 6
O14497	pS1195;pS735	AT-rich interactive domain-containing protein 1A	ARID1A
P29374	pS1164	AT-rich interactive domain-containing protein 4A	ARID4A
Q9UBL0	pS300;pS303;pS31;pS347;pS348;pS349;pS401;pS412;pT142;pT145;pT388;pT396;pT560	cAMP-regulated phosphoprotein 21	ARPP21
Q8TDY4	pS291	ANK repeat and PH domain-containing protein 3;Arf-GAP with SH3 domain	ASAP3
Q9ULI0	pS1379	ATPase family AAA domain-containing protein 2B	ATAD2B
Q96BY7	pS1576;pS1767	Autophagy-related protein 2 homolog B	ATG2B
P54259	pT736	Atrophin-1	ATN1
P98196	pT733	Probable phospholipid-transporting ATPase IH	ATP11A
Q9NQ11	pS433;pS443;pY442;pY448	Probable cation-transporting ATPase 13A2	ATP13A2
P20020-4	pS1139;pS1142	Plasma membrane calcium-transporting ATPase 1	ATP2B1
P46100	pS856;pT792		ATRX
P46379	pT102	Large proline-rich protein BAG6	BAG6
Q96PG8	pS160	Bcl-2-binding component 3	BBC3
P11274	pS1268	Breakpoint cluster region protein	BCR
Q96G01	pS610	Protein bicaudal D homolog 1	BICD1

O00499	pS286	Myc box-dependent-interacting protein 1	BIN1
O00499-10	pS320	Myc box-dependent-interacting protein 1	BIN1
Q9NR09	pT495	Baculoviral IAP repeat-containing protein 6	BIRC6
Q6QNY0	pT74	Biogenesis of lysosome-related organelles complex 1 subunit 3	BLOC1S3
P35226	pS320	Polycomb complex protein BMI-1	BMI1
Q9NSY1	pT1000;pT963		BMP2K
Q14692	pT265	Ribosome biogenesis protein BMS1 homolog	BMS1
Q8NFC6	pT489	Biorientation of chromosomes in cell division protein 1-like 1	BOD1L1
P55201	pS1081	Peregrin	BRPF1
Q8NE79	pS350	Blood vessel epicardial substance	BVES
Q711Q0	pS1246;pS160;pS517;pS844;pT680	Uncharacterized protein C10orf71	C10orf71
Q6NUN7	pS432;pS439;pT438	Uncharacterized protein C11orf63	C11orf63
Q6ZUT6	pS407	Uncharacterized protein C15orf52	C15orf52
Q8NEP4	pS486	Uncharacterized protein C17orf47	C17orf47
Q8N9M1	pS146	Uncharacterized protein C19orf47	C19orf47
Q9H425	pS167;pS171;pS173	Uncharacterized protein C1orf198	C1orf198
Q8TAB5	pS126	UPF0500 protein C1orf216	C1orf216
Q8NEQ6	pS56;pT60	Uncharacterized protein C1orf64	C1orf64
Q86YS7-3	pT445	C2 domain-containing protein 5	C2CD5
Q8WVR3-3	pS120;pS30;pS34	Uncharacterized protein C7orf43	C7orf43
Q1RMZ1	pT21	Probable methyltransferase BTM2 homolog	C7orf60
Q5VU97	pS265	VWFA and cache domain-containing protein 1	CACHD1
Q02641-2	pS46;pS513;pS62	Voltage-dependent L-type calcium channel subunit beta-1;Voltage-dependent L-type calcium channel subunit beta-2	CACNB1;CACNB2
Q8WUQ7	pS57;pS59	Cactin	CACTIN
Q8N1I8	pS44	Putative uncharacterized protein encoded by CACTIN-AS1	CACTIN-AS1
Q13554	pS367		CAMK2B
Q13557-10	pS348		CAMK2D
Q5T5Y3	pS1499	Calmodulin-regulated spectrin-associated protein 1	CAMSAP1
P40123	pS257;pT303	Adenylyl cyclase-associated protein 2	CAP2
P47756	pT267	F-actin-capping protein subunit beta	CAPZB

Q8WXE0	pS673;pS720;pT477	Caskin-2	CASKIN2
Q9NQ75	pS392	Cas scaffolding protein family member 4	CASS4
P20810-5	pS36;pT134	Calpastatin	CAST
Q03135-2	pS6	Caveolin-1	CAV1
Q6P1N0	pT460	Coiled-coil and C2 domain-containing protein 1A	CC2D1A
Q6DHV5-1	pY19	Protein CC2D2B	CC2D2B
Q6ZP82	pS282	Coiled-coil domain-containing protein 141	CCDC141
Q9Y3C0	pS185;pS186;pS188;pS190;pS193	WASH complex subunit CCDC53	CCDC53
Q96PX6	pS255;pS335;pS358	Coiled-coil domain-containing protein 85A	CCDC85A
Q9Y3X0	pS9	Coiled-coil domain-containing protein 9	CCDC9
Q567U6	pS490;pY497	Coiled-coil domain-containing protein 93	CCDC93
Q9BSQ5	pS287;pS292	Cerebral cavernous malformations 2 protein	CCM2
Q9HCU0	pT748;pT752	Endosialin	CD248
Q5VT25-6	pS1630		CDC42BPA
Q00587	pT377	Cdc42 effector protein 1	CDC42EP1
Q9UKI2	pT111;pT96	Cdc42 effector protein 3	CDC42EP3
Q9BXL8	pS36;pS41	Cell division cycle-associated protein 4	CDCA4
P55287	pS796	Cadherin-11	CDH11
P55291	pS198;pS801	Cadherin-15	CDH15
Q14004	pS1065		CDK13
Q00537	pS173		CDK17
Q9UKY7-3	pS5	Protein CDV3 homolog	CDV3
Q8N8U2	pS68;pS72;pS73;pS75	Chromodomain Y-like protein 2	CDYL2
Q15744	pS134	CCAAT/enhancer-binding protein epsilon	CEBPE
Q8N8E3	pT175;pT184	Centrosomal protein of 112 kDa	CEP112
Q9UPN4	pS83;pT50	Centrosomal protein of 131 kDa	CEP131
Q5SW79	pS1126;pS135;pS968;pS973;pT350	Centrosomal protein of 170 kDa	CEP170
Q9Y4F5	pY1314	Centrosomal protein of 170 kDa protein B	CEP170B
Q96ST8-2	pS9;pT11;pT16	Centrosomal protein of 89 kDa	CEP89
Q9Y281	pT6	Cofilin-2	CFL2

Q9BRQ6	pS81	MICOS complex subunit MIC25	CHCHD6
Q86WJ1	pS880		CHD1L
Q3L8U1	pT2071		CHD9
Q96EP1	pS205	E3 ubiquitin-protein ligase CHFR	CHFR
Q07001	pS378;pS379;pS385	Acetylcholine receptor subunit delta	CHRND
Q96RK0	pS154	Protein capicua homolog	CIC
Q86X95	pS390	Corepressor interacting with RBPJ 1	CIR1
P51797	pS684	Chloride transport protein 6	CLCN6
Q96DZ5	pT34	CAP-Gly domain-containing linker protein 3	CLIP3
Q00610-2	pS1638	Clathrin heavy chain 1	CLTC
Q96MX0	pS177;pS179;pS181	CKLF-like MARVEL transmembrane domain-containing protein 3	CMTM3
O95628	pT331	CCR4-NOT transcription complex subunit 4	CNOT4
Q13057	pY156	Phosphopantetheine adenylyltransferase	COASY
Q05707	pS1721;pS1724;pT1676	Collagen alpha-1(XIV) chain	COL14A1
Q07092	pS1043	Collagen alpha-1(XVI) chain	COL16A1
Q92793	pS2061	CREB-binding protein	CREBBP
P02511	pS153;pS66;pT63	Alpha-crystallin B chain	CRYAB
Q68DQ2	pS800		CRYBG3
P09603	pS541	Macrophage colony-stimulating factor 1;Processed macrophage colony-stimulating factor 1	CSF1
Q2NKJ3	pT301	CST complex subunit CTC1	CTC1
O43310	pS293	CBP80/20-dependent translation initiation factor	CTIF
P43235	pY307	Cathepsin K	CTSK
Q9NWM3	pS8	CUE domain-containing protein 1	CUEDC1
Q9HCG8	pS65		CWC22
A8MYA2	pS314	Uncharacterized protein CXorf49	CXorf49
Q7LFL8	pS48	CXXC-type zinc finger protein 5	CXXC5
Q9NYF0	pS485	Dapper homolog 1	DACT1
P53355	pS745		DAPK1
Q96JK2	pS533;pS627;pT650	DDB1- and CUL4-associated factor 5	DCAF5
O15075	pS174;pS294;pS302;pS355;pT168;pT296;pT354		DCLK1
Q8N568-3	pS317;pS358;pS705;pT700;pT710		DCLK2
Q9NPI6	pT409		DCP1A

Q9BW61	pT102	DET1- and DDB1-associated protein 1	DDA1
Q8NEL9	pS139;pS719;pT720	Phospholipase DDHD1	DDHD1
Q92499	pS486		DDX1
Q92841	pT55		DDX17
Q9BUQ8	pS39		DDX23
Q7L014	pS102;pS104		DDX46
Q8TEH3	pT470	DENN domain-containing protein 1A	DENND1A
Q6P3S1	pS654	DENN domain-containing protein 1B	DENND1B
P17661	pS266;pS46;pS460;pS47;pS48;pT431;pT463	Desmin	DES
O60231	pT110		DHX16
O60879	pS144;pY142	Protein diaphanous homolog 2	DIAPH2
O95661	pS117;pY116	GTP-binding protein Di-Ras3	DIRAS3
Q96QB1	pS856	Rho GTPase-activating protein 7	DLC1
Q8TDM6-5	pT4	Disks large homolog 5	DLG5
Q9Y2H0	pS620;pS946;pS977	Disks large-associated protein 4	DLGAP4
O00548	pS694;pS697;pT677	Delta-like protein 1	DLL1
P11532	pS2437	Dystrophin	DMD
Q9Y485	pY1643	DmX-like protein 1	DMXL1
Q14185	pS1861	Dedicator of cytokinesis protein 1	DOCK1
Q96BY6	pS1298	Dedicator of cytokinesis protein 10	DOCK10
Q96N67-2	pT933	Dedicator of cytokinesis protein 7	DOCK7
Q18PE1-3	pS542	Protein Dok-7	DOK7
Q9Y3R5	pT2203	Protein dopey-2	DOPEY2
Q03001	pS2225;pS2527;pS7364;pS7366;pS7367;pS7518;pT2211;pT2932;pT7369;pT7370	Dystonin	DST
Q96EV8	pS349;pS351;pT342	Dysbindin	DTNBP1
Q5VZP5	pS1005;pS1008;pS1010;pS1011;pS1030;pS1031;pS1032;pS1054;pS15;pS292;pS303;pS320;pS322;pS336;pS374;pS376;pS377;pS508;pS509;pS566;pS567;pS602;pS612;pS748;pT1029;pT340;pT889		DUSP27
Q99956	pS312	Dual specificity protein phosphatase 9	DUSP9
O14641	pS618;pS620	Segment polarity protein dishevelled homolog DVL-2	DVL2

O43237	pT220	Cytoplasmic dynein 1 light intermediate chain 2	DYNC1LI2
Q92630	pS571		DYRK2
P24534	pT153	Elongation factor 1-beta	EEF1B2
Q8NDI1	pS286;pS377	EH domain-binding protein 1	EHBP1
Q8N3D4	pS734;pT995	EH domain-binding protein 1-like protein 1	EHBP1L1
Q8N140	pS149	EP300-interacting inhibitor of differentiation 3	EID3
Q7L2H7	pS10	Eukaryotic translation initiation factor 3 subunit M	EIF3M
O43432	pS258	Eukaryotic translation initiation factor 4 gamma 3	EIF4G3
P55010	pT153	Eukaryotic translation initiation factor 5	EIF5
Q6PJG2	pS648	ELM2 and SANT domain-containing protein 1	ELMSAN1
Q05925	pS234	Homeobox protein engrailed-1	EN1
Q9Y6X5	pY360;pY371	Bis(5'-adenosyl)-triphosphatase ENPP4	ENPP4
Q9Y2J2-4	pT484	Band 4.1-like protein 3	EPB41L3
P29317	pS431	Ephrin type-A receptor 2	EPHA2
O95208-2	pS454	Epsin-2	EPN2
Q96RT1	pS1020;pS1140;pT1016	Protein LAP2	ERBB2IP
P28715	pS1038;pT528		ERCC5
P50548	pY116	ETS domain-containing transcription factor ERF	ERF
Q96HE7	pY305;pY308	ERO1-like protein alpha;ERO1-like protein beta	ERO1L;ERO1LB
Q9BSJ8	pT1032		ESYT1
Q9UI08	pS302		EVL
Q9BTL3	pS45	RNMT-activating mini protein	FAM103A1
Q969W3	pS177	Protein FAM104A	FAM104A
Q6P1L5	pS53	Protein FAM117B	FAM117B
Q5BKY9	pS246	Protein FAM133B	FAM133B
A8MVW0	pS411;pS476	Protein FAM171A2	FAM171A2
Q641Q2	pT479	WASH complex subunit FAM21A;WASH complex subunit FAM21C	FAM21A; FAM21C
Q9Y4E1	pS15	WASH complex subunit FAM21C	FAM21C
Q9Y4F9	pS42	Protein FAM65B	FAM65B
A6ND36	pS364	Protein FAM83G	FAM83G

P49327	pS2239;pS2240	[Acyl-carrier-protein] S-acetyltransferase;[Acyl-carrier-protein] S-malonyltransferase;3-hydroxyacyl-[acyl-carrier-protein] dehydratase;3-oxoacyl-[acyl-carrier-protein] reductase;3-oxoacyl-[acyl-carrier-protein] synthase;Enoyl-[acyl-carrier-protein] reductase;Fatty acid synthase;Oleoyl-[acyl-carrier-protein] hydrolase	FASN
Q9HCM7	pS830	Fibrosin-1-like protein	FBRSL1
Q9UK96	pY505	F-box only protein 10	FBXO10
P37268	pS89;pT87	Squalene synthase	FDFT1
Q96AC1	pT356	Fermitin family homolog 2	FERMT2
Q2V2M9-4	pS613;pS881;pT1474;pT1476;pT967	FH1/FH2 domain-containing protein 3	FHOD3
Q7Z7B0	pS1005;pT1011;pT622	Filamin-A-interacting protein 1	FILIP1
Q4L180	pT1008;pY1070	Filamin A-interacting protein 1-like	FILIP1L
Q5T1M5	pT355	FK506-binding protein 15	FKBP15
Q00688	pT103	Peptidyl-prolyl cis-trans isomerase FKBP3	FKBP3
Q13045	pY940	Protein flightless-1 homolog	FLII
Q14315	pS2152;pS2405;pS2461;pS2633;pT2149;pT2446	Filamin-C	FLNC
Q68DA7-5	pS88	Formin-1	FMN1
Q12778	pT317	Forkhead box protein O1	FOXO1
Q5H8C1-2	pS435	FRAS1-related extracellular matrix protein 1	FREM1
Q96NE9	pT613	FERM domain-containing protein 6	FRMD6
Q9BZ67	pS451	FERM domain-containing protein 8	FRMD8
Q5TBA9	pS1955;pS2649;pT940	Protein furry homolog	FRY
Q5CZC0	pS99	Fibrous sheath-interacting protein 2	FSIP2
Q8IY81	pS468		FTSJ3
Q96QD9	pS33	UAP56-interacting factor	FYTTD1
Q13480-2	pT377	GRB2-associated-binding protein 1	GAB1
Q9UQC2	pS212	GRB2-associated-binding protein 2	GAB2
P24522	pS28		GADD45A
Q14C86	pS772	GTPase-activating protein and VPS9 domain-containing protein 1	GAPVD1
Q86YP4	pT188		GATAD2A
P50395	pS65	Rab GDP dissociation inhibitor beta	GDI2

P55042	pS306	GTP-binding protein GEM;GTP-binding protein RAD	GEM;RRAD
P10912	pS375	Growth hormone-binding protein;Growth hormone receptor	GHR
Q14161	pT626	ARF GTPase-activating protein GIT2	GIT2
Q96KN9	pS277;pS327	Gap junction delta-4 protein	GJD4
Q86VQ1	pS226;pS397	Glucocorticoid-induced transcript 1 protein	GLCCI1
Q14789	pS1956	Golgin subfamily B member 1	GOLGB1
Q86SQ6-1	pS1065	Probable G-protein coupled receptor 123	GPR123
Q8TDV0	pS366;pS367;pS370	Probable G-protein coupled receptor 151	GPR151
Q9NZH0	pS360	G-protein coupled receptor family C group 5 member B	GPRC5B
Q96HH9	pT51	GRAM domain-containing protein 3	GRAMD3
Q13322	pS438	Growth factor receptor-bound protein 10	GRB10
P35269	pT400	General transcription factor IIF subunit 1	GTF2F1
Q8WUA4	pS219	General transcription factor 3C polypeptide 2	GTF3C2
P13807	pS701;pS702;pS704;pS706;pT703	Glycogen [starch] synthase;muscle	GYS1
Q9UJM8	pS218	Hydroxyacid oxidase 1	HAO1
P56524	pT244	Histone deacetylase 4;Histone deacetylase 5;Histone deacetylase 9	HDAC4;HDAC5;HDAC9
Q9UKV0-3	pS457;pS491	Histone deacetylase 9	HDAC9
Q7Z4V5	pS419	Hepatoma-derived growth factor-related protein 2	HDGFRP2
Q7Z4Q2	pT31	HEAT repeat-containing protein 3	HEATR3
Q9ULT8	pS1380;pS1517	E3 ubiquitin-protein ligase HECTD1	HECTD1
Q8WVB3	pS477	Hexosaminidase D	HEXDC
Q9NQ87	pS10	Hairy/enhancer-of-split related with YRPW motif-like protein	HEYL
Q96A08	pS86;pS92;pY85	Histone H2B type 1-A	HIST1H2BA
Q01581	pT490	cytoplasmic;Hydroxymethylglutaryl-CoA synthase	HMGCS1
Q9UK76	pT38	Hematological and neurological expressed 1 protein	HN1

Q99729-3	pS266	Heterogeneous nuclear ribonucleoprotein A/B	HNRNPAB
P07910-2	pS169	Heterogeneous nuclear ribonucleoproteins C1/C2	HNRNPC
Q5SSJ5	pS110;pT114	Heterochromatin protein 1-binding protein 3	HP1BP3
P23327	pS482	Sarcoplasmic reticulum histidine-rich calcium-binding protein	HRC
P51659	pT321	Enoyl-CoA hydratase 2	HSD17B4
Q00613	pT328	Heat shock factor protein 1	HSF1
P48723	pY119	Heat shock 70 kDa protein 13	HSPA13
Q12988	pS53	Heat shock protein beta-3	HSPB3
O14558	pS23	Heat shock protein beta-6	HSPB6
O43719	pS389	HIV Tat-specific factor 1	HTATSF1
P28223	pS219;pT201	5-hydroxytryptamine receptor 2A	HTR2A
Q0D2I5	pS377	Intermediate filament family orphan 1	IFFO1
Q9UG01	pY1388	Intraflagellar transport protein 172 homolog	IFT172
Q8WYA0	pS39	Intraflagellar transport protein 81 homolog	IFT81
Q96PD4	pS138;pS140	Interleukin-17F	IL17F
P24001	pT143;pT223	Interleukin-32	IL32
Q9Y2H2	pS881	Phosphatidylinositide phosphatase SAC2	INPP5F
F8WCM5	pS116	Insulin;isoform 2	INS-IGF2
P35568	pS272	Insulin receptor substrate 1	IRS1
Q9UKP3	pS107	Integrin beta-1-binding protein 2	ITGB1BP2
Q6UXX5	pS870	Inter-alpha-trypsin inhibitor heavy chain H6	ITIH6
Q15811	pT1146	Intersectin-1	ITSN1
Q9NZM3	pS216	Intersectin-2	ITSN2
Q9BR39	pS523;pT525	Junctophilin-2	JPH2
Q96MG2	pS320		JSRP1
Q63ZY3-2	pS151;pS155;pT149;pT472	KN motif and ankyrin repeat domain-containing protein 2	KANK2
Q9BVA0	pS356	Katanin p80 WD40 repeat-containing subunit B1	KATNB1
Q14721	pS783;pT733;pT782	Potassium voltage-gated channel subfamily B member 1	KCNB1
P51787	pS407	Potassium voltage-gated channel subfamily KQT member 1	KCNQ1
P56696	pS41	Potassium voltage-gated channel subfamily KQT member 4	KCNQ4

Q9H3F6	pS28	BTB/POZ domain-containing adapter for CUL3-mediated RhoA degradation protein 3	KCTD10
Q96CX2	pS162	BTB/POZ domain-containing protein KCTD12	KCTD12
Q9Y597-2	pT586	BTB/POZ domain-containing protein KCTD3	KCTD3
O60303	pS252;pS253	Uncharacterized protein KIAA0556	KIAA0556
Q5T5P2	pT465	Sickle tail protein homolog	KIAA1217
Q9BY89	pT1706	Uncharacterized protein KIAA1671	KIAA1671
Q9ULH0	pS1717		KIDINS220
P52732	pS758	Kinesin-like protein KIF11	KIF11
Q9H1H9-2	pT1385	Kinesin-like protein KIF13A	KIF13A
Q5T7B8	pS875;pS878	Kinesin-like protein KIF24	KIF24
Q2KJY2	pS1773	Kinesin-like protein KIF26B	KIF26B
O95239	pS936;pY933	Chromosome-associated kinesin KIF4A	KIF4A
P57682	pS70	Krueppel-like factor 3	KLF3
O95600	pS17;pS21	Krueppel-like factor 8	KLF8
Q9H511	pS626;pS628;pS629	Kelch-like protein 31	KLHL31
Q03164	pS3529	Histone-lysine N-methyltransferase 2A;MLL cleavage product C180;MLL cleavage product N320	KMT2A
O14686	pT4368	Histone-lysine N-methyltransferase 2D	KMT2D
Q8N9T8	pS182	Protein KRI1 homolog	KRI1
Q8IVT5	pS192		KSR1
Q9UN81	pS18	LINE-1 retrotransposable element ORF1 protein	L1RE1
Q6IAA8	pS113	Ragulator complex protein LAMTOR1	LAMTOR1
Q9BRS8	pT70	La-related protein 6	LARP6
Q14739	pS70;pS73;pT68	Lamin-B receptor	LBR
O75112-7	pS121;pS123;pS143;pS147;pS173;pS510;pT132;pT135;pT141;pT511	LIM domain-binding protein 3	LDB3
Q9UPQ0	pS1002;pS992;pS995	LIM and calponin homology domains-containing protein 1	LIMCH1
Q05469	pT868	Hormone-sensitive lipase	LIPE
Q8WWI1	pS1539;pS392	LIM domain only protein 7	LMO7

Q6P5Q4	pS186;pS24;pS26;pS386;pS387;pS388;pS392;pS396;pS399;pS400;pS515;pT197;pT516;pT59	Leiomodin-2	LMOD2
Q0VAK6	pS2;pS28;pS5	Leiomodin-3	LMOD3
Q0VAK6-2	pY2	Leiomodin-3	LMOD3
P57059	pS547;pT526		LOC102724428;SIK1
Q14693	pS598;pS599;pS600;pS601;pS723;pT733;pY721	Phosphatidate phosphatase LPIN1;Phosphatidate phosphatase LPIN2	LPIN1;LPIN2
O75427	pT19	Leucine-rich repeat and calponin homology domain-containing protein 4	LRCH4
Q3SXY7	pT503	immunoglobulin-like domain and transmembrane domain-containing protein 3;Leucine-rich repeat	LRIT3
Q5VZK9	pT1253	Leucine-rich repeat-containing protein 16A	LRRC16A
Q32MZ4	pS132;pS75	Leucine-rich repeat flightless-interacting protein 1	LRRFIP1
Q32MZ4-4	pS165;pS171;pS179;pS187;pS190;pS204;pY189	Leucine-rich repeat flightless-interacting protein 1	LRRFIP1
Q9Y608	pS195;pS276;pS285	Leucine-rich repeat flightless-interacting protein 2	LRRFIP2
Q86V48	pS667;pT998	Leucine zipper protein 1	LUZP1
Q9Y250	pS237;pT214	Leucine zipper putative tumor suppressor 1	LZTS1
Q9UPN3	pS2027;pS2836;pS3000;pS3168;pS3169;pS3259;pT2005;pT7246;pT7340	isoforms 1/2/3/5;Microtubule-actin cross-linking factor 1	MACF1
Q9H063	pS85		MAF1
Q9HCI5	pS619	Melanoma-associated antigen E1	MAGEE1
P78559	pS1154;pS2126;pS2135;pS2172;pS2237;pS2419;pS2652;pS2686;pS385;pS990;pT1084;pT2042;pT2137;pT2142;pT2468;pT2651;pT326	MAP1 light chain LC2;MAP1A heavy chain;Microtubule-associated protein 1A	MAP1A
P46821	pS2254;pS2255;pS770	MAP1 light chain LC1;MAP1B heavy chain;Microtubule-associated protein 1B	MAP1B

Q66K74	pT460	MAP1S heavy chain;MAP1S light chain;Microtubule-associated protein 1S	MAP1S
P11137	pS1011	Microtubule-associated protein 2	MAP2
O43318	pT446		MAP3K7
O95819-3	pS925;pS926		MAP4K4
O95819-6	pS548;pS604;pS878		MAP4K4
Q9UPT6	pS750;pS754;pT367;pT753		MAPK8IP3
Q15555	pS229	Microtubule-associated protein RP/EB family member 2	MAPRE2
Q7KZI7-14	pS602;pS7		MARK2
P27448	pS410;pS411		MARK3
Q6P0Q8	pT1036		MAST2
O60307	pT785		MAST3
P43243	pS705	Matrin-3	MATR3
O95983	pS60	Methyl-CpG-binding domain protein 3	MBD3
Q8IVS2	pY334	Malonyl-CoA-acyl carrier protein transacylase;mitochondrial	MCAT
Q9BTE3	pS156		MCMBP
Q15648	pS996;pT998		MED1
Q71F56	pS1071		MED13L
Q02078-3	pT242	Myocyte-specific enhancer factor 2A	MEF2A
Q06413-6	pS382;pT440	Myocyte-specific enhancer factor 2C	MEF2C
Q14814-5	pS97;pT107	Myocyte-specific enhancer factor 2D	MEF2D
Q7L2J0	pS370		MEPCE
Q14696	pS221	LDLR chaperone MESD	MESDC2
Q6ZN04	pS48		MEX3B
Q86XN8	pT516		MEX3D
O60291	pT498	E3 ubiquitin-protein ligase MGRN1	MGRN1
Q8TDZ2	pS887;pS962	Protein-methionine sulfoxide oxidase MICAL1	MICAL1
O94851	pY613	Protein-methionine sulfoxide oxidase MICAL2	MICAL2
Q7RTP6	pS1637	Protein-methionine sulfoxide oxidase MICAL3	MICAL3
Q8IY33	pS130	MICAL-like protein 2	MICALL2
Q5VWP3-3	pS348;pS408;pS432;pS468;pS470;pS509;pS520;pS595;pS704;pS815;pT458;pT526		MLIP
Q9H8L6	pT386;pT387	Multimerin-2	MMRN2

O00566	pS178	U3 small nucleolar ribonucleoprotein protein MPP10	MPHOSPH10
Q99549	pS425	M-phase phosphoprotein 8	MPHOSPH8
Q00013	pS237	55 kDa erythrocyte membrane protein	MPP1
Q6WCQ1	pS1022;pT1025	Myosin phosphatase Rho-interacting protein	MPRIP
Q6WCQ1-2	pT982	Myosin phosphatase Rho-interacting protein	MPRIP
P49959	pT700	Double-strand break repair protein MRE11A	MRE11A
Q9Y3D3	pT137	28S ribosomal protein S16;mitochondrial	MRPS16
P82909	pY67	28S ribosomal protein S36;mitochondrial	MRPS36
Q9Y4B5	pT1804	Microtubule cross-linking factor 1	MTCL1
Q96QG7	pT541	Myotubularin-related protein 9	MTMR9
P42345	pS2127;pY2125		MTOR
Q765P7	pT298;pT619;pT622	MTSS1-like protein	MTSS1L
Q5BKX8	pS172;pS173;pS19;pS258;pS260;pS302;pS307;pS311;pS315;pS363;pS364;pT32;pY310	Muscle-related coiled-coil protein	MURC
O15146	pS541;pS691;pT538	Muscle	MUSK
P84157-2	pS34	Matrix-remodeling-associated protein 7	MXRA7
P84157-3	pS176	Matrix-remodeling-associated protein 7	MXRA7
Q9BQG0	pS731;pS732;pS734;pS738;pS743	Myb-binding protein 1A	MYBBP1A
P10243	pS611	Myb-related protein A	MYBL1
Q00872-2	pT66	Myosin-binding protein C;slow-type	MYBPC1
Q13203	pS13;pS445;pS449	Myosin-binding protein H	MYBPH
O75592	pS2838;pS2898	E3 ubiquitin-protein ligase MYCBP2	MYCBP2
P11055	pS1020;pS1037;pS1038;pS1235;pS1270;pS1272;pS1279;pS1297;pS1303;pS1363;pS1438;pS1938;pS54;pS55;pS632;pS643;pS649;pT1275;pT5;pT624;pT647	Myosin-1;Myosin-13;Myosin-2;Myosin-3;Myosin-4;Myosin-8	MYH1;MYH13;MYH2;MYH3;MYH4;MYH8
P13535	pS1202;pS1742;pS1935	Myosin-8	MYH8
Q02045	pS20;pS21;pS25	Myosin light chain 5	MYL5
P14649	pS16;pS18;pS192	Myosin light chain 6B	MYL6B
Q96A32	pS132;pS20;pT114;pT81	Myosin regulatory light chain 2;skeletal muscle isoform	MYLPF

Q9HD67	pS2056		MYO10
Q8IUG5	pS114;pS1675;pS181;pS20;pS2147;pS2170;pS2217;pS2226;pS2232;pS2245;pS2247;pS2251;pS2302;pS24;pS2460;pS25;pS2542;pS31;pS62;pT180;pT2277;pT2541		MYO18B
Q12965	pS127;pT119;pY124;pY128		MYO1E
Q9NQX4	pT1708		MYO5C
P15172	pS263;pS278		MYOD1
P15173	pS43	Myogenin	MYOG
Q9NP98	pS116	Myozenin-1	MYOZ1
Q9NPC6	pS101	Myozenin-2	MYOZ2
Q86TC9	pS128;pS1317;pS386;pS613;pS766;pT420;pY422	Myopalladin	MYPN
A2RRP1	pS1937	Neuroblastoma-amplified sequence	NBAS
Q9HCH0	pS809;pS810;pS816;pS818	Nck-associated protein 5-like	NCKAP5L
O75376	pS1381;pT991	Nuclear receptor corepressor 1	NCOR1
Q9Y618	pT2392	Nuclear receptor corepressor 2	NCOR2
P20929-3	pS216;pS224;pS8396;pS8423;pS8458;pS8459;pT8421;pT8452;pY8367	Nebulin	NEB
Q96PY6	pS1057		NEK1
P48681	pS1261;pS1268;pS1462;pS1466;pS1506;pS465;pS666;pS873;pT1003;pT1294;pT1487;pT304;pT354	Nestin	NES
O95644	pS256;pS286;pT284	cytoplasmic 1;Nuclear factor of activated T-cells	NFATC1
Q6P4R8	pT1287;pT1288	Nuclear factor related to kappa-B-binding protein	NFRKB
Q14112	pY733	Nidogen-2	NID2
O15226	pS428;pT426	NF-kappa-B-repressing factor	NKRF
Q8TAU0	pS13	Homeobox protein Nkx-2.3	NKX2-3
O60551	pY42	Glycylpeptide N-tetradecanoyltransferase 2	NMT2
Q5SY16	pT90		NOL9
Q9Y314	pS147	Nitric oxide synthase-interacting protein	NOSIP
Q9UM47	pS2117	Neurogenic locus notch homolog protein 3;Notch 3 extracellular truncation;Notch 3 intracellular domain	NOTCH3

P49116	pS44	Nuclear receptor subfamily 2 group C member 2	NR2C2
Q9NSY0	pT419	Nuclear receptor-binding protein 2	NRBP2
Q02297	pS383	membrane-bound isoform;Neuregulin-1;Pro-neuregulin-1	NRG1
O60285	pS380;pT414		NUAK1
Q7Z417	pT117	Nuclear fragile X mental retardation-interacting protein 2	NUFIP2
P35658	pS991	Nuclear pore complex protein Nup214	NUP214
Q5VST9	pT6815	Obscurin	OBSCN
Q5VST9-3	pS4783;pS4801;pS4804;pS4815;pS5034;pS5252;pS5567;pS5573;pS5588;pS5589;pS5590;pS5592;pS5686;pS6245;pS6252;pS6256;pS6262;pS6345;pS6538;pT4803;pT5253;pT6240;pT6241;pY402	Obscurin	OBSCN
Q9NZT2	pS539	Opioid growth factor receptor	OGFR
O60890	pS654	Oligophrenin-1	OPHN1
Q96CV9	pT450	Optineurin	OPTN
Q9BXW6	pS890	Oxysterol-binding protein-related protein 1	OSBPL1A
Q9BZF3	pS344	Oxysterol-binding protein-related protein 6	OSBPL6
Q8N7B6	pS46	PACRG-like protein	PACRGL
Q9BY11	pS339;pS348;pS349;pT332		PACSIN1
P00439	pY179	Phenylalanine-4-hydroxylase	PAH
O96013	pY480		PAK4
Q8WX93	pS1167;pS206;pS236;pS399;pS400;pS74;pT100;pT55;pT70	Palladin	PALLD
Q8WX93-9	pS737	Palladin	PALLD
Q9NP74	pT387;pT494	Palmdelphin	PALMD
P51003	pT652	Poly(A) polymerase alpha	PAPOLA
Q9BVG4	pT187	Protein PBDC1	PBDC1
Q15366	pT169	Poly(rC)-binding protein 2	PCBP2
Q9HCL0	pS780;pS781	Protocadherin-18	PCDH18
Q9HC56	pS943	Protocadherin-9	PCDH9
Q15154-5	pT1557	Pericentriolar material 1 protein	PCM1
Q14123	pS669;pS677;pY667	5'-cyclic nucleotide phosphodiesterase 1C;Calcium/calmodulin-dependent 3'	PDE1C
Q53GG5-2	pS237;pT176;pT30	PDZ and LIM domain protein 3	PDLIM3

Q53GG5-3	pS169;pS170	PDZ and LIM domain protein 3	PDLIM3
P50479	pS132	PDZ and LIM domain protein 4	PDLIM4
O15530	pS250		PDPK1;PDPK2P
Q9NTI5	pS1406	Sister chromatid cohesion protein PDS5 homolog B	PDS5B
Q9H792	pS1169		PEAK1
Q5VY43	pS915;pS918	Platelet endothelial aggregation receptor 1	PEAR1
Q8IZL8	pT1069	glutamic acid- and leucine-rich protein 1;Proline-	PELP1
O95336	pS52		PGLS
O95394	pS50	Phosphoacetylglucosamine mutase	PGM3
Q8NDX5	pS277	Polyhomeotic-like protein 3	PHC3
Q86UU1	pS412;pS526;pS942;pT435;pT52;pT548	Pleckstrin homology-like domain family B member 1	PHLDB1
Q86SQ0	pS414;pS521	Pleckstrin homology-like domain family B member 2	PHLDB2
Q9P1Y6	pS1373	PHD and RING finger domain-containing protein 1	PHRF1
Q9H611	pS363		PIF1
Q16512	pT388;pT531;pT909		PKN1
Q15111	pS565;pS97		PLCL1
Q15149	pS2833	Plectin	PLEC
Q9HB20	pT246	Pleckstrin homology domain-containing family A member 3	PLEKHA3
Q9H4M7	pS567	Pleckstrin homology domain-containing family A member 4	PLEKHA4
Q9Y2H5	pT784	Pleckstrin homology domain-containing family A member 6	PLEKHA6
Q9H7P9	pS1254	Pleckstrin homology domain-containing family G member 2	PLEKHG2
O94827	pS957;pS990;pS993	Pleckstrin homology domain-containing family G member 5	PLEKHG5
Q8IWE5	pS264	Pleckstrin homology domain-containing family M member 2	PLEKHM2
O60664	pS137;pS138	Perilipin-3	PLIN3
Q8TF01	pS762;pS764;pT297	Arginine/serine-rich protein PNISR	PNISR
Q9UGP5	pT164		POLL
O15514	pS50;pS58		POLR2D
P0CAP2	pS268		POLR2M
O75335	pS612;pS635;pS644	Liprin-alpha-4	PPFIA4
Q86W92-2	pS447	Liprin-beta-1	PPFIBP1

Q13427	pS506;pS533;pS535;pS658;pS660	Peptidyl-prolyl cis-trans isomerase G	PPIG
O60437	pT19	Periplakin	PPL
O14974	pS455	Protein phosphatase 1 regulatory subunit 12A	PPP1R12A
O60237	pS391	Protein phosphatase 1 regulatory subunit 12B	PPP1R12B
Q6ZMI0	pS38	Protein phosphatase 1 regulatory subunit 21	PPP1R21
Q6ZSY5	pT4	Protein phosphatase 1 regulatory subunit 3F	PPP1R3F
Q9ULJ8	pS95	Neurabin-1	PPP1R9A
P30044	pS168;pS171	mitochondrial;Peroxiredoxin-5	PRDX5
Q8N945	pS70	PRELI domain-containing protein 2	PRELID2
Q7Z3G6	pS546	Prickle-like protein 2	PRICKLE2
O43741	pS44		PRKAB2
P17612	pY205		PRKACA;PRKACB;PRKACG
Q9UGI9	pS162;pS65		PRKAG3
Q15139	pS251;pS399;pT214		PRKD1;PRKD3
E7EW31	pS142;pS150;pS179;pS218;pS427;pS452;pS454;pS470;pS477;pS581;pS809;pS862;pS922;pT776;pT820;pT823	Proline-rich basic protein 1	PROB1
Q9UF12	pY157		PRODH2
O75400	pS826;pS830;pS914;pS918;pT368		PRPF40A
Q13523	pS230;pS376;pS379		PRPF4B
O94906	pY376		PRPF6
A8MZF0	pS59;pS67;pT171	Proline-rich protein 33	PRR33
P85299	pS309	Proline-rich protein 5	PRR5
P48634	pS1670	Protein PRRC2A	PRRC2A
Q9Y520	pS1545;pS2680	Protein PRRC2C	PRRC2C
C9JH25	pS707;pS731	Proline-rich transmembrane protein 4	PRRT4
Q8WUY3	pS1324;pS1326;pS1391;pS1527;pS1628;pS1788;pS1833;pS2181;pS2185;pS2249;pS2416;pS2571;pS2602;pS2626;pS2632;pS2864;pS693;pS701;pS707;pS827;pT1618;pT2137;pT2393	Protein prune homolog 2	PRUNE2

E9PB15	pS165;pT164	Putative protein PTGES3L	PTGES3L
Q05209	pT574;pT587;pT598	Tyrosine-protein phosphatase non-receptor type 12	PTPN12
Q15678	pY589	Tyrosine-protein phosphatase non-receptor type 14	PTPN14
Q16825	pS554;pS582;pT605;pT656;pY552	Tyrosine-protein phosphatase non-receptor type 21	PTPN21
Q9NQS3-3	pT386	Nectin-3	PVRL3
P49023	pS216	Paxillin	PXN
Q9Y2K5	pS336;pT331	R3H domain-containing protein 2	R3HDM2
Q9BXF6	pS407	Rab11 family-interacting protein 5	RAB11FIP5
Q12829	pS265	Ras-related protein Rab-40B	RAB40B
Q15276	pS386	Rab GTPase-binding effector protein 1	RABEP1
Q5R372	pS128	Rab GTPase-activating protein 1-like	RABGAP1L
P43351	pS157		RAD52
Q9P0K7-4	pS261	Ankycorbin	RAI14
Q13905-4	pS10;pS357;pS382	Rap guanine nucleotide exchange factor 1	RAPGEF1
Q70E73	pS139;pT1146	Ras-associated and pleckstrin homology domains-containing protein 1	RAPH1
P20936	pS582	Ras GTPase-activating protein 1	RASA1
Q9H2L5	pS144;pS147	Ras association domain-containing protein 4	RASSF4
Q7Z6E9	pS1535	E3 ubiquitin-protein ligase RBBP6	RBBP6
Q08999	pS941	Retinoblastoma-like protein 2	RBL2
Q8IXT5	pY285		RBM12B
Q96T37	pY302		RBM15
Q8NDT2	pS10		RBM15B
Q5T481	pT1042		RBM20
Q5T8P6	pT615		RBM26
Q5T8P6-3	pT615		RBM26
Q5TC82	pS690	Roquin-1	RC3H1
Q9H902	pS192	Receptor expression-enhancing protein 1	REEP1
Q9H902-4	pS134;pS136;pT135	Receptor expression-enhancing protein 1	REEP1
Q8NFH8	pS550	RalBP1-associated Eps domain-containing protein 2	REPS2
Q9P2R6	pT658	Arginine-glutamic acid dipeptide repeats protein	RERE
Q8N1G1	pS422		REXO1
Q14699	pS485	Raftlin	RFTN1

Q8NET4	pS464;pT472	Retrotransposon gag domain-containing protein 1	RGAG1
O15211	pT12	Ral guanine nucleotide dissociation stimulator-like 2	RGL2
Q9NPQ8	pT517	Synembryn-A	RIC8A
Q6R327	pT31	Rapamycin-insensitive companion of mTOR	RICTOR
Q5EBL4	pT345	RILP-like protein 1	RILPL1
Q06587	pT243	E3 ubiquitin-protein ligase RING1	RING1
O15541	pS95	RING finger protein 113A	RNF113A
Q6ZMZ0	pS674	E3 ubiquitin-protein ligase RNF19B	RNF19B
Q8ND24	pS4	RING finger protein 214	RNF214
Q969K3	pS268	E3 ubiquitin-protein ligase RNF34	RNF34
P05386	pS83	60S acidic ribosomal protein P1	RPLP1
Q5VT52	pS619		RPRD2
Q5VT52-5	pS914		RPRD2
P08708	pT120	40S ribosomal protein S17	RPS17
P62979	pT55	40S ribosomal protein S27a;60S ribosomal protein L40;Polyubiquitin-B;Polyubiquitin-C;Ubiquitin;Ubiquitin-40S ribosomal protein S27a;Ubiquitin-60S ribosomal protein L40	RPS27A;UBA52;UBB;UBC
P62857	pT28	40S ribosomal protein S28	RPS28
Q5VWQ0	pS96	Round spermatid basic protein 1	RSBN1
Q92681	pS28	Regulatory solute carrier protein family 1 member 1	RSC1A1
Q2I0M5	pY66	R-spondin-4	RSPO4
Q7L4I2	pS54	Arginine/serine-rich coiled-coil protein 2	RSRC2
Q16799	pT358	Reticulon-1	RTN1
Q9NQC3	pS196;pS218;pS239;pS302;pS303;pS307;pS446;pS664;pS666;pS738;pS739;pS749;pS752;pS802;pS806;pS860;pS862;pS909;pS933;pS997;pT445;pT551;pT813;pT890	Reticulon-4	RTN4
Q8WWV3	pY255	mitochondrial;Reticulon-4-interacting protein 1	RTN4IP1
P21817	pS2845;pY2849	Ryanodine receptor 1	RYR1
Q99500	pS346	Sphingosine 1-phosphate receptor 3	S1PR3
Q9NZJ4	pS2031;pS2032;pT2516	Sacsin	SACS
Q15424	pS619	Scaffold attachment factor B1	SAFB
Q9UPU9	pS586;pT670	Protein Smaug homolog 1	SAMD4A

Q15020	pT3	Squamous cell carcinoma antigen recognized by T-cells 3	SART3
O94885	pS706;pT252;pT414;pT444	SAM and SH3 domain-containing protein 1	SASH1
Q99590	pS834;pS901	Protein SCAF11	SCAF11
Q96GP6	pS693	Scavenger receptor class F member 2	SCARF2
Q14524	pS671	Sodium channel protein type 5 subunit alpha	SCN5A
P55735-3	pT7	Protein SEC13 homolog	SEC13
O15027	pS1228	Protein transport protein Sec16A	SEC16A
O94979	pT1167	Protein transport protein Sec31A	SEC31A
Q9H2E6	pS808;pS810;pT761	Semaphorin-6A	SEMA6A
Q9GZR1	pS358	Sentrin-specific protease 6	SENP6
P84101	pS19	Small EDRK-rich factor 2	SERF2
Q13530	pT377	Serine incorporator 3	SERINC3
Q01105-2	pS170	Protein SET;Protein SETSIP	SET;SET SIP
Q8WTS6	pS224	Histone-lysine N-methyltransferase SETD7	SETD7
Q16586-2	pS253	Alpha-sarcoglycan	SGCA
Q16585	pS31	Beta-sarcoglycan	SGCB
P55822	pS185	SH3 domain-binding glutamic acid-rich protein	SH3BGR
Q96B97-2	pS151		SH3KBP1
Q5TCZ1	pS1041	SH3 and PX domain-containing protein 2A	SH3PXD2A
Q9BYB0	pS1155	SH3 and multiple ankyrin repeat domains protein 3	SHANK3
B4DS77	pS337	Protein shisa-9	SHISA9
O60292	pS102		SIPA1L3
P78324	pS406	Tyrosine-protein phosphatase non-receptor type substrate 1	SIRPA
Q8IXJ6	pT365		SIRT2
P49281	pS63;pS66;pY62		SLC11A2
P55011	pS939	Solute carrier family 12 member 2	SLC12A2
Q9UP95	pS104	Solute carrier family 12 member 4	SLC12A4
P36021	pS512	Monocarboxylate transporter 8	SLC16A2
O60669	pS219	Monocarboxylate transporter 2	SLC16A7
Q8WUM9	pT285	Sodium-dependent phosphate transporter 1	SLC20A1
Q92504	pT283	Zinc transporter SLC39A7	SLC39A7
Q07837	pS450	Neutral and basic amino acid transport protein rBAT	SLC3A1
Q9Y6M7	pS279;pY1187		SLC4A7
Q9H2G2-2	pS378		SLK

Q9NWH9	pS374;pS922;pT372	SAFB-like transcription modulator	SLTM
Q8IYB5	pS152	Stromal membrane-associated protein 1	SMAP1
Q86US8	pS1191;pS1196	Telomerase-binding protein EST1A	SMG6
Q9H0W8	pT56	Protein SMG9	SMG9
Q9UHP9	pS50;pT49	Small muscular protein	SMPX
P53814	pS713;pT253	Smoothelin	SMTN
P57768	pT288	Sorting nexin-16	SNX16
Q9Y5X3	pS30	Sorting nexin-5	SNX5
O94964-2	pT1543	Protein SOGA1	SOGA1
Q9BX66	pS1000;pS1024;pS1057;pS484;pS640;pS704;pS949;pS957;pS960;pS978;pT409;pT985	Sorbin and SH3 domain-containing protein 1	SORBS1
Q9BX66-12	pS470;pS471;pS578;pS725;pT475	Sorbin and SH3 domain-containing protein 1	SORBS1
Q9BX66-3	pS491;pS800;pT802	Sorbin and SH3 domain-containing protein 1	SORBS1
Q9BX66-5	pS427	Sorbin and SH3 domain-containing protein 1	SORBS1
O94875-10	pS100;pS136;pS486;pS552;pS78;pT102;pT541	Sorbin and SH3 domain-containing protein 2	SORBS2
O94875-4	pS7;pT3	Sorbin and SH3 domain-containing protein 2	SORBS2
O94875-8	pT3	Sorbin and SH3 domain-containing protein 2	SORBS2
O60504	pT106	Vinexin	SORBS3
O60504-2	pS6	Vinexin	SORBS3
Q07889	pS1075	Son of sevenless homolog 1	SOS1
P35716	pT280	Transcription factor SOX-11	SOX11
Q8TC71	pS505	Mitochondria-eating protein	SPATA18
Q9NUQ6	pS117;pS141;pS392;pS73;pS75	SPATS2-like protein	SPATS2L
Q5M775	pS553	Cytospin-B	SPECC1
Q15772	pS1981;pS2004;pS2110;pS2171;pS2318;pS2443;pS2500;pS2941;pS417;pS861		SPEG
Q15772-4	pS4		SPEG
Q08AE8	pS714	Protein spire homolog 1	SPIRE1
P11277-2	pS2299;pS2304	erythrocytic;Spectrin beta chain	SPTB
Q8N9Q2	pS96;pS97;pS98	Protein SREK1IP1	SREK1IP1
O75044	pT989	SLIT-ROBO Rho GTPase-activating protein 2	SRGAP2
P78362	pS11		SRPK2
Q9UPE1	pS333;pS334;pS335;pS345;pS380;pS382		SRPK3

Q9UQ35	pS1565;pS2713;pS2715;pS2731;pS799;pS801;pS802;pS817	Serine/arginine repetitive matrix protein 2	SRRM2
A7MD48	pS127	Serine/arginine repetitive matrix protein 4	SRRM4
Q9BXP5	pS341		SRRT
O75494	pS213	Serine/arginine-rich splicing factor 10	SRSF10
P78524	pS651;pS653;pS655	Suppression of tumorigenicity 5 protein	ST5
Q96MF2	pS9	SH3 and cysteine-rich domain-containing protein 3	STAC3
Q96FJ0	pS240;pY238	AMSH-like protease	STAMBPL1
Q9Y3M8	pS593;pT546	StAR-related lipid transfer protein 13	STARD13
O95772	pY209		STARD3NL
P31948	pS189;pY27	Stress-induced-phosphoprotein 1	STIP1
Q8N1F8	pS743		STK11IP
Q9P289	pS246;pS311		STK26
Q5VSL9	pS65	Striatin-interacting protein 1	STRIP1
Q9UBS9	pT1085	SUN domain-containing ossification factor	SUCO
Q8IX01	pS92	SURP and G-patch domain-containing protein 2	SUGP2
Q6ZW31	pS159;pS648	Rho GTPase-activating protein SYDE1	SYDE1
Q92797	pS1170	Symplekin	SYMPK
Q9H7C4	pS132;pS335;pT131	Syncoilin	SYNC
Q8N3V7-2	pT217		SYNPO
Q9UMS6	pS1064;pS1065;pS595;pS805;pS943;pT1082;pT821		SYNPO2
Q9H987	pS130;pS134;pS180;pS197;pS331;pS333;pS341;pS731;pS744;pS878;pS945;pS947;pT319;pT330;pT870;pY137;pY356;pY813		SYNPO2L
Q8N5C8	pS383		TAB3
O95359	pT2387;pT2553	Transforming acidic coiled-coil-containing protein 2	TACC2
Q9HCD6	pS1571	Protein TANC2	TANC2
Q8TBP0	pS257	TBC1 domain family member 16	TBC1D16
O60343-3	pS673	TBC1 domain family member 4	TBC1D4
Q66K14	pS753	TBC1 domain family member 9B	TBC1D9B
Q96SF7-2	pT346	T-box transcription factor TBX15	TBX15
Q13207	pS680	T-box transcription factor TBX2	TBX2

O15119	pS705	T-box transcription factor TBX3	TBX3
Q13428	pS1469	Treacle protein	TCOF1
Q9NUJ3	pS46	T-complex protein 11-like protein 1	TCP11L1
Q8N4U5	pS55	T-complex protein 11-like protein 2	TCP11L2
Q2MV58	pY435	Tectonic-1	TCTN1
Q15569	pS440		TESK1
Q01664	pT92	Transcription factor AP-4	TFAP4
Q9NS62	pS619;pS775;pS776	Thrombospondin type-1 domain-containing protein 1	THSD1
Q9BV44	pS154;pS90;pY104	THUMP domain-containing protein 3	THUMPD3
Q04727	pS210	Transducin-like enhancer protein 4	TLE4
Q9Y490	pS1156;pT1639	Talin-1	TLN1
Q9Y4G6	pS732	Talin-2	TLN2
Q9ULS5	pT244	Transmembrane and coiled-coil domains protein 3	TMCC3
Q96HH4	pS20;pS47;pS51;pT5;pY55	Transmembrane protein 169	TMEM169
Q9NVA4	pS435;pS438	Transmembrane protein 184C	TMEM184C
Q9UKE5	pT676		TNIK
Q15025	pS428;pS82	TNFAIP3-interacting protein 1	TNIP1
Q07912	pS928		TNK2
P45379	pS73	cardiac muscle;Troponin T	TNNT2
Q8NDV7	pS942	Trinucleotide repeat-containing gene 6A protein	TNRC6A
Q9HBL0	pS1289;pS1505;pS678;pS828;pT760;pT932	Tensin-1	TNS1
Q63HR2	pS808;pT103;pY654	Tensin-2	TNS2
Q68CZ2	pS730;pT656	Tensin-3	TNS3
Q96GM8	pS11	Target of EGR1 protein 1	TOE1
O60784	pT372	Target of Myb protein 1	TOM1
Q6ZVM7-5	pS370;pS371;pT374	TOM1-like protein 2	TOM1L2
Q02880	pY1558		TOP2B
O95985	pY111		TOP3B
Q12888	pS721;pT357	Tumor suppressor p53-binding protein 1	TP53BP1
P60174	pS273	Triosephosphate isomerase	TPI1
P09493-10	pT282	Tropomyosin alpha-1 chain	TPM1
P62995	pS20;pS22	Transformer-2 protein homolog beta	TRA2B
Q9BUZ4	pS431;pY436	TNF receptor-associated factor 4	TRAF4
O15050	pY952	TPR and ankyrin repeat-containing protein 1	TRANK1
Q9Y2L5	pS1088;pS1090	Trafficking protein particle complex subunit 8	TRAPPC8

Q96DX7	pT344	Tripartite motif-containing protein 44	TRIM44
Q9BYV2	pS175	Tripartite motif-containing protein 54	TRIM54
Q9BRZ2	pS485	E3 ubiquitin-protein ligase TRIM56	TRIM56
Q15643	pS1858	Thyroid receptor-interacting protein 11	TRIP11
Q14669-3	pS1131;pS169	E3 ubiquitin-protein ligase TRIP12	TRIP12
Q12816	pT357	Trophinin	TRO
Q92574	pS530;pT1110	Hamartin	TSC1
P49815	pS1336	Tuberin	TSC2
Q9Y3Q8	pS203	TSC22 domain family protein 4	TSC22D4
Q5VTQ0	pS123	Tetratricopeptide repeat protein 39B	TTC39B
Q9ULT0	pS88	Tetratricopeptide repeat protein 7A	TTC7A
Q8WZ42-12	pS11956;pS12229;pS12480;pS23576;pS34625;pS34697;pS34832;pS34855;pS35557;pS773;pS892;pT10215;pT10465;pT11954;pT12015;pT14689;pT253;pT35269;pY34670	Titin	TTN
Q8WZ42-6	pS3457;pS3464;pS3475;pS4142;pS4570;pS4651;pS4771;pS4827;pS5043;pS5052;pS5164;pS5166;pT4111;pT4654;pT4659;pT4786;pT5030;pT5041;pT5053;pT5143;pY3501	Titin	TTN
Q3ZCM7	pT290	Tubulin beta-8 chain;Tubulin beta-8 chain-like protein LOC260334	TUBB8
Q96CW5	pT524	Gamma-tubulin complex component 3	TUBGCP3
Q9NNX1	pS374	Tuftelin	TUFT1
O00294	pS215	Tubby-related protein 1	TULP1
Q8N3L3	pS38;pS569;pS94;pT560	Beta-taxilin	TXLNB
Q6IPR3	pS236		TYW3
Q9BZF9	pT259	Uveal autoantigen with coiled-coil domains and ankyrin repeats	UACA
Q14157	pS1067;pS445	Ubiquitin-associated protein 2-like	UBAP2L
Q96LR5	pS13	Ubiquitin-conjugating enzyme E2 E2	UBE2E2
O95155	pS374	Ubiquitin conjugation factor E4 B	UBE4B
Q96S82	pS242;pT248	Ubiquitin-like protein 7	UBL7
Q16851-2	pS2	UTP--glucose-1-phosphate uridylyltransferase	UGP2
A0JNW5	pS994	UHRF1-binding protein 1-like	UHRF1BP1L
O75385	pT401;pT755		ULK1

Q8IYT8	pT837		ULK2
O14795	pS366	Protein unc-13 homolog B	UNC13B
Q9H3U1	pT2	Protein unc-45 homolog A	UNC45A
Q53GS9	pS19	U4/U6.U5 tri-snRNP-associated protein 2	USP39
Q70EL2	pS451		USP45
O14607	pS1008	Histone demethylase UTY	UTY
Q86V25	pT304	Vasohibin-2	VASH2
P50552	pS245	Vasodilator-stimulated phosphoprotein	VASP
Q8N8G2	pS114;pS264	Transcription cofactor vestigial-like protein 2	VGLL2
Q8NFZ6	pS250;pY248		VN1R2
Q709C8	pS463	Vacuolar protein sorting-associated protein 13C	VPS13C
Q5THJ4	pS2093	Vacuolar protein sorting-associated protein 13D	VPS13D
P49754	pS11;pS15;pS19;pT16;pT9	Vacuolar protein sorting-associated protein 41 homolog	VPS41
Q9UID3	pS641	Vacuolar protein sorting-associated protein 51 homolog	VPS51
Q8N3P4	pT18	Vacuolar protein sorting-associated protein 8 homolog	VPS8
Q8IW00	pS224	Peptide Lv;V-set and transmembrane domain-containing protein 4	VSTM4
A6NCI4	pS334	von Willebrand factor A domain-containing protein 3A	VWA3A
P23381	pS8	cytoplasmic;T1-TrpRS;T2-TrpRS	WARS
Q8TBZ3	pS438	WD repeat-containing protein 20	WDR20
A6NGB9	pS330;pS93;pT178;pT94	WAS/WASL-interacting protein family member 3	WIPF3
Q9Y4P8	pS388	WD repeat domain phosphoinositide-interacting protein 2	WIPI2
Q702N8	pS1057;pS1297;pS1395;pS1445;pS1666;pS1668;pS1737;pS1739;pS213;pS305;pS415;pS419;pS452;pS463;pT1671;pT530;pT991	Xin actin-binding repeat-containing protein 1	XIRP1
A4UGR9	pS1968;pS2321;pS2530;pS3042;pS3059;pS3295;pS3297;pS418;pS868	Xin actin-binding repeat-containing protein 2	XIRP2
Q9UBH6	pT696	Xenotropic and polytropic retrovirus receptor 1	XPR1
P61981	pT70	14-3-3 protein gamma	YWHAG
P86452	pT390	Zinc finger BED domain-containing protein 6	ZBED6

Q5T200	pS1025;pS1278;pS409	Zinc finger CCCH domain-containing protein 13	ZC3H13
Q6PJT7	pS135	Zinc finger CCCH domain-containing protein 14	ZC3H14
Q86VM9	pS836	Zinc finger CCCH domain-containing protein 18	ZC3H18
Q8IWR0	pS318	Zinc finger CCCH domain-containing protein 7A	ZC3H7A
Q9UGR2	pT407	Zinc finger CCCH domain-containing protein 7B	ZC3H7B
Q5TAX3	pS131;pS48		ZCCHC11
Q8WW38	pS238	Zinc finger protein ZFPM2	ZFPM2
Q68DK2	pS1762;pS617	Zinc finger FYVE domain-containing protein 26	ZFYVE26
Q9ULU4-19	pS505		ZMYND8
O15014	pS1317	Zinc finger protein 609	ZNF609
O75312	pS4	Zinc finger protein ZPR1	ZPR1
O95218-2	pS292;pS294;pS295	Zinc finger Ran-binding domain-containing protein 2	ZRANB2
Q15695	pS475	U2 small nuclear ribonucleoprotein auxiliary factor 35 kDa subunit-related protein 1	ZRSR1
Q15696	pS388	U2 small nuclear ribonucleoprotein auxiliary factor 35 kDa subunit-related protein 2	ZRSR2
Q8TBC5	pS25;pT22	Zinc finger and SCAN domain-containing protein 18	ZSCAN18
Q15942	pS153	Zyxin	ZYX
Q8IYH5-2	pS91	ZZ-type zinc finger-containing protein 3	ZZZ3
E9PAV3	pS1018;pS1022;pS1033;pS1042;pS1046;pS1066;pS1112;pS1190;pS1296;pS1304;pS1319;pS1323;pS1388;pS1397;pS1404;pS1429;pS1474;pS1487;pS1488;pS1489;pS1511;pS1557;pS1580;pS1581;pS1607;pS1609;pS1623;pS1639;pS1650;pS1653;pS1656;pS1713;pS1757;pS1799;pS1805;pS1820;pS1867;pS257;pS277;pS545;pS577;pS578;pS579;pS674;pS736;pS738;pS765;pS766;pS793;pS795;pS800	muscle-specific form	

	;pS802;pS826;pS829;pS840;pS855;pS860;pS868;pS874;pS915;pS916;pS917;pS933;pS935;pS949;pS958;pS972;pT1010;pT1015;pT1026;pT1034;pT1039;pT1109;pT1127;pT1128;pT1132;pT1142;pT1178;pT1257;pT1265;pT1270;pT1293;pT1303;pT1316;pT1326;pT1348;pT1362;pT1385;pT1418;pT1427;pT1434;pT1458;pT1471;pT1486;pT1504;pT1573;pT1606;pT1615;pT1620;pT1636;pT1638;pT1643;pT1652;pT744;pT853;pT857;pT871;pT914;pT941;pT946;pT956;pT969		
O75449	pT175;pT359	Katanin p60 ATPase-containing subunit A-like 1;Katanin p60 ATPase-containing subunit A1	
O95180	pS758	Voltage-dependent T-type calcium channel subunit alpha-1H	
P02545	pS428	Lamin-A/C;Prelamin-A/C	
P21333	pT2175;pT2179	Filamin-A	
P41227	pS233	N-alpha-acetyltransferase 10	
P54920	pT190	Alpha-soluble NSF attachment protein	
Q00975	pY59	Voltage-dependent N-type calcium channel subunit alpha-1B	
Q13698	pS5;pT395	Voltage-dependent L-type calcium channel subunit alpha-1S	
Q5SXM2	pT1228		
Q8IVF2	pS2661;pS337;pS38;pS5401;pS56;pS641;pT643		
Q8IVL0	pS1220;pS1221;pS278;pS358		
Q8N8S7	pS488;pT467		
Q8NEY1	pT292;pT726;pT98		
Q8TBM8	pY92		
Q96DT5	pT1767	axonemal;Dynein heavy chain 11	
Q9BXJ9	pS38	N-alpha-acetyltransferase 15	
Q9UFH2	pS3796	axonemal;Dynein heavy chain 17	
Q9Y4J8	pS365;pS366;pS563;pS645	Dystrobrevin alpha	

Table 8. Identified and quantified protein phosphatase in human skeletal muscle cells

Proteins	PhosphoSites	Protein Names	Gene Names	Rerpoted In
A2A3K4	S394	Protein tyrosine phosphatase domain-containing protein 1	PTPDC1	Homo sapiens (Human)
O14974	S202;S299;S304;S396;S401;S402;S409;S440;S445;S455;S479;S484;S507;S509;S527;S607;S608;S666;S667;S668;S669;S693;S694;S695;S696;S860;S862;S869;S871;S903;S910;S912;S994;S995;S997;T394;T396;T397;T399;T406;T408;T438;T443;T453;T482;T508;T647;T648;T649;T650;T694;T695;T696;T697;T698;T700;T701;T850;T852;T853;T855;T857;T858;T859;T861;T871;T873	Protein phosphatase 1 regulatory subunit 12A	PPP1R12A	Bos taurus (Bovine);Cricetulus griseus (Chinese hamster) (Cricetulus barabensis griseus);Gallus gallus (Chicken);Homo sapiens (Human);Mus musculus (Mouse);Rattus norvegicus (Rat);Sus scrofa (Pig)
O15084	S1011;S1036;S1041;S987;S988;S989;S990;T982	Serine/threonine-protein phosphatase 6 regulatory ankyrin repeat subunit A	ANKRD28	Homo sapiens (Human);Mus musculus (Mouse);Rattus norvegicus (Rat);Sus scrofa (Pig)
O15194	S33	CTD small phosphatase-like protein	CTDSPL	Homo sapiens (Human);Sus scrofa (Pig)
O15357	S1003;S132;S241	4;5-trisphosphate 5-phosphatase 2;Phosphatidylinositol 3	INPPL1	Homo sapiens (Human);Mus musculus (Mouse);Rattus norvegicus (Rat)
O60237	S391;S446;S447;S451;S452;S504;S506;S643;S644;S645;S656;S735;S839;S842;T444;T445;T505;T644;T645;T646;T657;T663;T731	Protein phosphatase 1 regulatory subunit 12B	PPP1R12B	Cricetulus griseus (Chinese hamster) (Cricetulus barabensis griseus);Homo sapiens (Human);Mus musculus (Mouse);Rattus

				norvegicus (Rat);Sus scrofa (Pig)
O60346	T409	PH domain leucine-rich repeat-containing protein phosphatase 1	PHLPP1	Homo sapiens (Human)
O60825	S13;S466;S467;S469;S493;S5;S6;T16	6-bisphosphatase;6-bisphosphatase 2;Fructose-2	PFKFB2	Bos taurus (Bovine);Homo sapiens (Human);Mus musculus (Mouse);Rattus norvegicus (Rat);Sus scrofa (Pig)
O75061	S570;T572	Putative tyrosine-protein phosphatase auxilin		Homo sapiens (Human)
O75167	S23;S237;S239;S34;S457;S481;S495;S520;S522;S534;S558;S560;S572;T20;T240;T25;T31;T36;T93	Phosphatase and actin regulator 2	PHACTR2	Homo sapiens (Human);Mus musculus (Mouse);Rattus norvegicus (Rat);Sus scrofa (Pig)
O75170	S436;S770;S771;T441	Serine/threonine-protein phosphatase 6 regulatory subunit 2	PPP6R2	Homo sapiens (Human)
O75864	S50;S54;S56;S561;S581;S583;S591;S597;S601;T588	Protein phosphatase 1 regulatory subunit 37	PPP1R37	Homo sapiens (Human);Mus musculus (Mouse);Rattus norvegicus (Rat)
O95685	S23;S25;S28;S46;S74;S78	Protein phosphatase 1 regulatory subunit 3D	PPP1R3D	Homo sapiens (Human);Sus scrofa (Pig)
P05186	S110;T113;T115;T116	Alkaline phosphatase;tissue-nonspecific isozyme	ALPL	Homo sapiens (Human);Mus musculus (Mouse);Rattus norvegicus (Rat);Sus scrofa (Pig)
P17706	S304	Tyrosine-protein phosphatase non-receptor type 2	PTPN2	Homo sapiens (Human)

P18433	S180;S183;S189;S196;S790;S796;S823;Y785;Y792;Y796;Y798;Y800;Y825;Y827	Receptor-type tyrosine-protein phosphatase alpha	PTPRA	Danio rerio (Zebrafish) (Brachydanio rerio);Homo sapiens (Human);Macaca fascicularis (Crab-eating macaque) (Cynomolgus monkey);Mus musculus (Mouse);Rattus norvegicus (Rat);Sus scrofa (Pig)
P41236	S121;S122;S127;S20;S77;S87;T19;T89;T92	Protein phosphatase inhibitor 2;Protein phosphatase inhibitor 2-like protein 3	PPP1R2;PPP1R2P3	Homo sapiens (Human);Macaca fascicularis (Crab-eating macaque) (Cynomolgus monkey)
P60484	S385	4;5-trisphosphate 3-phosphatase and dual-specificity protein phosphatase PTEN;Phosphatidylinositol 3	PTEN	Homo sapiens (Human);Mus musculus (Mouse);Rattus norvegicus (Rat)
P62140	T316	Serine/threonine-protein phosphatase PP1-beta catalytic subunit	PPP1CB	Homo sapiens (Human);Mus musculus (Mouse);Rattus norvegicus (Rat);Sus scrofa (Pig)
P78324	S406	Tyrosine-protein phosphatase non-receptor type substrate 1	SIRPA	Homo sapiens (Human)
Q05209	S323;S324;S332;S368;S369;S371;S372;S434;S435;S448;S449;S514;S517;S571;S575;S588;S597;S603;S606;S607;S608;S610;S612;S670;S673;S677;T318;T366;T367;T375;T376;T378;T379;T509;T569;T573;T574;T578;T587;T598	Tyrosine-protein phosphatase non-receptor type 12	PTPN12	Homo sapiens (Human);Mus musculus (Mouse);Rattus norvegicus (Rat);Sus scrofa (Pig)
Q05D32	S28;S33	CTD small phosphatase-like protein 2	CTDSPL2	Homo sapiens (Human);Mus musculus

				(Mouse);Rattus norvegicus (Rat)
Q06124	S562;Y546;Y62;Y63	Tyrosine-protein phosphatase non-receptor type 11	PTPN11	Homo sapiens (Human);Mus musculus (Mouse);Rattus norvegicus (Rat)
Q06190	S179;S180;S181;S686;S687	Serine/threonine-protein phosphatase 2A regulatory subunit B" subunit alpha	PPP2R3A	Homo sapiens (Human)
Q12923	S1033;S345;S348;S901;S908;S910;S911;S913;S936;S938;T902;T909;Y943	Tyrosine-protein phosphatase non-receptor type 13	PTPN13	Homo sapiens (Human);Mus musculus (Mouse);Sus scrofa (Pig)
Q13362	S497	Serine/threonine-protein phosphatase 2A 56 kDa regulatory subunit gamma isoform	PPP2R5C	Homo sapiens (Human)
Q14693	727;729;732;734;739;744;747;749;757;759;763;765;769;775;806;808;818;S162;S211;S293;S294;S444;S445;S449;S598;S599;S600;S601;S723;S887;S889;T733;Y721	Phosphatidate phosphatase LPIN1;Phosphatidate phosphatase LPIN2	LPIN1;LPIN2	Homo sapiens (Human);Sus scrofa (Pig)
Q14738	S10;S470;S516;S52;S53;S54;S55;S565;S566;S573;S60;S62;S81;S82;S83;S88;S89;S9;S90;T55;T56;T63	Serine/threonine-protein phosphatase 2A 56 kDa regulatory subunit delta isoform	PPP2R5D	Gallus gallus (Chicken);Homo sapiens (Human);Mus musculus (Mouse);Rattus norvegicus (Rat);Sus scrofa (Pig)
Q15172	S42;S43	Serine/threonine-protein phosphatase 2A 56 kDa regulatory subunit alpha isoform	PPP2R5A	Homo sapiens (Human);Mus musculus (Mouse);Rattus norvegicus (Rat);Sus scrofa (Pig)
Q15262	S856;S868;S896;Y858;Y870;Y898	Receptor-type tyrosine-protein phosphatase kappa	PTPRK	Homo sapiens (Human);Mus musculus (Mouse);Rattus norvegicus (Rat);Sus scrofa (Pig)

Q15435	S11;S12;S24;S27;S36	Protein phosphatase 1 regulatory subunit 7	PPP1R7	Bos taurus (Bovine);Homo sapiens (Human);Mus musculus (Mouse);Rattus norvegicus (Rat);Sus scrofa (Pig)
Q15678	S314;S461;S463;S465;S466;S486;S576;S578;S589;S591;S592;S593;S594;S598;S620;S760;S762;S809;S811;S831;S833;T577;T579;T597;T599;Y589	Tyrosine-protein phosphatase non-receptor type 14	PTPN14	Bos taurus (Bovine);Gallus gallus (Chicken);Homo sapiens (Human);Mus musculus (Mouse);Rattus norvegicus (Rat);Sus scrofa (Pig)
Q16537	S32;S33;S34;T7	Serine/threonine-protein phosphatase 2A 56 kDa regulatory subunit epsilon isoform	PPP2R5E	Gallus gallus (Chicken);Homo sapiens (Human);Mus musculus (Mouse);Rattus norvegicus (Rat)
Q16825	S442;S492;S538;S554;S577;S582;S589;S590;S602;S616;S637;S658;S660;S670;S673;S676;S702;S710;S711;S795;S797;S820;S821;S824;T578;T605;T656;Y552	Tyrosine-protein phosphatase non-receptor type 21	PTPN21	Cricetulus griseus (Chinese hamster) (Cricetulus barabensis griseus);Homo sapiens (Human);Mus musculus (Mouse);Rattus norvegicus (Rat)
Q4G0W2	S13	Dual specificity phosphatase 28	DUSP28	Homo sapiens (Human)
Q5H9R7	S588;S617;S622;S638;S648;S651;T602;T620;T631;T649	Serine/threonine-protein phosphatase 6 regulatory subunit 3	PPP6R3	Homo sapiens (Human);Mus musculus (Mouse);Rattus norvegicus (Rat);Sus scrofa (Pig)

Q5VZP5	S1005;S1008;S1010;S1011;S1015;S1016;S1030;S1031;S1032;S1036;S1054;S1065;S15;S292;S303;S32;S320;S322;S327;S328;S336;S34;S36;S374;S376;S377;S39;S42;S421;S425;S426;S48;S508;S509;S513;S566;S567;S597;S612;S748;S813;S876;S891;S895;S955;T1029;T301;T340;T433;T46;T889		DUSP27	Bos taurus (Bovine);Homo sapiens (Human);Mus musculus (Mouse);Rattus norvegicus (Rat)
Q6IN85	S117;S126;S127;S586;S629;S662;S665;S685;S698;S728;S741;S758;S761;S764;S768;S771;S774;S777;S780;T762;T763	Serine/threonine-protein phosphatase 4 regulatory subunit 3A	SMEK1	Homo sapiens (Human);Mus musculus (Mouse);Rattus norvegicus (Rat);Sus scrofa (Pig);Xenopus laevis (African clawed frog)
Q6WCQ1	S1013;S1014;S1015;S1016;S1018;S1020;S1022;T1025	Myosin phosphatase Rho-interacting protein	MPRIP	Homo sapiens (Human);Mus musculus (Mouse);Rattus norvegicus (Rat)
Q6WCQ1-2	S1013;S1014;S1015;S1016;S1341;S1770;S1772;S218;S220;S224;S2245;S2247;S226;S227;S253;S255;S265;S266;S269;S271;S289;S292;S294;S35;S360;S362;S365;S37;S377;S381;S538;S540;S543;S619;S820;S822;S824;S826;S891;S976;S977;S978;S979;S980;S984;S990;S991;S992;S993;S995;S997;T295;T378;T540;T542;T545;T889;T982;Y986	Myosin phosphatase Rho-interacting protein	MPRIP	Homo sapiens (Human);Macaca fascicularis (Crab-eating macaque) (Cynomolgus monkey);Mus musculus (Mouse);Rattus norvegicus (Rat)
Q6ZMI0	S38	Protein phosphatase 1	PPP1R21	

		regulatory subunit 21		
Q6ZSY5	S18;S400;S401;S545;S547;T4	Protein phosphatase 1 regulatory subunit 3F	PPP1R3F	Homo sapiens (Human);Mus musculus (Mouse)
Q76I76	S1216;S1217;S809;T795;T811	Protein phosphatase Slingshot homolog 2	SSH2	Homo sapiens (Human)
Q7L9B9	S173;S25	Endonuclease/exonuclease/phosphatase family domain-containing protein 1	EEPD1	Cricetulus griseus (Chinese hamster) (Cricetulus barabensis griseus);Homo sapiens (Human);Mus musculus (Mouse);Rattus norvegicus (Rat)
Q8IZ21-3	S116;S117;S118;S176;S177;S178;S270;S278;S283;S288;S291;S305;S342;S344;S464;S590;S615;S620;S628;S680;T11;T12;T27;T28;T285;T342;T349;T358;T362;T41;T42	Phosphatase and actin regulator 4	PHACTR4	Danio rerio (Zebrafish) (Brachydanio rerio);Homo sapiens (Human);Mus musculus (Mouse);Rattus norvegicus (Rat);Sus scrofa (Pig);Xenopus laevis (African clawed frog)
Q8N4L2	S16;S18;S32;S33;T22;T24	5-bisphosphate 4-phosphatase;Type 2 phosphatidylinositol 4	TMEM55A	Homo sapiens (Human);Mus musculus (Mouse);Rattus norvegicus (Rat)
Q8NBV4	S62	Probable lipid phosphate phosphatase PPAPDC3	PPAPDC3	Homo sapiens (Human);Macaca fascicularis (Crab-eating macaque) (Cynomolgus monkey);Mus musculus (Mouse);Rattus norvegicus (Rat);Sus scrofa (Pig)
Q8TAP8	S45;S47;S52	Protein phosphatase 1 regulatory subunit 35	PPP1R35	Homo sapiens (Human)
Q8TE77	S649;S653;S7;S87;S9;T5	Protein phosphatase Slingshot homolog 3	SSH3	Homo sapiens (Human)

Q8TF05	S944;S947;S948;S949;Y950;Y951	Serine/threonine-protein phosphatase 4 regulatory subunit 1	PPP4R1	Homo sapiens (Human);Mus musculus (Mouse);Rattus norvegicus (Rat)
Q8WYL5	S515;S521;S576;S583;S894;S897;S919;S920;S921;S928;S929;S930;S935;S936;S937;S938	Protein phosphatase Slingshot homolog 1	SSH1	Homo sapiens (Human);Mus musculus (Mouse);Rattus norvegicus (Rat)
Q92539	S106;S144;S186;S187;T105;T143	Phosphatidate phosphatase LPIN2	LPIN2	Cricetulus griseus (Chinese hamster) (Cricetulus barabensis griseus);Homo sapiens (Human);Mus musculus (Mouse);Rattus norvegicus (Rat)
Q92932	S230	Receptor-type tyrosine-protein phosphatase N2	PTPRN2	Homo sapiens (Human)
Q96A00	S128;S136;S26;S85;S93	Protein phosphatase 1 regulatory subunit 14A	PPP1R14A	Bos taurus (Bovine);Homo sapiens (Human);Macaca fascicularis (Crab-eating macaque) (Cynomolgus monkey)
Q96C86	S24;T25	m7GpppX diphosphatase	DCPS	Homo sapiens (Human)
Q96HS1	S106;S112;S113	mitochondrial;Serine/threonine-protein phosphatase PGAM5	PGAM5	Homo sapiens (Human);Mus musculus (Mouse)
Q96QC0	S313;S542;S545;T315;T536	Serine/threonine-protein phosphatase 1 regulatory subunit 10	PPP1R10	Cricetulus griseus (Chinese hamster) (Cricetulus barabensis griseus);Homo sapiens (Human);Mus musculus (Mouse);Rattus norvegicus (Rat);Sus scrofa (Pig)
Q96T60	T118;T122	Polynucleotide 3'-phosphatase	PNKP	Homo sapiens (Human)
Q99956	S312	Dual specificity protein phosphatase 9	DUSP9	

Q9BQK8	S204;S224	Phosphatidate phosphatase LPIN3	LPIN3	Homo sapiens (Human)
Q9BX95	S112	Sphingosine-1-phosphate phosphatase 1	SGPP1	Homo sapiens (Human)
Q9BZL4	S407	Protein phosphatase 1 regulatory subunit 12C	PPP1R12C	Homo sapiens (Human)
Q9BZL4-3	S364;S407;S427;S428;S450;S452;S453;S454;S498;S499;S509;S559;S560;T425;T489;T545;T560;T561	Protein phosphatase 1 regulatory subunit 12C	PPP1R12C	Homo sapiens (Human);Mus musculus (Mouse);Rattus norvegicus (Rat);Sus scrofa (Pig)
Q9H0C8	S13		ILKAP	Homo sapiens (Human);Sus scrofa (Pig)
Q9H2U2-2	S316;S317;S72	Inorganic pyrophosphatase 2;mitochondrial	PPA2	Homo sapiens (Human)
Q9H3S7	S1122;S1123;S1126;S1133;S1152;S1153;S1178;S1179;S1569;S1570;S1574;S1575;S1576;S1582;S985;S986;T1131	Tyrosine-protein phosphatase non-receptor type 23	PTPN23	Homo sapiens (Human);Mus musculus (Mouse);Rattus norvegicus (Rat)
Q9NQ88	S159	6-bisphosphatase TIGAR;Fructose-2	TIGAR	Homo sapiens (Human)
Q9ULR3	S112;S220;S221;S222;S223;T223;T224	Protein phosphatase 1H	PPM1H	Homo sapiens (Human);Mus musculus (Mouse);Rattus norvegicus (Rat)
Q9UPN7	S531;S558;S635;S638;S667;S670;S747;T524;T668	Serine/threonine-protein phosphatase 6 regulatory subunit 1	PPP6R1	Homo sapiens (Human);Mus musculus (Mouse);Rattus norvegicus (Rat);Sus scrofa (Pig)
Q9UQK1	S293;S33	Protein phosphatase 1 regulatory subunit 3C	PPP1R3C	Homo sapiens (Human)
Q9Y2H2	S881;S935;S940;S942	Phosphatidylinositide phosphatase SAC2	INPP5F	Homo sapiens (Human)

Q9Y570	S15;S217;S22;S243;S25;S42;S47;S52;T216;T242	Protein phosphatase methylesterase 1	PPME1	Homo sapiens (Human);Mus musculus (Mouse);Rattus norvegicus (Rat);Sus scrofa (Pig)
Q9Y5B0	S395;S474;S478;S740;S832;S841;S869;S872;S902		CTDP1	Homo sapiens (Human);Rattus norvegicus (Rat);Sus scrofa (Pig)
Q9Y6X5	S363;S439;T364;Y360;Y371	Bis(5'-adenosyl)-triphosphatase ENPP4	ENPP4	Homo sapiens (Human)

Table 9. Significant (P-Value< 0.05) protein phosphatases quantified in lean insulin-sensitive participants after metformin treatment in human skeletal muscle cells. Fold change is log2 transformed, zero indicates no change, while 1 indicates 2 fold increase and -1 indicates 50% decrease.

Accession	Protein	Gene Name	phospho-Sites	P-Value	Fold change (Metformin/No-Metformin, Lean)	SEM
O15084	Serine/threonine-protein phosphatase 6 regulatory ankyrin repeat subunit A	ANKRD28	S-1011	0.02157523	-2.500	3.317
Q9Y5B0	RNA polymerase II subunit A C-terminal domain phosphatase	CTDP1	S-740	3.63E-05	-4.523	3.689
Q5VZP5	Inactive dual specificity phosphatase 27	DUSP27	S-336	0.04852933	2.030	4.215
Q5VZP5	Inactive dual specificity phosphatase 27	DUSP27	S-566	0.0008924	3.499	3.513
Q5VZP5	Inactive dual specificity phosphatase 27	DUSP27	S-509	0.03195838	2.197	3.367
Q5VZP5	Inactive dual specificity phosphatase 27	DUSP27	S-602	0.00147706	3.448	3.838
Q5VZP5	Inactive dual specificity phosphatase 27	DUSP27	S-1065	0.0057526	-2.940	3.574
Q5VZP5	Inactive dual specificity phosphatase 27	DUSP27	S-1010	0.0364827	-2.248	3.944
Q5VZP5	Inactive dual specificity phosphatase 27	DUSP27	S-1031	0.03200627	-2.196	3.818
Q5VZP5	Inactive dual specificity phosphatase 27	DUSP27	T-340	0.04852933	2.030	4.215
Q99956	Dual specificity protein phosphatase 9	DUSP9	S-312	0.04801453	-2.217	3.803
Q9Y2H2	Phosphatidylinositide phosphatase SAC2	INPP5F	S-935	0.02277846	-2.361	3.664
Q9Y2H2	Phosphatidylinositide phosphatase SAC2	INPP5F	S-942	0.01321548	2.520	3.687
Q14693	Phosphatidate phosphatase LPIN1	LPIN1	S-889	0.00374119	-3.019	4.555
Q14693	Phosphatidate phosphatase LPIN1	LPIN1	S-294	0.02802896	-2.240	4.118

Q14693	Phosphatidate phosphatase LPIN1	LPIN1	S-162	0.03296795	2.172	3.728
Q6WCQ1-2	Myosin phosphatase Rho-interacting protein	MPRIP	S-289	0.00491936	-2.872	4.253
Q6WCQ1-2	Myosin phosphatase Rho-interacting protein	MPRIP	S-292	0.01031385	-2.608	4.256
Q6WCQ1-2	Myosin phosphatase Rho-interacting protein	MPRIP	S-365	0.00038393	-3.766	4.287
Q6WCQ1-2	Myosin phosphatase Rho-interacting protein	MPRIP	S-220	0.00713072	2.740	4.031
Q6WCQ1-2	Myosin phosphatase Rho-interacting protein	MPRIP	S-224	0.03448347	2.140	3.919
Q6WCQ1-2	Myosin phosphatase Rho-interacting protein	MPRIP	S-619	0.01890915	4.318	4.103
Q6WCQ1-2	Myosin phosphatase Rho-interacting protein	MPRIP	S-99	0.00134147	3.287	5.342
Q6WCQ1-2	Myosin phosphatase Rho-interacting protein	MPRIP	S-891	0.0062423	2.909	3.556
Q6WCQ1-2	Myosin phosphatase Rho-interacting protein	MPRIP	S-269	2.48E-05	4.443	4.024
Q6WCQ1	Myosin phosphatase Rho-interacting protein	MPRIP	T-1025	0.00389745	2.956	3.746
Q6WCQ1-2	Myosin phosphatase Rho-interacting protein	MPRIP	T-542	0.01507937	2.477	4.318
O60825	6-phosphofructo-2-kinase/fructose-2,6-bisphosphatase 2;6-phosphofructo-2-kinase;Fructose-2,6-bisphosphatase	PFKFB2	S-493	0.00013063	5.671	3.466
Q8IZ21-3	Phosphatase and actin regulator 4	PHACTR4	S-254	3.50E-06	6.415	3.593
Q8IZ21-3	Phosphatase and actin regulator 4	PHACTR4	S-272	0.00296843	3.769	3.608
Q8IZ21-3	Phosphatase and actin regulator 4	PHACTR4	S-574	1.03E-05	-5.392	3.562
Q96T60	Bifunctional polynucleotide phosphatase/kinase;Polynucleotide 3'-phosphatase;Polynucleotide 5'-hydroxyl-kinase	PNKP	T-118	0.03714791	2.109	4.055
Q9H2U2-2	Inorganic pyrophosphatase 2, mitochondrial	PPA2	S-332	0.04245739	2.173	3.451
Q9Y570	Protein phosphatase methylesterase 1	PPME1	S-42	0.00015588	4.385	3.445
Q9Y570	Protein phosphatase methylesterase 1	PPME1	S-25	0.04501069	2.064	3.535
O14974	Protein phosphatase 1 regulatory subunit 12A	PPP1R12A	S-299	5.22E-06	4.907	3.945

O14974	Protein phosphatase 1 regulatory subunit 12A	PPP1R12A	S-304	0.01511849	2.593	3.785
O14974	Protein phosphatase 1 regulatory subunit 12A	PPP1R12A	S-445	0.00707773	2.742	4.730
O14974	Protein phosphatase 1 regulatory subunit 12A	PPP1R12A	S-871	0.01221099	2.553	4.258
O14974	Protein phosphatase 1 regulatory subunit 12A	PPP1R12A	S-668	0.00395724	-7.240	4.263
O14974	Protein phosphatase 1 regulatory subunit 12A	PPP1R12A	T-453	0.00048811	3.665	4.086
O60237	Protein phosphatase 1 regulatory subunit 12B	PPP1R12B	S-735	1.52E-13	13.432	3.874
O60237	Protein phosphatase 1 regulatory subunit 12B	PPP1R12B	S-447	0.0480639	2.010	3.848
O60237	Protein phosphatase 1 regulatory subunit 12B	PPP1R12B	S-452	0.00052004	3.646	3.745
O60237	Protein phosphatase 1 regulatory subunit 12B	PPP1R12B	T-646	0.00079878	-3.565	3.624
Q9BZL4-3	Protein phosphatase 1 regulatory subunit 12C	PPP1R12C	S-452;451	0.01997983	2.471	3.652
Q9BZL4-3	Protein phosphatase 1 regulatory subunit 12C	PPP1R12C	T-425;424	0.00791359	-5.787	4.166
P41236	Protein phosphatase inhibitor 2	PPP1R2	S-87	0.000244	-5.266	4.292
O75864	Protein phosphatase 1 regulatory subunit 37	PPP1R37	S-591	0.00214194	-3.265	3.722
O75864	Protein phosphatase 1 regulatory subunit 37	PPP1R37	S-597	0.0021311	-3.267	3.614
O95685	Protein phosphatase 1 regulatory subunit 3D	PPP1R3D	S-74	0.01366628	-2.515	3.613
Q6ZSY5	Protein phosphatase 1 regulatory subunit 3F	PPP1R3F	S-547	9.10E-16	-13.779	3.888
Q15435	Protein phosphatase 1 regulatory subunit 7	PPP1R7	S-24	0.01982764	2.362	5.226
Q15435	Protein phosphatase 1 regulatory subunit 7	PPP1R7	S-27	0.00523392	2.846	5.343
Q13362	Serine/threonine-protein phosphatase 2A 56 kDa regulatory subunit gamma isoform	PPP2R5C	S-497	0.00727543	2.752	3.668
Q16537	Serine/threonine-protein phosphatase 2A 56 kDa regulatory subunit epsilon isoform	PPP2R5E	S-32	0.02481872	-2.296	3.684
Q16537	Serine/threonine-protein phosphatase 2A 56 kDa regulatory subunit epsilon isoform	PPP2R5E	S-33	0.0401951	2.075	3.942

Q5H9R7	Serine/threonine-protein phosphatase 6 regulatory subunit 3	PPP6R3	S-617	7.90E-05	4.119	4.259
P60484	Phosphatidylinositol 3,4,5-trisphosphate 3-phosphatase and dual-specificity protein phosphatase PTEN	PTEN	S-385	0.04946934	-2.200	3.433
Q06124	Tyrosine-protein phosphatase non-receptor type 11	PTPN11	Y-542	3.12E-05	-4.774	3.986
Q05209	Tyrosine-protein phosphatase non-receptor type 12	PTPN12	S-369	0.01651127	2.626	3.317
Q05209	Tyrosine-protein phosphatase non-receptor type 12	PTPN12	S-332	0.00032036	3.794	3.934
Q05209	Tyrosine-protein phosphatase non-receptor type 12	PTPN12	S-435	0.0030941	3.033	4.409
Q05209	Tyrosine-protein phosphatase non-receptor type 12	PTPN12	S-603	0.02457643	-2.280	4.257
Q05209	Tyrosine-protein phosphatase non-receptor type 12	PTPN12	S-606	0.01614317	-2.444	4.391
Q05209	Tyrosine-protein phosphatase non-receptor type 12	PTPN12	T-587	0.03130159	3.611	3.311
Q12923	Tyrosine-protein phosphatase non-receptor type 13	PTPN13	S-1033	0.00014719	-5.593	3.916
Q12923	Tyrosine-protein phosphatase non-receptor type 13	PTPN13	S-348	0.04189901	2.294	3.288
Q12923	Tyrosine-protein phosphatase non-receptor type 13	PTPN13	Y-943	0.0181716	2.760	3.358
Q15678	Tyrosine-protein phosphatase non-receptor type 14	PTPN14	S-831	0.00135874	-3.478	3.526
Q15678	Tyrosine-protein phosphatase non-receptor type 14	PTPN14	S-314	6.27E-05	4.240	3.837
Q15678	Tyrosine-protein phosphatase non-receptor type 14	PTPN14	S-578	0.02110938	-2.393	3.772
Q15678	Tyrosine-protein phosphatase non-receptor type 14	PTPN14	S-591	0.00163216	-4.112	3.967
Q15678	Tyrosine-protein phosphatase non-receptor type 14	PTPN14	S-593	0.01713328	-2.433	3.706
Q16825	Tyrosine-protein phosphatase non-receptor type 21	PTPN21	S-637	0.00248359	-3.120	4.056
Q16825	Tyrosine-protein phosphatase non-receptor type 21	PTPN21	S-554	0.03971547	-2.136	3.436

Q16825	Tyrosine-protein phosphatase non-receptor type 21	PTPN21	S-710	0.03885948	2.102	3.529
Q16825	Tyrosine-protein phosphatase non-receptor type 21	PTPN21	S-711	0.03885948	2.102	3.529
Q9H3S7	Tyrosine-protein phosphatase non-receptor type 23	PTPN23	S-1126	1.40E-06	-9.191	4.571
P18433	Receptor-type tyrosine-protein phosphatase alpha	PTPRA	S-189	0.00067587	-3.727	3.113
Q92932	Receptor-type tyrosine-protein phosphatase N2	PTPRN2	S-230	0.00043099	-14.466	4.707
Q9BX95	Sphingosine-1-phosphate phosphatase 1	SGPP1	S-112	4.02E-06	-8.267	3.944
Q8WYL5	Protein phosphatase Slingshot homolog 1	SSH1	S-576	0.00012885	3.985	4.094
Q8WYL5	Protein phosphatase Slingshot homolog 1	SSH1	S-515	0.01482191	-2.676	3.698
Q8WYL5	Protein phosphatase Slingshot homolog 1	SSH1	S-521	0.00736136	-5.926	3.749
Q8WYL5	Protein phosphatase Slingshot homolog 1	SSH1	S-897	0.00120475	3.466	3.662
Q8TE77	Protein phosphatase Slingshot homolog 3	SSH3	S-9	0.01193088	-2.694	4.021
Q8TE77	Protein phosphatase Slingshot homolog 3	SSH3	S-87	0.000169	-5.502	3.931
Q8TE77	Protein phosphatase Slingshot homolog 3	SSH3	S-653	0.03571314	-2.157	3.357

Table 10. Significant (P-Value <0.05) protein phosphatase quantified in obese insulin-resistant participants after metformin treatments in human skeletal muscle cells. Fold change is log2 transformed, zero indicates no change, while 1 indicates 2 fold increase and -1 indicates 50% decrease.

Accession	Protein	Gene Name	phosphoSites	P-Value	Fold change (Metformin/NoMetformin, OIR)	SEM
Q9Y5B0	RNA polymerase II subunit A C-terminal domain phosphatase	CTDP1	S-395	0.0014	4.214	3.235
O15194	CTD small phosphatase-like protein	CTDSPL	S-33	0.0012	-4.275	3.351
Q5VZP5	Inactive dual specificity phosphatase 27	DUSP27	S-376	0.0417	2.089	3.098
Q9Y6X5	Bis(5'-adenosyl)-triphosphatase ENPP4	ENPP4	S-439	0.0000	-5.722	3.686
Q9Y6X5	Bis(5'-adenosyl)-triphosphatase ENPP4	ENPP4	Y-360	0.0083	-5.709	3.175
Q9Y6X5	Bis(5'-adenosyl)-triphosphatase ENPP4	ENPP4	Y-371	0.0083	-5.709	3.175
O60825	6-phosphofructo-2-kinase/fructose-2,6-bisphosphatase 2;6-phosphofructo-2-kinase;Fructose-2,6-bisphosphatase	PFKFB2	S-466	0.0033	-3.111	3.226
Q8IZ21-3	Phosphatase and actin regulator 4	PHACTR4	S-574	0.0428	2.125	2.934
P62140	Serine/threonine-protein phosphatase PP1-beta catalytic subunit	PPP1CB	T-316	0.0127	-2.958	3.153
Q96QC0	Serine/threonine-protein phosphatase 1 regulatory subunit 10	PPP1R10	T-315	0.0024	-3.140	3.876
O14974	Protein phosphatase 1 regulatory subunit 12A	PPP1R12A	T-453	0.0378	-2.119	3.776
O14974	Protein phosphatase 1 regulatory subunit 12A	PPP1R12A	T-696	0.0182	-2.398	4.450
O60237	Protein phosphatase 1 regulatory subunit 12B	PPP1R12B	S-735	0.0251	2.370	3.160

O60237	Protein phosphatase 1 regulatory subunit 12B	PPP1R12B	S-452	0.0201	-2.380	3.728
P41236	Protein phosphatase inhibitor 2;Protein phosphatase inhibitor 2-like protein 3	PPP1R2;PPP1R2P3	S-121	0.0006	3.516	4.313
P41236	Protein phosphatase inhibitor 2;Protein phosphatase inhibitor 2-like protein 3	PPP1R2;PPP1R2P3	S-122	0.0002	3.866	4.481
P41236	Protein phosphatase inhibitor 2;Protein phosphatase inhibitor 2-like protein 3	PPP1R2;PPP1R2P3	S-127	0.0011	3.401	4.075
O95685	Protein phosphatase 1 regulatory subunit 3D	PPP1R3D	S-46	0.0013	3.318	3.565
O95685	Protein phosphatase 1 regulatory subunit 3D	PPP1R3D	S-74	0.0003	3.790	3.515
O95685	Protein phosphatase 1 regulatory subunit 3D	PPP1R3D	S-78	0.0009	3.440	3.500
Q15435	Protein phosphatase 1 regulatory subunit 7	PPP1R7	S-24	0.0039	2.943	5.081
Q15435	Protein phosphatase 1 regulatory subunit 7	PPP1R7	S-27	0.0052	2.846	5.134
Q14738	Serine/threonine-protein phosphatase 2A 56 kDa regulatory subunit delta isoform	PPP2R5D	S-89	0.0439	2.041	4.098
Q14738	Serine/threonine-protein phosphatase 2A 56 kDa regulatory subunit delta isoform	PPP2R5D	S-90	0.0348	2.141	4.026
Q14738	Serine/threonine-protein phosphatase 2A 56 kDa regulatory subunit delta isoform	PPP2R5D	S-573	0.0313	-2.182	3.849
Q06124	Tyrosine-protein phosphatase non-receptor type 11	PTPN11	S-558	0.0008	-3.957	3.099
Q05209	Tyrosine-protein phosphatase non-receptor type 12	PTPN12	S-369	0.0072	-3.006	3.193
Q12923	Tyrosine-protein phosphatase non-receptor type 13	PTPN13	S-345	0.0394	-2.328	2.956
Q15678	Tyrosine-protein phosphatase non-receptor type 14	PTPN14	S-465	0.0208	-2.347	4.061
Q15678	Tyrosine-protein phosphatase non-receptor type 14	PTPN14	S-591	0.0443	-2.263	3.783
P18433	Receptor-type tyrosine-protein phosphatase alpha	PTPRA	Y-798	0.0497	-2.019	3.152

Table 11. Significant (P-Value <0.05) protein phosphatase quantified in both groups after metformin treatments when comparing Lean vs OIR in human skeletal muscle cells. Fold change is log2 transformed and zero indicates no change, while 1 indicates 2 fold increase and -1 indicates 50% decrease.

Accession	**Protein**	**Gene Name**	**phosphoproteins**	**P-Value**	**Fold change (Metformin (Lean)/ Metformin (OIR))**	**SEM**
Q5VZP5	Inactive dual specificity phosphatase 27	DUSP27	S-15	0.036029	2.123	3.990
Q5VZP5	Inactive dual specificity phosphatase 27	DUSP27	S-748	0.047408	-2.118	3.525
Q5VZP5	Inactive dual specificity phosphatase 27	DUSP27	S-1005	0.009627	-2.784	3.634
Q8IZ21-3	Phosphatase and actin regulator 4	PHACTR4	S-574	0.027182	-2.334	3.048
O14974	Protein phosphatase 1 regulatory subunit 12A	PPP1R12A	S-479	0.042299	2.175	3.429
O14974	Protein phosphatase 1 regulatory subunit 12A	PPP1R12A	S-527	6.07E-06	-4.804	4.278
Q06190	Serine/threonine-protein phosphatase 2A regulatory subunit B" subunit alpha	PPP2R3A	S-181	0.018933	-2.438	3.497
Q05209	Tyrosine-protein phosphatase non-receptor type 12	PTPN12	S-369	0.004734	3.192	3.320

Table 12. Significant (P-Value <0.05) protein phosphatase quantified in lean insulin-sensitive participants upon insulin stimulation in human skeletal muscle cell. Fold change is log2 transformed and zero indicates no change, while 1 indicates 2 fold increase and -1 indicates 50% decrease.

Acces-sion	**protein**	**Gene Name**	**phos-pho-Sites**	**P-Value**	**Fold change(Insu-lin/No-Insulin, Lean)**	**SEM**
Q9Y5B0	RNA polymer-ase II subunit A C-terminal domain phos-phatase	CTDP1	S-395	0.00529272	3.443	3.568
Q9Y5B0	RNA polymer-ase II subunit A C-terminal domain phos-phatase	CTDP1	S-740	0.00776547	-2.771	3.676
Q5VZP5	Inactive dual specificity phosphatase 27	DUSP27	S-336	0.00221509	3.253	4.299
Q5VZP5	Inactive dual specificity phosphatase 27	DUSP27	S-566	0.00305354	3.089	3.563
Q5VZP5	Inactive dual specificity phosphatase 27	DUSP27	S-421	0.04591632	2.026	4.002
Q5VZP5	Inactive dual specificity phosphatase 27	DUSP27	S-602	5.68E-05	4.574	3.936
Q5VZP5	Inactive dual specificity phosphatase 27	DUSP27	S-377	0.04406314	-2.039	3.511
Q5VZP5	Inactive dual specificity phosphatase 27	DUSP27	S-1065	0.00094394	-3.609	3.622
Q5VZP5	Inactive dual specificity phosphatase 27	DUSP27	S-1010	0.04747456	-2.117	4.021
Q5VZP5	Inactive dual specificity phosphatase 27	DUSP27	T-340	0.00221509	3.253	4.299

Q7L9B9	Endonuclease/exonuclease/phosphatase family domain-containing protein 1	EEPD1	S-173	0.0222445	-2.648	3.614
Q9H0C8	Integrin-linked kinase-associated serine/threonine phosphatase 2C	ILKAP	S-13	0.03186098	-2.173	4.926
O15357	Phosphatidylinositol 3,4,5-trisphosphate 5-phosphatase 2	INPPL1	S-132	0.00012549	3.970	5.456
Q14693	Phosphatidate phosphatase LPIN1	LPIN1	S-889	0.00546631	-2.884	4.640
Q14693	Phosphatidate phosphatase LPIN1	LPIN1	S-162	0.00061458	3.576	3.822
Q6WCQ1-2	Myosin phosphatase Rho-interacting protein	MPRIP	S-977	0.00920225	-2.727	3.857
Q6WCQ1-2	Myosin phosphatase Rho-interacting protein	MPRIP	S-289	0.0004471	-3.623	4.339
Q6WCQ1-2	Myosin phosphatase Rho-interacting protein	MPRIP	S-292	0.00127243	-3.303	4.342
Q6WCQ1-2	Myosin phosphatase Rho-interacting protein	MPRIP	S-365	1.22E-05	-4.774	4.376
Q6WCQ1-2	Myosin phosphatase Rho-interacting protein	MPRIP	S-220	0.00658216	2.768	4.105
Q6WCQ1-2	Myosin phosphatase Rho-interacting protein	MPRIP	S-993	0.00060305	3.528	5.421
Q6WCQ1	Myosin phosphatase Rho-	MPRIP	S-1016	0.01240404	2.678	3.284

	interacting protein					
Q6WCQ1-2	Myosin phosphatase Rho-interacting protein	MPRIP	S-891	0.00914793	2.758	3.627
Q6WCQ1-2	Myosin phosphatase Rho-interacting protein	MPRIP	S-269	0.00755424	2.732	4.025
Q6WCQ1	Myosin phosphatase Rho-interacting protein	MPRIP	T-1025	0.00902539	2.663	3.754
O60825	6-phosphofructo-2-kinase/fructose-2,6-bisphosphatase 2;6-phosphofructo-2-kinase;Fructose-2,6-bisphosphatase	PFKFB2	S-493	8.67E-06	7.638	3.573
O75167	Phosphatase and actin regulator 2	PHACTR2	S-237	0.01466027	-2.543	3.727
Q8IZ21-3	Phosphatase and actin regulator 4	PHACTR4	S-254	0.000261	4.458	3.471
Q8IZ21-3	Phosphatase and actin regulator 4	PHACTR4	S-272	0.03426579	2.407	3.467
Q8IZ21-3	Phosphatase and actin regulator 4	PHACTR4	S-574	1.54E-08	-7.913	3.657
Q9Y570	Protein phosphatase methylesterase 1	PPME1	S-42	0.00094701	3.706	3.493
Q9Y570	Protein phosphatase methylesterase 1	PPME1	S-25	0.0472203	2.043	3.601
O14974	Protein phosphatase 1 regulatory subunit 12A	PPP1R12A	S-299	0.00026997	3.823	3.993

O14974	Protein phosphatase 1 regulatory subunit 12A	PPP1R12A	S-445	0.00102961	3.368	4.818
O14974	Protein phosphatase 1 regulatory subunit 12A	PPP1R12A	S-479	0.03932213	-2.211	3.387
O14974	Protein phosphatase 1 regulatory subunit 12A	PPP1R12A	S-871	0.01253345	2.543	4.340
O14974	Protein phosphatase 1 regulatory subunit 12A	PPP1R12A	S-910	0.02037348	2.527	4.268
O14974	Protein phosphatase 1 regulatory subunit 12A	PPP1R12A	S-668	0.00636801	-6.212	4.331
O14974	Protein phosphatase 1 regulatory subunit 12A	PPP1R12A	S-527	0.0414854	2.068	4.184
O14974	Protein phosphatase 1 regulatory subunit 12A	PPP1R12A	T-443	0.0028601	3.053	4.008
O14974	Protein phosphatase 1 regulatory subunit 12A	PPP1R12A	T-453	0.00144653	3.322	4.159
O60237	Protein phosphatase 1 regulatory subunit 12B	PPP1R12B	S-735	2.64E-16	17.405	3.980
O60237	Protein phosphatase 1 regulatory subunit 12B	PPP1R12B	T-646	5.85E-06	-5.055	3.709
Q9BZL4-3	Protein phosphatase 1 regulatory subunit 12C	PPP1R12C	T-425;424	0.02457234	-3.940	4.184
Q96A00	Protein phosphatase 1 regulatory subunit 14A	PPP1R14A	S-26	0.00017742	-4.043	4.107

P41236	Protein phosphatase inhibitor 2	PPP1R2	S-87	2.29E-07	-10.971	4.401
Q8TAP8	Protein phosphatase 1 regulatory subunit 35	PPP1R35	S-52	0.03468539	-2.156	4.147
O75864	Protein phosphatase 1 regulatory subunit 37	PPP1R37	S-591	5.55E-05	-4.471	3.806
O75864	Protein phosphatase 1 regulatory subunit 37	PPP1R37	S-597	5.51E-05	-4.473	3.698
Q9UQK1	Protein phosphatase 1 regulatory subunit 3C	PPP1R3C	S-293	0.0332413	3.533	3.869
Q6ZSY5	Protein phosphatase 1 regulatory subunit 3F	PPP1R3F	S-547	4.75E-16	-14.080	3.942
Q6ZSY5	Protein phosphatase 1 regulatory subunit 3F	PPP1R3F	S-401	0.02414463	2.447	3.169
Q15435	Protein phosphatase 1 regulatory subunit 7	PPP1R7	S-12	0.04859862	-2.210	3.977
Q15435	Protein phosphatase 1 regulatory subunit 7	PPP1R7	S-27	0.01788489	2.402	5.383
Q13362	Serine/threonine-protein phosphatase 2A 56 kDa regulatory subunit gamma isoform	PPP2R5C	S-497	0.01800698	2.413	3.733
Q14738	Serine/threonine-protein phosphatase 2A 56 kDa regulatory subunit delta isoform	PPP2R5D	S-89	0.0386936	2.095	3.993

Q14738	Serine/threonine-protein phosphatase 2A 56 kDa regulatory subunit delta isoform	PPP2R5D	S-90	0.01775354	2.411	3.987
Q16537	Serine/threonine-protein phosphatase 2A 56 kDa regulatory subunit epsilon isoform	PPP2R5E	S-32	0.03591954	-2.141	3.744
Q5H9R7	Serine/threonine-protein phosphatase 6 regulatory subunit 3	PPP6R3	S-617	0.00057646	3.557	4.324
P60484	Phosphatidylinositol 3,4,5-trisphosphate 3-phosphatase and dual-specificity protein phosphatase PTEN	PTEN	S-385	0.01164622	-3.006	3.531
Q06124	Tyrosine-protein phosphatase non-receptor type 11	PTPN11	Y-542	0.00022141	-4.114	4.047
Q05209	Tyrosine-protein phosphatase non-receptor type 12	PTPN12	S-673	0.00810178	2.695	4.232
Q05209	Tyrosine-protein phosphatase non-receptor type 12	PTPN12	S-332	0.02811565	2.244	3.964
Q05209	Tyrosine-protein phosphatase non-receptor type 12	PTPN12	S-435	0.00060957	3.541	4.497
Q05209	Tyrosine-protein phosphatase non-receptor type 12	PTPN12	S-603	0.00591639	-2.808	4.343

Q05209	Tyrosine-protein phosphatase non-receptor type 12	PTPN12	S-606	0.00482508	-2.878	4.478
Q05209	Tyrosine-protein phosphatase non-receptor type 12	PTPN12	S-514	0.03641523	-3.416	3.743
Q05209	Tyrosine-protein phosphatase non-receptor type 12	PTPN12	T-573	0.03584007	-2.166	3.413
Q12923	Tyrosine-protein phosphatase non-receptor type 13	PTPN13	S-1033	0.00016125	-5.533	4.003
Q12923	Tyrosine-protein phosphatase non-receptor type 13	PTPN13	S-348	0.01515415	2.860	3.367
Q12923	Tyrosine-protein phosphatase non-receptor type 13	PTPN13	Y-943	0.04908539	2.205	3.396
Q15678	Tyrosine-protein phosphatase non-receptor type 14	PTPN14	S-831	0.00052177	-3.818	3.603
Q15678	Tyrosine-protein phosphatase non-receptor type 14	PTPN14	S-465	0.0125604	-2.539	4.317
Q15678	Tyrosine-protein phosphatase non-receptor type 14	PTPN14	S-314	4.16E-06	4.965	3.888
Q15678	Tyrosine-protein phosphatase non-receptor type 14	PTPN14	S-578	0.04508345	-2.064	3.846
Q15678	Tyrosine-protein phosphatase non-receptor type 14	PTPN14	S-591	0.00072607	-4.591	4.037
Q16825	Tyrosine-protein phosphatase non-receptor type 21	PTPN21	S-673	0.00156558	-3.245	4.143

Q16825	Tyrosine-protein phosphatase non-receptor type 21	PTPN21	S-637	0.00096966	-3.421	4.141
Q16825	Tyrosine-protein phosphatase non-receptor type 21	PTPN21	S-554	0.00612893	-2.916	3.519
Q16825	Tyrosine-protein phosphatase non-receptor type 21	PTPN21	S-616	0.02581209	-2.308	3.257
Q16825	Tyrosine-protein phosphatase non-receptor type 21	PTPN21	T-605	0.01884477	-2.564	3.247
Q16825	Tyrosine-protein phosphatase non-receptor type 21	PTPN21	Y-552	0.04881489	-2.018	3.596
Q9H3S7	Tyrosine-protein phosphatase non-receptor type 23	PTPN23	S-1126	7.68E-07	-9.756	4.636
P18433	Receptor-type tyrosine-protein phosphatase alpha	PTPRA	S-189	0.03900058	-2.144	3.115
Q92932	Receptor-type tyrosine-protein phosphatase N2	PTPRN2	S-230	0.00033649	-15.610	4.799
Q9BX95	Sphingosine-1-phosphate phosphatase 1	SGPP1	S-112	1.76E-05	-7.088	4.008
P78324	Tyrosine-protein phosphatase non-receptor type substrate 1	SIRPA	S-406	0.00459705	-2.989	3.597
Q8WYL5	Protein phosphatase Slingshot homolog 1	SSH1	S-576	0.00068587	3.505	4.166
Q8WYL5	Protein phosphatase Slingshot homolog 1	SSH1	S-515	0.01028973	-2.843	3.775

Q8WYL5	Protein phosphatase Slingshot homolog 1	SSH1	S-521	0.007734	-5.831	3.835
Q8WYL5	Protein phosphatase Slingshot homolog 1	SSH1	S-897	1.49E-05	4.878	3.754
Q8TE77	Protein phosphatase Slingshot homolog 3	SSH3	S-9	0.02975912	-2.293	4.100
Q8TE77	Protein phosphatase Slingshot homolog 3	SSH3	S-87	1.17E-05	-7.401	4.018
Q8TE77	Protein phosphatase Slingshot homolog 3	SSH3	S-653	0.04471384	-2.058	3.440

Table 13. Significant protein phosphatase quantified in obese insulin-resistant participants upon insulin-stimulation in human skeletal muscle cells. Fold change is log2 transformed, zero indicates no change, while 1 indicates 2 fold increase and -1 indicates 50% decrease. P-Value <0.05

Accession	Protein	Gene Name	phospho-Sites	P-Value	Fold change (Insulin/No-Insulin, OIR)	SEM
Q9Y5B0	RNA polymerase II subunit A C-terminal domain phosphatase	CTDP1	S474	0.0492	2.203	2.948
Q05D32	CTD small phosphatase-like protein 2	CTDSPL2	S33	0.0009	4.442	3.516
Q5VZP5	Inactive dual specificity phosphatase 27	DUSP27	S1005	0.0194	-2.484	3.787
Q9Y6X5	Bis(5'-adenosyl)-triphosphatase ENPP4	ENPP4	S439	0.0007	-3.978	3.717
Q9Y6X5	Bis(5'-adenosyl)-triphosphatase ENPP4	ENPP4	Y360	0.01941	-4.279	3.222
Q9Y6X5	Bis(5'-adenosyl)-triphosphatase ENPP4	ENPP4	Y371	0.01941	-4.279	3.222
O14974	Protein phosphatase 1 regulatory subunit 12A	PPP1R12A	S527	5.65E-05	-4.225	4.249
O60237	Protein phosphatase 1 regulatory subunit 12B	PPP1R12B	S735	0.02284	2.412	3.218
P41236	Protein phosphatase inhibitor 2;Protein phosphatase inhibitor 2-like protein 3	PPP1R2;PPP1R2P3	S121	0.042801	2.048	4.336
P41236	Protein phosphatase inhibitor	PPP1R2;PPP1R2P3	S122	0.02424	2.283	4.501

	2;Protein phosphatase inhibitor 2-like protein 3					
P41236	Protein phosphatase inhibitor 2;Protein phosphatase inhibitor 2-like protein 3	PPP1R2;PPP1R2P3	S127	0.00547	2.860	4.104
Q14738	Serine/threonine-protein phosphatase 2A 56 kDa regulatory subunit delta isoform	PPP2R5D	S88	0.00138	3.299	4.095
Q14738	Serine/threonine-protein phosphatase 2A 56 kDa regulatory subunit delta isoform	PPP2R5D	S89	0.00024	3.809	4.154
Q14738	Serine/threonine-protein phosphatase 2A 56 kDa regulatory subunit delta isoform	PPP2R5D	S90	3.74E-05	4.318	4.079
Q5H9R7	Serine/threonine-protein phosphatase 6 regulatory subunit 3	PPP6R3	S617	0.024704	2.281	4.245
Q06124	Tyrosine-protein phosphatase non-receptor type 11	PTPN11	S558	0.00209	-3.550	3.147
Q12923	Tyrosine-protein phosphatase non-receptor type 13	PTPN13	T909	0.03240	-2.438	2.966
Q16825	Tyrosine-protein phosphatase non-receptor type 21	PTPN21	S590	0.006323	-2.790	3.283
Q8WYL5	Protein phosphatase Slingshot homolog 1	SSH1	S937	0.013579	-2.522	3.484

Table 14. Significant (P<0.05) protein phosphatase quantified in both groups upon insulin-stimulation when comparing Lean vs OIR in human skeletal muscle cells. Fold change is log2 transformed and zero indicates no change, while 1 indicates 2 fold increase and -1 indicates 50% decrease.

Accession	Protein	Gene Name	phos-phoSites	P-Value	Fold change (Insulin (Lean)/ Insulin (OIR))	SEM
Q5VZP5	Inactive dual specificity phosphatase 27	DUSP27	S426	0.017301	0.37223	3.9297
Q5VZP5	Inactive dual specificity phosphatase 27	DUSP27	S1036	0.027385	-1.18313	3.8307
Q5VZP5	Inactive dual specificity phosphatase 27	DUSP27	S376	0.019985	0.25724	3.1880
Q5VZP5	Inactive dual specificity phosphatase 27	DUSP27	S1065	0.012526	-1.75607	3.5936
Q8IZ21-3	Phosphatase and actin regulator 4	PHACTR4	S574	0.002812	-2.33429	3.1239
O14974	Protein phosphatase 1 regulatory subunit 12A	PPP1R12A	S479	0.00132	2.174591	3.5694
O14974	Protein phosphatase 1 regulatory subunit 12A	PPP1R12A	S862	0.013451	-1.28702	4.093
O14974	Protein phosphatase 1 regulatory subunit 12A	PPP1R12A	S871	0.028793	-0.25054	4.1937
Q15678	Tyrosine-protein phosphatase non-receptor type 14	PTPN14	S831	0.031934	-0.78283	3.1845

Table 15. Effect of metformin on phosphorylation of protein phosphatases 2A subunits in human skeletal muscle cells in lean insulin-sensitive and obese insulin-resistant participants. Fold change is log2 transformed and zero indicates no change, while 1 indicates 2 fold increase and -1 indicates 50% decrease.

Accession	Protein	Gene Name	phospho-Sites	Fold change ± SEM (Lean)	Fold change ± SEM (OIR)
Q06190	Serine/threonine-protein phosphatase 2A regulatory subunit B" subunit alpha	PPP2R3A	S181	1.1 ±3.4	1.2 ±3.4
Q13362	Serine/threonine-protein phosphatase 2A 56 kDa regulatory subunit gamma isoform	PPP2R5C	S497*	2.8 ± 3.7	-1.3 ±3.5
Q14738	Serine/threonine-protein phosphatase 2A 56 kDa regulatory subunit delta isoform	PPP2R5D	S88	0.58± 3.8	1.50± 4.01
Q14738	Serine/threonine-protein phosphatase 2A 56 kDa regulatory subunit delta isoform	PPP2R5D	S89*	1.12 ± 4.0	2.04± 4.1
Q14738	Serine/threonine-protein phosphatase 2A 56 kDa regulatory subunit delta isoform	PPP2R5D	S90*	1.28± 4.0	2.14± 4.0
Q14738	Serine/threonine-protein phosphatase 2A 56 kDa regulatory subunit delta isoform	PPP2R5D	S573*	1.85± 3.8	-2.18± 3.9
Q14738	Serine/threonine-protein phosphatase 2A 56 kDa regulatory subunit delta isoform	PPP2R5D	S62	NA	-1.1± 2.6
Q15172	Serine/threonine-protein phosphatase 2A 56 kDa regulatory subunit alpha isoform	PPP2R5A	S42	-0.24± 3.6	-1.62± 3.3
Q16537	Serine/threonine-protein phosphatase 2A 56 kDa regulatory subunit epsilon isoform	PPP2R5E	S32*	-2.30± 3.7	0.46± 3.4

Q16537	Serine/threonine-protein phosphatase 2A 56 kDa regulatory subunit epsilon isoform	PPP2R5E	S33*	2.08± 4.0	1.29± 4.0
Q16537	Serine/threonine-protein phosphatase 2A 56 kDa regulatory subunit epsilon isoform	PPP2R5E	S34	1.88± 4.0	1.79 ± 4.0
O43815	Protein Phosphatase 2 Regulatory Subunit B''' Alpha	STRN	S245	1.42± 4.5	-1.36± 4.6
Q13033	Protein Phosphatase 2 Regulatory Subunit B''' Beta	STRN3	S229	0.62± 3.4	-0.93± 3.6
Q13033	Protein Phosphatase 2 Regulatory Subunit B''' Beta	STRN3	S257*	2.65± 4.3	0.24± 4.5
Q9NRL3	Protein Phosphatase 2 Regulatory Subunit B''' Gamma	STRN4	S276*	2.39± 3.6	-5.63± 3.8
Q9NRL3	Protein Phosphatase 2 Regulatory Subunit B''' Gamma	STRN4	T377*	-2.54± 4.0	-0.89± 3.3

*: P- Value <0.05, the phosphosites are highlighted with green indicated that sites were significant change in Lean and the sites highlighted with yellow indicated that sites were significant change in OIR.

Table 16. Effect of metformin on phosphorylation of protein kinases in human skeletal muscle cells in lean insulin-sensitive and OIR participants. Fold change is log2 transformed and zero indicates no change, while 1 indicates 2 fold increase and -1 indicates 50% decrease. * P-Value <0.05; ND: not detectable

Acces-sion	Protein	Gene Name	Sites	Fold change ±SEM, Lean	Fold change ±SEM,OIR
P42684	Abelson tyrosine-protein kinase 2	ABL2	S936	2.08±3.18*	-2.1±3.06*
P25098	Beta-adrenergic receptor kinase 1	ADRBK1	S670	-3.51±3.89*	-0.38±3.74
Q96L96	Alpha-protein kinase 3	ALPK3	S1844	-0.86±4.41	-2.09±4.74*
Q96L96	Alpha-protein kinase 3	ALPK3	S1401	0.94±3.29	3.11±3.5*
Q96L96	Alpha-protein kinase 3	ALPK3	S1209	-0.05±3.5	-2.81±3.65*
Q96L96	Alpha-protein kinase 3	ALPK3	S430	0.93±3.99	-2.05±4.02*
Q96L96	Alpha-protein kinase 3	ALPK3	S1235	1.8±3.69	-3.18±3.71*
Q96L96	Alpha-protein kinase 3	ALPK3	T1190	-0.96±3.07	-2.13±3.19*
P15056	Serine/threonine-protein kinase B-raf	BRAF	S365		-3±3.34*
Q13557-10	Calcium/calmodulin-dependent protein kinase type II subunit delta;Calcium/calmodulin-dependent protein kinase type II subunit alpha	CAMK2D;CAMK2A	T287	-1.57±3.29	2.19±4.18*
Q5VT25-6	Serine/threonine-protein kinase MRCK alpha	CDC42BPA	S1638;1665	4.45±3.35*	-6.11±3.91*
Q5VT25-6	Serine/threonine-protein kinase MRCK alpha	CDC42BPA	S1630	-1.19±3.02	-2.23±2.92*
P21127	Cyclin-dependent kinase 11B;Cyclin-dependent kinase 11A	CDK11B;CDK11A	S277;265	0.87±2.95	-3±2.84*
Q9NYV4-2	Cyclin-dependent kinase 12	CDK12	S644	3.5±3.6*	-2.9±3.44*

Q00536	Cyclin-dependent kinase 16	CDK16	S138	2.39±3.86*	-2.66±3.7*
Q00536	Cyclin-dependent kinase 16	CDK16	S153	-0.81±3.52	-2.77±3.58*
Q07002	Cyclin-dependent kinase 18	CDK18	S16	3.25±3.46*	-8.55±4.03*
P49918	Cyclin-dependent kinase inhibitor 1C	CDKN1C	S297	2.84±3.08*	2.98±3.39*
P12277	Creatine kinase B-type	CKB	S164	-2.31±3.32*	-2.32±3.24*
P12277	Creatine kinase B-type	CKB	S4	-1.01±3.27	-2.44±3.13*
Q68DQ2	Very large A-kinase anchor protein	CRYBG3	S931	ND	-2.78±3.3*
P53355	Death-associated protein kinase 1	DAPK1	S745	0.95±2.52	-3.34±3.21*
O15075	Serine/threonine-protein kinase DCLK1	DCLK1	S298	ND	-2.7±5.75*
Q8N568-3	Serine/threonine-protein kinase DCLK2	DCLK2	S308	2.79±4.07*	-2.56±4.3*
O00418	Eukaryotic elongation factor 2 kinase	EEF2K	Y443	ND	3.01±3.35*
P16591	Tyrosine-protein kinase Fer	FER	S434	ND	-6.74±3.33*
Q5VSY0	G kinase-anchoring protein 1	GKAP1	S360	-1.18±2.45	-2.29±2.43*
Q9ULH0	Kinase D-interacting substrate of 220 kDa	KIDINS220	S1555	1.33±3.36	-2.11±3.47*
Q8IVT5	Kinase suppressor of Ras 1	KSR1	S406	-2.51±3.77*	-2.05±3.66*
Q8WXG6	MAP kinase-activating death domain protein	MADD	S1059	3.82±3.2*	-3.35±3.02*
Q96QZ7	Membrane-associated guanylate kinase, WW and PDZ domain-containing protein 1	MAGI1	S1361	-1.66±3.54	2.13±3.17*
Q02750	Dual specificity mitogen-activated protein kinase kinase 1	MAP2K1	T292	ND	-2.84±3.59*
P36507	Dual specificity mitogen-activated protein kinase kinase 2	MAP2K2	S306	ND	3.6±3.5*
Q16584	Mitogen-activated protein kinase kinase kinase 11	MAP3K11	S740	ND	-4.96±3.66*
Q16584	Mitogen-activated protein kinase kinase kinase 11	MAP3K11	S705	0.86±3.1	-2.35±3.55*

Q9Y6R4	Mitogen-activated protein kinase kinase kinase 4	MAP3K4	S431	6.89±3.57*	-5.05±3.56*
O43318	Mitogen-activated protein kinase kinase kinase 7	MAP3K7	T444	1.06±3.13	-2.14±3.55*
O95819-6	Mitogen-activated protein kinase kinase kinase kinase 4	MAP4K4	S550;519	1.49±3.24	-2.54±3.5*
O95819-6	Mitogen-activated protein kinase kinase kinase kinase 4	MAP4K4	S631;708;623;600	-1.73±4.29	-2.54±4.24*
O95819-3	Mitogen-activated protein kinase kinase kinase kinase 4	MAP4K4	T846;927;841	-0.2±3.21	-3.05±3.31*
O95819-6	Mitogen-activated protein kinase kinase kinase kinase 4;Misshapen-like kinase 1;TRAF2 and NCK-interacting protein kinase	MAP4K4;MINK1;TNIK	T181	-0.34±3.16	-3.44±3.35*
O60336	Mitogen-activated protein kinase-binding protein 1	MAP-KBP1	S18	2.82±3.19*	-3.91±3.27*
O60336	Mitogen-activated protein kinase-binding protein 1	MAP-KBP1	S761	1.07±2.95	2.67±3.26*
P29966	Myristoylated alanine-rich C-kinase substrate	MARCKS	S145	-0.39±4.52	5.2±4.6*
P29966	Myristoylated alanine-rich C-kinase substrate	MARCKS	S147	0.84±4.45	2.45±4.36*
P29966	Myristoylated alanine-rich C-kinase substrate	MARCKS	S131	-0.54±3.12	4.14±3.54*
P29966	Myristoylated alanine-rich C-kinase substrate	MARCKS	S26	1.35±3.49	4.4±3.75*
P29966	Myristoylated alanine-rich C-kinase substrate	MARCKS	S27	-0.24±4.59	6.47±4.71*
P29966	Myristoylated alanine-rich C-kinase substrate	MARCKS	S101	-0.04±4.54	2.92±4.57*
P29966	Myristoylated alanine-rich C-kinase substrate	MARCKS	S170	ND	4.92±5.47*
P29966	Myristoylated alanine-rich C-kinase substrate	MARCKS	T143	1.57±4.04	2.83±4.39*
P29966	Myristoylated alanine-rich C-kinase substrate	MARCKS	T150	ND	7.78±5.7*
Q7KZI7-14	Serine/threonine-protein kinase MARK2	MARK2	S422	ND	2.22±3.97*

P27448	MAP/microtubule affinity-regulating kinase 3	MARK3	S601	-0.36±3.13	-2.18±3.91*
P27448	MAP/microtubule affinity-regulating kinase 3;Serine/threonine-protein kinase MARK1;Serine/threonine-protein kinase MARK2;MAP/microtubule affinity-regulating kinase 4	MARK3;MARK1;MARK2;MARK4	T211;175;214	-0.09±3.4	-3.55±3.53*
Q6P0Q8	Microtubule-associated serine/threonine-protein kinase 2	MAST2	S1381	-3.87±3.48*	-5.94±3.45*
O60307	Microtubule-associated serine/threonine-protein kinase 3	MAST3	S774	-0.54±2.81	-3.11±3.32*
O15021	Microtubule-associated serine/threonine-protein kinase 4	MAST4	S1467	-3.46±3.4*	-2.41±3.49*
P42345	Serine/threonine-protein kinase mTOR	MTOR	S1261	1.65±3.03	-4.88±3.39*
Q15746	Myosin light chain kinase, smooth muscle;Myosin light chain kinase, smooth muscle, deglutamylated form	MYLK	S1776	8.13±3.98*	2.28±3.44*
O95544	NAD kinase	NADK	S48		-3.43±3.29*
P22392-2	Putative nucleoside diphosphate kinase;Nucleoside diphosphate kinase B	NME2P1;NME2	S105;235	1.86±3.87	2.2±3.75*
O15530	3-phosphoinositide-dependent protein kinase 1;Putative 3-phosphoinositide-dependent protein kinase 2	PDPK1;PDPK2P	S241	-1.45±3.72	-2.3±3.49*
O15530	3-phosphoinositide-dependent protein kinase 1;Putative 3-phosphoinositide-dependent protein kinase 2	PDPK1;PDPK2P	Y248	-1.12±3.6	-2.06±3.33*
Q9H792	Pseudopodium-enriched atypical kinase 1	PEAK1	Y635	1.72±3.12	-3.56±3.21*

O60825	6-phosphofructo-2-kinase/fructose-2,6-bisphosphatase 2;6-phosphofructo-2-kinase;Fructose-2,6-bisphosphatase	PFKFB2	S466	-0.73±2.95	-3.11±3.22*
Q9BTU6	Phosphatidylinositol 4-kinase type 2-alpha	PI4K2A	S47	-1.18±4.26	-2.21±4.05*
P42356	Phosphatidylinositol 4-kinase alpha	PI4KA	S256	3.42±3.54*	-2.15±3.25*
Q16513	Serine/threonine-protein kinase N2	PKN2	S302	-0.2±3.48	-4.38±3.71*
Q16513	Serine/threonine-protein kinase N2	PKN2	S306	ND	-2.31±3.25*
Q9Y478	5'-AMP-activated protein kinase subunit beta-1	PRKAB1	S24	ND	3.36±4.62*
O43741	5'-AMP-activated protein kinase subunit beta-2	PRKAB2	T40	3.04±3.34*	-2.1±3.13*
O43741	5'-AMP-activated protein kinase subunit beta-2	PRKAB2	T40		-2.1±3.13*
P17612	cAMP-dependent protein kinase catalytic subunit alpha;cAMP-dependent protein kinase catalytic subunit gamma;cAMP-dependent protein kinase catalytic subunit beta	PRKACA;PRKACG;PRKACB	Y205	ND	-2.46±3.29*
Q05655	Protein kinase C delta type;Protein kinase C delta type regulatory subunit;Protein kinase C delta type catalytic subunit	PRKCD	S664	ND	-3.07±3.08*
O94806	Serine/threonine-protein kinase D3	PRKD3	S213	ND	-3.3±3.31*
Q15139	Serine/threonine-protein kinase D3;Serine/threonine-protein kinase D1	PRKD3;PRKD1	S391;397	ND	-2.86±3.52*
P78527	DNA-dependent protein kinase catalytic subunit	PRKDC	S893	ND	-5.63±2.9*
O75569	Interferon-inducible double-stranded RNA-dependent protein kinase activator A	PRKRA	T20	-0.86±4.06	2.97±3.99*

Q13523	Serine/threonine-protein kinase PRP4 homolog	PRPF4B	S257	-1.25±4.52	-2.54±4.77*
Q13523	Serine/threonine-protein kinase PRP4 homolog	PRPF4B	S431	-0.18±4.42	2.06±4.33*
P10398	RAF proto-oncogene serine/threonine-protein kinase;Serine/threonine-protein kinase A-Raf	RAF1;ARAF	S621;582	-2.45±4.58*	2.07±4.29*
P57059	Serine/threonine-protein kinase SIK1	SIK1	S547	ND	-4.36±3.29*
P57059	Serine/threonine-protein kinase SIK1	SIK1;LOC102724428	T577	ND	-2.02±3.29*
Q9NRH2	SNF-related serine/threonine-protein kinase	SNRK	S569	ND	5.16±3.15*
O60271	C-Jun-amino-terminal kinase-interacting protein 4	SPAG9	S203	2.44±3.83*	-2.71±3.64*
Q15772	Striated muscle preferentially expressed protein kinase	SPEG	S2458		-2.05±3.12*
Q15772	Striated muscle preferentially expressed protein kinase	SPEG	S419	ND	-4.41±3.41*
O94804	Serine/threonine-protein kinase 10	STK10	S13	ND	-2.83±3.62*
Q13188	Serine/threonine-protein kinase 3;Serine/threonine-protein kinase 3 36kDa subunit;Serine/threonine-protein kinase 3 20kDa subunit	STK3	S385	0.02±3.12	2.12±3.48*
Q8TEA7	TBC domain-containing protein kinase-like protein	TBCK	S890	1.96±3.47	-2.68±3.32*
Q86UE8	Serine/threonine-protein kinase tousled-like 2	TLK2	T72	-0.2±3.79	-3.13±3.51*
Q9UKE5	TRAF2 and NCK-interacting protein kinase	TNIK	S548	1±3.4	-2.43±4.07*
Q07912	Activated CDC42 kinase 1	TNK2	S102	2.13±3.38	-3.31±3.47*
Q9NWZ5	Uridine-cytidine kinase-like 1	UCKL1	S56		-3.92±3.37*
O75385	Serine/threonine-protein kinase ULK1	ULK1	S556	-5.82±3.82*	-3.69±3.37*

O75385	Serine/threonine-protein kinase ULK1	ULK1	T636	3.59±3.4*	-2.49±3.23*
O75385	Serine/threonine-protein kinase ULK1	ULK1	S588	ND	-2.65±3.23*
Q9H4A3	Serine/threonine-protein kinase WNK1	WNK1	S1261	-2.52±3.77*	2.36±3.46*
Q9H4A3	Serine/threonine-protein kinase WNK1	WNK1	S2027	ND	-2.64±3.62*
Q9H4A3	Serine/threonine-protein kinase WNK1	WNK1	S2032	ND	-2.44±3.84*
Q9NYL2	Mitogen-activated protein kinase kinase kinase MLT	ZAK	S633	ND	-2.95±3.44*
Q9UIG0	Tyrosine-protein kinase BAZ1B	BAZ1B	S312	ND	-3.6±3.24*
Q9NSY1	BMP-2-inducible protein kinase	BMP2K	T1000	ND	4.43±3.56*
Q9NYV4-2	Cyclin-dependent kinase 12	CDK12	S420	ND	-2.19±3.7*
Q9NYV4-2	Cyclin-dependent kinase 12	CDK12	S423	ND	-2.17±3.73*
Q9NYV4-2	Cyclin-dependent kinase 12	CDK12	S332	ND	2.93±3.89*
Q9NYV4-2	Cyclin-dependent kinase 12	CDK12	S644	ND	-2.9±3.44*
Q9NYV4-2	Cyclin-dependent kinase 12	CDK12	T692	ND	-2.29±3.37*
Q14004	Cyclin-dependent kinase 13	CDK13	S1054	ND	-2.26±3.64*
Q14004	Cyclin-dependent kinase 13	CDK13	T1058	ND	-2.64±3.43*
Q00537	Cyclin-dependent kinase 17	CDK17	S180	ND	-3.05±3.77*
Q07002	Cyclin-dependent kinase 18	CDK18	S134	ND	2.02±4.12*
P46527	Cyclin-dependent kinase inhibitor 1B	CDKN1B	S10	ND	3.37±3.78*
O95747	Serine/threonine-protein kinase OSR1	OXSR1	S339	2.67±4.33*	-3.15±3.17*
O60271	C-Jun-amino-terminal kinase-interacting protein 4	SPAG9	T217	2.58±4.2*	-2.52±4.04*
P17612	cAMP-dependent protein kinase catalytic subunit alpha;cAMP-dependent protein kinase catalytic subunit	PRKACA;PRKACG;PRKACB	T198	ND	-3.76±3.74*

	gamma;cAMP-dependent protein kinase catalytic subunit beta				
Q2M2I8	AP2-associated protein kinase 1	AAK1	S637	3.23±3.55*	-1.28±3.57
Q2M2I8	AP2-associated protein kinase 1	AAK1	S670	2.48±3.73*	0.07±3.38
Q2M2I8	AP2-associated protein kinase 1	AAK1	T640	2.75±4.22*	-0.05±3.69
Q2M2I8	AP2-associated protein kinase 1	AAK1	T672	2.74±3.77*	0.18±3.56
Q2M2I8	AP2-associated protein kinase 1	AAK1	T620	2.01±4.89*	-1.02±4.6
Q2M2I8	AP2-associated protein kinase 1	AAK1	T606	3.24±4.33*	0.64±4.12
P00519	Tyrosine-protein kinase ABL1	ABL1	S569	-4.16±3.94*	0.61±2.88
P42684	Abelson tyrosine-protein kinase 2	ABL2	S631	4.09±3.87*	0.2±3.21
Q92667	A-kinase anchor protein 1, mitochondrial	AKAP1	S445	4.49±3.61*	-1.03±3.16
Q9Y243	RAC-gamma serine/threonine-protein kinase	AKT3	S476	2.85±3.5*	-0.24±3.22
Q96L96	Alpha-protein kinase 3	ALPK3	S1394	-2.21±4.65*	-0.54±3.97
Q96L96	Alpha-protein kinase 3	ALPK3	S1865	-2.92±4.94*	0.64±4.36
Q96L96	Alpha-protein kinase 3	ALPK3	T1383	-3.25±4.67*	-0.46±3.85
Q96L96	Alpha-protein kinase 3	ALPK3	T728	-2.3±4.42*	-1.04±3.98
P10398	Serine/threonine-protein kinase A-Raf	ARAF	S257	-3.22±4.11*	1.03±3.64
P10398	Serine/threonine-protein kinase A-Raf	ARAF	S157	-7.45±3.72*	0.31±2.96
P10398	Serine/threonine-protein kinase A-Raf	ARAF	T181	-4.12±3.88*	ND
P15056	Serine/threonine-protein kinase B-raf	BRAF	S419	-4.76±4.12*	-2.14±3.68
P15056	Serine/threonine-protein kinase B-raf	BRAF	S446	-7.94±3.83*	0.31±2.83
P15056	Serine/threonine-protein kinase B-raf	BRAF	S151	2.65±3.92*	-0.63±3.65
Q13557	Calcium/calmodulin-dependent protein kinase type II subunit delta	CAMK2D	S334	5.27±3.72*	0.17±3.14

Q13557-10	Calcium/calmodulin-dependent protein kinase type II subunit delta	CAMK2D	S348	2.12±4.04*	0.15±3.53
Q5VT25-6	Serine/threonine-protein kinase MRCK alpha	CDC42BPA	S1673;1700	2.76±3.77*	0.59±3.41
Q5VT25-6	Serine/threonine-protein kinase MRCK alpha	CDC42BPA	T1640;1667	3.19±3.67*	ND
P06493	Cyclin-dependent kinase 1;Cyclin-dependent kinase 2;Cyclin-dependent kinase 3	CDK1;CDK2;CDK3	T14	-5.1±4.4*	ND
P21127	Cyclin-dependent kinase 11B	CDK11B	S115	3.26±4.33*	0.47±4.13
P21127	Cyclin-dependent kinase 11B	CDK11B	T600	4.84±4.16*	ND
P21127	Cyclin-dependent kinase 11B;Cyclin-dependent kinase 11A	CDK11B;CDK11A	S65	-3.69±3.87*	ND
P21127	Cyclin-dependent kinase 11B;Cyclin-dependent kinase 11A	CDK11B;CDK11A	S47	-2.16±4.14*	0.61±3.32
Q14004	Cyclin-dependent kinase 13	CDK13	S662	8.91±3.85*	-1.71±3.2
Q14004	Cyclin-dependent kinase 13	CDK13	S1065	3.8±3.97*	-1.08±3.71
Q14004	Cyclin-dependent kinase 13	CDK13	T494	-2.57±3.99*	1.28±3.41
Q14004	Cyclin-dependent kinase 13	CDK13	T1147	7.7±3.71*	-0.6±3.33
O94921	Cyclin-dependent kinase 14	CDK14	T79	3.08±3.41*	0.41±3.26
Q00536	Cyclin-dependent kinase 16	CDK16	S65	-5.25±3.87*	0.25±2.77
Q00536	Cyclin-dependent kinase 16	CDK16	S110	3.65±3.38*	-0.29±3.21
Q00536	Cyclin-dependent kinase 16;Cyclin-dependent kinase 17	CDK16;CDK17	S119;146	-2.61±3.82*	0.48±3.5
Q07002	Cyclin-dependent kinase 18	CDK18	S132	3.82±4.37*	-0.7±4.33
Q07002	Cyclin-dependent kinase 18	CDK18	S14	2.06±3.95*	-1.8±3.83
Q07002	Cyclin-dependent kinase 18	CDK18	S117	2.09±4.29*	-0.94±3.99

P50613	Cyclin-dependent kinase 7	CDK7	T170	-2.43±4.02*	0.13±3.26
P06732	Creatine kinase M-type;Creatine kinase M-type, N-terminally processed	CKM	S199	3.9±3.75*	-1.67±3.72
P06732	Creatine kinase M-type;Creatine kinase M-type, N-terminally processed	CKM	S164	2.29±3.34*	-0.43±3.1
P06732	Creatine kinase M-type;Creatine kinase M-type, N-terminally processed	CKM	T166	2.97±3.44*	-0.31±3.13
P49761	Dual specificity protein kinase CLK3	CLK3	S157	-3.94±3.46*	-0.74±2.96
Q9HAZ1	Dual specificity protein kinase CLK4	CLK4	S138	-9.1±3.97*	ND
Q6P9H4	Connector enhancer of kinase suppressor of ras 3	CNKSR3	S383	-3.98±4.44*	0.06±3.13
Q68DQ2	Very large A-kinase anchor protein	CRYBG3	S800	7.46±4.34*	ND
Q68DQ2	Very large A-kinase anchor protein	CRYBG3	S802	7.46±4.34*	ND
P48729	Casein kinase I isoform alpha	CSNK1A1	T321	-2.11±3.19*	-0.93±3.14
P48730-2	Casein kinase I isoform delta	CSNK1D	S383	-2.59±3.53*	0.51±2.98
P48730-2	Casein kinase I isoform delta	CSNK1D	S384	-2.54±3.55*	ND
P48730-2	Casein kinase I isoform delta	CSNK1D	S328	-3.7±4.2*	0.28±3.53
P48730-2	Casein kinase I isoform delta	CSNK1D	S331	-2.38±4.61*	-0.32±4.22
P48730-2	Casein kinase I isoform delta	CSNK1D	S401	-2.48±3.5*	-0.52±3.21
P49674	Casein kinase I isoform epsilon	CSNK1E	S363	2.67±4.41*	-1.43±4.33
P49674	Casein kinase I isoform epsilon	CSNK1E	T362	2.04±3.07*	-1.89±3.31
O43293	Death-associated protein kinase 3	DAPK3	S311	-2.34±3.34*	0.57±3.05
O43293	Death-associated protein kinase 3	DAPK3	S312	-3.79±3.82*	0.46±3.25
O15075	Serine/threonine-protein kinase DCLK1	DCLK1	S720	-3.33±3.73*	0.72±3.13

O15075	Serine/threonine-protein kinase DCLK1	DCLK1	S294	2.23±4.34*	0.85±4.16
O15075	Serine/threonine-protein kinase DCLK1	DCLK1	S298	2±5.55*	
O15075	Serine/threonine-protein kinase DCLK1	DCLK1	S310	-2.94±3.34*	1.63±3.03
O15075	Serine/threonine-protein kinase DCLK1	DCLK1	T296	3.51±4.2*	0.34±3.88
O15075	Serine/threonine-protein kinase DCLK1	DCLK1	T311	2.58±3.93*	0.55±3.63
O15075	Serine/threonine-protein kinase DCLK1	DCLK1	T317	8.61±3.88*	-0.05±3.31
Q8N568-3	Serine/threonine-protein kinase DCLK2	DCLK2	S688; 705	3.23±3.35*	ND
Q8N568-3	Serine/threonine-protein kinase DCLK2	DCLK2	S6	-2.87±3.29*	0.45±3.05
Q8N568-3	Serine/threonine-protein kinase DCLK2	DCLK2	S362; 379	-2.39±3.72*	0.93±3.16
Q8N568-3	Serine/threonine-protein kinase DCLK2	DCLK2	S317	3.34±3.79*	0.19±3.63
Q8N568-3	Serine/threonine-protein kinase DCLK2	DCLK2	T683; 700	3.6±3.03*	ND
Q8N568-3	Serine/threonine-protein kinase DCLK2	DCLK2	T693; 710	7.7±3.67*	ND
Q13574	Diacylglycerol kinase zeta	DGKZ	S894	3.5±3.47*	ND
Q09013	Myotonin-protein kinase	DMPK	S540	2.59±3.31*	-0.55±2.89
Q13627	Dual specificity tyrosine-phosphorylation-regulated kinase 1A;Dual specificity tyrosine-phosphorylation-regulated kinase 1B	DYRK1A;DYRK1B	Y321	2.97±4.34*	-1.55±4.12
Q92630	Dual specificity tyrosine-phosphorylation-regulated kinase 2	DYRK2	S48	2.25±3.34*	-0.86±2.9
O00418	Eukaryotic elongation factor 2 kinase	EEF2K	S462	-3.15±3.62*	-0.24±2.79
O00418	Eukaryotic elongation factor 2 kinase	EEF2K	S474	-2.16±3.17*	0.46±2.87
O00418	Eukaryotic elongation factor 2 kinase	EEF2K	S72	-2.21±3.71*	-0.02±3.39
Q9BQI3	Eukaryotic translation initiation factor 2-alpha kinase 1	EIF2AK1	S258	-5.56±3.41*	ND
Q9P2K8	Eukaryotic translation initiation factor 2-alpha kinase 4	EIF2AK4	T667	2.77±3.83*	-1.54±3.66

Q12929	Epidermal growth factor receptor kinase substrate 8	EPS8	S625	2.04±4.05*	-1.68±3.95
Q12929	Epidermal growth factor receptor kinase substrate 8	EPS8	S659	-5.01±4.66*	-0.15±3.48
Q12929	Epidermal growth factor receptor kinase substrate 8	EPS8	S661	-3.28±4.65*	-0.14±3.34
Q12929	Epidermal growth factor receptor kinase substrate 8	EPS8	S664	-11.88±4.62*	0.28±3.31
Q9H6S3	Epidermal growth factor receptor kinase substrate 8-like protein 2	EPS8L2	S570	2.28±3.49*	-0.44±3.03
P04626	Receptor tyrosine-protein kinase erbB-2	ERBB2	T1240	-8.22±3.58*	-1.74±2.74
P21860	Receptor tyrosine-protein kinase erbB-3	ERBB3	S686	-2.1±3.83*	0±3.08
O14976	Cyclin-G-associated kinase	GAK	S826	-2.1±2.99*	0.45±2.38
O14976	Cyclin-G-associated kinase	GAK	S829	-2.1±2.99*	0.45±2.38
P49841	Glycogen synthase kinase-3 alpha;Glycogen synthase kinase-3 beta	GSK3A; GSK3B	S282; 219	-4.23±3.91*	-0.96±3.46
P49841	Glycogen synthase kinase-3 alpha;Glycogen synthase kinase-3 beta	GSK3A; GSK3B	Y279 ;216	-2.3±5.26*	-0.16±4.76
P49841	Glycogen synthase kinase-3 beta	GSK3B	S9	2.09±4.43*	-0.08±3.91
P49841	Glycogen synthase kinase-3 beta	GSK3B	S21	5.93±4.1*	-0.12±3.76
P49841	Glycogen synthase kinase-3 beta	GSK3B	S25	3.13±3.51*	-0.75±3.2
Q86Z02	Homeodomain-interacting protein kinase 1;Homeodomain-interacting protein kinase 2	HIPK1; HIPK2	Y352	-2.34±3.57*	-0.25±3.09
Q8NE63	Homeodomain-interacting protein kinase 4	HIPK4	S337	-3.78±3.17*	ND
Q8NE63	Homeodomain-interacting protein kinase 4	HIPK4	S339	-3.78±3.17*	ND
Q9P2D0	Inhibitor of Bruton tyrosine kinase	IBTK	S1083	7.74±3.78*	-2.19±3.4
Q9P2D0	Inhibitor of Bruton tyrosine kinase	IBTK	S999	5.17±4.11*	ND

O14920	Inhibitor of nuclear factor kappa-B kinase subunit beta	IKBKB	S672	-3.46±4.06*	0.88±3.27
Q8IVT5	Kinase suppressor of Ras 1	KSR1	S267	-3.29±4.25*	-0.6±3.59
Q8IVT5	Kinase suppressor of Ras 1	KSR1	S409	2.51±3.19*	1.08±2.71
Q8WXG6	MAP kinase-activating death domain protein	MADD	S1239	-2.21±3.64*	0.04±3.5
Q8WXG6	MAP kinase-activating death domain protein	MADD	S1241	-3.75±4.14*	0.41±3.49
Q8WXG6	MAP kinase-activating death domain protein	MADD	T1245	-4.21±3.77*	ND
Q02750	Dual specificity mitogen-activated protein kinase kinase 1	MAP2K1	T292	3.33±3.83*	0.56±4.73
P36507	Dual specificity mitogen-activated protein kinase kinase 2	MAP2K2	T394	2.24±5.02*	ND
P36507	Dual specificity mitogen-activated protein kinase kinase 2;Dual specificity mitogen-activated protein kinase kinase 1	MAP2K2;MAP2K1	S222;218	3.1±3.39*	ND
Q13233	Mitogen-activated protein kinase kinase kinase 1	MAP3K1	S21	-2.49±3.83*	-0.58±3.1
Q16584	Mitogen-activated protein kinase kinase kinase 11	MAP3K11	S507	-7.41±3.63*	-1.29±3.14
Q9Y2U5	Mitogen-activated protein kinase kinase kinase 2	MAP3K2	S248	-7.6±4.26*	0.18±3.19
Q99759	Mitogen-activated protein kinase kinase kinase 3	MAP3K3	S250	-2.73±4.11*	0.84±3.58
Q9Y6R4	Mitogen-activated protein kinase kinase kinase 4	MAP3K4	S1251	-2.21±3.68*	ND
Q9Y6R4	Mitogen-activated protein kinase kinase kinase 4	MAP3K4	S1252	-3.05±4.1*	0.27±3.04
Q8IVH8	Mitogen-activated protein kinase kinase kinase kinase 3	MAP4K3	S329	6.09±3.69*	-1.53±3.39

O95819-6	Mitogen-activated protein kinase kinase kinase kinase 4	MAP4K4	S579;548	-3.16±3.18*	-1.01±2.86
O95819-6	Mitogen-activated protein kinase kinase kinase kinase 4	MAP4K4	S580;549	-3.96±3.73*	-1.5±3.47
O95819-6	Mitogen-activated protein kinase kinase kinase kinase 4	MAP4K4	S700;778;692;670	-2.84±3.08*	-1.96±2.93
O95819-6	Mitogen-activated protein kinase kinase kinase kinase 4	MAP4K4	S639;716;631;608	-2.34±3.74*	0.22±3.45
O95819-6	Mitogen-activated protein kinase kinase kinase kinase 4	MAP4K4	S710;788;702;680	2.1±4.44*	-1.73±4.51
O95819-6	Mitogen-activated protein kinase kinase kinase kinase 4	MAP4K4	S635;712;627;604	-2.47±4.41*	-1.06±4.04
O95819-6	Mitogen-activated protein kinase kinase kinase kinase 4	MAP4K4	S879	6.99±3.95*	ND
Q9Y4K4	Mitogen-activated protein kinase kinase kinase kinase 5	MAP4K5	S335	2.86±4.23*	-0.26±3.87
P28482	Mitogen-activated protein kinase 1	MAPK1	T181	2.32±3.85*	-0.96±3.83
Q16539	Mitogen-activated protein kinase 14	MAPK14	S2	-6.32±3.79*	ND
P27361	Mitogen-activated protein kinase 3	MAPK3	T202	-2.46±4.01*	-1.01±3.99
Q16659	Mitogen-activated protein kinase 6	MAPK6	S684	2.97±3.1*	ND
Q16659	Mitogen-activated protein kinase 6	MAPK6	S688	2.97±3.1*	ND
Q13164	Mitogen-activated protein kinase 7	MAPK7	S731	-3.27±3.53*	-2.6±3.28
Q9UPT6	C-Jun-amino-terminal kinase-interacting protein 3	MAPK8IP3	S207	-2.21±3.4*	-0.74±2.97
Q9UPT6	C-Jun-amino-terminal kinase-interacting protein 3	MAPK8IP3	S584	4.32±4.29*	-0.35±3.91
Q9UPT6	C-Jun-amino-terminal kinase-interacting protein 3	MAPK8IP3	S585	3.56±4.12*	-0.06±3.64

O60336	Mitogen-activated protein kinase-binding protein 1	MAP-KBP1	S1198	-5.59±3.87*	-0.61±2.78
P29966	Myristoylated alanine-rich C-kinase substrate	MARCKS	S170	3.92±5.42*	
P29966	Myristoylated alanine-rich C-kinase substrate	MARCKS	T150	2.8±5.62*	
Q7KZI7-14	Serine/threonine-protein kinase MARK2	MARK2	S357	2.61±3.51*	-1.66±3.35
Q7KZI7-14	Serine/threonine-protein kinase MARK2	MARK2	S376	4.66±3.56*	ND
Q7KZI7-14	Serine/threonine-protein kinase MARK2	MARK2	S422	2.34±4*	ND
P27448	MAP/microtubule affinity-regulating kinase 3	MARK3	S455	2.82±3.61*	-0.43±3.37
P27448	MAP/microtubule affinity-regulating kinase 3	MARK3	T507	-5.01±3.53*	-0.45±2.55
P27448	MAP/microtubule affinity-regulating kinase 3;Serine/threonine-protein kinase MARK1;Serine/threonine-protein kinase MARK2;MAP/microtubule affinity-regulating kinase 4	MARK3;MARK1;MARK2;MARK4	S215;179;218	2.03±4.01*	-1.4±3.72
P27448	MAP/microtubule affinity-regulating kinase 3;Serine/threonine-protein kinase MARK1;Serine/threonine-protein kinase MARK2;MAP/microtubule affinity-regulating kinase 4	MARK3;MARK1;MARK2;MARK4	Y218;182;221	7.27±3.79*	-1.38±3.57
Q6P0Q8	Microtubule-associated serine/threonine-protein kinase 2	MAST2	S209	-3.14±3.4*	ND
Q6P0Q8	Microtubule-associated serine/threonine-protein kinase 2	MAST2	S883	7.25±4.15*	-0.3±3.36
Q6P0Q8	Microtubule-associated serine/threonine-protein kinase 2	MAST2	S900	2.39±3.31*	-1.74±3.21
Q6P0Q8	Microtubule-associated serine/threonine-protein kinase 2	MAST2	T1036	3.21±3.92*	-1.58±3.53

O60307	Microtubule-associated serine/threonine-protein kinase 3	MAST3	S348	-7.18±3.66*	0.66±2.42
O60307	Microtubule-associated serine/threonine-protein kinase 3	MAST3	S793	2.09±3.3*	0.32±3.17
O60307	Microtubule-associated serine/threonine-protein kinase 3	MAST3	S146	-9.41±4.17*	0.84±2.85
O15021	Microtubule-associated serine/threonine-protein kinase 4	MAST4	S1391	-5.24±3.9*	ND
O15021	Microtubule-associated serine/threonine-protein kinase 4	MAST4	S1779	7.05±3.67*	0.08±2.35
O15021	Microtubule-associated serine/threonine-protein kinase 4	MAST4	T1382	-5.24±3.9*	ND
Q6P0Q8	Microtubule-associated serine/threonine-protein kinase 4;Microtubule-associated serine/threonine-protein kinase 2	MAST4; MAST2	S864; 806	-6.44±3.35*	ND
Q6P0Q8	Microtubule-associated serine/threonine-protein kinase 4;Microtubule-associated serine/threonine-protein kinase 2;Microtubule-associated serine/threonine-protein kinase 1	MAST4; MAST2; MAST1	S1432;1393	-2.26±3.51*	0.2±3.41
Q8N4C8	Misshapen-like kinase 1	MINK1	S733	2.92±3.58*	-0.39±3.24
P51948	CDK-activating kinase assembly factor MAT1	MNAT1	S279	-6.71±4.33*	0.05±1.98
P42345	Serine/threonine-protein kinase mTOR	MTOR	S2478	7.43±3.69*	ND
P42345	Serine/threonine-protein kinase mTOR	MTOR	S2481	7.43±3.69*	ND
O15146	Muscle, skeletal receptor tyrosine-protein kinase	MUSK	S541	-3.89±3.96*	ND
Q15746	Myosin light chain kinase, smooth muscle;Myosin light chain kinase, smooth muscle, deglutamylated form	MYLK	S305	-2.42±3.74*	ND
Q15746	Myosin light chain kinase, smooth muscle;Myosin light chain	MYLK	S1779	7.42±3.79*	0.2±2.99

	kinase, smooth muscle, deglutamylated form				
Q9UJ70	N-acetyl-D-glucosamine kinase	NAGK	S76	3.05±4.25*	0.27±3.87
Q96PY6	Serine/threonine-protein kinase Nek1	NEK1	S1126	-4.59±3.97*	0.2±3.22
Q96PY6	Serine/threonine-protein kinase Nek1	NEK1	S1057	3.04±3.8*	-0.16±3.31
Q8TD19	Serine/threonine-protein kinase Nek9	NEK9	S29	3.62±2.82*	ND
Q8TD19	Serine/threonine-protein kinase Nek9	NEK9	T333	-2.43±3.43*	ND
P15531	Nucleoside diphosphate kinase A	NME1	S120	2.05±3.45*	1.04±3.06
P15531	Nucleoside diphosphate kinase A	NME1	S122	2.55±3.5*	1.18±3.36
P22392-2	Putative nucleoside diphosphate kinase;Nucleoside diphosphate kinase A;Nucleoside diphosphate kinase B	NME2P1;NME1;NME2	T79;94	3.26±3.66*	0.31±3.41
Q5SY16	Polynucleotide 5'-hydroxyl-kinase NOL9	NOL9	S487	2.28±3.64*	-1.53±3.29
O60285	NUAK family SNF1-like kinase 1	NUAK1	S380	-3.37±4.02*	0.45±3.25
O60285	NUAK family SNF1-like kinase 1	NUAK1	S22	-2.86±3.98*	0.15±3.16
Q9H1E3	Nuclear ubiquitous casein and cyclin-dependent kinase substrate 1	NUCKS1	S130	3.17±3.69*	ND
Q9H1E3	Nuclear ubiquitous casein and cyclin-dependent kinase substrate 1	NUCKS1	S132	3.17±3.69*	ND
Q9H1E3	Nuclear ubiquitous casein and cyclin-dependent kinase substrate 1	NUCKS1	S144	3.17±3.69*	ND
Q9H1E3	Nuclear ubiquitous casein and cyclin-dependent kinase substrate 1	NUCKS1	S214	2.38±5.91*	1.79±5.66
Q9H1E3	Nuclear ubiquitous casein and cyclin-dependent kinase substrate 1	NUCKS1	S223	2.11±4.56*	0.64±4.16
Q9BY11	Protein kinase C and casein kinase substrate in neurons protein 1	PACSIN1	T184	2.14±3.45*	1.19±3.26
Q9UKS6	Protein kinase C and casein kinase substrate in neurons protein 3	PACSIN3	S383	-3.93±3.32*	ND

Q9UKS6	Protein kinase C and casein kinase substrate in neurons protein 3	PACSIN3	S319	-2.6±3.64*	-0.46±3.03
Q13153	Serine/threonine-protein kinase PAK 1	PAK1	S137	3.53±4.37*	1.19±3.9
Q13153	Serine/threonine-protein kinase PAK 1	PAK1	S115	5.67±3.47*	-1.57±3.07
Q13153	Serine/threonine-protein kinase PAK 1	PAK1	S204	-5.59±3.49*	ND
Q13177	Serine/threonine-protein kinase PAK 2;PAK-2p27;PAK-2p34	PAK2	S132	3.39±3.87*	-0.06±2.85
Q13177	Serine/threonine-protein kinase PAK 2;PAK-2p27;PAK-2p34	PAK2	S58	2.41±3.4*	-1.25±3.13
Q13177	Serine/threonine-protein kinase PAK 2;PAK-2p27;PAK-2p34	PAK2	S64	5.02±3.33*	-1.37±3.24
Q13177	Serine/threonine-protein kinase PAK 2;PAK-2p27;PAK-2p34	PAK2	S19	3.93±3.87*	ND
Q13177	Serine/threonine-protein kinase PAK 2;PAK-2p27;PAK-2p34	PAK2	S2	-3.45±4.54*	1.09±3.81
Q13177	Serine/threonine-protein kinase PAK 2;PAK-2p27;PAK-2p34	PAK2	T169	-2.67±4.17*	-1.11±3.85
O96013	Serine/threonine-protein kinase PAK 4	PAK4	S104	-2.7±4.44*	1.82±3.78
O96013	Serine/threonine-protein kinase PAK 4	PAK4	Y480	3.08±3.25*	-1.16±3.1
Q9Y2D5-6	Paralemmin-2;A-kinase anchor protein 2	PALM2;AKAP2	S155	2.05±3.43*	-0.92±3.07
O15530	3-phosphoinositide-dependent protein kinase 1;Putative 3-phosphoinositide-dependent protein kinase 2	PDPK1;PDPK2P	T245	3.11±3.9*	-1±3.31
Q9H792	Pseudopodium-enriched atypical kinase 1	PEAK1	S1169	-4.78±4.02*	ND
Q9H792	Pseudopodium-enriched atypical kinase 1	PEAK1	S1217	-2.99±4.31*	0.07±3.59
Q9H792	Pseudopodium-enriched atypical kinase 1	PEAK1	S648	-2.18±3.44*	ND
Q9H792	Pseudopodium-enriched atypical kinase 1	PEAK1	S1036	3.58±3.98*	-1.83±3.74
Q9H792	Pseudopodium-enriched atypical kinase 1	PEAK1	S1038	-2.46±3.37*	ND

Q9H792	Pseudopodium-enriched atypical kinase 1	PEAK1	S587	2.36±3.85*	-0.3±3.39
O60825	6-phosphofructo-2-kinase/fructose-2,6-bisphosphatase 2;6-phosphofructo-2-kinase;Fructose-2,6-bisphosphatase	PFKFB2	S493	5.67±3.46*	-0.72±2.77
Q93100	Phosphorylase b kinase regulatory subunit beta	PHKB	S701	5.02±3.58*	0.96±3.28
Q9BTU6	Phosphatidylinositol 4-kinase type 2-alpha	PI4K2A	S44	-2.75±3.77*	-1.98±3.84
Q9BTU6	Phosphatidylinositol 4-kinase type 2-alpha	PI4K2A	S51	-2.31±4.35*	-0.35±4
P42356	Phosphatidylinositol 4-kinase alpha	PI4KA	S1436	-16.06±4.7*	0.38±2.81
P42356	Phosphatidylinositol 4-kinase alpha	PI4KA	T255	-5.51±3.72*	-0.26±2.98
Q9UBF8-2	Phosphatidylinositol 4-kinase beta	PI4KB	S266	2.22±3.51*	ND
Q9UBF8-2	Phosphatidylinositol 4-kinase beta	PI4KB	T280	2.87±4*	0.6±3.59
Q9UBF8-2	Phosphatidylinositol 4-kinase beta	PI4KB	T292	3.83±3.52*	-0.66±3.26
O00443	Phosphatidylinositol 4-phosphate 3-kinase C2 domain-containing subunit alpha	PIK3C2A	S259	3.17±3.57*	-1.13±3.28
Q9Y2I7	1-phosphatidylinositol 3-phosphate 5-kinase	PIKFYVE	S1758	2.88±3.62*	-0.92±3.15
Q16512	Serine/threonine-protein kinase N1	PKN1	S916	3.49±4.28*	-0.54±4.07
Q16513	Serine/threonine-protein kinase N2	PKN2	S306	-3.35±2.99*	ND
Q16513	Serine/threonine-protein kinase N2	PKN2	S110	-4.09±3.57*	0.14±2.16
Q16513	Serine/threonine-protein kinase N2	PKN2	T820	-4.54±3.17*	ND
Q96T60	Bifunctional polynucleotide phosphatase/kinase;Polynucleotide 3'-phosphatase;Polynucleotide 5'-hydroxyl-kinase	PNKP	T118	2.1±4.05*	1.02±4.07
Q6PFW1	Inositol hexakisphosphate and diphosphoinositol-pentakisphosphate kinase 1	PPIP5K1	S1152	-3±3.5*	-0.54±3

Q13131	5'-AMP-activated protein kinase catalytic subunit alpha-1	PRKAA1	S508	3.27±4.16*	1.33±3.75
Q13131	5'-AMP-activated protein kinase catalytic subunit alpha-1	PRKAA1	S498	-2.35±4.46*	-0.08±3.59
O43741	5'-AMP-activated protein kinase subunit beta-2	PRKAB2	S108	2.47±3.5*	0.27±3.3
P17612	cAMP-dependent protein kinase catalytic subunit alpha	PRKACA	Y331	-3.53±3.07*	-1.21±2.73
P17612	cAMP-dependent protein kinase catalytic subunit alpha;cAMP-dependent protein kinase catalytic subunit gamma;cAMP-dependent protein kinase catalytic subunit beta	PRKACA;PRKACG;PRKACB	T202	2.19±4.19*	-1.98±3.89
P17612	cAMP-dependent protein kinase catalytic subunit alpha;cAMP-dependent protein kinase catalytic subunit gamma;cAMP-dependent protein kinase catalytic subunit beta	PRKACA;PRKACG;PRKACB	Y205	3.92±3.55*	ND
P22694	cAMP-dependent protein kinase catalytic subunit beta	PRKACB	S339	-5.85±3.97*	-1.38±3.23
P10644	cAMP-dependent protein kinase type I-alpha regulatory subunit;cAMP-dependent protein kinase type I-alpha regulatory subunit, N-terminally processed	PRKAR1A	S77	3.42±4.43*	1.22±4.25
P31321	cAMP-dependent protein kinase type I-beta regulatory subunit	PRKAR1B	S3	-3.55±3.7*	-0.29±3.42
P31321	cAMP-dependent protein kinase type I-beta regulatory subunit	PRKAR1B	S77	2.37±3.56*	0.72±3.14
P13861	cAMP-dependent protein kinase type II-alpha regulatory subunit	PRKAR2A	S78	2.03±4.97*	-1.37±5.05

P13861	cAMP-dependent protein kinase type II-alpha regulatory subunit	PRKAR2A	S80	2.08±4.96*	-1.42±5.04
P13861	cAMP-dependent protein kinase type II-alpha regulatory subunit	PRKAR2A	S99	-2.09±3.95*	0±3.66
P31323	cAMP-dependent protein kinase type II-beta regulatory subunit	PRKAR2B	S114	-4.6±3.91*	-1.86±3.29
P17252	Protein kinase C alpha type	PRKCA	S226	3.84±4.01*	-0.97±3.48
P17252	Protein kinase C alpha type	PRKCA	S319	-4.54±3.91*	ND
P17252	Protein kinase C alpha type;Protein kinase C beta type;Protein kinase C gamma type	PRKCA;PRKCB;PRKCG	T497	-2.54±3.8*	-1.8±3.44
P17252	Protein kinase C alpha type;Protein kinase C beta type;Protein kinase C gamma type	PRKCA;PRKCB;PRKCG	Y504	-4.95±3.49*	ND
Q05655	Protein kinase C delta type;Protein kinase C delta type regulatory subunit;Protein kinase C delta type catalytic subunit	PRKCD	S658	6.49±3.75*	ND
Q969G5	Protein kinase C delta-binding protein	PRKCDBP	S62	-2.03±3.02*	1.04±2.98
Q02156	Protein kinase C epsilon type	PRKCE	T710	-2.96±3.51*	-1.47±3.1
Q15139	Serine/threonine-protein kinase D1	PRKD1	S251	-3.13±3.65*	ND
Q15139	Serine/threonine-protein kinase D1	PRKD1	T214	-2.49±3.71*	-0.46±3.1
Q9BZL6	Serine/threonine-protein kinase D2	PRKD2	S396	3.11±4.03*	0.2±3.59
O94806	Serine/threonine-protein kinase D3	PRKD3	S27	5.88±3.21*	-1.61±2.75
Q15139	Serine/threonine-protein kinase D3;Serine/threonine-protein kinase D1	PRKD3;PRKD1	S393;399	2.31±3.2*	-1.97±3.24
Q15139	Serine/threonine-protein kinase D3;Serine/threonine-protein kinase D1	PRKD3;PRKD1	T389;395	3.31±3.67*	ND
Q13523	Serine/threonine-protein kinase PRP4 homolog	PRPF4B	S87	2.51±4.06*	1.74±3.97

Q13523	Serine/threonine-protein kinase PRP4 homolog	PRPF4B	S93	2.8±4.24*	0.76±4.1
Q13523	Serine/threonine-protein kinase PRP4 homolog	PRPF4B	S20	3.8±3.83*	0.53±3.29
Q13523	Serine/threonine-protein kinase PRP4 homolog	PRPF4B	S23	3.8±3.83*	0.53±3.29
Q13523	Serine/threonine-protein kinase PRP4 homolog	PRPF4B	S277	3.05±4.73*	-0.06±4.34
Q13523	Serine/threonine-protein kinase PRP4 homolog	PRPF4B	S283	2.27±3.74*	-0.73±3.52
Q13523	Serine/threonine-protein kinase PRP4 homolog	PRPF4B	S379	3.6±4.03*	0.6±3.63
Q13523	Serine/threonine-protein kinase PRP4 homolog	PRPF4B	S381	4.1±4.12*	0.3±3.73
Q13523	Serine/threonine-protein kinase PRP4 homolog	PRPF4B	S383	4.04±4.33*	0.55±3.83
Q13523	Serine/threonine-protein kinase PRP4 homolog	PRPF4B	S376	14.71±4.18*	1.33±3.51
Q05397	Focal adhesion kinase 1	PTK2	S716	2.67±3.35*	1.22±3.16
P04049	RAF proto-oncogene serine/threonine-protein kinase	RAF1	S642	-3.31±3.8*	-0.58±3.04
P04049	RAF proto-oncogene serine/threonine-protein kinase	RAF1	S29	-2.97±3.16*	ND
P10398	RAF proto-oncogene serine/threonine-protein kinase;Serine/threonine-protein kinase A-Raf	RAF1;ARAF	S624;585	-3.44±3.94*	0.26±3.18
Q9BVS4	Serine/threonine-protein kinase RIO2	RIOK2	S332	-3.57±3.66*	ND
Q9BVS4	Serine/threonine-protein kinase RIO2	RIOK2	S335	-3.18±3.44*	ND
Q9BVS4	Serine/threonine-protein kinase RIO2	RIOK2	S337	-2.28±3.49*	ND
Q9BVS4	Serine/threonine-protein kinase RIO2	RIOK2	S380	4.13±3.34*	0.69±3.12
Q9BVS4	Serine/threonine-protein kinase RIO2	RIOK2	S442	-5.59±3.6*	ND
O43353	Receptor-interacting serine/threonine-protein kinase 2	RIPK2	S531	2.43±3.02*	-0.03±2.61
Q13464	Rho-associated protein kinase 1	ROCK1	S1341	2.35±4.47*	-0.01±4.4
O75116	Rho-associated protein kinase 2	ROCK2	S1137	-2.6±3.35*	ND
P51812	Ribosomal protein S6 kinase alpha-3	RPS6KA3	S375	2.94±3.12*	ND

P51812	Ribosomal protein S6 kinase alpha-3;Ribosomal protein S6 kinase alpha-1;Ribosomal protein S6 kinase alpha-6	RPS6KA3;RPS6KA1;RPS6KA6	S227	-3.8±3.9*	ND
P51812	Ribosomal protein S6 kinase alpha-3;Ribosomal protein S6 kinase alpha-1;Ribosomal protein S6 kinase alpha-6	RPS6KA3;RPS6KA1;RPS6KA6	Y234	-3.59±3.76*	ND
Q96S38	Ribosomal protein S6 kinase delta-1	RPS6KC1	S282	-11.35±4.44*	-0.2±2.77
Q86YV5	Tyrosine-protein kinase SgK223	SGK223	S510	-2.85±3.65*	-0.04±2.86
Q86YV5	Tyrosine-protein kinase SgK223	SGK223	T1227	3.65±3.45*	-0.15±2.91
Q96B97-2	SH3 domain-containing kinase-binding protein 1	SH3KBP1	S550	4.02±4.92*	1.73±4.66
Q96B97-2	SH3 domain-containing kinase-binding protein 1	SH3KBP1	S552	5.51±4.04*	0.12±3.52
Q96B97-2	SH3 domain-containing kinase-binding protein 1	SH3KBP1	S128	4.19±3.66*	ND
Q96B97-2	SH3 domain-containing kinase-binding protein 1	SH3KBP1	S146	3.21±4.29*	1.3±3.79
Q96B97-2	SH3 domain-containing kinase-binding protein 1	SH3KBP1	S151	5.1±4.26*	0.15±3.65
Q9H0K1	Serine/threonine-protein kinase SIK2	SIK2	S534	2.95±3.41*	ND
Q9H0K1	Serine/threonine-protein kinase SIK2	SIK2	S576	-9.15±3.97*	ND
Q9H0K1	Serine/threonine-protein kinase SIK2	SIK2	S358	-2.44±3.98*	ND
Q9Y2K2	Serine/threonine-protein kinase SIK3	SIK3	S730	2.13±3.5*	-1.02±3.17
Q9Y2K2	Serine/threonine-protein kinase SIK3	SIK3	S731	2.15±3.77*	-0.76±3.63
Q9Y2K2	Serine/threonine-protein kinase SIK3	SIK3	S34	2.88±3.23*	-1.49±3.07
Q9H2G2-2	STE20-like serine/threonine-protein kinase	SLK	S348	-2.38±3.32*	-1.14±3
Q9H2G2-2	STE20-like serine/threonine-protein kinase	SLK	S354	4.37±3.49*	-1.82±2.99
Q9H2G2-2	STE20-like serine/threonine-protein kinase	SLK	S781	-2.59±3.74*	-0.01±3.32
Q9H2G2-2	STE20-like serine/threonine-protein kinase	SLK	S565	2.86±4.42*	0.86±3.77
Q9H2G2-2	STE20-like serine/threonine-protein kinase	SLK	S372	2.66±4.28*	0.49±3.75

Q9H2G2-2	STE20-like serine/threonine-protein kinase	SLK	S655	-2.46±3.76*	ND
O60271	C-Jun-amino-terminal kinase-interacting protein 4	SPAG9	S728	3.51±4.55*	0.13±4.19
O60271	C-Jun-amino-terminal kinase-interacting protein 4	SPAG9	S732	3.74±4.69*	0.64±4.49
O60271	C-Jun-amino-terminal kinase-interacting protein 4	SPAG9	S733	3.42±5.05*	0.95±4.77
O60271	C-Jun-amino-terminal kinase-interacting protein 4	SPAG9	S251	2.14±4.11*	-0.24±3.68
O60271	C-Jun-amino-terminal kinase-interacting protein 4	SPAG9	T595	-4.12±4.03*	ND
Q15772	Striated muscle preferentially expressed protein kinase	SPEG	S2037	-2.32±4.34*	0.65±3.75
Q15772	Striated muscle preferentially expressed protein kinase	SPEG	S2004	-2.41±3.67*	0.06±2.94
Q15772	Striated muscle preferentially expressed protein kinase	SPEG	S2941	-2.92±4.43*	1.01±3.52
Q15772	Striated muscle preferentially expressed protein kinase	SPEG	S2443	-4.83±3.71*	ND
Q15772	Striated muscle preferentially expressed protein kinase	SPEG	S2448	-2.98±3.61*	ND
Q15772	Striated muscle preferentially expressed protein kinase	SPEG	S1172	-2.35±3.68*	0.28±2.99
Q15772	Striated muscle preferentially expressed protein kinase	SPEG	S2458	-2.87±2.97*	ND
Q15772	Striated muscle preferentially expressed protein kinase	SPEG	S861;12	-2.28±3.66*	0.84±3.53
Q15772	Striated muscle preferentially expressed protein kinase	SPEG	S313	4.57±3.69*	ND
Q15772	Striated muscle preferentially expressed protein kinase	SPEG	S488	-6.95±3.67*	0.3±2.84

Q15772	Striated muscle preferentially expressed protein kinase	SPEG	S2948	-19.64±4.06*	0.62±2.42
Q15772	Striated muscle preferentially expressed protein kinase	SPEG	S853	2.31±3.67*	0.37±3.21
Q15772	Striated muscle preferentially expressed protein kinase	SPEG	S2284	2.63±3.41*	-0.53±2.73
Q15772-4	Striated muscle preferentially expressed protein kinase	SPEG	S4	-2.79±3.81*	1.16±3.47
Q96SB4	SRSF protein kinase 1	SRPK1	S51	-4.41±4.11*	-1.5±3.29
Q96SB4	SRSF protein kinase 1	SRPK1	S311	-3.48±4.49*	1.93±3.84
P78362	SRSF protein kinase 2;SRSF protein kinase 2 N-terminal;SRSF protein kinase 2 C-terminal	SRPK2	S497	3.29±3.92*	0.17±3.6
P78362	SRSF protein kinase 2;SRSF protein kinase 2 N-terminal;SRSF protein kinase 2 C-terminal	SRPK2	T498	2.7±4.08*	0.3±3.82
Q9UPE1	SRSF protein kinase 3	SRPK3	S330	-2.06±3.72*	-0.08±3.46
Q9UPE1	SRSF protein kinase 3	SRPK3	S382	10.64±4.13*	-0.83±2.94
O94804	Serine/threonine-protein kinase 10	STK10	S191	2.59±3.51*	ND
O94804	Serine/threonine-protein kinase 10	STK10	S417	-4.63±3.63*	0.31±3.25
Q8N1F8	Serine/threonine-protein kinase 11-interacting protein	STK11IP	S761	2.3±4.21*	0.36±4.09
Q8N1F8	Serine/threonine-protein kinase 11-interacting protein	STK11IP	S387	-4.77±3.93*	0.65±3.41
Q8N1F8	Serine/threonine-protein kinase 11-interacting protein	STK11IP	S482	-2.61±4.23*	1.05±3.87
Q9UEE5	Serine/threonine-protein kinase 17A	STK17A	S28	-4.2±3.48*	-0.97±2.94
Q9Y6E0-2	Serine/threonine-protein kinase 24;Serine/threonine-protein kinase 24 36 kDa subunit;Serine/threonine-protein kinase 24 12 kDa subunit	STK24	S4	-5.01±4.27*	-0.51±3.34
O00506	Serine/threonine-protein kinase 25	STK25	S231	2.8±3.14*	ND

Q9P289	Serine/threonine-protein kinase 26	STK26	S300	-3.14±2.88*	0.2±2.79
Q13188	Serine/threonine-protein kinase 3;Serine/threonine-protein kinase 3 36kDa subunit;Serine/threonine-protein kinase 3 20kDa subunit	STK3	S392	6.05±3.85*	-0.59±3.37
Q86UX6	Serine/threonine-protein kinase 32C	STK32C	S18	-3.12±3.95*	0.06±3.4
Q9UEW8	STE20/SPS1-related proline-alanine-rich protein kinase	STK39	S385	3.31±4.36*	-0.29±4.17
Q9UKE5	TRAF2 and NCK-interacting protein kinase	TNIK	S707	-2.81±3.46*	ND
Q07912	Activated CDC42 kinase 1	TNK2	S728	-2.46±4.1*	1.02±3.63
Q07912	Activated CDC42 kinase 1	TNK2	Y284	-4.07±3.77*	0.42±2.92
Q07912	Activated CDC42 kinase 1	TNK2	Y827	4.97±3.55*	1.16±3.18
P29597	Non-receptor tyrosine-protein kinase TYK2	TYK2	Y292	-9.08±4.3*	ND
O75385	Serine/threonine-protein kinase ULK1	ULK1	S450	6.77±3.61*	-1.61±3.27
O75385	Serine/threonine-protein kinase ULK1	ULK1	S623	3.12±3.63*	-1.46±3.57
Q6PHR2	Serine/threonine-protein kinase ULK3	ULK3	S464	3.29±3.69*	ND
Q9H4A3	Serine/threonine-protein kinase WNK1	WNK1	S174	2.94±3.16*	-0.05±2.33
P07947	Tyrosine-protein kinase Yes;Tyrosine-protein kinase Fyn;Tyrosine-protein kinase Lck;Proto-oncogene tyrosine-protein kinase Src	YES1;FYN;LCK;SRC	Y426;419	-4.86±3.81*	-1.9±3.23
Q9NYL2	Mitogen-activated protein kinase kinase kinase MLT	ZAK	S637	3.43±3.84*	-0.9±3.6
Q9ULU4-19	Protein kinase C-binding protein 1	ZMYND8	S433	2.13±3.6*	0.05±3.19
Q9ULU4-19	Protein kinase C-binding protein 1	ZMYND8	S682	2.64±3.78*	-0.65±3.41
Q9ULU4-19	Protein kinase C-binding protein 1	ZMYND8	S522	2.32±3.74*	-0.75±3.45

Table 17. Effect of metformin on phosphorylation of protein kinases in human skeletal muscle cells when comparing Lean vs OIR participants

Accession	Protein	Gene Name	PhosphoSites	P-Value	Fold change (Metformin (Lean)/ Metformin (OIR))	SEM
Q2M2I8	AP2-associated protein kinase 1	AAK1	S-676	0.023042	-2.334	3.011
Q9UKA4	A-kinase anchor protein 11	AKAP11	T-1100	0.025228	2.337	2.915
Q02952	A-kinase anchor protein 12	AKAP12	S-1391	0.009128	2.759	3.775
Q12802-4	A-kinase anchor protein 13	AKAP13	S-2703;2683	0.022809	4.045	3.560
Q12802-4	A-kinase anchor protein 13	AKAP13	S-1602;1584	0.038906	2.091	3.693
Q12802-4	A-kinase anchor protein 13	AKAP13	S-2563;2543	0.001906	3.218	3.678
Q12802-4	A-kinase anchor protein 13	AKAP13	T-953	0.004586	3.088	3.552
Q9Y2D5-6	A-kinase anchor protein 2	AKAP2	S-383	0.025695	2.260	3.849
Q96L96	Alpha-protein kinase 3	ALPK3	S-1401	0.004625	3.202	3.714
P10398	Serine/threonine-protein kinase A-Raf	ARAF	S-272	0.018063	-2.458	3.560
Q13557-10	Calcium/calmodulin-dependent protein kinase type II subunit delta	CAMK2D	S-315	0.001048	-3.410	4.148
Q13557-10	Calcium/calmodulin-dependent protein kinase type II subunit delta	CAMK2D	S-319	0.001048	-3.410	4.148
Q00536	Cyclin-dependent kinase 16;Cyclin-dependent kinase 17	CDK16; CDK17	S-119;146	0.019511	-2.371	3.596
Q00537	Cyclin dependent kinase 17	CDK17	S-180	0.040698	-2.072	3.503
Q07002	Cyclin-dependent kinase 18	CDK18	S-89	0.009431	-2.648	4.182
Q5VSY0	G kinase-anchoring protein 1	GKAP1	S-360	0.032253	2.441	2.277

P49841	Glycogen synthase kinase-3 beta	GSK3B	S-25	0.027886	-2.378	3.313
Q9P2D0	Inhibitor of Bruton tyrosine kinase	IBTK	S-1083	0.007343	3.261	3.451
Q8IVT5	Kinase suppressor of Ras 1	KSR1	T-425	0.03297	-2.183	3.296
O95819-6	Mitogen-activated protein kinase kinase kinase kinase 4	MAP4K4	S-700;778;692;670	0.023938	-2.397	2.993
P28482	Mitogen-activated protein kinase 1	MAPK1	T-181	0.0012	3.615	3.905
P28482	Mitogen-activated protein kinase 1	MAPK1	T-185	0.012959	2.524	4.616
P28482	Mitogen-activated protein kinase 1	MAPK1	Y-187	0.002814	3.053	4.833
Q9UPT6	C-Jun-amino-terminal kinase-interacting protein 3	MAPK8IP3	T-206	0.001056	-3.569	3.125
Q9UPT6	C-Jun-amino-terminal kinase-interacting protein 3	MAPK8IP3	T-753	0.037829	-2.142	3.464
O60336	Mitogen-activated protein kinase-binding protein 1	MAPKBP1	S-18	0.040802	2.309	3.127
P27448	MAP/microtubule affinity-regulating kinase 3	MARK3	S-411	0.012261	-2.640	3.760
P42345	Serine/threonine-protein kinase mTOR	MTOR	S-1261	0.032916	2.192	3.042
O95747	Serine/threonine-protein kinase OSR1	OXSR1	S-325	0.000713	-3.516	4.058
Q9H792	Pseudopodium-enriched atypical kinase 1	PEAK1	S-572	0.019344	2.390	3.529
Q9H792	Pseudopodium-enriched atypical kinase 1	PEAK1	S-587	0.014377	2.534	3.523
A2A3N6	Putative PIP5K1A and PSMD4-like protein;Phosphatidylinositol 4-phosphate 5-kinase type-1 alpha	PIPSL;PIP5K1A	S-405	0.014734	-2.524	3.651
Q9Y478	5'-AMP-activated protein kinase subunit beta-1	PRKAB1	S-25	0.013649	-2.918	4.209
O43741	5'-AMP-activated protein kinase subunit beta-2	PRKAB2	T-40	0.008189	2.751	3.428

Q13523	Serine/threonine-protein kinase PRP4 homolog	PRPF4B	S-32	0.029489	2.239	3.463
Q13464	Rho-associated protein kinase 1	ROCK1	S-1105	0.022265	2.319	3.682
Q13464	Rho-associated protein kinase 1	ROCK1	S-1341	0.011499	-2.568	4.415
Q9Y2K2	Serine/threonine-protein kinase SIK3	SIK3	S-626	0.035725	-2.132	3.542
Q9NRH2	SNF-related serine/threonine-protein kinase	SNRK	S-569	0.020856	-2.683	3.076
O60271	C-Jun-amino-terminal kinase-interacting protein 4	SPAG9	T-217	0.019936	2.366	3.909
Q15772	Striated muscle preferentially expressed protein kinase	SPEG	S-2496	0.004338	-2.966	3.331
O94804	Serine/threonine-protein kinase 10	STK10	S-450	0.029174	2.209	4.061
O94804	Serine/threonine-protein kinase 10	STK10	T-459	0.04718	2.012	4.004
Q9P289	Serine/threonine-protein kinase 26	STK26	S-300	0.046476	-3.116	3.011
Q9UEW8	STE20/SPS1-related proline-alanine-rich protein kinase	STK39	S-371	0.004424	-2.903	4.067
O75385	Serine/threonine-protein kinase ULK1	ULK1	T-636	0.006584	2.816	3.291

Table 18. Pathways significantly enriched for the differential phosphoproteins in metformin-treated cells, as measured by KEGG analysis.

No	Path-way ID	KEGG Pathway	Count	P-Value
1	hsa03040	Spliceosome	95	1.46E-26
2	hsa04144	Endocytosis	139	2.00E-24
3	hsa03013	RNA transport	105	4.16E-21
4	hsa03010	Ribosome	81	1.90E-15
5	hsa03050	Proteasome	35	3.47E-12
6	hsa01130	Biosynthesis of antibiotics	99	5.10E-10
7	hsa03015	mRNA surveillance pathway	53	7.44E-10
8	hsa04141	Protein processing in endoplasmic reticulum	83	7.74E-10
9	hsa01200	Carbon metabolism	57	1.57E-07
10	hsa04910	Insulin signaling pathway	66	1.86E-07
11	hsa04150	mTOR signaling pathway	35	2.88E-07
12	hsa04510	Focal adhesion	89	3.62E-07
13	hsa04810	Regulation of actin cytoskeleton	88	2.02E-06
14	hsa05131	Shigellosis	35	6.23E-06
15	hsa05100	Bacterial invasion of epithelial cells	40	9.11E-06
16	hsa04722	Neurotrophin signaling pathway	55	1.10E-05
17	hsa04120	Ubiquitin mediated proteolysis	60	2.28E-05
18	hsa03008	Ribosome biogenesis in eukaryotes	42	3.33E-05
19	hsa04012	ErbB signaling pathway	42	3.33E-05
20	hsa01230	Biosynthesis of amino acids	36	5.55E-05
21	hsa05130	Pathogenic Escherichia coli infection	28	6.06E-05
22	hsa00020	Citrate cycle (TCA cycle)	19	1.26E-04
23	hsa04010	MAPK signaling pathway	95	1.43E-04
24	hsa05220	Chronic myeloid leukemia	35	1.46E-04
25	hsa04919	Thyroid hormone signaling pathway	50	1.52E-04
26	hsa05205	Proteoglycans in cancer	78	1.55E-04
27	hsa04666	Fc gamma R-mediated phagocytosis	39	1.89E-04
28	hsa04520	Adherens junction	34	2.65E-04
29	hsa03018	RNA degradation	36	2.98E-04
30	hsa05132	Salmonella infection	38	3.27E-04
31	hsa00620	Pyruvate metabolism	22	4.61E-04
32	hsa00520	Amino sugar and nucleotide sugar metabo-lism	25	4.77E-04
33	hsa05211	Renal cell carcinoma	31	7.90E-04
34	hsa04530	Tight junction	38	9.82E-04
35	hsa00010	Glycolysis / Gluconeogenesis	31	1.07E-03
36	hsa05120	Epithelial cell signaling in Helicobacter py-lori infection	31	1.07E-03
37	hsa05169	Epstein-Barr virus infection	49	1.51E-03
38	hsa05134	Legionellosis	26	1.53E-03
39	hsa04152	AMPK signaling pathway	49	1.84E-03
40	hsa00310	Lysine degradation	25	1.99E-03
41	hsa04962	Vasopressin-regulated water reabsorption	22	2.25E-03
42	hsa05212	Pancreatic cancer	29	3.12E-03

43	hsa04961	Endocrine and other factor-regulated calcium reabsorption	22	3.17E-03
44	hsa04066	HIF-1 signaling pathway	39	3.96E-03
45	hsa05410	Hypertrophic cardiomyopathy (HCM)	33	4.15E-03
46	hsa05110	Vibrio cholerae infection	24	4.77E-03
47	hsa05213	Endometrial cancer	24	4.77E-03
48	hsa04114	Oocyte meiosis	43	6.55E-03
49	hsa00071	Fatty acid degradation	20	7.42E-03
50	hsa04330	Notch signaling pathway	22	7.97E-03
51	hsa05215	Prostate cancer	35	9.53E-03
52	hsa05210	hsa00030:Pentose phosphate pathway	15	1.05E-02
53	hsa05230	Central carbon metabolism in cancer	27	1.07E-02
54	hsa04921	Oxytocin signaling pathway	54	1.20E-02
55	hsa00270	Cysteine and methionine metabolism	18	1.26E-02
56	hsa04922	Glucagon signaling pathway	38	1.28E-02
57	hsa05223	Non-small cell lung cancer	24	1.37E-02
58	hsa04261	Adrenergic signaling in cardiomyocytes	50	1.38E-02
59	hsa04912	GnRH signaling pathway	35	1.66E-02
60	hsa04540	Gap junction	34	1.71E-02
61	hsa00480	Glutathione metabolism	22	1.75E-02
62	hsa04931	Insulin resistance	40	1.97E-02
63	hsa04142	Lysosome	44	1.99E-02
64	hsa04022	cGMP-PKG signaling pathway	55	2.24E-02
65	hsa05203	Viral carcinogenesis	69	2.29E-02
66	hsa05414	Dilated cardiomyopathy	32	2.58E-02
67	hsa05210	Colorectal cancer	25	2.61E-02
68	hsa05221	Acute myeloid leukemia	23	2.72E-02
69	hsa00630	Glyoxylate and dicarboxylate metabolism	13	3.56E-02
70	hsa04320	Dorso-ventral axis formation	13	3.56E-02
71	hsa04915	Estrogen signaling pathway	36	3.59E-02
72	hsa04068	FoxO signaling pathway	46	4.63E-02
73	hsa04110	Cell cycle	43	4.64E-02

Table 19. Significant enriched pathways for differential PP2Ac protein interaction partners in upon the metformin treatment, as measured by KEGG analysis

Term	Count	P-Value	Genes
hsa04144:Endocytosis	48	5.57E-12	TSG101, TFRC, SH3KBP1, VPS4A, CLTC, ARPC5L, KIAA1033,NEDD4L, AP2A1,AP2A2,SNX3, EEA1, SNX1, CAPZB, KIF5B, FAM21A, VPS35, AP2M1, RAB8A, SH3GL1, SH3GLB1, SH3GLB2, GIT2, HSPA8, RAB4A, SMAD3, GBF1, KIAA0196, VPS37B, ARPC5, ARFGAP1, ARFGAP2, RAB11B, RUFY1, EHD2, EHD4, ARPC2, ARPC3, HGS, CAPZA1, CHMP2B, CAPZA2, CHMP2A, CHMP4B, VPS25, ARF5, SPG20, ARF6
hsa03050:Proteasome	19	7.53E-11	PSMD11, PSMD14, PSMA7, PSMD8, PSMA6, PSMD6, PSMC5, PSMA3, PSMB5, PSMC3, PSMD4, PSMB2, PSMC4, PSMC1, PSMD3, PSMB1, PSME1, PSMD1, PSME2
hsa04141:Protein processing in endoplasmic reticulum	36	6.07E-10	UFD1L, SEC23A, HSP90AB1, SAR1A, PRKCSH, CUL1, RRBP1, DNAJB1, LMAN1, HSPH1, LMAN2, CAPN2, SSR1, CAPN1, SEC31A, UBQLN2, SEC63, HSPA8, SSR4, EIF2AK2, TRAF2, PDIA6, RAD23B, CKAP4, DNAJA1, DNAJC3, NSFL1C, NPLOC4, DNAJB11, DNAJA2, ERP29, PLAA, STUB1, P4HB, CRYAB, SEC24C
hsa03010:Ribosome	25	6.61E-06	RPL10, RPL34, RPLP0, RPL36A, RPL9, RPS17, RPS15A, RPL18A, RPS3, RPS2, RPS11, RPL18, RPL17, RPS10, RPS9, RPS7, RPL35A, RPL23A, RPS3A, RPS26, RPS28, RPS27, RPL27A, RPL24, RPL28
hsa01130:Biosynthesis of antibiotics	31	4.55E-05	FH, ECHS1, PYCRL, SHMT2, AK1, AK2, DLST, HSD17B10, ACAT1, LDHA, NSDHL, UGP2, ALDH1B1, PHGDH, PGLS, HADH, FDFT1, TPI1, MDH2, ARG1, ALDH3A2, HADHA, PFKL, PKM, SUCLA2, OGDH, ALDOC, ALDOA, PFKM, GAPDH, PFKP
hsa03013:RNA transport	27	4.74E-05	EIF4A2, CYFIP1, EIF4A1, EIF4A3, FXR2, NUP88, EIF4B, EIF2B5, EIF5B, EIF2B4, PABPC4, EIF2S2, NUP93, EIF2S3, XPOT, EIF3I, EIF3J, EEF1A2,

			GEMIN5, EIF3H, EIF3E, EIF3F, EIF4E2, EIF3D, EIF4G3, RAN, EIF4G1
hsa01200:Carbon metabolism	19	3.59E-04	FH, ECHS1, TPI1, SHMT2, MDH2, DLST, ACAT1, HADHA, PFKL, SUCLA2, PKM, OGDH, ALDOC, PHGDH, PGLS, ALDOA, GAPDH, PFKM, PFKP
hsa05132:Salmonella infection	15	8.92E-04	DYNC1H1, DYNC1I2, ROCK2, RHOG, ARPC5L, ARPC5, KLC1, TJP1, DYNC1LI2, KLC2, ARPC2, ARPC3, FLNB, PKN2, FLNC
hsa00970:Aminoacyl-tRNA biosynthesis	13	0.001	YARS, WARS, TARS, SARS, QARS, KARS, LARS, MARS, GARS, HARS, FARSA, FARSB, AARS
hsa03018:RNA degradation	14	0.001	HSPA9, PABPC4, CNOT10, WDR61, HSPD1, EDC4, PFKL, CNOT7, XRN1, CNOT1, CNOT3, SKIV2L, PFKM, PFKP
hsa04810:Regulation of actin cytoskeleton	26	0.003	ITGB1, CYFIP1, NCKAP1, ROCK2, ARPC5L, ARAF, MYL12A, CFL2, CFL1, ITGAV, PAK2, ITGA3, ACTN1, RDX, FN1, ARPC5, GNG12, MYLPF, ENAH, DIAPH1, ARPC2, ARPC3, ITGA7, ITGA6, ARHGEF1, ARHGEF6
hsa00010:Glycolysis / Gluconeogenesis	12	0.004	ALDH3A2, LDHA, PFKL, PKM, TPI1, ALDH1B1, ADH1B, ALDOC, ALDOA, GAPDH, PFKM, PFKP
hsa00071:Fatty acid degradation	9	0.005	ALDH3A2, HADHA, ECHS1, ALDH1B1, ACSL1, ADH1B, ACSL3, HADH, ACAT1
hsa05169:Epstein-Barr virus infection	17	0.006	MAP2K3, CDKN1A, PSMD11, PSMD14, EIF2AK2, TRAF2, PSMD8, PSMD6, PSMC5, TBK1, PSMC3, PSMD4, PSMC4, PSMC1, PSMD3, PSMD1, VIM
hsa00310:Lysine degradation	10	0.006	ALDH3A2, HADHA, ECHS1, ALDH1B1, OGDH, DLST, PLOD2, HADH, COLGALT1, ACAT1
hsa01230:Biosynthesis of amino acids	12	0.007	PFKL, PKM, TPI1, PYCRL, SHMT2, ARG1, PHGDH, ALDOC, ALDOA, GAPDH, PFKM, PFKP
hsa04962:Vasopressin-regulated water reabsorption	9	0.007	NSF, DYNC1H1, DCTN5, DYNC1I2, DYNC1LI2, ARHGDIA, GNAS, PRKACA, RAB11B
hsa00030:Pentose phosphate pathway	7	0.010	PFKL, ALDOC, PGLS, ALDOA, PFKM, PFKP, DERA
hsa00620:Pyruvate metabolism	8	0.014	ALDH3A2, GRHPR, LDHA, FH, PKM, ALDH1B1, MDH2, ACAT1
hsa00051:Fructose and mannose metabolism	7	0.016	PFKL, TPI1, GMPPA, ALDOC, ALDOA, PFKM, PFKP

hsa05130:Pathogenic Escherichia coli infection	9	0.017	ITGB1, TUBB6, ARPC2, ROCK2, ARPC3, ARPC5L, ARPC5, ARHGEF2, TUBA4A
hsa04961:Endocrine and other factor-regulated calcium reabsorption	8	0.026	CLTC, GNAS, AP2A1, ATP1B3, ATP1A1, PRKACA, AP2A2, AP2M1
hsa04152:AMPK signaling pathway	15	0.030	RAB2A, PRKAA1, CAB39, PRKAG1, TSC2, PPP2R5C, ELAVL1, RAB11B, PFKL, PPP2R1B, FASN, PPP2R2D, PFKM, RAB8A, PFKP
hsa05410:Hypertrophic cardiomyopathy (HCM)	11	0.030	ITGB1, PRKAA1, DES, ITGA3, TNNT2, TNNC1, LMNA, PRKAG1, ITGA7, ITGAV, ITGA6
hsa01212:Fatty acid metabolism	8	0.035	HADHA, ECHS1, ACSL1, FASN, ACSL3, HSD17B12, HADH, ACAT1
hsa00380:Tryptophan metabolism	7	0.044	ALDH3A2, HADHA, ECHS1, ALDH1B1, OGDH, HADH, ACAT1
hsa05012:Parkinson's disease	16	0.045	COX4I1, ATP5A1, ATP5C1, ATP5F1, COX5B, COX5A, UBE2L3, GNAI2, UQCRC1, VDAC3, VDAC2, UBA1, VDAC1, SLC25A5, PRKACA, SLC25A6
hsa05414:Dilated cardiomyopathy	11	0.047	ITGB1, DES, ITGA3, TNNT2, TNNC1, LMNA, GNAS, ITGA7, ITGAV, ITGA6, PRKACA
hsa05010:Alzheimer's disease	18	0.048	APP, MME, COX4I1, ATP5A1, ATP5C1, ATP5F1, COX5B, COX5A, HSD17B10, PPP3CA, NCSTN, CDK5, CAPN2, UQCRC1, CAPN1, APOE, BID, GAPDH
hsa04510:Focal adhesion	21	0.049	ITGB1, ROCK2, ITGA3, ACTN1, TNC, FN1, LAMC1, MYL12A, MYLPF, DIAPH1, COL3A1, COL6A1, RAPGEF1, CAPN2, COL6A3, ITGA7, ITGAV, ITGA6, FLNB, FLNC, PAK2

Table 20. Identification of PP2Ac-interacting proteins by UPLC-ESI-MS/MS analyses of human skeletal muscle cells after metformin treatment in lean insulin-sensitive participants.

accession	Protein names	Unique peptides	Gene	Fold change*	P-Value
O14745	Na(+)/H(+) exchange regulatory cofactor NHE-RF1	3	SLC9A3R1	Infinite	
O14773-2	Tripeptidyl-peptidase 1	4	TPP1	Infinite	
O15084-2	Serine/threonine-protein phosphatase 6 regulatory ankyrin repeat subunit A	2	ANKRD28	Infinite	
O75223	Gamma-glutamylcyclotransferase	5	GGCT	Infinite	
P04040	Catalase	12	CAT	Infinite	
P05067-10	Amyloid beta A4 protein;N-APP;Soluble APP-alpha;Soluble APP-beta;C99;Beta-amyloid protein 42;Beta-amyloid protein 40;C83;P3(42);P3(40);C80;Gamma-secretase C-terminal fragment 59;Gamma-secretase C-terminal fragment 57;Gamma-secretase C-terminal fragment 50;C31	4	APP	Infinite	
P08243-2	Asparagine synthetase [glutamine-hydrolyzing]	5	ASNS	Infinite	
P10606	Cytochrome c oxidase subunit 5B, mitochondrial	4	COX5B	Infinite	
P11166	Solute carrier family 2, facilitated glucose transporter member 1	4	SLC2A1	Infinite	
P20674	Cytochrome c oxidase subunit 5A, mitochondrial	2	COX5A	Infinite	
P22307-6	Non-specific lipid-transfer protein	7	SCP2	Infinite	
P22735	Protein-glutamine gamma-glutamyltransferase K	11	TGM1	Infinite	
P29508	Serpin B3	6	SERPINB3	Infinite	
P31483	Nucleolysin TIA-1 isoform p40	2	TIA1	Infinite	

P38936	Cyclin-dependent kinase inhibitor 1	3	CDKN1A	Infinite	
P52294	Importin subunit alpha-5;Importin subunit alpha-5, N-terminally processed	2	KPNA1	Infinite	
P55042	GTP-binding protein RAD	3	RRAD	Infinite	
Q13136-2	Liprin-alpha-1	9	PPFIA1	Infinite	
Q16537-2	Serine/threonine-protein phosphatase 2A 56 kDa regulatory subunit epsilon isoform	5	PPP2R5E	Infinite	
Q567U6	Coiled-coil domain-containing protein 93	14	CCDC93	Infinite	
Q8N8A2	Serine/threonine-protein phosphatase 6 regulatory ankyrin repeat subunit B	10	ANKRD44	Infinite	
Q8WXI4-2	Acyl-coenzyme A thioesterase 11	9	ACOT11	Infinite	
Q96P16	Regulation of nuclear pre-mRNA domain-containing protein 1A	4	RPRD1A	Infinite	
Q99985	Semaphorin-3C	5	SEMA3C	Infinite	
Q9HC07	Transmembrane protein 165	2	TMEM165	Infinite	
Q9NS86	LanC-like protein 2	4	LANCL2	Infinite	
Q9NUP9	Protein lin-7 homolog C	3	LIN7C	Infinite	
Q9Y2B0	Protein canopy homolog 2	2	CNPY2	Infinite	
Q14693	Phosphatidate phosphatase LPIN1	12	LPIN1	0.232	0.034
Q5VIR6-4	Vacuolar protein sorting-associated protein 53 homolog	17	VPS53	0.230	0.036
Q14161-5	ARF GTPase-activating protein GIT2	8	GIT2	0.213	0.022

***: The normalized peak area after metformin divided by the normalized peak area of basal**

Infinite: The proteins were not quantified in control (basal) samples

Table 21. PP2Ac-interacting proteins by UPLC-ESI-MS/MS analyses of human skeletal muscle cells after metformin treatment in obese insulin-resistant participants

accession	Protein names	Unique peptides	Gene	Fold change*	P-Value
O14920	Inhibitor of nuclear factor kappa-B kinase subunit beta	5	IKBKB	Infinite	
P12931	Proto-oncogene tyrosine-protein kinase Src	2	SRC	Infinite	
O14972-2	Down syndrome critical region protein 3	4	DSCR3	Infinite	
P12110-3	Collagen alpha-2(VI) chain	6	COL6A2	Infinite	
P13798	Acylamino-acid-releasing enzyme	8	APEH	Infinite	
P60033	CD81 antigen	2	CD81	Infinite	
Q5T5Y3-2	Calmodulin-regulated spectrin-associated protein 1	8	CAMSAP1	Infinite	
Q8NEV1	Casein kinase II subunit alpha 3;Casein kinase II subunit alpha	5	CSNK2A3	Infinite	
Q8NHG8	E3 ubiquitin-protein ligase ZNRF2	4	ZNRF2	Infinite	
Q8TC07-2	TBC1 domain family member 15	12	TBC1D15	Infinite	
Q8TD55-2	Pleckstrin homology domain-containing family O member 2	5	PLEKHO2	Infinite	
Q96EY5-3	Multivesicular body subunit 12A	2	MVB12A	Infinite	
Q9BRX2	Protein pelota homolog	6	PELO	Infinite	
Q8WUI4-3	Histone deacetylase 7	9	HDAC7	2.776	0.041
P50395	Rab GDP dissociation inhibitor beta	10	GDI2	0.317	0.035

***: The normalized peak area after metformin divided by the normalized peak area of basal**

Infinite: The proteins were not quantified in control (basal) samples

Table 22. Significant metformin responsive PP2Ac interaction partners in lean insulin-sensitive participants and obese insulin-resistant participants by UPLC-ESI-MS/MS analyses of human skeletal muscle cells

Significant metformin responsive PP2Ac interaction partners in lean insulin-sensitive participants					
Accession No	**Protein Names**	**Gene**	**Uniquep eptide**	**Fold change**	**P-Value**
P33176	Kinesin-1 heavy chain	KIF5B	45	1.937	0.049
Q13310-2	Polyadenylate-binding protein 4	PABPC4	11	1.794	0.047
Q14161-5	ARF GTPase-activating protein GIT2	GIT2	8	4.705	0.022
Q14444-2	Caprin-1	CAPRIN1	11	2.413	0.017
Q14693	Phosphatidate phosphatase LPIN1	LPIN1	12	4.313	0.034
Q5VIR6-4	Vacuolar protein sorting-associated protein 53 homolog	VPS53	17	4.339	0.036
P06702	Protein S100-A9	S100A9	7	Infinite	
Q9BVG4	Protein PBDC1	PBDC1	8	2.980	0.043
P26447	Protein S100-A4	S100A4	6	Infinite	
P38936	Cyclin-dependent kinase inhibitor 1	CDKN1A	3	Infinite	
Q567U6	Coiled-coil domain-containing protein 93	CCDC93	14	Infinite	
Q16537-2	Serine/threonine-protein phosphatase 2A 56 kDa regulatory subunit epsilon isoform	PPP2R5E	5	Infinite	
Significant metformin responsive PP2Ac interaction partners in obese insulin-resistant participants					
accession	**Protein.names**	**Gene**	**Uniquep eptide**	**Fold change**	**P-Value**
O43617	Trafficking protein particle complex subunit 3	TRAPPC3	4	zero	0.003
P22392-2	Nucleoside diphosphate kinase B	NME2	3	0.062	0.002
Q9UBS4	DnaJ homolog subfamily B member 11	DNAJB11	8	Infinite	
Q9BRX2	Protein pelota homolog	PELO	6	Infinite	
P30044	Peroxiredoxin-5, mitochondrial	PRDX5	7	0.241	0.043
P38606-2	V-type proton ATPase catalytic subunit A	ATP6V1A	9	zero	0.044
Q9NP79	Vacuolar protein sorting-associated protein VTA1 homolog	VTA1	5	zero	

Infinite: The proteins were not quantified in control (basal) samples

Table 23. PP2Ac-interacting proteins by UPLC-ESI-MS/MS analyses of human skeletal muscle cells upon insulin-stimulation in lean insulin-sensitive participants

accession	Protein Name	Unique peptide	Gene Name	Fold change*	P-Value
A1X283	SH3 and PX domain-containing protein 2B	9	SH3PXD2B	Infinite	
O43583	Density-regulated protein	2	DENR	Infinite	
O43813	LanC-like protein 1	4	LANCL1	Infinite	
O95456-2	Proteasome assembly chaperone 1	3	PSMG1	Infinite	
P0DN76	Splicing factor U2AF 35 kDa subunit; Splicing factor U2AF 26 kDa subunit	4	U2AF1	Infinite	
P17931	Galectin-3	5	LGALS3	Infinite	
P26447	Protein S100-A4	5	S100A4	Infinite	
P38936	Cyclin-dependent kinase inhibitor 1	3	CDKN1A	Infinite	
P41227	N-alpha-acetyltransferase 10	6	NAA10	Infinite	
P42025	Beta-centractin	3	ACTR1B	Infinite	
P42765	3-ketoacyl-CoA thiolase, mitochondrial	7	ACAA2	Infinite	
P49674	Casein kinase I isoform epsilon	3	CSNK1E	Infinite	
P55039	Developmentally-regulated GTP-binding protein 2	5	DRG2	Infinite	
Q16537-2	Serine/threonine-protein phosphatase 2A 56 kDa regulatory subunit epsilon isoform	5	PPP2R5E	Infinite	
Q52LJ0	Protein FAM98B	2	FAM98B	Infinite	
Q567U6	Coiled-coil domain-containing protein 93	14	CCDC93	Infinite	
Q96EE3	Nucleoporin SEH1	4	SEH1L	Infinite	
Q96MF2-2	SH3 and cysteine-rich domain-containing protein 3	5	STAC3	Infinite	
Q9BQS8	FYVE and coiled-coil domain-containing protein 1	11	FYCO1	Infinite	
Q9NRN7	L-aminoadipate-semialdehyde dehydrogenase-phosphopantetheinyl transferase	3	AASDHPPT	Infinite	
Q5VIR6-4	Vacuolar protein sorting-associated protein 53 homolog	17	VPS53	0.324	0.050
O75962	Triple functional domain protein	38	TRIO	0.159	0.030

***: The normalized peak area upon insulin-stimulation divided by the normalized peak area of basal**

Infinite: The proteins were not quantified in control (basal) samples

Table 24. Identification of PP2Ac-interacting proteins by UPLC-ESI-MS/MS analyses of human skeletal muscle cells upon insulin-stimulation in obese insulin-resistant participants

Accession No	Protein Name	Unique peptides	Gene Name	Fold change*	P-Value
A1X283	SH3 and PX domain-containing protein 2B	8	SH3PXD2B	Infinite	
O43670-2	BUB3-interacting and GLEBS motif-containing protein ZNF207	6	ZNF207	Infinite	
P13798	Acylamino-acid-releasing enzyme	8	APEH	Infinite	
P57723	Poly(rC)-binding protein 4	2	PCBP4	Infinite	
Q12778	Forkhead box protein O1	5	FOXO1	Infinite	
Q14232	Translation initiation factor eIF-2B subunit alpha	6	EIF2B1	Infinite	
Q16513-2	Serine/threonine-protein kinase N2	15	PKN2	Infinite	
Q5JTD0-2	Tight junction-associated protein 1	11	TJAP1	Infinite	
Q6ZMI0	Protein phosphatase 1 regulatory subunit 21	13	PPP1R21	Infinite	
Q7LBC6	Lysine-specific demethylase 3B	8	KDM3B	Infinite	
Q86VN1-2	Vacuolar protein-sorting-associated protein 36	7	VPS36	Infinite	
Q86XZ4	Spermatogenesis-associated serine-rich protein 2	4	SPATS2	Infinite	
Q8NHG8	E3 ubiquitin-protein ligase ZNRF2	4	ZNRF2	Infinite	
Q8NHV4	Protein NEDD1	7	NEDD1	Infinite	
Q96CV9-3	Optineurin	13	OPTN	Infinite	
Q96P16	Regulation of nuclear pre-mRNA domain-containing protein 1A	7	RPRD1A	Infinite	
Q9BQ69	O-acetyl-ADP-ribose deacetylase MACROD1	3	MACROD1	Infinite	

Q9H1I8-3	Activating signal cointegrator 1 complex subunit 2	9	ASCC2	Infinite	
Q9H7E2-3	Tudor domain-containing protein 3	14	TDRD3	Infinite	
Q9NWS0	PIH1 domain-containing protein 1	6	PIH1D1	Infinite	
Q8WUI4-3	Histone deacetylase 7	9	HDAC7	2.776	0.041
P50395	Rab GDP dissociation inhibitor beta	10	GDI2	0.317	0.035

***: The normalized peak area upon insulin-stimulation divided by the normalized peak area of basal**

Infinite: The proteins were not quantified in control (basal) samples

Table 25. AMPK and AMPK substrates identified in human skeletal muscle cells from phosphoproteome experiment.

Protein	Protein Name	Gene Name	Phos-phoSite	Known In
Q86TI0-2	TBC1 domain family member 1	TBC1D1	T596	Homo sapiens (Human)
Q9BZL4-3	Protein phosphatase 1 regulatory subunit 12C	PPP1R12C	S452	Homo sapiens (Human)
Q13177	Serine/threonine-protein kinase PAK 2;PAK-2p27;PAK-2p34	PAK2	S20	Sus scrofa (Pig), Homo sapiens (Human), Rattus norvegicus (Rat), Mus musculus (Mouse)
Q13131	5'-AMP-activated protein kinase catalytic subunit alpha-1	PRKAA1	S496	Homo sapiens (Human)
Q06210	Glutamine--fructose-6-phosphate aminotransferase [isomerizing] 1	GFPT1	S261, S176, S243	Sus scrofa (Pig), Macaca fascicularis (Crab-eating macaque) (Cynomolgus monkey), Homo sapiens (Human), Gallus gallus (Chicken)
Q13131	5'-AMP-activated protein kinase catalytic subunit alpha-1	PRKAA1	S486	Rattus norvegicus (Rat), Homo sapiens (Human), Mus musculus (Mouse)
Q14694	Ubiquitin carboxyl-terminal hydrolase 10	USP10	S76	Homo sapiens (Human)
Q9Y478	5'-AMP-activated protein kinase subunit beta-1	PRKAB1	S183, S182	Cricetulus griseus (Chinese hamster) (Cricetulus barabensis griseus), Rattus norvegicus (Rat), Mus musculus (Mouse), Homo sapiens (Human)
Q07866-6	Kinesin light chain 1	KLC1	S696, S549, S522, S123, S104, S524	Homo sapiens (Human), Homo sapiens (Human), Homo sapiens (Human), Homo sapiens (Human), Homo sapiens (Human), Rattus norvegicus (Rat), Homo sapiens (Human)

Q07866-6	Kinesin light chain 1	KLC1	S693, S546, S519, S526, S120, S101, S521	Homo sapiens (Human), Homo sapiens (Human), Homo sapiens (Human), Macaca fascicularis (Crab-eating macaque) (Cynomolgus monkey), Homo sapiens (Human), Homo sapiens (Human), Homo sapiens (Human)
Q05469	Hormone-sensitive lipase	LIPE	S605, S128, S855, S554	Sus scrofa (Pig), Homo sapiens (Human), Homo sapiens (Human), Sus scrofa (Pig)
O75385	Serine/threonine-protein kinase ULK1	ULK1	S638	Homo sapiens (Human)
P56524	Histone deacetylase 4;Histone deacetylase 9;Histone deacetylase 5	HDAC4;HDAC9;HDAC5	S266, S251, S223, S84, S220, S259, S250	Sus scrofa (Pig), Sus scrofa (Pig), Rattus norvegicus (Rat), Rattus norvegicus (Rat), Mus musculus (Mouse), Homo sapiens (Human), Homo sapiens (Human), Mus musculus (Mouse)
P50552	Vasodilator-stimulated phosphoprotein	VASP	S239, S235	Homo sapiens (Human), Mus musculus (Mouse)
Q92538-2	Golgi-specific brefeldin A-resistance guanine nucleotide exchange factor 1	GBF1	T1325, T1337	Sus scrofa (Pig), Homo sapiens (Human)
Q9Y478	5'-AMP-activated protein kinase subunit beta-1	PRKAB1	S24	Rattus norvegicus (Rat), Homo sapiens (Human)
P46937	Transcriptional coactivator YAP1	YAP1	S61, S21	Homo sapiens (Human), Danio rerio (Zebrafish) (Brachydanio rerio)
P06400	Retinoblastoma-associated protein	RB1	S811, S804, S803	Homo sapiens (Human), Mus musculus (Mouse), Rattus norvegicus (Rat)
Q86TI0-2	TBC1 domain family member 1	TBC1D1	S702, S301, S700, S707	Rattus norvegicus (Rat), Homo sapiens (Human), Mus musculus (Mouse)

Q9UQB8	Brain-specific angiogenesis inhibitor 1-associated protein 2	BAIAP2	S367, S387, S366	Sus scrofa (Pig), Cricetulus griseus (Chinese hamster) (Cricetulus barabensis griseus), Rattus norvegicus (Rat), Mus musculus (Mouse), Homo sapiens (Human)
Q9Y478	5'-AMP-activated protein kinase subunit beta-1	PRKAB1	S25, S25	Rattus norvegicus (Rat), Homo sapiens (Human)
Q9UQK1	Protein phosphatase 1 regulatory subunit 3C	PPP1R3C	S293	Homo sapiens (Human)
Q13085	Acetyl-CoA carboxylase 1;Biotin carboxylase	ACACA	S117, S80	Macaca fascicularis (Crab-eating macaque) (Cynomolgus monkey), Homo sapiens (Human)
Q9UQK1	Protein phosphatase 1 regulatory subunit 3C	PPP1R3C	S33	Homo sapiens (Human)
P42345	Serine/threonine-protein kinase mTOR	MTOR	T2446	Homo sapiens (Human), Rattus norvegicus (Rat), Mus musculus (Mouse)
Q9Y2I7	1-phosphatidylinositol 3-phosphate 5-kinase	PIKFYVE	S319, S307	Sus scrofa (Pig), Rattus norvegicus (Rat), Macaca fascicularis (Crab-eating macaque) (Cynomolgus monkey), Homo sapiens (Human), Mus musculus (Mouse)
P49815	Tuberin	TSC2	S1448, S1452, S1451	Homo sapiens (Human), Rattus norvegicus (Rat), Mus musculus (Mouse)
P10398	RAF proto-oncogene serine/threonine-protein kinase;Serine/threonine-protein kinase A-Raf	RAF1;ARAF	S628, S621, S234, S604, S641	Bos taurus (Bovine), Danio rerio (Zebrafish) (Brachydanio rerio), Sus scrofa (Pig), Homo sapiens (Human), Rattus norvegicus (Rat), Mus musculus (Mouse)
Q8N122	Regulatory-associated protein of mTOR	RPTOR	S722	Rattus norvegicus (Rat), Sus scrofa (Pig), Mus musculus (Mouse), Homo sapiens (Human)
Q9H0B6	Kinesin light chain 2	KLC2	S443, S582	Homo sapiens (Human), Sus scrofa (Pig), Macaca fascicularis (Crab-eating macaque) (Cynomolgus monkey), Homo sapiens (Human)

O60825	6-phosphofructo-2-kinase/fructose-2,6-bisphosphatase 2;6-phosphofructo-2-kinase;Fructose-2,6-bisphosphatase	PFKFB2	S466, S467, S469	Sus scrofa (Pig), Homo sapiens (Human), Bos taurus (Bovine), Mus musculus (Mouse), Rattus norvegicus (Rat)
Q14247	Src substrate cortactin	CTTN	T401	Homo sapiens (Human)
P35222	Catenin beta-1	CTNNB1	S560, S552, S541	Gallus gallus (Chicken), Danio rerio (Zebrafish) (Brachydanio rerio), Mus musculus (Mouse), Macaca fascicularis (Crab-eating macaque) (Cynomolgus monkey), Homo sapiens (Human), Mus musculus (Mouse), Bos taurus (Bovine), Sus scrofa (Pig), Rattus norvegicus (Rat)
P49674	Casein kinase I isoform epsilon	CSNK1E	S352, S389	Sus scrofa (Pig), Cricetulus griseus (Chinese hamster) (Cricetulus barabensis griseus), Homo sapiens (Human), Rattus norvegicus (Rat), Mus musculus (Mouse)
P56524	Histone deacetylase 4	HDAC4	S467, S465, S466	Sus scrofa (Pig), Homo sapiens (Human), Mus musculus (Mouse), Rattus norvegicus (Rat)
Q9UQL6	Histone deacetylase 5	HDAC5	S323, S498, S488	Rattus norvegicus (Rat), Homo sapiens (Human), Mus musculus (Mouse)
Q86TI0-2	TBC1 domain family member 1	TBC1D1	S234, S231, S237	Rattus norvegicus (Rat), Sus scrofa (Pig), Mus musculus (Mouse), Homo sapiens (Human)
Q9Y478	5'-AMP-activated protein kinase subunit beta-1	PRKAB1	S108, S73	Sus scrofa (Pig), Macaca fascicularis (Crab-eating macaque) (Cynomolgus monkey), Sus scrofa (Pig), Bos taurus (Bovine), Homo sapiens (Human)

P04049	RAF proto-oncogene serine/threonine-protein kinase	RAF1	S259	Bos taurus (Bovine), Sus scrofa (Pig), Homo sapiens (Human), Rattus norvegicus (Rat), Mus musculus (Mouse)
O00418	Eukaryotic elongation factor 2 kinase	EEF2K	S78	Homo sapiens (Human)
Q15036	Sorting nexin-17	SNX17	S424, S437	Cricetulus griseus (Chinese hamster) (Cricetulus barabensis griseus), Macaca fascicularis (Crab-eating macaque) (Cynomolgus monkey), Sus scrofa (Pig), Homo sapiens (Human), Rattus norvegicus (Rat), Mus musculus (Mouse)
Q13131	5'-AMP-activated protein kinase catalytic subunit alpha-1	PRKAA1	T490, T505	Homo sapiens (Human)
Q13131	5'-AMP-activated protein kinase catalytic subunit alpha-1	PRKAA1	T488, T503	Rattus norvegicus (Rat), Homo sapiens (Human), Mus musculus (Mouse)
Q13131	5'-AMP-activated protein kinase catalytic subunit alpha-1	PRKAA1	S506, S521	Rattus norvegicus (Rat), Homo sapiens (Human), Mus musculus (Mouse)
Q13131	5'-AMP-activated protein kinase catalytic subunit alpha-1	PRKAA1	S498,S513	Homo sapiens (Human)
Q13131	5'-AMP-activated protein kinase catalytic subunit alpha-1	PRKAA1	S508, S523	Rattus norvegicus (Rat), Homo sapiens (Human), Mus musculus (Mouse)
Q13131	5'-AMP-activated protein kinase catalytic subunit alpha-1	PRKAA1	T482, T497	Rattus norvegicus (Rat), Homo sapiens (Human), Mus musculus (Mouse)
Q9Y478	5'-AMP-activated protein kinase subunit beta-1	PRKAB1	S181	Rattus norvegicus (Rat), Mus musculus (Mouse), Homo sapiens (Human)

Table 26. PP2A regulatory subunits identified by UPLC-ESI-MS/MS analyses of human skeletal muscle cells in lean insulin-sensitive participants.

Accession	Gene Name	protein Name	Mol Wt	Fold Change (Control /Control)	Fold Change (Metfromin/control)	Fold Change (Insulin/ control)	Fold Change (Okadaic Acid/control)	Fold Change (Metformin &Okadaic Acid/control)
P63151	PPP2R2A	Serine/threonine-protein phosphatase 2A 55 kDa regulatory subunit B alpha isoform	51.691	1.000	0.913	1.324	0.904	1.127
P30153	PPP2R1A	Serine/threonine-protein phosphatase 2A 65 kDa regulatory subunit A alpha isoform	65.308	1.000	0.734	1.109	0.803	0.954
P30154	PPP2R1B	Serine/threonine-protein phosphatase 2A 65 kDa regulatory subunit A beta isoform	66.213	1.000	1.146	1.069	0.971	1.268
Q06190	PPP2R3A	Serine/threonine-protein phosphatase 2A regulatory subunit B subunit alpha	130.28	1.000	0.699	0.996	0.785	0.521

Q13362-3	PPP2R5C	Serine/threonine-protein phosphatase 2A 56 kDa regulatory subunit gamma isoform	56.66	1.000	0.737	1.130	1.223	0.730
Q14738	PPP2R5D	Serine/threonine-protein phosphatase 2A 56 kDa regulatory subunit delta isoform	69.991	1.000	1.016	1.296	1.199	0.968
Q15173-2	PPP2R5B	Serine/threonine-protein phosphatase 2A 56 kDa regulatory subunit beta isoform	57.293	NA	NA	NA	Infinite	NA
Q15257-3	PPP2R4	Serine/threonine-protein phosphatase 2A activator	33.467	1.000	0.411	0.635	0.000	0.000
Q16537-2	PPP2R5E	Serine/threonine-protein phosphatase 2A 56 kDa regulatory subunit epsilon isoform	54.042	NA	Infinite	Infinite	Infinite	NA
Q66LE6	PPP2R2D	Serine/threonine-protein phosphatase 2A 55 kDa regulatory subunit B	52.042	1.000	0.877	1.039	0.987	1.186

		delta isoform						
Q9Y5P8	PPP2R3B	Serine/threonine-protein phosphatase 2A regulatory subunit B subunit beta	65.06	1.000	0.849	1.399	0.927	0.941
Q9Y5P8	PPP2R3B	Serine/threonine-protein phosphatase 2A regulatory subunit B subunit beta	65.06	1.000	0.848	1.399	0.927	0.940
O43815	STRN	Striatin	86.131	1.000	0.710	0.845	0.983	0.883
Q13033	STRN3	Striatin-3	87.208	1.000	0.868	0.989	0.955	0.953
Q9NRL3	STRN4	Striatin-4	80.595	1.000	0.791	0.856	0.808	0.816

Infinite: The proteins were not quantified in control (basal) samples

Table 27. PP2A regulatory subunits identified by UPLC-ESI-MS/MS analyses of human skeletal muscle cells in obese insulin-resistant participants

Accession No	Gene	Protein Name	Mol Wt	Fold Change (Control/control)	Fold Change (Metfromin/control)	Fold Change (Insulin/control)	Fold Change (Okadaic Acid/control)	Fold Change (Metformin &Okadaic Acid/control)
P63151	PPP2R2A	Serine/threonine-protein phosphatase 2A 55 kDa regulatory subunit B alpha isoform	51.69	1.000	1.179	0.980	0.876	0.996
P30153	PPP2R1A	Serine/threonine-protein phosphatase 2A 65 kDa regulatory subunit A alpha isoform	65.30	1.000	1.111	1.024	0.852	0.930
P30154	PPP2R1B	Serine/threonine-protein phosphatase 2A 65 kDa regulatory subunit A beta isoform	66.21	1.000	1.209	1.273	0.899	1.157
Q06190	PPP2R3A	Serine/threonine-protein phosphatase 2A regulatory subunit B subunit alpha	130.2	1.000	0.982	0.882	0.548	0.592
Q13362-3	PPP2R5C	Serine/threonine-protein phosphatase 2A 56 kDa regulatory subunit gamma isoform	56.66	1.000	0.000	0.000	0.000	0.000
Q13362-4	PPP2R5C	Serine/threonine-protein phosphatase 2A 56 kDa regulatory subunit	62.75	1.000	0.857	0.850	0.928	0.788

		gamma isoform						
Q14738	PPP2R5D	Serine/threonine-protein phosphatase 2A 56 kDa regulatory subunit delta isoform	69.99	1.000	0.913	0.825	0.369	0.508
Q15173	PPP2R5B	Serine/threonine-protein phosphatase 2A 56 kDa regulatory subunit beta isoform	57.39	1.000	0.000	0.537	0.952	0.936
Q15257-3	PPP2R4	Serine/threonine-protein phosphatase 2A activator	33.46	NA	NA	NA	Infinite	Infinite
Q16537-2	PPP2R5E	Serine/threonine-protein phosphatase 2A 56 kDa regulatory subunit epsilon isoform	54.04	1.000	0.000	0.000	0.000	0.000
Q66LE6	PPP2R2D	Serine/threonine-protein phosphatase 2A 55 kDa regulatory subunit B delta isoform	52.04	1.000	1.362	1.043	1.229	1.235
Q9Y5P8	PPP2R3B	Serine/threonine-protein phosphatase 2A regulatory subunit B subunit beta	65.06	1.000	0.780	1.012	0.531	0.597
O43815	STRN	Striatin	86.13	1.000	0.736	1.097	0.667	0.714
O43815-2	STRN	Striatin	80.76	NA	NA	NA	Infinite	NA
Q13033	STRN3	Striatin-3	87.20	1.000	0.863	1.152	0.774	0.731
Q13033-2	STRN3	Striatin-3	77.74	1.000	0.828	0.717	1.367	0.000
Q9NRL3	STRN4	Striatin-4	80.59	1.000	1.110	1.255	0.832	0.934

Infinite: The proteins were not quantified in control (basal) samples

REFERENCES

1 New WHO statistics highlight increases in blood pressure and diabetes, other noncommunicable risk factors. *Cent Eur J Public Health* **20**, 134, 149 (2012).

2 World Health Organization,Global report on diabetes. **2020** (2020).

3 CDC. National Diabetes Statistics Report. *US Department of Health and Human Services* (2020).

4 American Diabetes, A. Economic Costs of Diabetes in the U.S. in 2017. *Diabetes Care* **41**, 917-928, doi:10.2337/dci18-0007 (2018).

5 De Meyts, P. in *Endotext* (eds K. R. Feingold *et al.*) (MDText.com, Inc. Copyright © 2000-2020, MDText.com, Inc., 2000).

6 Kamei, Y., Hatazawa, Y., Uchitomi, R., Yoshimura, R. & Miura, S. Regulation of Skeletal Muscle Function by Amino Acids. *Nutrients* **12**, 261, doi:10.3390/nu12010261 (2020).

7 Merz, K. E. & Thurmond, D. C. Role of Skeletal Muscle in Insulin Resistance and Glucose Uptake. *Comprehensive Physiology* **10**, 785-809, doi:10.1002/cphy.c190029 (2020).

8 Handschin, C. *et al.* Skeletal muscle fiber-type switching, exercise intolerance, and myopathy in PGC-1alpha muscle-specific knock-out animals. *The Journal of biological chemistry* **282**, 30014-30021, doi:10.1074/jbc.M704817200 (2007).

9 DeFronzo, R. A. & Tripathy, D. Skeletal muscle insulin resistance is the primary defect in type 2 diabetes. *Diabetes Care* **32 Suppl 2**, S157-163, doi:10.2337/dc09-S302 (2009).

10 Saltiel, A. R. & Kahn, C. R. Insulin signalling and the regulation of glucose and lipid metabolism. *Nature* **414**, 799-806, doi:10.1038/414799a (2001).

11 Boucher, J., Kleinridders, A. & Kahn, C. R. Insulin receptor signaling in normal and insulin-resistant states. *Cold Spring Harb Perspect Biol* **6**, a009191, doi:10.1101/cshperspect.a009191 (2014).

12 Wu, H. & Ballantyne, C. M. Metabolic Inflammation and Insulin Resistance in Obesity. *Circulation research* **126**, 1549-1564, doi:10.1161/circresaha.119.315896 (2020).

13 Prevention, C. f. D. C. a. Adult obesity facts. *https://www.cdc.gov/obesity/data/adult.html*. **Accessed 25** (November 2019).

14 Wu, H. & Ballantyne, C. M. Skeletal muscle inflammation and insulin resistance in obesity. *The Journal of clinical investigation* **127**, 43-54, doi:10.1172/jci88880 (2017).

15 Blouin, C. M. *et al.* Plasma membrane subdomain compartmentalization contributes to distinct mechanisms of ceramide action on insulin signaling. *Diabetes* **59**, 600-610, doi:10.2337/db09-0897 (2010).

16 Fan, Y. *et al.* Lysine 63-linked polyubiquitination of TAK1 at lysine 158 is required for tumor necrosis factor alpha- and interleukin-1beta-induced IKK/NF-kappaB and JNK/AP-1 activation. *The Journal of biological chemistry* **285**, 5347-5360, doi:10.1074/jbc.M109.076976 (2010).

17 Booth, F. W., Roberts, C. K. & Laye, M. J. Lack of exercise is a major cause of chronic diseases. *Comprehensive Physiology* **2**, 1143-1211, doi:10.1002/cphy.c110025 (2012).

18 Brown, R. J. & Yanovski, J. A. Estimation of insulin sensitivity in children: methods, measures and controversies. *Pediatr Diabetes* **15**, 151-161, doi:10.1111/pedi.12146 (2014).

19 Lee, J. S. *et al.* Saturated, but not n-6 polyunsaturated, fatty acids induce insulin resistance: role of intramuscular accumulation of lipid metabolites. *Journal of applied physiology (Bethesda, Md. : 1985)* **100**, 1467-1474, doi:10.1152/japplphysiol.01438.2005 (2006).

20 Raschke, S., Eckardt, K., Bjørklund Holven, K., Jensen, J. & Eckel, J. Identification and validation of novel contraction-regulated myokines released from primary human skeletal muscle cells. *PloS one* **8**, e62008, doi:10.1371/journal.pone.0062008 (2013).

21 Khan, I. M. *et al.* Intermuscular and perimuscular fat expansion in obesity correlates with skeletal muscle T cell and macrophage infiltration and insulin resistance. *International journal of obesity (2005)* **39**, 1607-1618, doi:10.1038/ijo.2015.104 (2015).

22 Fan, W. & Evans, R. M. Exercise Mimetics: Impact on Health and Performance. *Cell metabolism* **25**, 242-247, doi:10.1016/j.cmet.2016.10.022 (2017).

23 Mammucari, C., Schiaffino, S. & Sandri, M. Downstream of Akt: FoxO3 and mTOR in the regulation of autophagy in skeletal muscle. *Autophagy* **4**, 524-526, doi:10.4161/auto.5905 (2008).

24 Nadeau, L. *et al.* IL-15 improves skeletal muscle oxidative metabolism and glucose uptake in association with increased respiratory chain supercomplex formation and AMPK pathway activation. *Biochimica et biophysica acta. General subjects* **1863**, 395-407, doi:10.1016/j.bbagen.2018.10.021 (2019).

25 Vosseller, K., Wells, L., Lane, M. D. & Hart, G. W. Elevated nucleocytoplasmic glycosylation by O-GlcNAc results in insulin resistance associated with defects in Akt activation in 3T3-L1 adipocytes. *Proc Natl Acad Sci U S A* **99**, 5313-5318, doi:10.1073/pnas.072072399 (2002).

26 Mueckler, M. & Thorens, B. The SLC2 (GLUT) family of membrane transporters. *Molecular aspects of medicine* **34**, 121-138, doi:10.1016/j.mam.2012.07.001 (2013).

27 Sheppeck, J. E., 2nd, Gauss, C. M. & Chamberlin, A. R. Inhibition of the Ser-Thr phosphatases PP1 and PP2A by naturally occurring toxins. *Bioorganic & medicinal chemistry* **5**, 1739-1750, doi:10.1016/s0968-0896(97)00146-6 (1997).

28 Seshacharyulu, P., Pandey, P., Datta, K. & Batra, S. K. Phosphatase: PP2A structural importance, regulation and its aberrant expression in cancer. *Cancer Lett* **335**, 9-18, doi:10.1016/j.canlet.2013.02.036 (2013).

29 Alonso, A. *et al.* Protein tyrosine phosphatases in the human genome. *Cell* **117**, 699-711, doi:10.1016/j.cell.2004.05.018 (2004).

30 Baskaran, R. & Velmurugan, B. K. Protein phosphatase 2A as therapeutic targets in various disease models. *Life sciences* **210**, 40-46, doi:https://doi.org/10.1016/j.lfs.2018.08.063 (2018).

31 Cho, U. S. & Xu, W. Crystal structure of a protein phosphatase 2A heterotrimeric holoenzyme. *Nature* **445**, 53-57, doi:10.1038/nature05351 (2007).

32 Lin, X. H. *et al.* Protein phosphatase 2A is required for the initiation of chromosomal DNA replication. *Proc Natl Acad Sci U S A* **95**, 14693-14698, doi:10.1073/pnas.95.25.14693 (1998).

33 Shi, Y. Serine/threonine phosphatases: mechanism through structure. *Cell* **139**, 468-484, doi:10.1016/j.cell.2009.10.006 (2009).

34 Guo, F. *et al.* Structural basis of PP2A activation by PTPA, an ATP-dependent activation chaperone. *Cell research* **24**, 190-203, doi:10.1038/cr.2013.138 (2014).

35 Yabe, R. *et al.* Protein Phosphatase Methyl-Esterase PME-1 Protects Protein Phosphatase 2A from Ubiquitin/Proteasome Degradation. *PloS one* **10**, e0145226, doi:10.1371/journal.pone.0145226 (2015).

36 Chen, J., Martin, B. L. & Brautigan, D. L. Regulation of protein serine-threonine phosphatase type-2A by tyrosine phosphorylation. *Science (New York, N.Y.)* **257**, 1261-1264 (1992).

37 Caruso, M. *et al.* Increased interaction with insulin receptor substrate 1, a novel abnormality in insulin resistance and type 2 diabetes. *Diabetes* **63**, 1933-1947, doi:10.2337/db13-1872 (2014).

38 Srinivasan, M. & Begum, N. Regulation of protein phosphatase 1 and 2A activities by insulin during myogenesis in rat skeletal muscle cells in culture. *The Journal of biological chemistry* **269**, 12514-12520 (1994).

39 Cazzolli, R., Carpenter, L., Biden, T. J. & Schmitz-Peiffer, C. A role for protein phosphatase 2A-like activity, but not atypical protein kinase Czeta, in the inhibition of protein kinase B/Akt and glycogen synthesis by palmitate. *Diabetes* **50**, 2210-2218 (2001).

40 Hojlund, K., Poulsen, M., Staehr, P., Brusgaard, K. & Beck-Nielsen, H. Effect of insulin on protein phosphatase 2A expression in muscle in type 2 diabetes. *European journal of clinical investigation* **32**, 918-923 (2002).

41 Nardi, F. *et al.* Enhanced insulin sensitivity associated with provision of mono and polyunsaturated fatty acids in skeletal muscle cells involves counter

modulation of PP2A. *PloS one* **9**, e92255, doi:10.1371/journal.pone.0092255 (2014).

42 Mandavia, C. & Sowers, J. R. Phosphoprotein Phosphatase PP2A Regulation of Insulin Receptor Substrate 1 and Insulin Metabolic Signaling. *Cardiorenal medicine* **2**, 308-313, doi:10.1159/000343889 (2012).

43 Feingold, K. R. in *Endotext* (eds K. R. Feingold *et al.*) (MDText.com, Inc. Copyright © 2000-2020, MDText.com, Inc., 2000).

44 Sivalingam, V. N., Myers, J., Nicholas, S., Balen, A. H. & Crosbie, E. J. Metformin in reproductive health, pregnancy and gynaecological cancer: established and emerging indications. *Hum Reprod Update* **20**, 853-868, doi:10.1093/humupd/dmu037 (2014).

45 Graham, G. G. *et al.* Clinical Pharmacokinetics of Metformin. *Clinical Pharmacokinetics* **50**, 81-98, doi:10.2165/11534750-000000000-00000 (2011).

46 Rena, G., Hardie, D. G. & Pearson, E. R. The mechanisms of action of metformin. *Diabetologia* **60**, 1577-1585, doi:10.1007/s00125-017-4342-z (2017).

47 Miller, R. A. *et al.* Biguanides suppress hepatic glucagon signalling by decreasing production of cyclic AMP. *Nature* **494**, 256-260, doi:10.1038/nature11808 (2013).

48 Madiraju, A. K. *et al.* Metformin suppresses gluconeogenesis by inhibiting mitochondrial glycerophosphate dehydrogenase. *Nature* **510**, 542-546, doi:10.1038/nature13270 (2014).

49 Gong, L., Goswami, S., Giacomini, K. M., Altman, R. B. & Klein, T. E. Metformin pathways: pharmacokinetics and pharmacodynamics.

Pharmacogenet Genomics **22**, 820-827, doi:10.1097/FPC.0b013e3283559b22 (2012).

50 Asagami, T. *et al.* Metformin treatment lowers asymmetric dimethylarginine concentrations in patients with type 2 diabetes. *Metabolism* **51**, 843-846, doi:10.1053/meta.2002.33349 (2002).

51 Musi, N. *et al.* Metformin increases AMP-activated protein kinase activity in skeletal muscle of subjects with type 2 diabetes. *Diabetes* **51**, 2074-2081, doi:10.2337/diabetes.51.7.2074 (2002).

52 Sarabia, V., Lam, L., Burdett, E., Leiter, L. A. & Klip, A. Glucose transport in human skeletal muscle cells in culture. Stimulation by insulin and metformin. *The Journal of clinical investigation* **90**, 1386-1395, doi:10.1172/jci116005 (1992).

53 Galuska, D., Nolte, L. A., Zierath, J. R. & Wallberg-Henriksson, H. Effect of metformin on insulin-stimulated glucose transport in isolated skeletal muscle obtained from patients with NIDDM. *Diabetologia* **37**, 826-832, doi:10.1007/bf00404340 (1994).

54 Bailey, C. J. & Puah, J. A. Effect of metformin on glucose metabolism in mouse soleus muscle. *Diabete & metabolisme* **12**, 212-218 (1986).

55 Menendez, J. A. & Lupu, R. Fatty acid synthase and the lipogenic phenotype in cancer pathogenesis. *Nature reviews. Cancer* **7**, 763-777, doi:10.1038/nrc2222 (2007).

56 Pollak, M. N. Investigating Metformin for Cancer Prevention and Treatment: The End of the Beginning. *Cancer Discovery* **2**, 778-790, doi:10.1158/2159-8290.cd-12-0263 (2012).

57 Liu, B. *et al.* Metformin induces unique biological and molecular responses in triple negative breast cancer cells. *Cell cycle (Georgetown, Tex.)* **8**, 2031-2040, doi:10.4161/cc.8.13.8814 (2009).

58 Malki, A. & Youssef, A. Antidiabetic drug metformin induces apoptosis in human MCF breast cancer via targeting ERK signaling. *Oncology research* **19**, 275-285, doi:10.3727/096504011x13021877989838 (2011).

59 He, G. *et al.* AMP-activated protein kinase induces p53 by phosphorylating MDMX and inhibiting its activity. *Mol Cell Biol* **34**, 148-157, doi:10.1128/MCB.00670-13 (2014).

60 Lund, S. S. *et al.* Impact of metformin versus repaglinide on non-glycaemic cardiovascular risk markers related to inflammation and endothelial dysfunction in non-obese patients with type 2 diabetes. *European Journal of Endocrinology* **158**, 631, doi:10.1530/eje-07-0815 (2008).

61 Deng, X. S. *et al.* Metformin targets Stat3 to inhibit cell growth and induce apoptosis in triple-negative breast cancers. *Cell cycle (Georgetown, Tex.)* **11**, 367-376, doi:10.4161/cc.11.2.18813 (2012).

62 Garabadu, D. & Krishnamurthy, S. Metformin attenuates hepatic insulin resistance in type-2 diabetic rats through PI3K/Akt/GLUT-4 signalling independent to bicuculline-sensitive GABA(A) receptor stimulation. *Pharmaceutical biology* **55**, 722-728, doi:10.1080/13880209.2016.1268635 (2017).

63 Tao, X., Cai, L., Chen, L., Ge, S. & Deng, X. Effects of metformin and Exenatide on insulin resistance and AMPKα-SIRT1 molecular pathway in PCOS rats. *Journal of Ovarian Research* **12**, 86, doi:10.1186/s13048-019-0555-8 (2019).

64 Chutkow, W. A. *et al.* Deletion of the alpha-arrestin protein Txnip in mice promotes adiposity and adipogenesis while preserving insulin sensitivity. *Diabetes* **59**, 1424-1434, doi:10.2337/db09-1212 (2010).

65 Parikh, H. *et al.* TXNIP regulates peripheral glucose metabolism in humans. *PLoS medicine* **4**, e158, doi:10.1371/journal.pmed.0040158 (2007).

66 MacNeil, L. T., Schertzer, J. D. & Steinberg, G. R. Bacteria transmit metformin-associated lifespan extension. *Nature Reviews Endocrinology* **16**, 9-10, doi:10.1038/s41574-019-0278-3 (2020).

67 Kim, Y. S. *et al.* Metformin protects against retinal cell death in diabetic mice. *Biochemical and Biophysical Research Communications* **492**, 397-403, doi:https://doi.org/10.1016/j.bbrc.2017.08.087 (2017).

68 Hirsch, A. *et al.* Metformin inhibits human androgen production by regulating steroidogenic enzymes HSD3B2 and CYP17A1 and complex I activity of the respiratory chain. *Endocrinology* **153**, 4354-4366, doi:10.1210/en.2012-1145 (2012).

69 Algire, C. *et al.* Metformin reduces endogenous reactive oxygen species and associated DNA damage. *Cancer prevention research (Philadelphia, Pa.)* **5**, 536-543, doi:10.1158/1940-6207.capr-11-0536 (2012).

70 Saisho, Y. Metformin and Inflammation: Its Potential Beyond Glucose-lowering Effect. *Endocrine, metabolic & immune disorders drug targets* **15**, 196-205, doi:10.2174/1871530315666150316124019 (2015).

71 Chen, X. *et al.* Immunomodulatory and Antiviral Activity of Metformin and Its Potential Implications in Treating Coronavirus Disease 2019 and Lung Injury. *Front Immunol* **11**, 2056-2056, doi:10.3389/fimmu.2020.02056 (2020).

72 Luo, P. *et al.* Metformin Treatment Was Associated with Decreased Mortality in COVID-19 Patients with Diabetes in a Retrospective Analysis. *The American journal of tropical medicine and hygiene* **103**, 69-72, doi:10.4269/ajtmh.20-0375 (2020).

73 Gordon, D. E. *et al.* A SARS-CoV-2-Human Protein-Protein Interaction Map Reveals Drug Targets and Potential Drug-Repurposing. *bioRxiv*, 2020.2003.2022.002386, doi:10.1101/2020.03.22.002386 (2020).

74 Soto-Acosta, R., Bautista-Carbajal, P., Cervantes-Salazar, M., Angel-Ambrocio, A. H. & Del Angel, R. M. DENV up-regulates the HMG-CoA reductase activity through the impairment of AMPK phosphorylation: A potential antiviral target. *PLoS pathogens* **13**, e1006257, doi:10.1371/journal.ppat.1006257 (2017).

75 Xie, W. *et al.* Activation of AMPK restricts coxsackievirus B3 replication by inhibiting lipid accumulation. *Journal of molecular and cellular cardiology* **85**, 155-167, doi:10.1016/j.yjmcc.2015.05.021 (2015).

76 Cheng, F., He, M., Jung, J. U., Lu, C. & Gao, S. J. Suppression of Kaposi's Sarcoma-Associated Herpesvirus Infection and Replication by 5'-AMP-Activated Protein Kinase. *Journal of virology* **90**, 6515-6525, doi:10.1128/jvi.00624-16 (2016).

77 Zhang, J. *et al.* AMP-activated Protein Kinase Phosphorylation of Angiotensin-Converting Enzyme 2 in Endothelium Mitigates Pulmonary Hypertension. *American journal of respiratory and critical care medicine* **198**, 509-520, doi:10.1164/rccm.201712-2570OC (2018).

78 Sharma, S., Ray, A. & Sadasivam, B. Metformin in COVID-19: A possible role beyond diabetes. *Diabetes research and clinical practice* **164**, 108183, doi:10.1016/j.diabres.2020.108183 (2020).

79 Simões e Silva, A. C., Silveira, K. D., Ferreira, A. J. & Teixeira, M. M. ACE2, angiotensin-(1-7) and Mas receptor axis in inflammation and fibrosis. *British journal of pharmacology* **169**, 477-492, doi:10.1111/bph.12159 (2013).

80 Deepa, S. S. *et al.* APPL1 mediates adiponectin-induced LKB1 cytosolic localization through the PP2A-PKCzeta signaling pathway. *Mol Endocrinol* **25**, 1773-1785, doi:10.1210/me.2011-0082 (2011).

81 Kickstein, E. *et al.* Biguanide metformin acts on tau phosphorylation via mTOR/protein phosphatase 2A (PP2A) signaling. *Proc Natl Acad Sci U S A* **107**, 21830-21835, doi:10.1073/pnas.0912793107 (2010).

82 Zhou, X. *et al.* Metformin Inhibit Lung Cancer Cell Growth and Invasion in Vitro as Well as Tumor Formation in Vivo Partially by Activating PP2A. *Medical science monitor : international medical journal of experimental and clinical research* **25**, 836-846, doi:10.12659/msm.912059 (2019).

83 Shouse, G. P., Nobumori, Y. & Liu, X. A B56gamma mutation in lung cancer disrupts the p53-dependent tumor-suppressor function of protein phosphatase 2A. *Oncogene* **29**, 3933-3941, doi:10.1038/onc.2010.161 (2010).

84 Sacco, F. *et al.* Deep Proteomics of Breast Cancer Cells Reveals that Metformin Rewires Signaling Networks Away from a Pro-growth State. *Cell systems* **2**, 159-171, doi:10.1016/j.cels.2016.02.005 (2016).

85 Hanawa, S., Mitsuhashi, A. & Shozu, M. Antitumor effects of metformin via indirect inhibition of protein phosphatase 2A in patients with endometrial cancer. *PloS one* **13**, e0192759, doi:10.1371/journal.pone.0192759 (2018).

86 Zhang, L. *et al.* Metformin reduced NLRP3 inflammasome activity in Ox-LDL stimulated macrophages through adenosine monophosphate activated protein kinase and protein phosphatase 2A. *European journal of pharmacology* **852**, 99-106, doi:10.1016/j.ejphar.2019.03.006 (2019).

87 Zhao, Y. & Sun, M. Metformin rescues Parkin protein expression and mitophagy in high glucose-challenged human renal epithelial cells by inhibiting NF-κB via PP2A activation. *Life sciences* **246**, 117382, doi:10.1016/j.lfs.2020.117382 (2020).

88 Auger, C. *et al.* Metformin prevents the pathological browning of subcutaneous white adipose tissue. *Molecular metabolism* **29**, 12-23, doi:10.1016/j.molmet.2019.08.011 (2019).

89 Kawashima, I. & Kirito, K. Metformin inhibits JAK2V617F activity in MPN cells by activating AMPK and PP2A complexes containing the B56α subunit. *Exp Hematol* **44**, 1156-1165.e1154, doi:10.1016/j.exphem.2016.08.005 (2016).

90 Cheng, G. & Li, L. High-glucose-induced apoptosis, ROS production and pro-inflammatory response in cardiomyocytes is attenuated by metformin treatment via PP2A activation. *Journal of biosciences* **45** (2020).

91 Tang, B. L. Could metformin be therapeutically useful in Huntington's disease? *Reviews in the neurosciences* **31**, 297-317, doi:10.1515/revneuro-2019-0072 (2020).

92 Dephoure, N., Gould, K. L., Gygi, S. P. & Kellogg, D. R. Mapping and analysis of phosphorylation sites: a quick guide for cell biologists. *Mol Biol Cell* **24**, 535-542, doi:10.1091/mbc.E12-09-0677 (2013).

93 Chatr-Aryamontri, A., Ceol, A., Licata, L. & Cesareni, G. Protein interactions: integration leads to belief. *Trends in biochemical sciences* **33**, 241-242; author reply 242-243, doi:10.1016/j.tibs.2008.04.002 (2008).

94 Rao, V. S., Srinivas, K., Sujini, G. N. & Kumar, G. N. Protein-protein interaction detection: methods and analysis. *International journal of proteomics* **2014**, 147648, doi:10.1155/2014/147648 (2014).

95 Vermeulen, M., Hubner, N. C. & Mann, M. High confidence determination of specific protein-protein interactions using quantitative mass spectrometry. *Current opinion in biotechnology* **19**, 331-337, doi:10.1016/j.copbio.2008.06.001 (2008).

96 Angel, T. E. *et al.* Mass spectrometry-based proteomics: existing capabilities and future directions. *Chem Soc Rev* **41**, 3912-3928, doi:10.1039/c2cs15331a (2012).

97 Shanely, R. A. *et al.* Human skeletal muscle biopsy procedures using the modified Bergström technique. *Journal of visualized experiments : JoVE*, 51812-51812, doi:10.3791/51812 (2014).

98 Bourlier, V. *et al.* Enhanced Glucose Metabolism Is Preserved in Cultured Primary Myotubes From Obese Donors in Response to Exercise Training. *The Journal of Clinical Endocrinology & Metabolism* **98**, 3739-3747, doi:10.1210/jc.2013-1727 (2013).

99 Larsen, M. R., Thingholm, T. E., Jensen, O. N., Roepstorff, P. & Jørgensen, T. J. D. Highly Selective Enrichment of Phosphorylated Peptides from Peptide Mixtures Using Titanium Dioxide Microcolumns. *Molecular & Cellular Proteomics* **4**, 873, doi:10.1074/mcp.T500007-MCP200 (2005).

100 Cox, J. & Mann, M. MaxQuant enables high peptide identification rates, individualized p.p.b.-range mass accuracies and proteome-wide protein quantification. *Nature Biotechnology* **26**, 1367-1372, doi:10.1038/nbt.1511 (2008).

101 Zhang, X. *et al.* Quantitative proteomics reveals novel protein interaction partners of PP2A catalytic subunit in pancreatic β-cells. *Molecular and cellular endocrinology* **424**, 1-11, doi:10.1016/j.mce.2016.01.008 (2016).

102 Lefort, N. *et al.* Proteome profile of functional mitochondria from human skeletal muscle using one-dimensional gel electrophoresis and HPLC-ESI-MS/MS. *Journal of proteomics* **72**, 1046-1060, doi:10.1016/j.jprot.2009.06.011 (2009).

103 Owen, M. R., Doran, E. & Halestrap, A. P. Evidence that metformin exerts its anti-diabetic effects through inhibition of complex 1 of the mitochondrial respiratory chain. *Biochem J* **348 Pt 3**, 607-614 (2000).

104 Hartley, D. & Cooper, G. M. Role of mTOR in the degradation of IRS-1: regulation of PP2A activity. *J Cell Biochem* **85**, 304-314, doi:10.1002/jcb.10135 (2002).

105 Dowling, R. J., Zakikhani, M., Fantus, I. G., Pollak, M. & Sonenberg, N. Metformin inhibits mammalian target of rapamycin-dependent translation initiation in breast cancer cells. *Cancer Res* **67**, 10804-10812, doi:10.1158/0008-5472.can-07-2310 (2007).

106 Stein, B. D. *et al.* Quantitative In Vivo Proteomics of Metformin Response in Liver Reveals AMPK-Dependent and -Independent Signaling Networks. *Cell reports* **29**, 3331-3348.e3337, doi:10.1016/j.celrep.2019.10.117 (2019).

107 Xie, M. *et al.* A pivotal role for endogenous TGF-beta-activated kinase-1 in the LKB1/AMP-activated protein kinase energy-sensor pathway. *Proc Natl Acad Sci U S A* **103**, 17378-17383, doi:10.1073/pnas.0604708103 (2006).

108 Alessi, D. R., Sakamoto, K. & Bayascas, J. R. LKB1-dependent signaling pathways. *Annual review of biochemistry* **75**, 137-163, doi:10.1146/annurev.biochem.75.103004.142702 (2006).

109 Hardie, D. G. AMP-activated/SNF1 protein kinases: conserved guardians of cellular energy. *Nature reviews. Molecular cell biology* **8**, 774-785, doi:10.1038/nrm2249 (2007).

110 Mihaylova, M. M. & Shaw, R. J. The AMPK signalling pathway coordinates cell growth, autophagy and metabolism. *Nat Cell Biol* **13**, 1016-1023, doi:10.1038/ncb2329 (2011).

111 Zang, M. *et al.* Polyphenols stimulate AMP-activated protein kinase, lower lipids, and inhibit accelerated atherosclerosis in diabetic LDL receptor-deficient mice. *Diabetes* **55**, 2180-2191, doi:10.2337/db05-1188 (2006).

112 Egan, D. F. *et al.* Phosphorylation of ULK1 (hATG1) by AMP-activated protein kinase connects energy sensing to mitophagy. *Science* **331**, 456-461, doi:10.1126/science.1196371 (2011).

113 Sakamoto, K. & Holman, G. D. Emerging role for AS160/TBC1D4 and TBC1D1 in the regulation of GLUT4 traffic. *American journal of physiology. Endocrinology and metabolism* **295**, E29-37, doi:10.1152/ajpendo.90331.2008 (2008).

114 Beurel, E., Grieco, S. F. & Jope, R. S. Glycogen synthase kinase-3 (GSK3): regulation, actions, and diseases. *Pharmacology & therapeutics* **148**, 114-131, doi:10.1016/j.pharmthera.2014.11.016 (2015).

115 Bungard, D. *et al.* Signaling kinase AMPK activates stress-promoted transcription via histone H2B phosphorylation. *Science* **329**, 1201-1205, doi:10.1126/science.1191241 (2010).

116 Hoffman, N. J. *et al.* Global Phosphoproteomic Analysis of Human Skeletal Muscle Reveals a Network of Exercise-Regulated Kinases and AMPK Substrates. *Cell metabolism* **22**, 922-935, doi:10.1016/j.cmet.2015.09.001 (2015).

117 Khan, A. S. & Frigo, D. E. A spatiotemporal hypothesis for the regulation, role, and targeting of AMPK in prostate cancer. *Nat Rev Urol* **14**, 164-180, doi:10.1038/nrurol.2016.272 (2017).

118 Hahn, K. *et al.* PP2A Regulatory Subunit PP2A-B′ Counteracts S6K Phosphorylation. *Cell metabolism* **11**, 438-444, doi:https://doi.org/10.1016/j.cmet.2010.03.015 (2010).

119 Hein, Marco Y. *et al.* A Human Interactome in Three Quantitative Dimensions Organized by Stoichiometries and Abundances. *Cell* **163**, 712-723, doi:https://doi.org/10.1016/j.cell.2015.09.053 (2015).

120 Miller, R. A. *et al.* Biguanides suppress hepatic glucagon signalling by decreasing production of cyclic AMP. *Nature* **494**, 256-260, doi:10.1038/nature11808 (2013).

121 He, L. *et al.* Activation of the cAMP-PKA pathway Antagonizes Metformin Suppression of Hepatic Glucose Production. *The Journal of biological chemistry* **291**, 10562-10570, doi:10.1074/jbc.M116.719666 (2016).

122 Ji, X. *et al.* PPP1R3C mediates metformin-inhibited hepatic gluconeogenesis. *Metabolism* **98**, 62-75, doi:10.1016/j.metabol.2019.06.002 (2019).

123 Takahashi, A. *et al.* Metformin impairs growth of endometrial cancer cells via cell cycle arrest and concomitant autophagy and apoptosis. *Cancer Cell International* **14**, 53, doi:10.1186/1475-2867-14-53 (2014).

124 Cuadrado, A. & Nebreda, Angel R. Mechanisms and functions of p38 MAPK signalling. *Biochemical Journal* **429**, 403-417, doi:10.1042/bj20100323 (2010).

125 Pryor, P. R. *et al.* Chronic insulin effects on insulin signalling and GLUT4 endocytosis are reversed by metformin. *Biochem J* **348 Pt 1**, 83-91 (2000).

126 Tsuchiya, A., Kanno, T. & Nishizaki, T. PI3 kinase directly phosphorylates Akt1/2 at Ser473/474 in the insulin signal transduction pathway. *J Endocrinol* **220**, 49-59, doi:10.1530/JOE-13-0172 (2013).

127 Granado, M. *et al.* Caloric restriction attenuates aging-induced cardiac insulin resistance in male Wistar rats through activation of PI3K/Akt pathway. *Nutrition, metabolism, and cardiovascular diseases : NMCD* **29**, 97-105, doi:10.1016/j.numecd.2018.09.005 (2019).

128 Beg, M., Abdullah, N., Thowfeik, F. S., Altorki, N. K. & McGraw, T. E. Distinct Akt phosphorylation states are required for insulin regulated Glut4 and Glut1-mediated glucose uptake. *Elife* **6**, e26896, doi:10.7554/eLife.26896 (2017).

129 Zhang, Z., Liu, H. & Liu, J. Akt activation: A potential strategy to ameliorate insulin resistance. *Diabetes research and clinical practice* **156**, 107092, doi:10.1016/j.diabres.2017.10.004 (2019).

130 Goudreault, M. *et al.* A PP2A Phosphatase High Density Interaction Network Identifies a Novel Striatin-interacting Phosphatase and Kinase Complex Linked to the Cerebral Cavernous Malformation 3 (CCM3) Protein. *Molecular &*

Cellular Proteomics **8**, 157-171, doi:https://doi.org/10.1074/mcp.M800266-MCP200 (2009).

131 McCright, B., Rivers, A. M., Audlin, S. & Virshup, D. M. The B56 family of protein phosphatase 2A (PP2A) regulatory subunits encodes differentiation-induced phosphoproteins that target PP2A to both nucleus and cytoplasm. *Journal of Biological Chemistry* **271**, 22081-22089 (1996).

132 Nakanishi, Y. *et al.* Dclk1 distinguishes between tumor and normal stem cells in the intestine. *Nature genetics* **45**, 98-103, doi:10.1038/ng.2481 (2013).

133 Berggard, T. *et al.* 140 Mouse brain proteins identified by Ca2+-calmodulin affinity chromatography and tandem mass spectrometry. *Journal of Proteome Research* **5**, 669-687, doi:10.1021/pr050421l (2006).

134 Ballif, B. A., Villen, J., Beausoleil, S. A., Schwartz, D. & Gygi, S. P. Phosphoproteomic analysis of the developing mouse brain. *Molecular & Cellular Proteomics* **3**, 1093-1101, doi:10.1074/mcp.M400085-MCP200 (2004).

135 Phanstiel, D. H. *et al.* Proteomic and phosphoproteomic comparison of human ES and iPS cells. *Nature Methods* **8**, 821-U884, doi:10.1038/nmeth.1699 (2011).

136 Rigbolt, K. T. G. *et al.* System-Wide Temporal Characterization of the Proteome and Phosphoproteome of Human Embryonic Stem Cell Differentiation. *Science Signaling* **4**, doi:10.1126/scisignal.2001570 (2011).

137 Van Hoof, D. *et al.* Phosphorylation Dynamics during Early Differentiation of Human Embryonic Stem Cells. *Cell Stem Cell* **5**, 214-226, doi:10.1016/j.stem.2009.05.021 (2009).

138 Huttlin, E. L. *et al.* A Tissue-Specific Atlas of Mouse Protein Phosphorylation and Expression. *Cell* **143**, 1174-1189, doi:https://doi.org/10.1016/j.cell.2010.12.001 (2010).

139 Humphrey, S. J. *et al.* Dynamic adipocyte phosphoproteome reveals that Akt directly regulates mTORC2. *Cell metabolism* **17**, 1009-1020, doi:10.1016/j.cmet.2013.04.010 (2013).

140 Zhang, X. *et al.* Quantitative phosphoproteomics reveals novel phosphorylation events in insulin signaling regulated by protein phosphatase 1 regulatory subunit 12A. *J Proteomics* **109**, 63-75, doi:10.1016/j.jprot.2014.06.010 (2014).

141 Sakashita, G. *et al.* Regulation of type 1 protein phosphatase/inhibitor-2 complex by glycogen synthase kinase-3beta in intact cells. *Journal of biochemistry* **133**, 165-171, doi:10.1093/jb/mvg020 (2003).

142 Ma, T. *et al.* Microcystin-LR exposure disrupts the insulin signaling pathway in C2C12 mice muscle cell line. *Environmental toxicology* **35**, 194-202, doi:10.1002/tox.22856 (2020).

143 Cameron, A. R. *et al.* Anti-Inflammatory Effects of Metformin Irrespective of Diabetes Status. *Circulation research* **119**, 652-665, doi:10.1161/CIRCRESAHA.116.308445 (2016).

144 Mashili, F., Chibalin, A. V., Krook, A. & Zierath, J. R. Constitutive STAT3 phosphorylation contributes to skeletal muscle insulin resistance in type 2 diabetes. *Diabetes* **62**, 457-465, doi:10.2337/db12-0337 (2013).

145 Jatiani, S. S., Baker, S. J., Silverman, L. R. & Reddy, E. P. Jak/STAT pathways in cytokine signaling and myeloproliferative disorders: approaches for targeted therapies. *Genes & cancer* **1**, 979-993, doi:10.1177/1947601910397187 (2010).

146 Jablonski, K. A. *et al.* Common variants in 40 genes assessed for diabetes incidence and response to metformin and lifestyle intervention in the diabetes prevention program. *Diabetes* **59**, 2672-2681, doi:10.2337/db10-0543 (2010).

147 Wang, Z. & Thurmond, D. C. Mechanisms of biphasic insulin-granule exocytosis - roles of the cytoskeleton, small GTPases and SNARE proteins. *Journal of cell science* **122**, 893-903, doi:10.1242/jcs.034355 (2009).

148 Kowluru, A. Small G proteins in islet beta-cell function. *Endocrine reviews* **31**, 52-78, doi:10.1210/er.2009-0022 (2010).

149 Andjelkovic, M. *et al.* Activation and phosphorylation of a pleckstrin homology domain containing protein kinase (RAC-PK/PKB) promoted by serum and protein phosphatase inhibitors. *Proceedings of the National Academy of Sciences of the United States of America* **93**, 5699-5704 (1996).

150 Galbo, T., Olsen, G. S., Quistorff, B. & Nishimura, E. Free fatty acid-induced PP2A hyperactivity selectively impairs hepatic insulin action on glucose metabolism. *PloS one* **6**, e27424, doi:10.1371/journal.pone.0027424 (2011).

151 Galbo, T. *et al.* PP2A inhibition results in hepatic insulin resistance despite Akt2 activation. *Aging* **5**, 770-781, doi:10.18632/aging.100611 (2013).

152 Laplante, M. & Sabatini, D. M. mTOR signaling at a glance. *Journal of cell science* **122**, 3589-3594, doi:10.1242/jcs.051011 (2009).

153 Lizcano, J. M. & Alessi, D. R. The insulin signalling pathway. *Current biology : CB* **12**, R236-238 (2002).

154 Ragolia, L. & Begum, N. Protein phosphatase-1 and insulin action. *Molecular and cellular biochemistry* **182**, 49-58 (1998).

155 Berdeaux, R. & Stewart, R. cAMP signaling in skeletal muscle adaptation: hypertrophy, metabolism, and regeneration. *American journal of physiology.*

Endocrinology and metabolism **303**, E1-17, doi:10.1152/ajpendo.00555.2011 (2012).

156 Steinberg, G. R. & Jorgensen, S. B. The AMP-activated protein kinase: role in regulation of skeletal muscle metabolism and insulin sensitivity. *Mini reviews in medicinal chemistry* **7**, 519-526 (2007).

157 Steinberg, G. R. & Kemp, B. E. AMPK in Health and Disease. *Physiological reviews* **89**, 1025-1078, doi:10.1152/physrev.00011.2008 (2009).

158 Nakashima, A. *et al.* A positive role of mammalian Tip41-like protein, TIPRL, in the amino-acid dependent mTORC1-signaling pathway through interaction with PP2A. *FEBS letters* **587**, 2924-2929, doi:10.1016/j.febslet.2013.07.027 (2013).

159 Kowluru, A., Seavey, S. E., Rabaglia, M. E., Nesher, R. & Metz, S. A. Carboxylmethylation of the catalytic subunit of protein phosphatase 2A in insulin-secreting cells: evidence for functional consequences on enzyme activity and insulin secretion. *Endocrinology* **137**, 2315-2323, doi:10.1210/endo.137.6.8641181 (1996).

160 Arora, D. K. *et al.* High glucose exposure promotes activation of protein phosphatase 2A in rodent islets and INS-1 832/13 beta-cells by increasing the posttranslational carboxylmethylation of its catalytic subunit. *Endocrinology* **155**, 380-391, doi:10.1210/en.2013-1773 (2014).

161 Kowluru, A. & Matti, A. Hyperactivation of protein phosphatase 2A in models of glucolipotoxicity and diabetes: potential mechanisms and functional consequences. *Biochem Pharmacol* **84**, 591-597, doi:10.1016/j.bcp.2012.05.003 (2012).

162 Li, L., Ren, C. H., Tahir, S. A., Ren, C. & Thompson, T. C. Caveolin-1 maintains activated Akt in prostate cancer cells through scaffolding domain binding site interactions with and inhibition of serine/threonine protein phosphatases PP1 and PP2A. *Mol Cell Biol* **23**, 9389-9404, doi:10.1128/mcb.23.24.9389-9404.2003 (2003).

163 Habersetzer, J. *et al.* ATP synthase oligomerization: from the enzyme models to the mitochondrial morphology. *The international journal of biochemistry & cell biology* **45**, 99-105, doi:10.1016/j.biocel.2012.05.017 (2013).

164 Hojlund, K. *et al.* Human ATP synthase beta is phosphorylated at multiple sites and shows abnormal phosphorylation at specific sites in insulin-resistant muscle. *Diabetologia* **53**, 541-551, doi:10.1007/s00125-009-1624-0 (2010).

165 JeBailey, L. *et al.* Skeletal muscle cells and adipocytes differ in their reliance on TC10 and Rac for insulin-induced actin remodeling. *Molecular endocrinology (Baltimore, Md.)* **18**, 359-372, doi:10.1210/me.2003-0294 (2004).

166 Ueda, S., Kataoka, T. & Satoh, T. Activation of the small GTPase Rac1 by a specific guanine-nucleotide-exchange factor suffices to induce glucose uptake into skeletal-muscle cells. *Biology of the cell* **100**, 645-657, doi:10.1042/bc20070160 (2008).

167 Sylow, L. *et al.* Rac1 is a novel regulator of contraction-stimulated glucose uptake in skeletal muscle. *Diabetes* **62**, 1139-1151, doi:10.2337/db12-0491 (2013).

168 ten Klooster, J. P., Leeuwen, I., Scheres, N., Anthony, E. C. & Hordijk, P. L. Rac1-induced cell migration requires membrane recruitment of the nuclear

oncogene SET. *The EMBO journal* **26**, 336-345, doi:10.1038/sj.emboj.7601518 (2007).

169 Sents, W., Ivanova, E., Lambrecht, C., Haesen, D. & Janssens, V. The biogenesis of active protein phosphatase 2A holoenzymes: a tightly regulated process creating phosphatase specificity. *The FEBS journal* **280**, 644-661, doi:10.1111/j.1742-4658.2012.08579.x (2013).

170 Kong, M., Ditsworth, D., Lindsten, T. & Thompson, C. B. Alpha4 is an essential regulator of PP2A phosphatase activity. *Molecular cell* **36**, 51-60, doi:10.1016/j.molcel.2009.09.025 (2009).

171 McConnell, J. L. *et al.* Alpha4 is a ubiquitin-binding protein that regulates protein serine/threonine phosphatase 2A ubiquitination. *Biochemistry* **49**, 1713-1718, doi:10.1021/bi901837h (2010).

172 Scott, R. W. & Olson, M. F. LIM kinases: function, regulation and association with human disease. *Journal of molecular medicine (Berlin, Germany)* **85**, 555-568, doi:10.1007/s00109-007-0165-6 (2007).

173 Bernard, O. Lim kinases, regulators of actin dynamics. *The international journal of biochemistry & cell biology* **39**, 1071-1076, doi:10.1016/j.biocel.2006.11.011 (2007).

174 Manetti, F. LIM kinases are attractive targets with many macromolecular partners and only a few small molecule regulators. *Medicinal research reviews* **32**, 968-998, doi:10.1002/med.20230 (2012).

175 Hein, M. Y. *et al.* A human interactome in three quantitative dimensions organized by stoichiometries and abundances. *Cell* **163**, 712-723, doi:10.1016/j.cell.2015.09.053 (2015).

176 Thanasopoulou, A., Stravopodis, D. J., Dimas, K. S., Schwaller, J. & Anastasiadou, E. Loss of CCDC6 affects cell cycle through impaired intra-S-phase checkpoint control. *PloS one* **7**, e31007, doi:10.1371/journal.pone.0031007 (2012).

177 Lecker, S. H., Goldberg, A. L. & Mitch, W. E. Protein Degradation by the Ubiquitin–Proteasome Pathway in Normal and Disease States. *Journal of the American Society of Nephrology* **17**, 1807, doi:10.1681/ASN.2006010083 (2006).

178 Lee, W. J., Kim, D. U., Lee, M. Y. & Choi, K. Y. Identification of proteins interacting with the catalytic subunit of PP2A by proteomics. *Proteomics* **7**, 206-214, doi:10.1002/pmic.200600480 (2007).

179 Self, A. J., Caron, E., Paterson, H. F. & Hall, A. Analysis of R-Ras signalling pathways. *Journal of Cell Science* **114**, 1357 (2001).

180 Rachek, L. I. Free fatty acids and skeletal muscle insulin resistance. *Progress in molecular biology and translational science* **121**, 267-292, doi:10.1016/b978-0-12-800101-1.00008-9 (2014).

181 Tillander, V. *et al.* Acyl-CoA thioesterase 9 (ACOT9) in mouse may provide a novel link between fatty acid and amino acid metabolism in mitochondria. *Cellular and molecular life sciences : CMLS* **71**, 933-948, doi:10.1007/s00018-013-1422-1 (2014).

182 Okuma, T., Honda, R., Ichikawa, G., Tsumagari, N. & Yasuda, H. In vitro SUMO-1 modification requires two enzymatic steps, E1 and E2. *Biochemical and biophysical research communications* **254**, 693-698, doi:10.1006/bbrc.1998.9995 (1999).

183 Tsakiridis, T. *et al.* Role of the actin cytoskeleton in insulin action. *Microscopy research and technique* **47**, 79-92, doi:10.1002/(sici)1097-0029(19991015)47:2<79::aid-jemt1>3.0.co;2-s (1999).

184 Patel, N., Rudich, A., Khayat, Z. A., Garg, R. & Klip, A. Intracellular segregation of phosphatidylinositol-3,4,5-trisphosphate by insulin-dependent actin remodeling in L6 skeletal muscle cells. *Molecular and cellular biology* **23**, 4611-4626 (2003).

185 Bisht, B. & Dey, C. S. Focal Adhesion Kinase contributes to insulin-induced actin reorganization into a mesh harboring Glucose transporter-4 in insulin resistant skeletal muscle cells. *BMC cell biology* **9**, 48, doi:10.1186/1471-2121-9-48 (2008).

186 Noritake, J., Watanabe, T., Sato, K., Wang, S. & Kaibuchi, K. IQGAP1: a key regulator of adhesion and migration. *Journal of cell science* **118**, 2085-2092, doi:10.1242/jcs.02379 (2005).

187 Suzuki, K. & Takahashi, K. Reduced cell adhesion during mitosis by threonine phosphorylation of beta1 integrin. *Journal of cellular physiology* **197**, 297-305, doi:10.1002/jcp.10354 (2003).

188 Suzuki, K., Chikamatsu, Y. & Takahashi, K. Requirement of protein phosphatase 2A for recruitment of IQGAP1 to Rac-bound beta1 integrin. *Journal of cellular physiology* **203**, 487-492, doi:10.1002/jcp.20249 (2005).

189 Abel, A. M. *et al.* IQGAP1: insights into the function of a molecular puppeteer. *Molecular immunology* **65**, 336-349, doi:10.1016/j.molimm.2015.02.012 (2015).

190 Cersosimo, E., Triplitt, C., Solis-Herrera, C., Mandarino, L. J. & DeFronzo, R. A. in *Endotext* (eds K. R. Feingold *et al.*) (MDText.com, Inc. Copyright © 2000-2020, MDText.com, Inc., 2000).

191 Ahmad, F. & Goldstein, B. J. Increased abundance of specific skeletal muscle protein-tyrosine phosphatases in a genetic model of insulin-resistant obesity and diabetes mellitus. *Metabolism* **44**, 1175-1184 (1995).

192 Zierath, J. R., Krook, A. & Wallberg-Henriksson, H. Insulin action and insulin resistance in human skeletal muscle. *Diabetologia* **43**, 821-835, doi:10.1007/s001250051457 (2000).

ABSTRACT

PROTEIN PHOSPHATASE 2A IN METFORMIN'S ACTION IN PRIMARY HUMAN SKELETAL MUSCLE CELLS

by

AKTHAM MESTAREEHI

August 2021

Advisors: Dr. Zhengping Yi & Dr. Anjaneyulu Kowluru

Major: Pharmaceutical Sciences (Pharmacology)

Degree: Doctor of Philosophy

Diabetes is a group of metabolic diseases characterized by hyperglycemia caused by defects in insulin secretion, insulin action, or both. Diabetes is associated with damage, dysfunction, and failure of various organs, such as the eyes, heart, kidneys, and brain. Diabetes is mainly classified into type 1 (T1DM) and type 2 diabetes (T2D). Diabetes affects more than 34 million people in the USA (about 1 in 10) and more than 90% of diabetic patients have type 2 diabetes (T2D). Insulin resistance is a main characteristic feature of type 2 diabetes. Skeletal muscle insulin resistance is considered to be the primary defect that is evident decades before β-cell failure and overt T2D. Skeletal muscle is the major site of insulin-stimulated glucose uptake (>70%) in the postprandial state in humans. Metformin (N, N-dimethylbiguanide) is an effective oral biguanide antihyperglycemic drug and the most frequently prescribed as a first-line therapy for type 2 diabetes mellitus. It is widely accepted that metformin can reduce glucose production by the liver, and increase insulin sensitivity (i.e., decrease insulin resistance) in skeletal muscles. Metformin stimulates insulin-mediated glucose uptake in skeletal muscle in T2D patients by increasing Thr172 phosphorylation (pThr172)

and activity of AMP-activated protein kinase (AMPK). However, the molecular mechanism of metformin's action in skeletal muscle is not well understood.

Protein phosphorylation, regulated by kinases and phosphatases, plays a key role in many cell signaling events, including insulin signaling. Abnormal protein phosphorylation has been implicated in the development of skeletal muscle insulin resistance and T2D[191,192191,192190,191]. However, most studies on protein phosphorylation in insulin resistance and T2D have been focused on kinases and little is known regarding the role of phosphatases. Protein Phosphatase 2A (PP2A) is a ubiquitously expressed serine/threonine phosphatase and plays a pivotal role in cellular processes, such as signal transduction, cell proliferation, and apoptosis, through dephosphorylating key signaling molecules such as AKT, AMPK, etc. Structurally, PP2A is composed of catalytic subunit C (PP2Ac), scaffold subunit A and a regulatory subunit B. PP2Ac and scaffold subunit A have two isoforms and the regulatory subunit B has four different families containing different isoforms. Whether PP2A plays a role in metformin-induced insulin sensitivity improvement in human skeletal muscle remains to be elucidated. Here, we investigated and measured PP2A activity, novel PPAc interaction partners, and novel PP2A substrates in human skeletal muscle cells derived from lean insulin-sensitive and obese insulin-resistant participants.

Hyperinsulinemic-euglycemic clamp was performed to assess insulin sensitivity in human subjects and skeletal muscle biopsy samples were obtained. Primary human skeletal muscle cells were cultured from these muscle biopsies that included 8 lean insulin-sensitive and 8 obese insulin-resistance participants. The cells were expanded, differentiated into myotubes, and treated with/without 50μM metformin for 24 hours, okadaic acid 5nM for 30 minutes, and/or Insulin 100nM for 15 minutes, before harvesting. The PP2A activity was performed and measured according to the manufacturer's

protocol. The phosphoproteome and proteome were performed according to our protocol using Orbitrap Fusion Lumos UPLC- ESI-MS/MS. We have identified >24,700 phosphorylation sites in 7,037 proteins, which is one of the largest catalogs of experimentally determined phosphorylation sites in primary human skeletal muscle cells. Among all phosphorylation sites identified 1,958 were not reported in human and 1,756 were not reported in any species in the PhosphositePlus database, thus appears to be novel. We identified phosphorylation sites in 291 kinases/kinases subunits and 18 phosphatases subunits of protein phosphatase 2A. Bioinformatics analysis indicated that subcellular localizations, multiple biological processes, molecular functions, and KEGG pathway (e.g., insulin signaling pathway, AMPK signaling, mTOR signaling, MAPK signaling, and ErbB signaling) were significantly enriched for these phosphoproteins. Furthermore, we identified proteins that potentially interact with PP2Ac and several proteins previously known to interact with PP2Ac such as CaMK II and GSK3. Many of the newly identified PP2Ac-binding proteins were associated with growth control. We identified 1377 interaction partners in human skeletal muscle cells with 19 partners classified as metformin responsive. Moreover, 450 interaction partners are identified in human skeletal muscle cells in insulin stimulation responsive, and 44 proteins presented a significant difference among the two groups. We observed several proteins associated with insulin signaling as PP2Ac interaction partners in human skeletal muscle cells like Rac1, Akt2, MAPK, and Limk1. We reported that metformin reversed the abnormality in PP2Ac interaction partners in obese insulin-resistant and rendered them similar to lean insulin-sensitive participants.

AUTOBIOGRAPHICAL STATEMENT

AKTHAM MESTAREEHI

EDUCATION

- Masters in Separation Sciences, Northeastern Illinois, USA
- Bachelors in Pharmacy, Rochville University, USA

PROFESSIONAL ASSOCIATIONS

- American Society for Mass Spectrometry (ASMS)
- American Association for Pharmaceutical Scientists (AAPS)

PUBLICATIONS & PRESENTATIONS

- Divyasri Damacharla; Vijayalakshmi Thamilselvan; Xiangmin Zhang; **Aktham Mestareehi**; Zhengping Yi; and Anjan Kowluru, "Quantitative proteomics reveals novel interaction partners of Rac1 in pancreatic beta-cells: Evidence for increased interaction with Rac1 under glucotoxic conditions", Molecular and Cellular Endocrinology, 2019 Jun 13:110489. doi: 10.1016/j.mce.2019.110489. [Epub ahead of print]. PMID: 31202817. (Impact Factor: 3.693).

- Yue Qi; Xiangmin Zhang; Berhane Seyoum; Zaher Msallaty; Abdullah Mallisho; Michael Caruso; Divyasri Damacharla; Danjun Ma; Wissam Al-janabi; Rebecca Tagett; Majed Alharbi; Griffin Calme; **Aktham Mestareehi**; Sorin Draghici, Abdul Abou-Samra, Anjaneyulu Kowluru, and Zhengping Yi, "Kinome profiling reveals abnormal activity of kinases in skeletal muscle from adults with obesity and insulin resistance", Journal of Clinical Endocrinology & Metabolism, 2020 Mar 1;105(3). DOI: 10.1210/clinem/dgz115, PMID: 31652310 (Impact Factor: 5.605).

- **Aktham Mestareehi;** Xiangmin Zhang; Berhane Seyoum; Zaher Msallaty; Abdullah Mallisho; Kyle Jon Burghardt; Anjaneyulu Kowluru and Zhengping Yi "Metformin Increases Protein Phosphatase 2A Activity In Primary Human Skeletal Muscle Cells", In review.

- **Aktham Mestareehi**#; Hainan Li#; Xiangmin Zhang; Zhengping Yi; and Jiemei Wang, "Trans-resveratrol (tRES) and Hesperetin (HESP) Rescued Disrupted Angiogenesis in Endothelial Cells from Type 2 Diabetic Patients", In Preparation. # Co-1st author.

- **Aktham Mestareehi**; Xiangmin Zhang; Berhane Seyoum; Zaher Msallaty; Abdullah Mallisho; Kyle Jon Burghardt; Anjaneyulu Kowluru and Zhengping Yi "Effect of Metformin on Protein Phosphatase 2A Complexes In Primary Human Skeletal Muscle Cells", In Preparation.

- **Aktham Mestareehi**; Xiangmin Zhang; Berhane Seyoum; Zaher Msallaty; Abdullah Mallisho; Kyle Jon Burghardt; Anjaneyulu Kowluru and Zhengping Yi "Effect of Metformin on Global Phosphorylation Profiles In Primary Human Skeletal Muscle Cells Derived from Insulin Resistant Participants", In Preparation.